NGU Report 97.014

Core-drilling at the Engebø-fjell rutile-bearing eclogite 1995/96; Dh1 to Dh10

NGU
Norges geologiske undersøkelse
Geological Survey of Norway

Geological Survey of Norway
P.O.Box 3006 - Lade
N-7002 Trondheim, Norway
Tel.: 47 73 90 40 11
Telefax 47 73 92 16 20

REPORT

Report no.: 97.014	ISSN 0800-3416	Grading: ~~Confidential until 31 Des. 2001~~ Åpen

Title:
Core-drilling at the Engebøfjell rutile-bearing eclogite 1995-96. Summary report.

Authors:
Are Korneliussen and Muriel Erambert

Client:
DuPont/Conoco

County: Sogn og Fjordane

Commune: Naustdal

Map-sheet name (M=1:250.000)
Florø

Map-sheet no. og -name (M=1:50.000)
1117.1 Dale

Deposit name and grid-reference:
Engebøfjellet (310300 6823100)

Number of pages: 141 Price (NOK) Kr. 1065,-
Map enclosures: 2

Fieldwork carried out:	Date of report:	Project no.:	Person responsible:
Oct.95-June 96	7 May 1996	1900.05	

Summary:

Engebøfjellet is situated on the northern side of Førdefjord within an area characterized by a series of Proterozoic felsic and mafic rocks heavily affected by Caledonian deformation and metamorphism. During the Caledonian high-pressure metamorphism Proterozoic mafic rocks were transformed into eclogites. In this transformation ilmenite was replaced by rutile. The protolith to the Engebøfjell eclogite is believed to be a layered, Ti-rich, Proterozoic gabbroic complex; it now has the form of a highly irregular, east-west trending, 2.5 km long and up to 0.5 km broad lens dipping steeply to the north. It consists of two major eclogite varieties: a leucogabbroic eclogite with low Ti-and Fe-content, and a ferrogabbroic, Ti-and Fe-rich eclogite. This ferrogabbroic eclogite is the rutile ore that has been the focus of the rutile exploration work at Engebøfjellet. In the period October 1995 to June 1996 ten reconnaissance bore-holes were drilled to investigate the character of the Engebøfjell ferrogabbroic eclogite at depth; altogether 2340 meters of core w ere recovered. This report gives a summary of these drilling results with analytical data and mineralogical descriptions.

Keywords: industrimineraler	kjerneboring	titan
rutil	eklogitt	fagrapport

Contents

page

1. Introduction 4
2. Primary geologic relations 7
3. The drilling 9
4. Core logging 9
5. Microscopy results 25
6. Analytical results
   - 6.1. X-Met TiO_2 and Fe_2O_3 analyses 35
   - 6.2. Major and trace element analyses 35
   - 6.3. The reliability of the X-Met TiO_2-analyses 37
   - 6.4. Petrophysical data 40
7. Summary and conclusion 43
8. References 45

Figures

Fig. 1: Geological map of the Førdefjord region (after Lutro and Ragnhildstveit, in prep.).
Fig. 2: Vertical profile - Dh 1.
Fig. 3: Vertical profile - Dh 2.
Fig. 4: Vertical profile - Dh 3.
Fig. 5: Vertical profile - Dh 4.
Fig. 6: Vertical profile - Dh 5.
Fig. 7: Vertical profile - Dh 6.
Fig. 8: Vertical profile - Dh 7.
Fig. 9: Vertical profile - Dh 8.
Fig. 10: Vertical profile - Dh 9.
Fig. 11: Vertical profile - Dh 10.
Fig. 12: Ferrogabbroic eclogite, core- and photomicrographs.
Fig. 13: Ferrogabbroic eclogite, core-photographs.
Fig. 14: Retrograded ferrogabbroic eclogite, photomicrographs.
Fig. 15: Retrograded ferrogabbroic eclogite, photomicrographs.
Fig. 16: Leucogabbroic eclogite, core- and photomicrographs.
Fig. 17: Amphibolites, core-photographs.
Fig. 18: Amphibolite unit rocks, core-photographs.
Fig. 19: Ferrogabbroic eclogite / amphibolite contact, core photograph.
Fig. 20: X-Met TiO_2 analyses vs. laboratory XRF-analyses.
Fig. 21: Scattergram plot of TiO_2 (X-Met) vs. TiO_2 (XRF-lab.).
Fig. 22: Scattergram plot of TiO_2 (X-Met) curved core surface vs. cut surface.
Fig. 23: Histogram showing specific gravity distribution for eclogite.
Fig. 24: Scattergram plots of TiO_2 vs. density and magnetic susceptibility.
Fig. 25: Scattergram plot showing Fe_2O_3, TiO_2 and density relations.
Fig. 26: Magnetic susceptibility distribution (histogram).

Tables

Table 1: Review of the exploration of the Engebøfjell eclogite deposit.
Table 2: Major lithologic units, Engebø-Vevring area.
Table 3: Bore-hole information.
Table 4: Dh 1 summary.
Table 5: Dh 2 summary.
Table 6: Dh 3 summary.
Table 7: Dh 4 summary.
Table 8: Dh 5 summary.
Table 9: Dh 6 summary.
Table 10: Dh 7 summary.
Table 11: Dh 8 summary.

Table 12: Dh 9 summary.
Table 13: Dh 10 summary.
Table 14: Core sample analyses summary.
Table 15: Average major- and trace-elements for characteristic Engebøfjellet rock-types.
Table 16: Petrophysical parameters.

Appendix

1. Miscellaneous scattergram plots showing TiO_2, Fe_2O_3, density and magn. susc. relations.
2. Petrophfysical data, core-samples.
3. Major and trace element analyses of core-samples.
4. Comparison of different X-Met analyses of the same core-sections.
5. Microscopy results.
6. Geologic map of the Førdefjord region.
7. Geologic map, Engebøfjellet.
8. Photographs of 10m core sections, Dh6 - Dh10, Dh3 (163 - 215 m).

Acknowledgements
We would like to thank Odd Sagegg, Gunnar Fossflaten,, Gudmund Grammeltvedt, Jomar Staw and Leif Furuhaug for miscellaneous work on cores at NGU's core storage at Løkken as well as in Trondheim, and Carl O. Mathiesen and Elisabeth Eide for reviewing the manuscript.

1. Introduction

Since 1992 NGU has collaborated with DuPont in a project for the investigation of rutile-bearing eclogites in W. Norway. This has resulted in a significant amount of new information including several new discoveries of rutile-rich eclogite. Existence of the Engebøfjell eclogite has been known since the 1970s (Korneliussen 1980 b; Korneliussen & Foslie 1985, Korneliussen & Furuhaug 1991); it has the form of an E-W-trending 2.5 km long, irregular zone of rutile-bearing eclogite at the northern side of Førdefjord at Engebø (Fig. 1, Appendix 4 and 5) in Naustdal kommune. For several years it had been considered to be of economic interest for rutile, but was not previously well investigated in the DuPont/NGU collaboration project due to mineral-right complications. In 1995, the company Fjord Blokk started production of eclogite blocks for breakwater material at the eastern end of the deposit, based on an eclogite mining-concession. The eastern half of Engebøfjellet had then been assigned for industry in the «reguleringsplan» of Naustdal kommune.

A meeting was held between Fjord Blokk and DuPont/Conoco in July 1995 which resulted in a collaboration in the continued investigation of Engebøfjellet and establishment of a core-drilling program. At first, the intent was to drill 400 m in the eastern part of Engebøfjellet near Fjord Blokk's quarry and financial support was given by the Prospecting Fund. The drilling started in October 1995. Shortly afterwards, the drilling program was extended and at the end of this first drilling program in June, 10 holes had been drilled, which comprised 2340 drill-meters. Some events in the long investigation history of the Engebøfjell eclogite are listed in Table 1.

Table 1: Review of the exploration of the Engebøfjell eclogite deposit.

Early 1970's	The Elkem geologist Hans-Peter Geis was probably the first geologist to recognize the Engebøfjell eclogite as a rutile deposit in the early '70's. He made a sampling profile through the road-tunnel.
1978-89	Additional sampling was done within a cooperation project between NGU and Elkem on rutile-bearing eclogites in Sunnfjord.
1979	Frank Barkve and geologist Tore Birkeland focused on Engebøfjellet in an investigation of heavy rocks as breakwater material. That was the start of a long and complex process which resulted in Fjord Blokk's eclogite mining operation in 1995.
1984-85	Three or four companies were active at Engebøfjellet in the mid-80's investigating the rutile and breakwater material/aggregate possibilities.
1990	NGU made a W-E sampling profile along the deposit (Korneliussen & Furuhaug 1991).
1992	Signing of agreement between DuPont and NGU to jointly investigate the rutile potential of eclogites in W.Norway.
1991	R. McLimans (DuPont), S. Parr (Stokke Industri) and A. Korneliussen (NGU) visited Engebøfjellet on a rutile/eclogite excursion in W. Norway, followed by a sample profile through the road tunnel later the same year by McLimans and K. Davies (also from DuPont).
1995	Fjord Blokk and Conoco/DuPont made an agreement for a joint rutile investigation of Engebøfjellet, followed by core-drilling, beneficiation tests, surface sampling and geologic mapping activities.

The purpose of this report is to summarize the results of the 2340 m of core-drilling that was done in the period October '95 to June '96. Additional drilling in the autumn 1996 will be reported separately. Another report (in prep) will focus on the geology of the Engebøfjell eclogite.

2. Primary geologic relations

The Førdefjord region is characterized by a variety of Proterozoic granitoid rocks which were strongly deformed and metamorphosed into gneisses during the Caledonian orogeny. Eclogitized mafic units including some major eclogite bodies such as the Engebøfjell eclogite are found within these granitoid gneisses on both sides of Førdefjord and eastwards from Naustdal (Fig. 1 and Appendix 6). The geologic relations at Engebøfjellet will be described very briefly in this report since they will be the subject of another report.

The Engebø - Vevring area is characterized by a series of mafic rocks (eclogitic and amphibolitic) intermixed with gray gneisses. These eclogites are mainly of a garnet-poor, amphibole-rich type, with gradational transitions into garnet-amphibolites and amphibolites. Generally, the eclogite to amphibolite transition is an effect of retrogression. The gray gneisses are of two types, (a) as cm-dm thick leucocratic bands (quartz + feldspar + white-mica) alternating with mafic bands of garnet amphibolitic to eclogitic composition, and (b) units of granodioritic gneiss several meters thick. These surrounding, gneissose rocks are called the «amphibolite unit» in this report.

Table 2: Major lithologic units in the Engebøfjell - Vevring area.

The surrounding rocks	
Granitoid gneisses (undifferentiated)	Variably deformed granitoid gneisses.
Amphibolite unit (undifferentiated)	Amphibolitic to eclogitic rocks intermixed with gray gneisses. A characteristic feature is a cm-dm thick alternating amphibolite/eclogite and gray gneiss bands (see e.g. Fig. 19 and later explanation). The gray gneiss also occur in several meters thick units of granodioritic composition.
The Engebøfjell eclogite rocks	
Leucogabbroic eclogite (< 14% Fe_2O_3, < 2 % TiO_2)	Fine-grained eclogite with a fairly low garnet content. In varieties with minor deformation a gabbroic texture is preserved (see e.g. Fig. 17 and later explanation).
Transitional eclogite (14-16% Fe_2O_3, 2-3 % TiO_2)	Eclogite intermediate between the leucogabbroic and the ferrogabbroic eclogite (not shown in the geologic map of Appendix 6).
Ferrogabbroic eclogite (>16% Fe_2O_3, >3 % TiO_2)	Fine-grained, dark, garnet-rich eclogite, often with a more massive character than the other eclogite varieties.

The Engebøfjell eclogite is an E-W-trending lens with a distinct massive character compared to the surrounding amphibolite unit rocks. The body is subdivided into two major eclogite types based on their varying iron and titanium contents:

(1), The ***ferrogabbroic eclogite*** is Fe_2O_3 -, TiO_2 - and garnet-rich. In general, it has a more massive character than the other eclogite varieties found at Engebøfjellet, although in parts it is significantly banded and folded. This eclogite is the rutile ore-type eclogite with the major volume found in the central and western parts of the deposit. This eclogite occasionally shows intrusive relations into the leucogabbroic eclogite (see below), but usually the contacts are gradational via a «transitional» eclogite variety. Rutile- and garnet-rich, and fairly massive eclogite layers in the Fjord Blokk quarry, and the rutile-rich parts of Dh1, 2 and 3 (see Chapter 3), are eastward extensions of this eclogite type.

(2) The ***leucogabbroic eclogite*** is TiO_2 - and Fe_2O_3-poor, locally with preserved gabbroic textures. In general, the the most distinct gabbroic character is in the western parts of the eclogite. However, this rock-type has not been mapped in the eastern part of Engebøfjellet; i.e. it is not distinguished from the amphibolite unit on the geologic map of Fig. 2 and Appendix 6.

Eclogite varieties intermediate between the leucogabbroic eclogite and the ferrogabbroic eclogite are called ***transitional eclogite***. The transitions between these eclogite varieties are usually gradational but can also be sharp. ***Granitoid gneisses*** including granitic gneiss, granitic augen gneiss and granitic mylonite belong to the surrounding gneiss complex and will not be discussed in this report.

The main features of the internal structure of the body were acquired during eclogite-facies metamorphism. The intense eclogite-facies deformation is marked by isoclinal folding, shear deformation and boudinage. Infolding of «gneiss» with eclogite-facies mineralogy (quartz, clinozoisite, phengite, omphacite) and quartz mobilizats are found along the main shear zones. Evidence of fluid activity during the high-pressure metamorphism include veins (with quartz, omphacite, rutile, mica) and pegmatoid pods, as well as the ubiquitous presence of eclogite-facies hydrous and volatile-bearing minerals (amphibole, white mica, clinozoisite, carbonate and apatite). Syn-eclogitic metasomatic veins (abundant carbonate ± garnet, quartz, amphibole and sulfides) are particularly abundant in the mafic eclogite mylonites in the east (e.g. in the Fjord Blokk quarries at the eastern end of Engebøfjellet).

A large part of the leucogabbro appears to have escaped the deformation and is statically eclogitized ("coronitic eclogite"), except at the contacts with the ferrogabbroic unit and along internal shear zones where foliated eclogites formed. Original banding of the magmatic protolith can locally be seen as dm-thick darker layers. Most light eclogites within the layered unit of eclogites, amphibolites and gneisses probably represent metasomatized and deformed leucogabbro.

The ferrogabbro appears totally eclogitized and recrystallised. In the field, differences in composition inherited from the magmatic protolith are now seen as a contrast in color between very dark- and fine-grained eclogites (those including the Ti "ore") and green eclogites, often with visible amphibole porphyroblasts (towards "intermediate" eclogites, with $TiO_2 < 3$ wt%?).

Because of the very fine grain size and dark color of the eclogites, and especially of the Ti-rich ones, it is often difficult in the field to estimate the extent of retrogression for individual samples. However, where visible, extensive amphibolite-facies retrogression is linked mainly to the margins of the body and internal shear-zones. The central part of the lens appears to have been little affected, having behaved mainly as a rigid core. Thus, the main ferrogabbroic body, the coronitic leucogabbroic eclogite and the central part of the layered unit suffered only minor retrogression. Apart from some discrete shear zones, most of the retrogression generally may be linked to the late fractures. Also, a large fold nose within mafic eclogite to the east of the Vevring farms is remarkably fresh. Both the western and eastern parts of the Engebøfjell body have been strongly sheared; lenses of coronites and eclogites are divided by amphibolite-facies shear zones.

3. The drilling

The drilling started in October 1995. The original plan was to drill only 400 m in 2-3 holes in the eastern part of Engebøfjellet because of unresolved property issues and industrial zoning boundaries. Additional holes were planned when progress was made in resolving the W. Engebøfjell property status. The drilling continued throughout the autumn '95, winter '96 and spring '96, the total core length recovered for 10 holes was 2340 m.

The drilling of Dh1 and Dh2 in October-November 1995 was done without particular complications. At Dh3 (Nov. - Dec.), however, severe water supply problems occurred due to an unusually dry and frosty autumn, and the hole was stopped at 160 m due to lack of water. Dh3 was later in the spring of 1996 extended to 215 m. At Dh4 a small water source and some additional water from Dh3-hole made it possible to drill to 160m. At this depth open fractures caused a fall in water pressure and the hole was stopped.

To be able to continue drilling during the winter, a reliable water supply was needed. An arrangement with an electric pump, electric pre-heating of the water, and a 1 km-long pipe from the stream 60 m.a.s.l. near the western road-tunnel opening was set up. While weather conditions were warmer this arrangement worked perfectly, but when the air-temperature sank below - 10° C combined with strong wind, the water in the pipes froze, again causing significant delays in the drilling. Another complication was unreliability in the supply of electricity. However, the drilling was able to continue throughout the winter 1996 and Dh5, Dh6 and Dh7 were drilled in Feb.- March and Dh8, and an extension of Dh3 from 160 m to 215 m, in April. The Dh-positions are shown on the Engebøfjell geologic map (Appendix 7) and in Figs. 2 to 11.

Table 3: Bore-hole information. The complete deviation measurement results are given in a separate report by Devico A/S (Tokle 1996).

Bore-hole #	Direction ¤	Dip ¤	Length (m)	East *	North *	D.a.s.l. #
1	163°	44.8°	196,4	311457	6823546	142
2	161°	45.2°	334,6	311099	6823529	229
3	190°	45°	215,0	310602	6823378	318
4	184°	45.0°	159,6	310352	6823310	294
5	178°	59.4°	180,0	310067	6823209	248
6	169°	59.8°	126,1	309936	6823151	237
7	178°	59.0°	215,4	310223	6823199	283
8	174°	60.0°	299,7	310504	6823276	314
9	356°	24.5°	290,0	310165	6822976	50
10	159°	25.3°	323,0	309653	6823340	58
			2339,8			

* UTM-coord. in meters (wgs84) # Distance above sea-level (m)
¤ Direction according to deviation measurements by Devico. Dh3 excluded.

4. Core logging

A preliminary logging of Dh1, 2 and 3 was done in the field by Eric Ahrenberg and Magnus Garson from DuPont, Oddvin Hansen from Fjord Blokk A/S, and Are Korneliussen from NGU, including X-Met analyses directly on the cores by a portable XRF-instrument (Outokumpu X-Met 880), and measurements of magnetic susceptibility by a hand-held susceptibility meter. The cores were taken to NGU's core storage facility at Løkken where the logging was done in more detail; selected parts of the cores were split (sawed) and

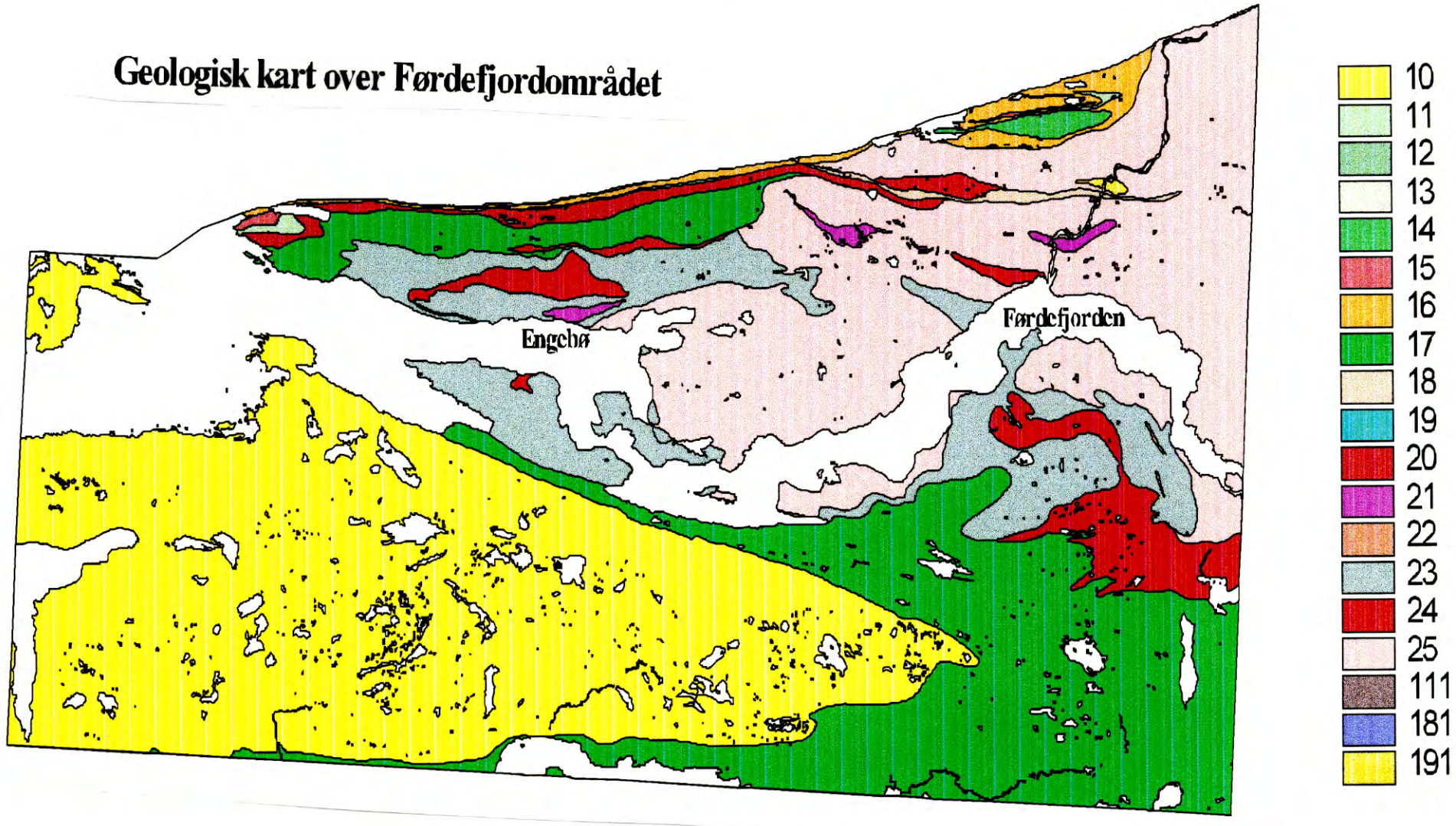

Fig. 1: Simplified geologic map of the Førdefjord region (after Lutro and Ragnhildstveit, in prep.).
See also the 1:50,000 scale version of this map in Appendix 4 and the Engebøfjell geologic map in Appendix 5.

supplementary X-Met analyses were done. Petrophysical parameters such as specific gravity and magnetic susceptibility were measured at NGU's petrophysical laboratory on a fairly large number of core samples.

Vertical geologic profiles showing the bore-holes and the TiO_2-content in the cores are given in Figs. 2 to 11. Profiles are indicated on map of Appendix 7. Tables 4 - 13 summarize individual core lithlogies.

Table 4: Dh1 summary. This is the first bore-hole drilled at Engebøfjellet (in October.96) and is the easternmost of the holes drilled. It starts well into the amphibolitic unit north of Fjord Blokk's quarry and cuts through the ferrogabbroic unit well under the quarry, and ends in amphibolite unit rocks on the southern side of the eclogite body. Its starting direction is 163° (clockwise from N) with dip 44.8° (Tokle 1996). The X-Met analyses were done directly on the core in the field by DuPont's X-Met. Experience has shown that such analyses directly on the round core surface might be slightly too low.

Position (m)	Rock	TiO_2 *	Comments
6 -54	amph. unit	0.5 - 1.0 % TiO_2	Banded amphibolitic eclogite with numerous thin (< 1 dm), leucocratic gneiss-zones (quartz-rich). Locally distinctly folded.
54 - 60	trans. eclogite	0.5 - 1.0 % 0.6 (3 %) TiO_2.	Gradually fewer gneiss zones, the eclogite becomes more massive. Distinct TiO_2-enrichment in the massive eclogite bands. Scattered quartz veins.
60 - 152	ferrog. eclogite	2.0 - 4.0 % TiO_2	Fairly massive, ferrogabbroic eclogite, locally banded, with scattered quartz veins. Low to distinct retrogression. The rutile/ilmenite-ratio is generally high.
152 - end of hole:	amph. unit	0.5 - 1.0 % TiO_2	Amphibolitic eclogite with alternating thin bands rich in quartz and feldspar (gneissic).

Table 5: Dh2 summary. This bore-hole is in an area with significant variation in rocktypes; in the field, amphibolite unit rocks can frequently be observed alternating with eclogite and amphibolite facies shear-zones give distinct retrogression effects on the eclogite.

Position (m)	Rock	TiO_2 *	Comments
1 - 3	ferrog. eclogite	1.0 - 2.0 % TiO_2	Fairly massive (transitional) eclogite with scattered quartz veins.
3 - 35	amph. unit	2.0 - 4.0 % TiO_2 in massive eclogite bands; < 1.0 % TiO_2 in gneiss bands.	Banded amphibolitic eclogite with numerous thin (1 dm), leucocratic gneiss zones.
35 - 90	amph. unit	Insignificant TiO_2- and rutile content.	Amphibolite unit rocks: Alternating eclogite/amphibolite and gneissic zones. Gneiss dominates from 54 m.
90 - 111	amph. unit	0.5 - 2.0 % TiO_2	Strongly deformed amph./eclogite with numerous, thin gneissic bands.
111 - 243	ferrog. eclogite	2 - 4 % TiO_2	Fairly massive, ferrogabbroic eclogite with scattered quartz veins. Low to distinct retrogression.
246 - end of hole	amph. unit	0.5 - 2 % TiO_2	Amphibolitic eclogite with numerous gneissic bands. Gneiss domination from 259 to 305m, then amphibolitic eclogite with gneiss bands from 305 m.

* The X-Met analyses were done in the field in Oct.-Nov. 1995 directly on the core surface (unsplit) by DuPont's X-Met.

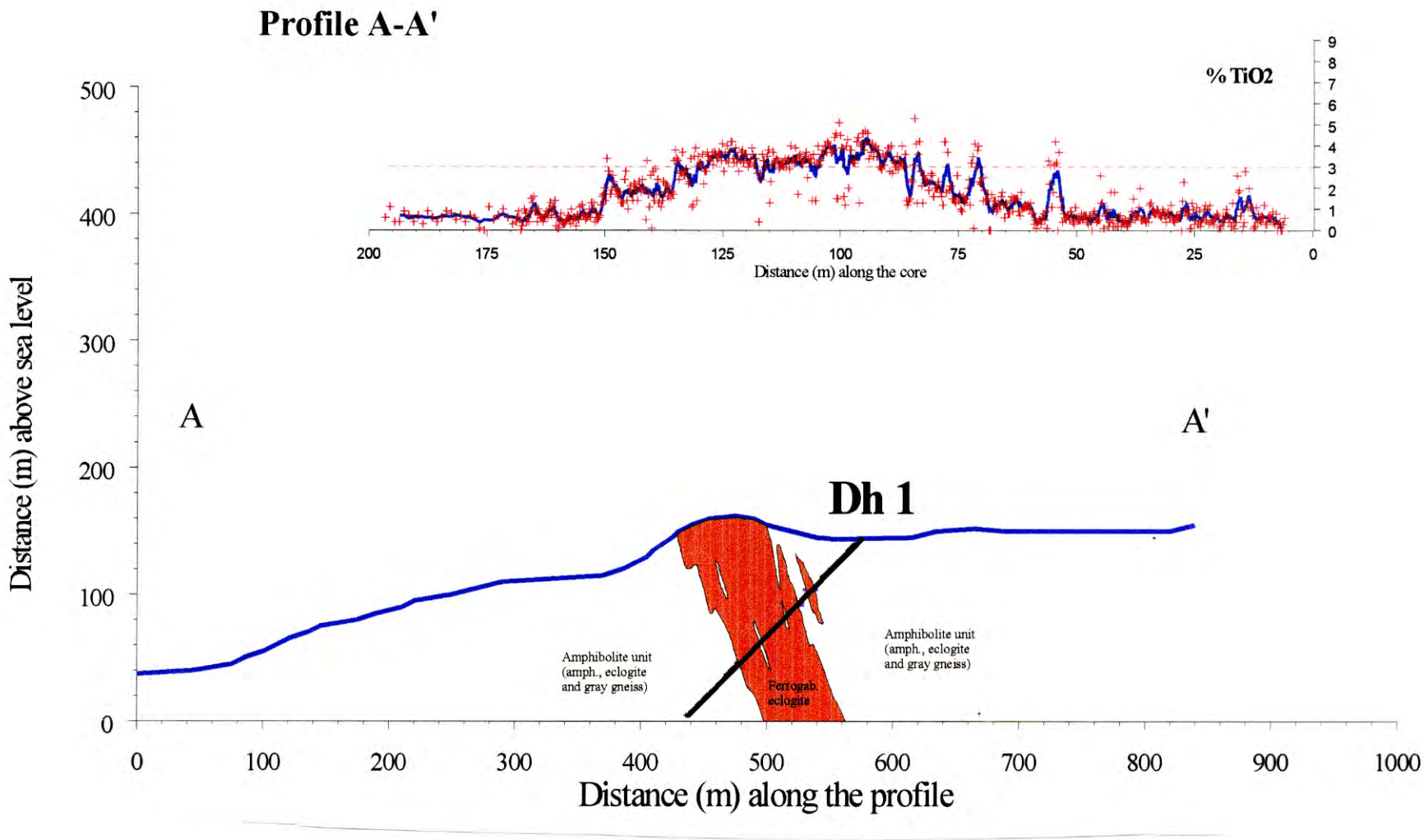

Fig. 2: Dh1 vertical profile (profile A-A' on the map of Appendix 7). Geologic profile showing the major geologic relations, the position of Dh1 in the profile and the TiO_2-distribution along the bore-hole. Due to the strongly deformed character of the eclogite, it has not been possible to distinguish ferrogabbroic from leucogabbroic varieties, i.e. the ferrogabbroic eclogite unit shown in the profile (as well as in the map of Fig. 2) contains leucogabbroic as well as transitional eclogite varieties. The amphibolitic unit rocks are the same on both sides of the ferrogabbroic eclogite zone, but the relative proportions of the mafic vs. felsic rocks are highly variable. The ferrogabbroic eclogite, as seen in the core, is very well exposed in the overlying quarry. The steeply dipping character of the ferrogabbroic eclogite zone is consistant with gravimetric results (Mauring 1996).

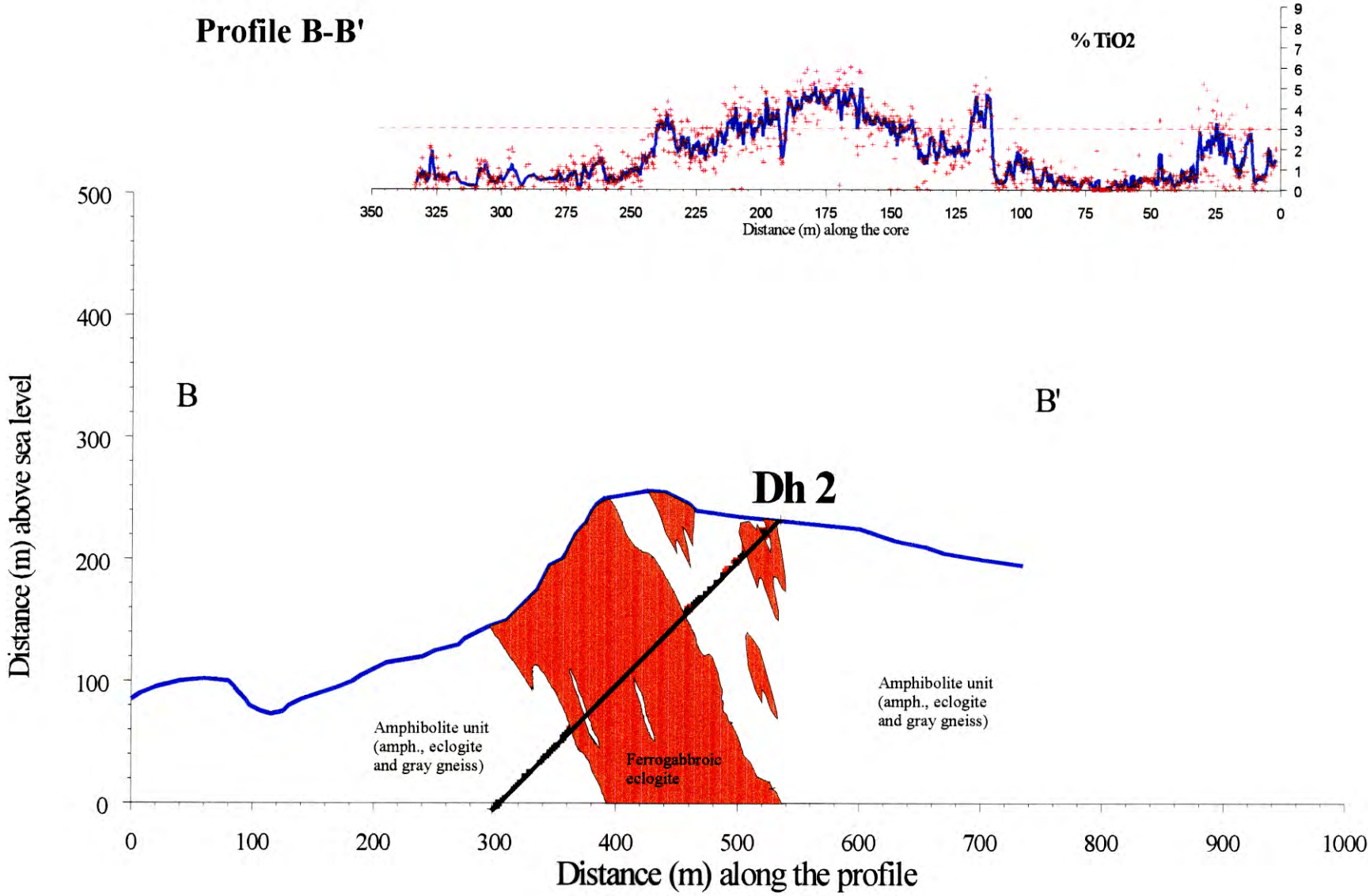

Fig. 3: Geologic profile showing the major geologic relations, the position of Dh2 in the profile and the TiO_2-distribution along the bore-hole.

Table 6: Dh3 summary.

Position (m)	Rock	TiO_2*	Comments
2 - 76	leucog. eclogite	< 1% TiO_2	Sheared metagabbro/amphibolite/eclogite, i.e. eclogitized metagabbro with variably preserved gabbroic textures.
76 - 91	gneiss	< 1 % TiO_2	Fairly homogeneous felsic rock (quartz-feldspar-phengite-clinozoisite).
91 - 127	leucog. eclogite	No rutile	Fairly light greenish, amphibolitic eclogite with quartzo-feldspathic layers/zones. Variations from massive to distinctly sheared/banded eclogite. Scattered quartz veins (< 1 dm thick)
127 - 130	leucog. eclogite	1-2% TiO_2 (gradually increasing)	Fairly massive, fine-grained eclogite with scattered quartz veins.
130 - 140	leucog. / trans. ecl.	1-2.5 % TiO_2 (gradually increasing)	The eclogite gradually becomes less sheared and contain less felsic (quartz-feldspatic) material down-hole.
140 - 154	trans. eclogite	1-3% TiO_2	Fairly massive eclogite, slightly banded (due to shearing). A few quartz veins.
154 - end of hole	ferrog. eclogite	2-5% TiO_2 High rut./ilm.-ratio	Fairly homogeneous, massive, garnet-rich eclogite. Locally some variation in garnet grain size.

* The X-Met analyses from 0 to 160m were done in the field on round core surface and on cut surface at Løkken from160 to 225m (end of hole). DuPont's X-Met.

Table 7: Dh4 summary.

Position (m)	Rock	TiO_2*	Comments
1.5 - 38	leucog. Eclogite	1-2% TiO_2	Low-Ti, fairly massive, leucogabbroic eclogite, locally with preserved gabbroic textures.
38 - 68	trans. eclogite	2-3 TiO_2	Fairly garnet-rich, leucogabbroic eclogite with increased Ti- and Fe-content down-hole
68 - 160 (end of hole)	ferrog. Eclogite	3-6 % TiO_2. High rut./ilm.-ratio.	Massive, ferrogabbroic eclogite, locally distinctly deformed and banded. Scattered quartz veins.

* X-Met analyses on cut core (DuPont's X-Met).

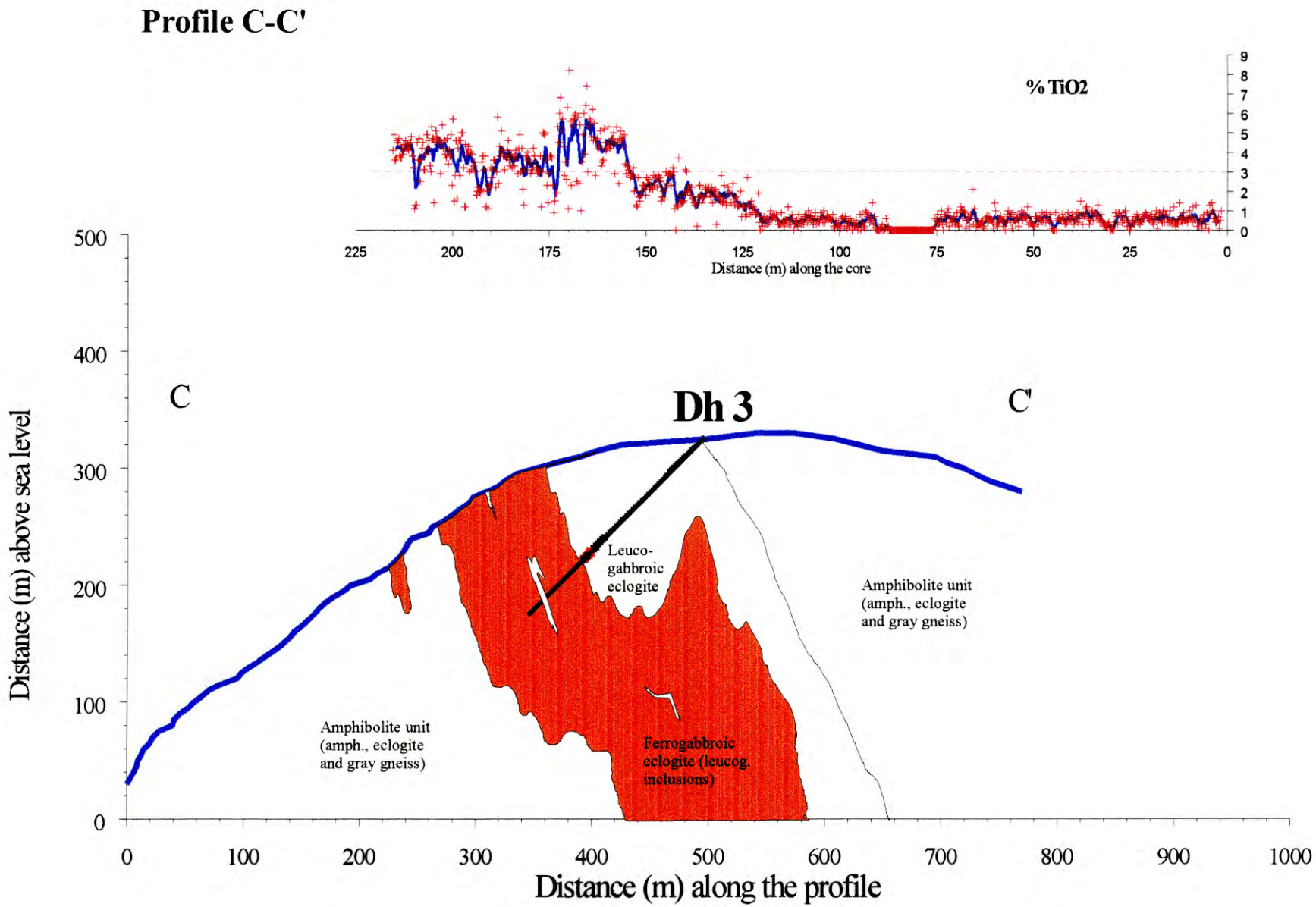

Fig. 4: Geologic profile showing the major geologic relations, the position of Dh3 in the profile and the TiO_2-distribution along the bore-hole.

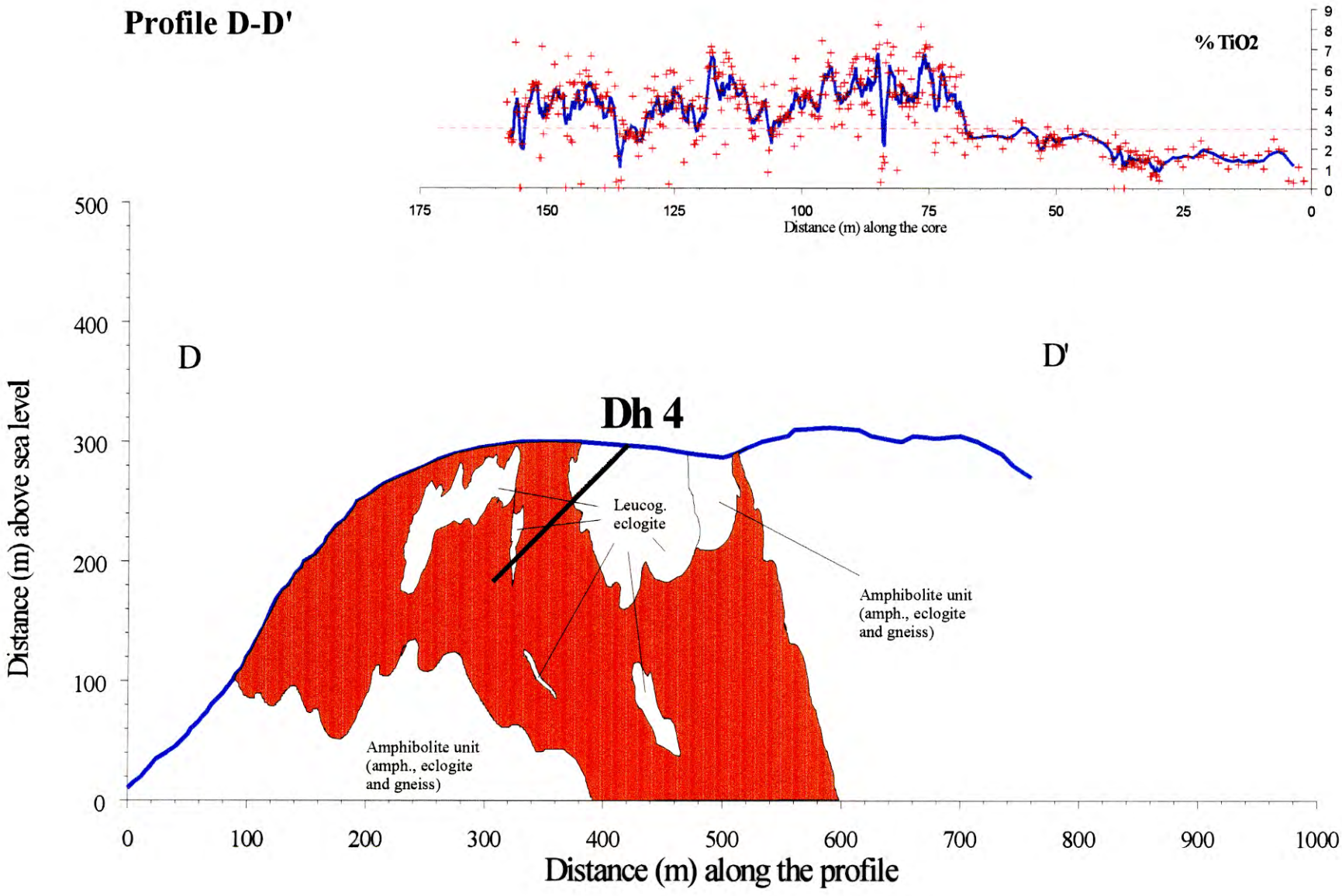

Fig. 5: Geologic profile showing the major geologic relations, the position of Dh4 in the profile and the TiO_2-distribution along the bore-hole. The indicated geologic relations at depth are speculative.

Table 8: Dh5 summary.

Position (m)	Rock	TiO_2*	Comments
1.5 - 4	trans. eclogite	2 - 3 % TiO_2	Transitional eclogite.
4 - 124	ferrog. eclogite	3 - 4 % TiO_2 High rut./ilm.-ratio	Ferrogabbroic eclogite with gradually increasing Ti-content down the hole. Scattered quartz veins are indicated by low Ti-values.
124 - 180 (end of hole)	ferrog. eclogite	3.5 - 6 % TiO_2 High rut./ilm.-ratio	

* X-Met analyses by DuPont's X-Met on cut core.

Table 9: Dh6 summary.

Position (m)	Rock	TiO_2*	Comments
2 - 9	ferrog. ecl.	3 - 4 % TiO_2	Massive, ferrogabbroic eclogite (leucog. / trans. eclogite from 5 to 7 m).
9 - 28	leucog. eclogite	< 1 % TiO_2	Massive, leucogabbroic eclogite.
28 - 46	trans. eclogite	1.5 - 2.5 % TiO_2 (<1% TiO_2)	Transitional eclogite (leucogabbroic eclogite from 32 to 36m). Locally distinctly banded and folded. Slightly variable garnet grain size. Locally relict gabbroic texture.
46 - 64	ferrog. eclogite	3 - 4 % TiO_2 High rut./ilm.-ratio.	Massive, ferrogabbroic eclogite.
64 - 70	trans. eclogite	1 - 1.5 % TiO_2	Massive, transitional (/ leucogabbroic) eclogite. Locally distinctly banded and folded. Locally relict gabbroic texture.
70 - 79	trans. eclogite	1 - 4 % TiO_2	Massive, transitional to ferrogabbroic eclogite with quartz veins.
79 - end of hole	ferrog. eclogite	3 - 4 % TiO_2 High rut./ilm.-ratio.	Primarily ferrogabbroic eclogite. Locally distinctly banded and folded. Slightly variable garnet grain size. Locally relict gabbroic texture.

* X-Met analyses by DuPont's X-Met on cut core.

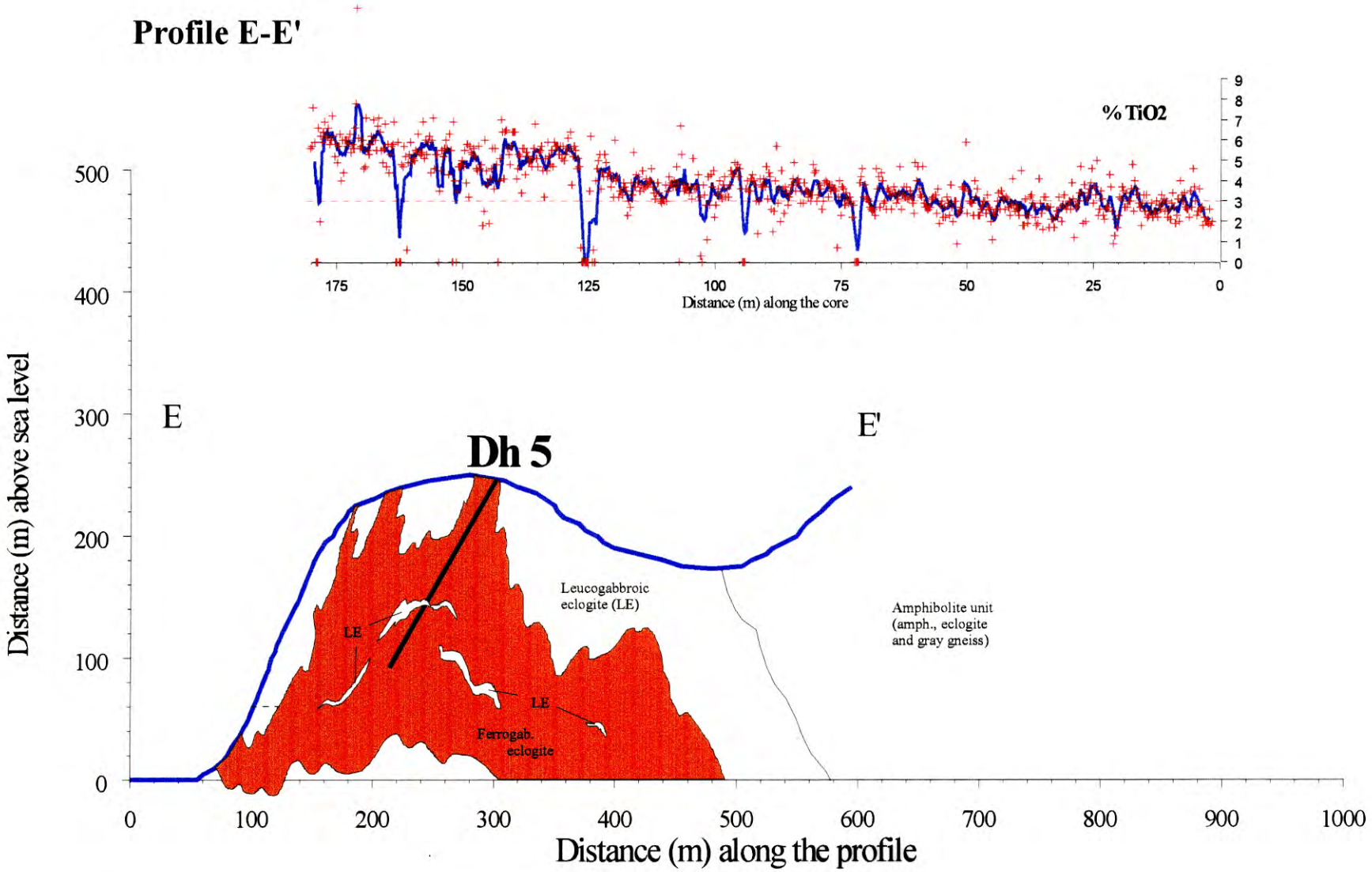

Fig. 6: Geologic profile showing the major geologic relations, the position of Dh5 in the profile and the TiO_2-distribution along the bore-hole. The indicated geologic relations at depth are speculative.

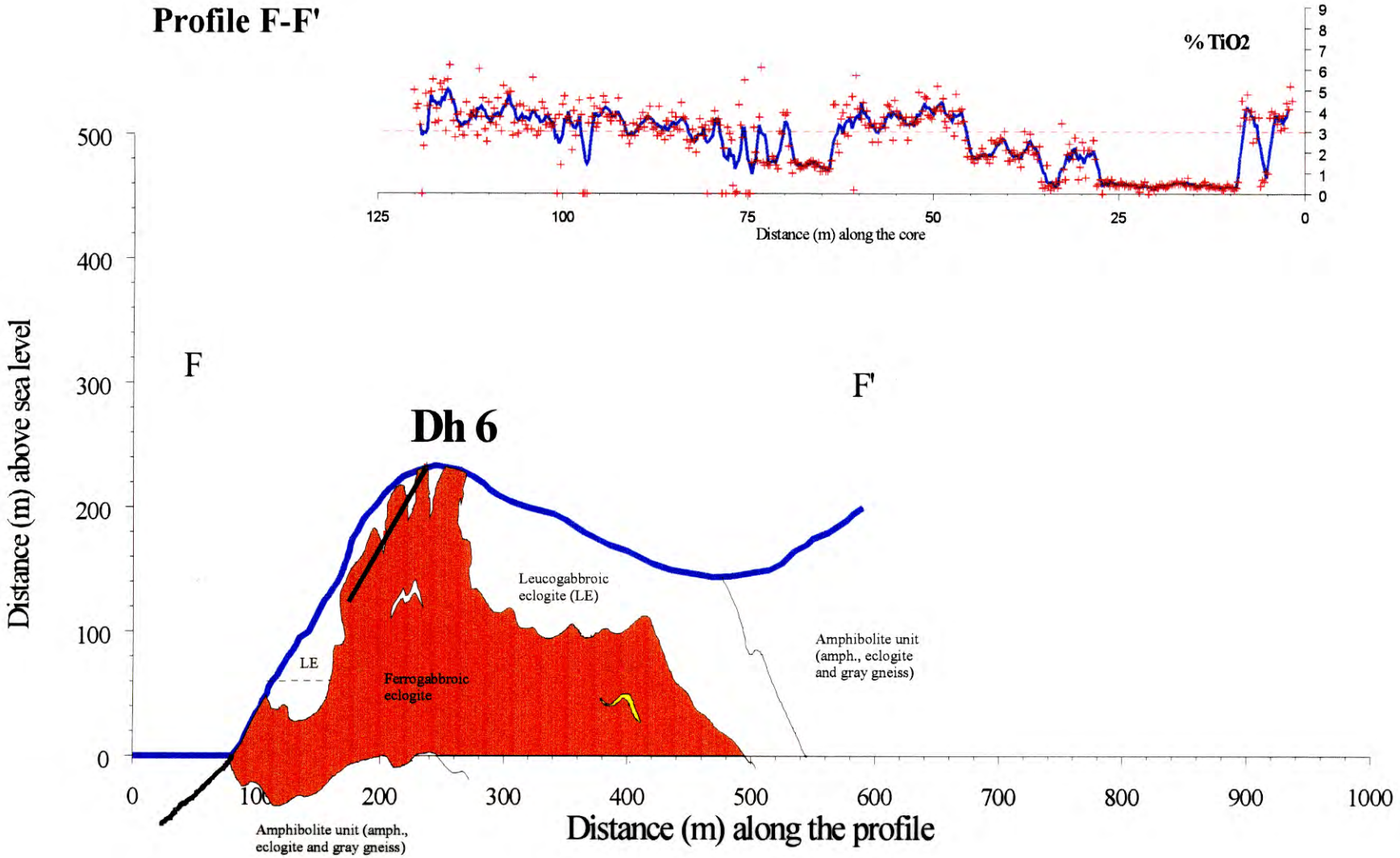

Fig. 7: Geologic profile showing the major geologic relations, the position of Dh6 in the profile and the TiO_2-distribution along the bore-hole. The indicated geologic relations at depth are speculative.

Table 10: Dh7 summary.

Position (m)	Rock	TiO_2*	Comments
1 - 7	ferrog. eclogite	4 - 6 % TiO_2	Massive, ferrogabbroic eclogite with quartz veins.
7 - 70	ferrog. eclogite	4 - 6 % TiO_2	Fairly massive, ferrogabbroic eclogite.
70 - 71	gneiss		Quarz-rich leucocratic gneiss.
71 - 85	ferrog. eclogite	2 - 6 % TiO_2	Fairly massive, ferrogabbroic eclogite with quartz veins.
85 - 89	ferrog. eclogite		Strongly sheared / brecciated, ferrogabbroic eclogite with hydrothermal quartz.
89 - 215 (end of hole)	mixed eclogite	1 - 6 % TiO_2	Generally fairly massive leucogabbroic-, transitional- and ferrogabbroic eclogite (gradual variations). Occasionally small-scale banding. Scattered quartz veins.

* X-Met analyses by DuPont's X-Met on cut core.

Table 11: Dh8 summary.

Position (m)	Rock	TiO_2	Comments
0 - 22	leucog. eclogite	0.5 - 1 % TiO_2	Slightly sheared leucogabbroic eclogite with low TiO_2-content. Scattered quartz veins.
22 - 27	leucog. eclogite	1 - 2 % TiO_2	Leucogabbroic eclogite / garnet-amphibolite with coarse-grained garnet. Distinctly quartz- and white mica-bearing.
27 - 76	trans. eclogite	2 - 3 % TiO_2	Fairly massive leucogabbroic to ferrogabbroic (transitional) eclogite. Occasionally mm-sized caves after leached carbonate. Scattered mm-thick retrograde (amphibolitized, occasionally with some chlorite) veinlets. Some quartz veins.
76 - 141	ferrog. eclogite	3 - 5 % TiO_2	Massive ferrogabbroic eclogite. Scattered quartz veins.
141- 164	leucog. eclogite	0.5 - 1 % TiO_2	Massive leucogabbroic eclogite (141 - 164m), partly amphibolitized, some chloritized cracks.
164 - 190	trans. eclogite	1.5 - 2.5 % TiO_2	Some amphibolitic (retrograde) zones with gradual transition into eclogite. Scattered quartz veins.
190 - 205	trans. eclogite	1.5 - 2.5 % TiO_2	Massive transitional eclogite with quartz veins. Variably retrograded.
205 - 227	trans. eclogite	1.5 - 2.5 % TiO_2	Slightly more heterogeneous eclogite (transitional) with small-scale banding and folding. Variably retrograded.
227 - 253	ferrog. eclogite	2.4 - 4 % TiO_2	Distinctively retrograded (amphibolitized) and heterogeneous ferrogabbroic eclogite with scattered quartz veins and a few up to 0.5 m thick quartz-rich, gneissic zones. Variable garnet grain sizes (0.2 mm to 1-3 mm). The larger garnets tend to occur in eclogite varieties (/ garnet amphibolites) that are enriched in quartz and white mica.
253 - 294	amph. unit	1 - 2 % TiO_2	Alternating amphibolite and gneiss. The gneiss is a fine-grained, banded, gray muscovite-bearing gneiss which occurs as cm - dm - m thick bands within amphibolitized eclogite. Occasionally the eclogite has a massive character.
294 - 300		1 - 2.5 % TiO_2	Eclogite / amphibolite with thin quartz-rich bands (end of hole)

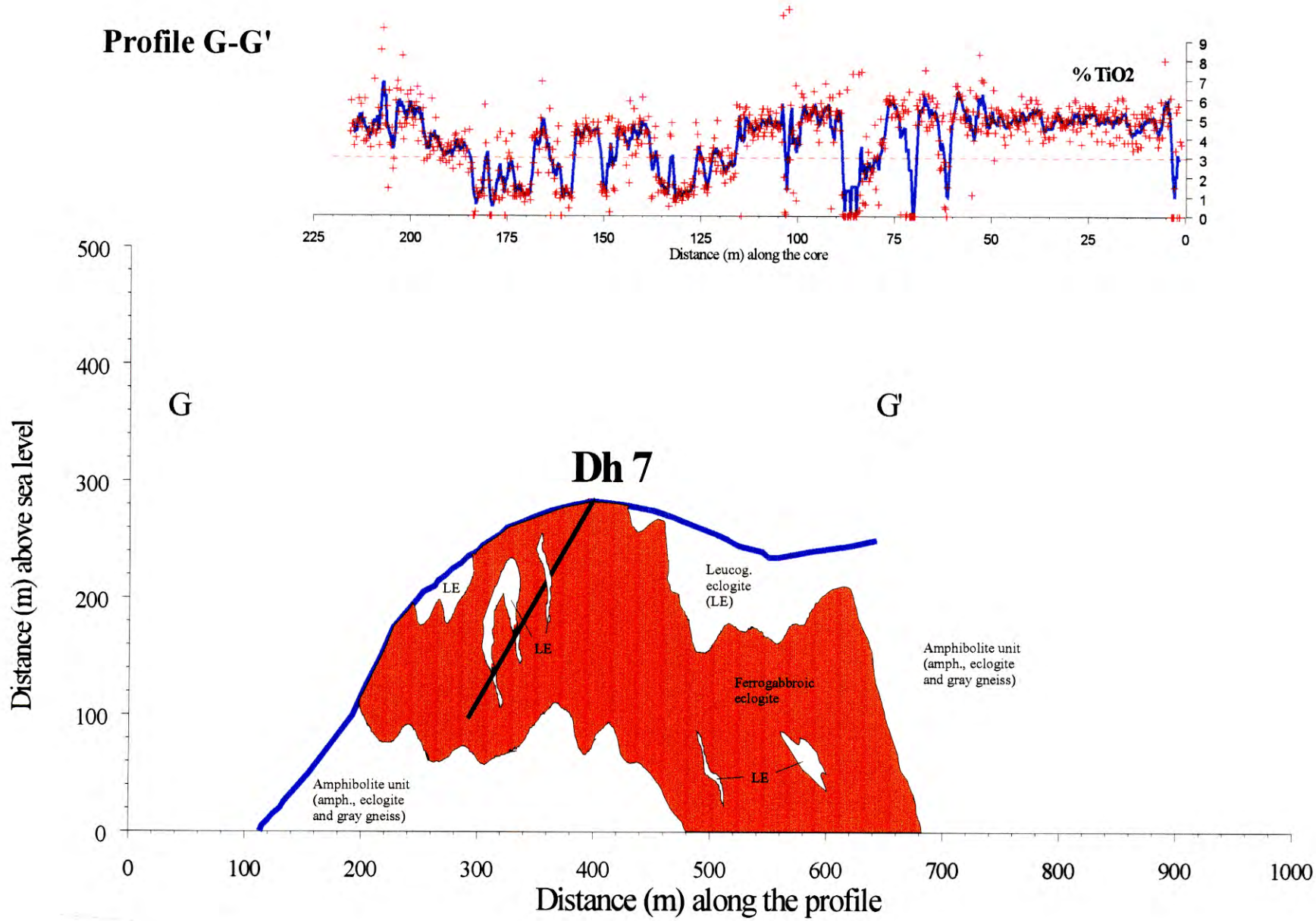

Fig. 8: Geologic profile showing the major geologic relations, the position of Dh7 in the profile and the TiO_2-distribution along the bore-hole. The indicated geologic relations at depth are speculative.

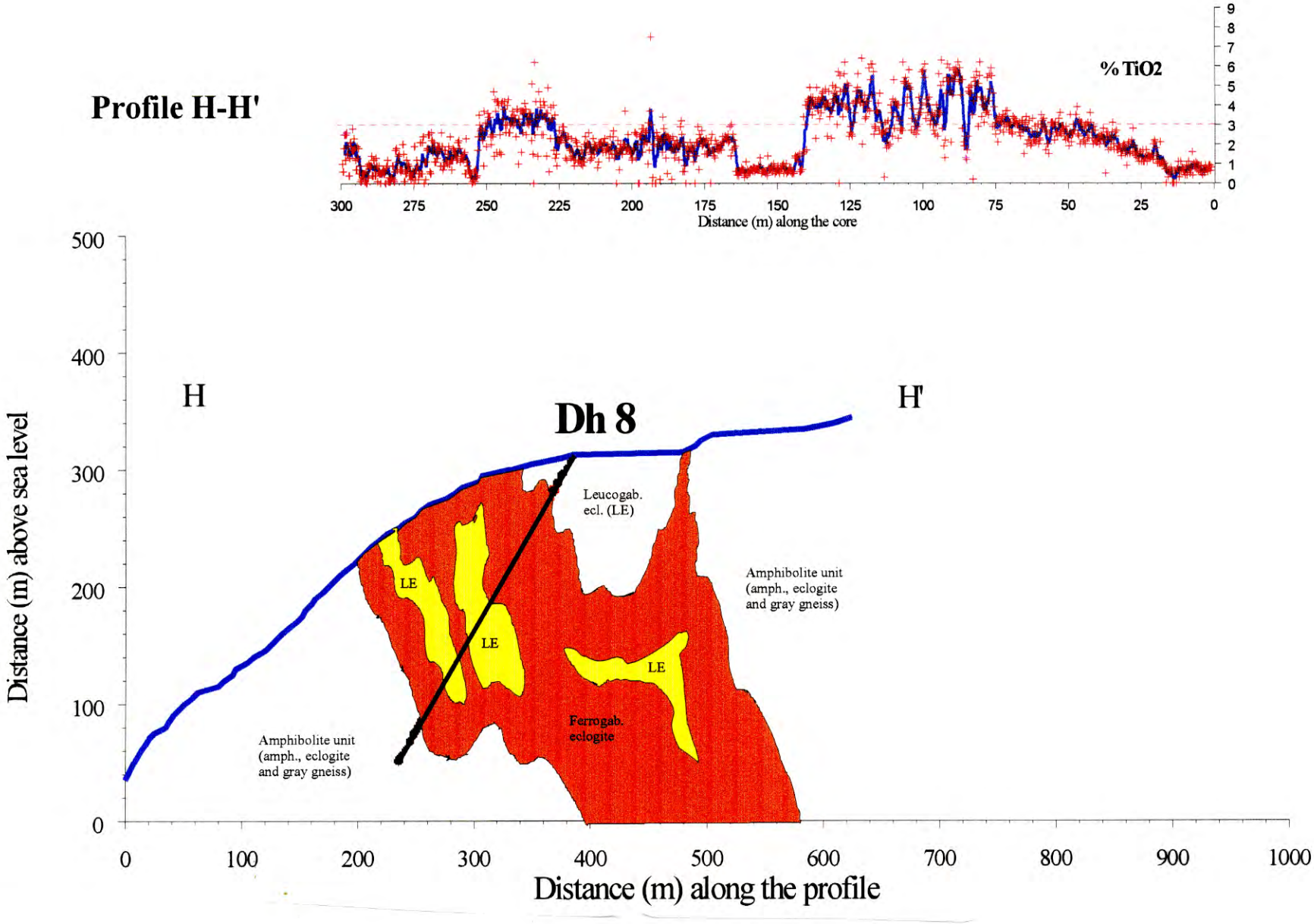

Fig. 9: Geologic profile showing the major geologic relations, the position of Dh8 in the profile and the TiO_2-distribution along the bore-hole. The indicated geologic relations at depth are speculative.

Table 12: Dh9 summary.

Position (m)	Rock	TiO_2*	Comments
			Up to 271 meters Dh9 go mostly through amphibolite unit rocks (amphibolite/eclogite with numerous thin leucocratic bands). At 271 m there is a sharp contact to ferrogabbroic eclogite.
2.0 - 82	amph. unit	1 - 2 % TiO_2	Amphibolite (retrograde) / eclogite with leucocratic (gneiss) bands. Two gneiss types are characteristic: (1) A garnet-bearing granodioritic gneiss that occurs in 1 dm to 3-4 m-thick bands, and (2) a quartz-, feldspar- and white mica-rich leucocratic gneissic rock that frequently occurs in cm-dm thick alternations with eclogite/amphibolite. The latter is the dominant gneiss type. Numerous eclogitic bands (or boudins), 1-5 dm thick, have a massive character, but are significantly retrograded.
88 - 91	trans. eclogite	2 - 3 % TiO_2	Massive, transitional type eclogite.
91 - 191	amph. unit	1 - 2 % TiO_2	Amphibolites with gneissic bands.
191 - 207	ferrog. eclogite	3 - 4 % TiO_2	Massive, ferrogabbroic eclogite (sharp contact) with scattered quartz veins.
207 - 234:	amph. unit	1 - 2 % TiO_2	Amphibolites with gneissic bands.
234 - 236	ferrog. eclogite	2.5 - 3.5 % TiO_2	Massive, ferrogabbroic eclogite with scattered quartz veins.
236 - 259	amph. unit	1 - 2 % TiO_2	Banded amphibolites (partly eclogitic) with felsic bands.
259 - 271	amph. unit	1 - 2 % TiO_2	Eclogite / amphibolite with a less distinct mafic/felsic banding.
271 - 290 (end of hole) #	ferrog. eclogite	2 - 5 % TiO_2	Sharp contact to ferrogabbroic eclogite (scattered quartz veins). Variable garnet grain size. The larger garnets tend to occur in quartz-rich eclogite varieties which are distinctly retrograded.

* X-Met analyses on round core surface by NGU's X-Met.
# Dh9 was extended from 290m to 385m in Nov.96; these results are to be presented in a later report.

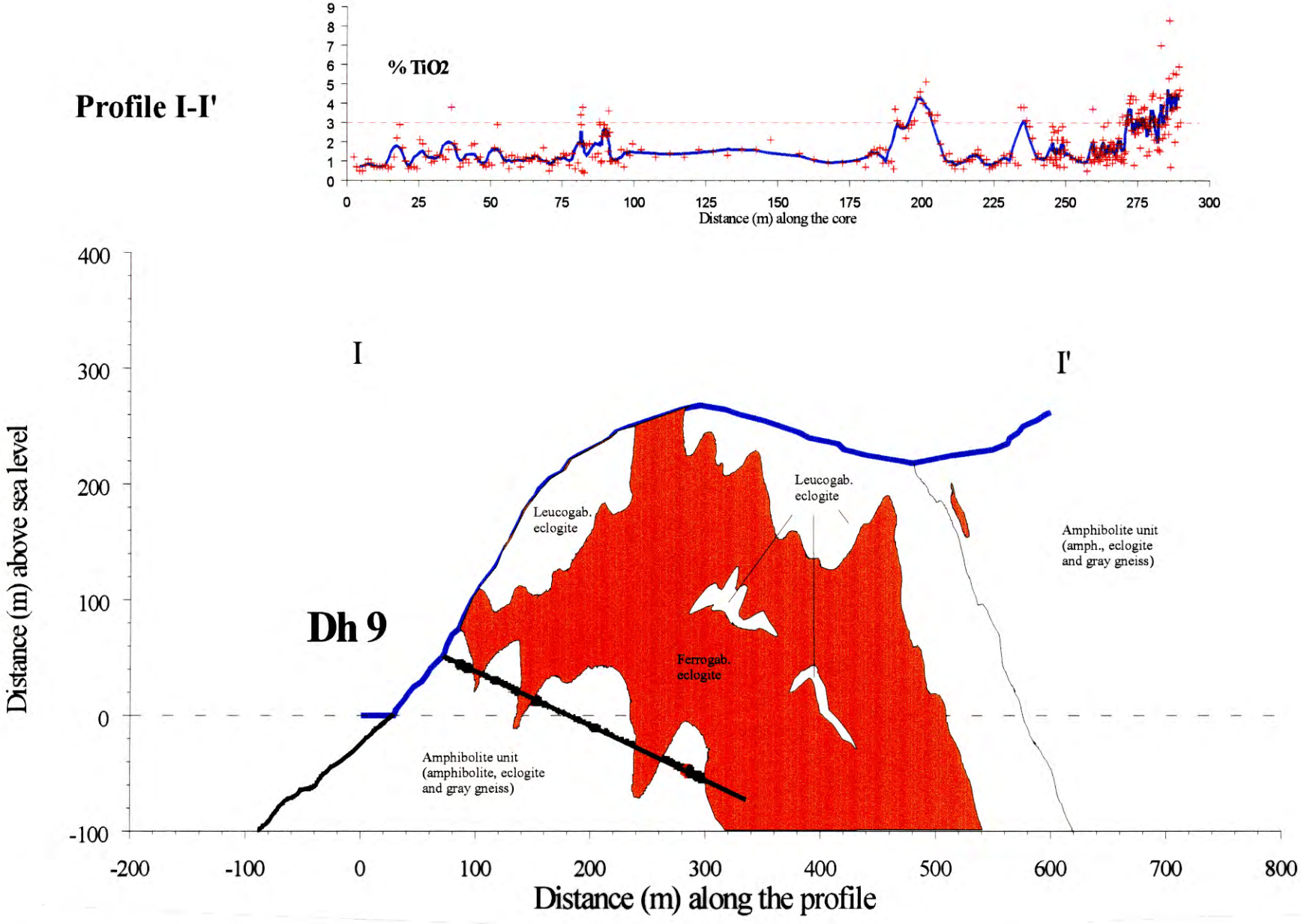

Fig. 10: Geologic profile showing the major geologic relations, the position of Dh9 in the profile and the TiO_2-distribution along the bore-hole. The indicated geologic relations at depth are speculative.

Table 13: Dh10 summary. Dh10 starts in leucogabbroic eclogite near the western road-tunnel opening, and enters ferrogabbroic eclogite at 96 m.

Position (m)	Rock	TiO_2*	Comments
2 - 96	leucog. eclogite	0.5 - 1. 5 (3.5) % TiO_2	Variably sheared leucogabbroic eclogite with distinct relict gabbroic textures in the least deformed eclogite varieties. Some quartz veins. Distinctly amphibolitized in shear-zones. A few 1-6 dm-thick quartz- and white mica-rich gneiss zones.
96 - 116	ferrog. Eclogite	2 - 3 % TiO_2	Distinctly Ti-enriched, ferrogabbroic eclogite with scattered quartz veins (varies from pure hydrothermal quartz to gneissic zones with quartz + white mica). A few 1-5 dm-thick zones of a leucocratic gneiss, occasionally with a reddish color.
116 - 226	ferrog. Eclogite	3 - 5 % TiO_2	Variably transitional to ferrogabbroic eclogite with distinct retrogression along mm-thick veins as well as in dm-m thick layers / bands (gradual contacts) in the eclogite.
226 - 229	leucog. eclogite	1.5 - 2.5 TiO_2	Whitemica- and quartz-rich eclogite with coarse garnets (up to 1-2 mm).
229 - 256	ferrog. eclogite	4 - 5.5 TiO_2	Ferrogabbroic eclogite with scattered quartz veins.
256 - 263	leucog. eclogite	1 - 2 % TiO_2	Variable amphibolite / leucogabbroic eclogite, locally folded, scattered quartz veins, variable garnet grain size.
263 - 274	amph. unit	1 % TiO_2	Amphibolite unit rocks with amph./ecl./gneiss alternations.
274 - end of hole:	ferrog. eclogite	4 - 6 % TiO_2	Ferrogabbroic eclogite. Scattered quartz veins.

* X-Met analyses on round core surface by NGU's X-Met.

5. Microscopy results

About 100 thin sections cut from drill cores (Dh 1, 2, 3, 4, 5, 7, 8, and 10) and surface samples have been studied, including "fresh" and retrograded leucogabbroic and ferrogabbroic eclogites, amphibolites and eclogite-facies "gneisses". Results are summarized in Table 14a.

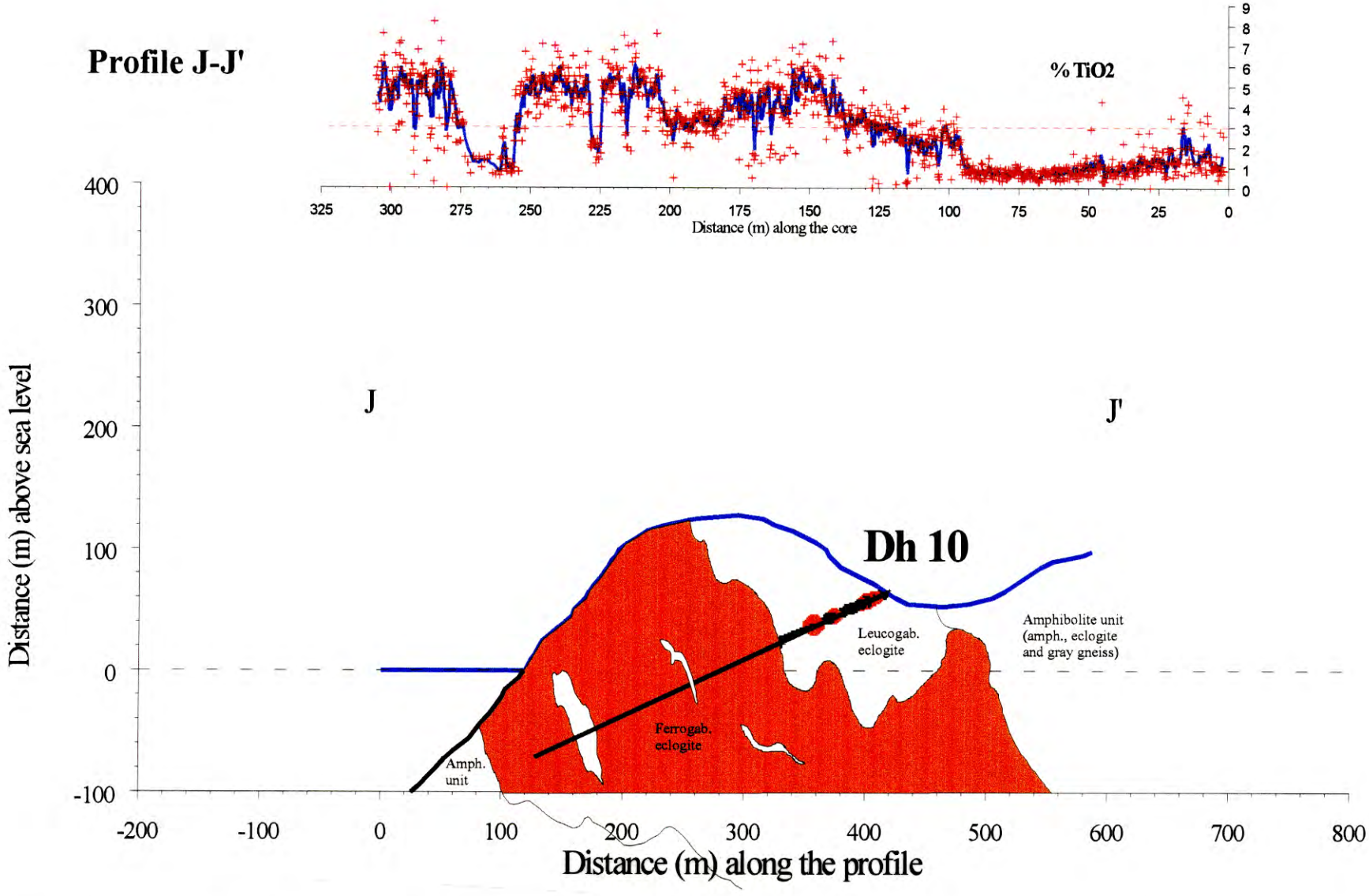

Fig. 11: Geologic profile showing the major geologic relations, the position of Dh10 in the profile and the TiO_2-distribution along the bore-hole. The indicated geologic relations at depth are speculative.

Fig. 12: Photographs of representative ferrogabbroic eclogite. The upper photo is a core sample from Dh10 (sample 10/97.1) of a garnet-rich, massive ferrogabbroic eclogite. Retrogression is minimal; omphacite (light green) is unaltered. The brown dots are small cavities after leached carbonate. The central photo is a microphotograph (transmitted light) of a similar rutile- (black) and garnet-rich fresh eclogite from Dh10 at 292.9 m (thin-section 10/292.9). Other minerals are omphacite (light green), minor amphibole (blue-green) and colorless minerals (phengite, quartz, carbonate). The lower photo shows the same thin-section seen in reflected light, with rutile (gray) and pyrite (white).

Fig. 13: Representative, massive ferrogabbroic eclogite from Dh9 at 87.7 m (upper photo) and Dh10 at 282.5 m (lower photo). For the darker part of sample 9/87.7 there are two possible explanations that both are fairly common: (a) during retrogression (amphibolitization) the primary amphibole * and the omphacitic clinopyroxene are replaced by a secondary amphibole (hornblende). Such retrogression occurs in gradual variations from hardly noticeable to very extensive. In the very extensive retrogression, rutile is often altered to ilmenite or even to titanite. (b) Alternatively, the darker area in the eclogite corresponds to an infiltration of fluid during eclogite facies metamorphism; in such cases the darker rock is due to the abundance of blue-green eclogite facies amphibole. Another common retrogression occurs along thin veins in the eclogite, as most clearly seen in the lower photo. In such retrograde veins, rutile is often partly retrograded to ilmenite and occasionally also to titanite (see Fig. 16).

* New electron microprobe analyses indicate that the primary amphibole in the fresh ferrogabbroic eclogite is an actinolitic hornblende, not barroisite as previously regarded. A possibility is that the composition of the primary eclogite-facies amphibole varies (Erambert; report in progress).

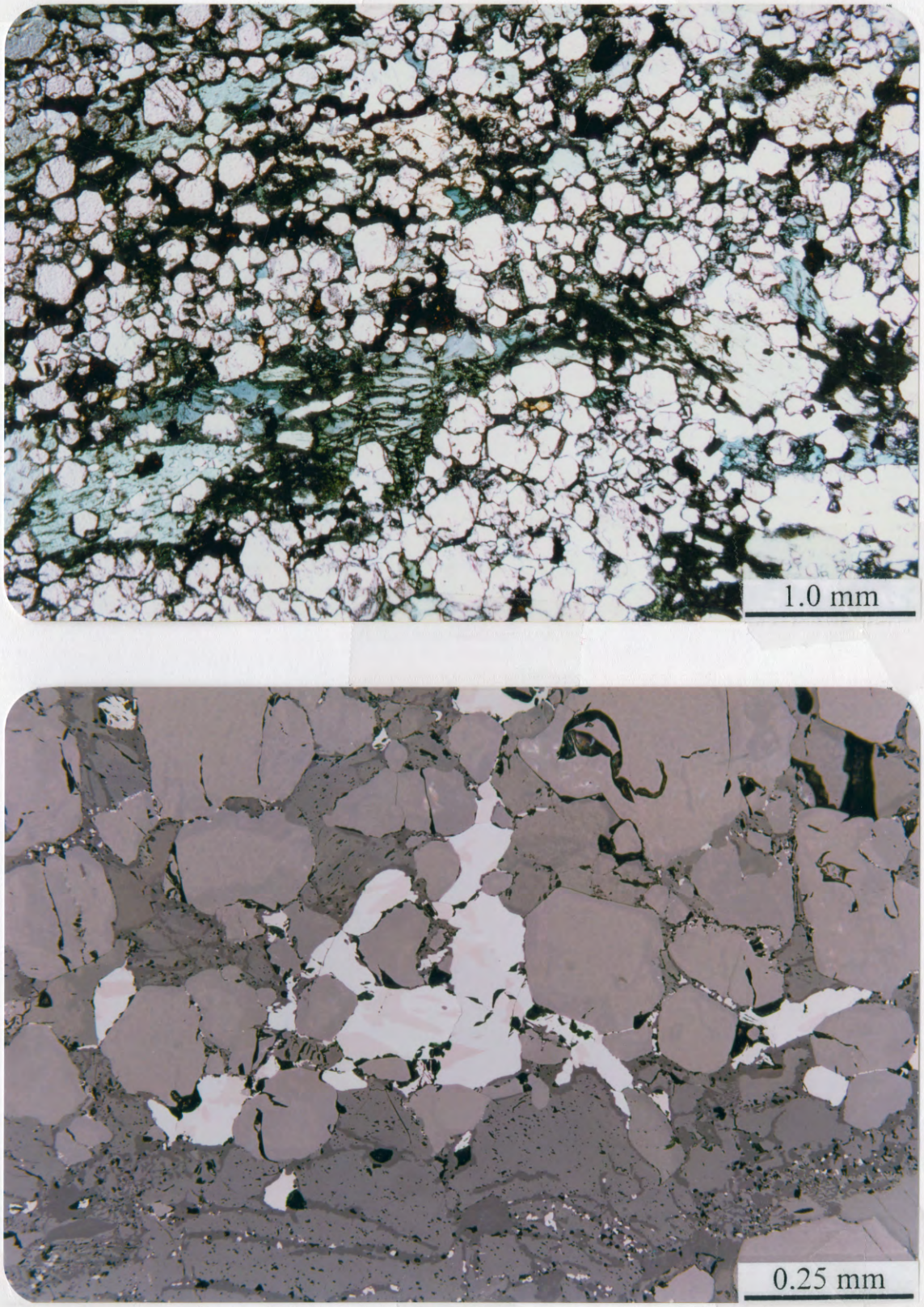

Fig. 14: Microphotographs of retrograded eclogite from Dh8 (thin section 8/229.0). In the upper photo (transmitted light), the barroisitic (?) amphibole is altered to hornblende (green) and the omphacite to very fine-grained symplectitic aggregates of hornblende-plagioclase-diopside-magnetite (dark green to black). Alteration happens along lines and fractures within minerals. The lower photo (reflected light) shows rutile (gray) with ilmenite exsolutions (brownish) and fine-grained secondary magnetite (white patches mainly within symplectites after omphacite).

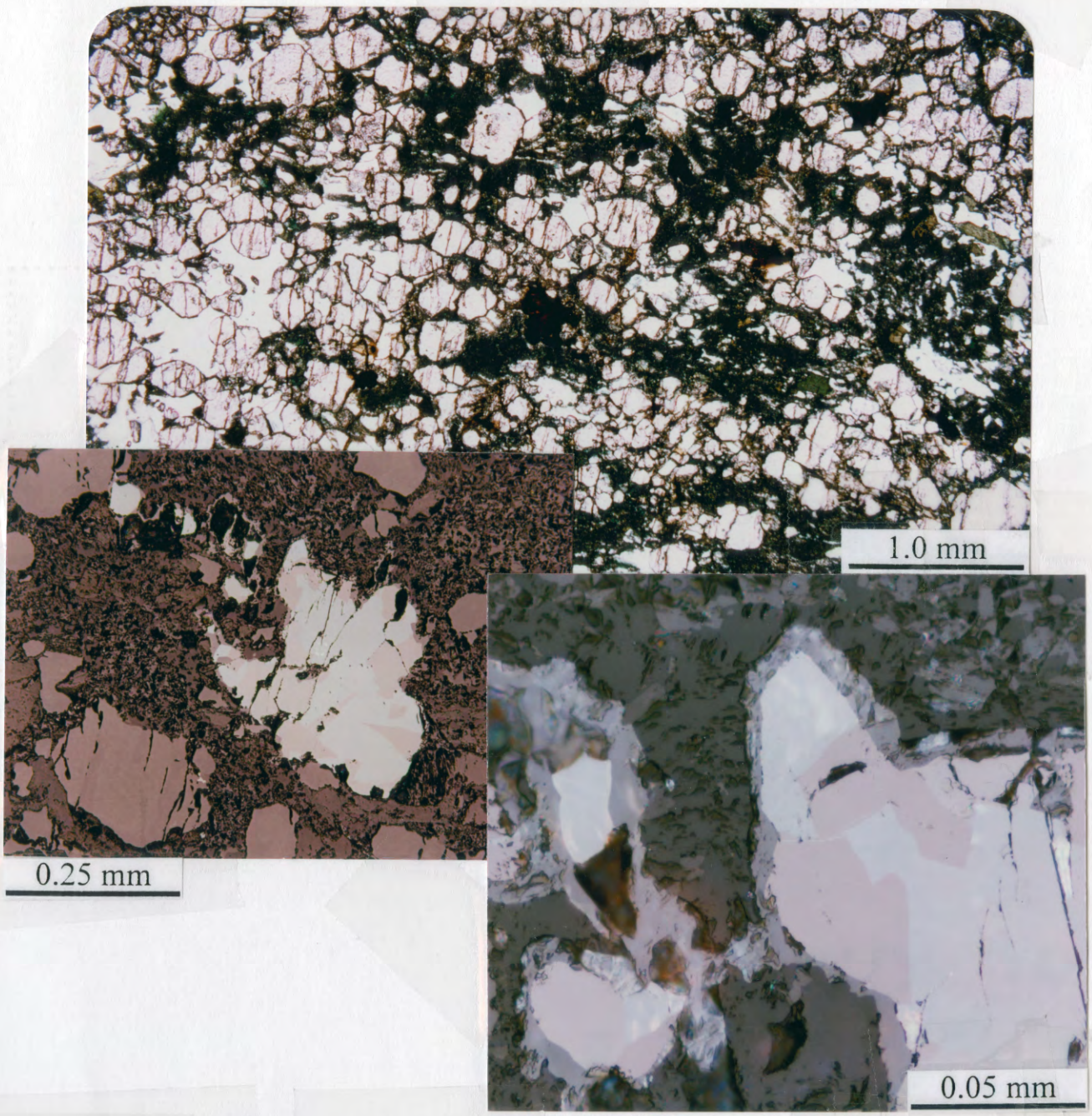

Fig. 15: Microphotographs of strongly retrograded, garnet- and rutile-rich ferrogabbroic eclogite from Dh8 (thin-section 8/170.0). The dark green to black fine-grained matrix in the upper photo (transmitted light) is an alteration product after barroisite and omphacite. Rutile (gray) - ilmenite (brownish) intergrowths (reflected light) are shown in the central photo. The lower photo is an enlargement of the previous image showing titanite corona at the rim of the rutile/ilmenite grain.

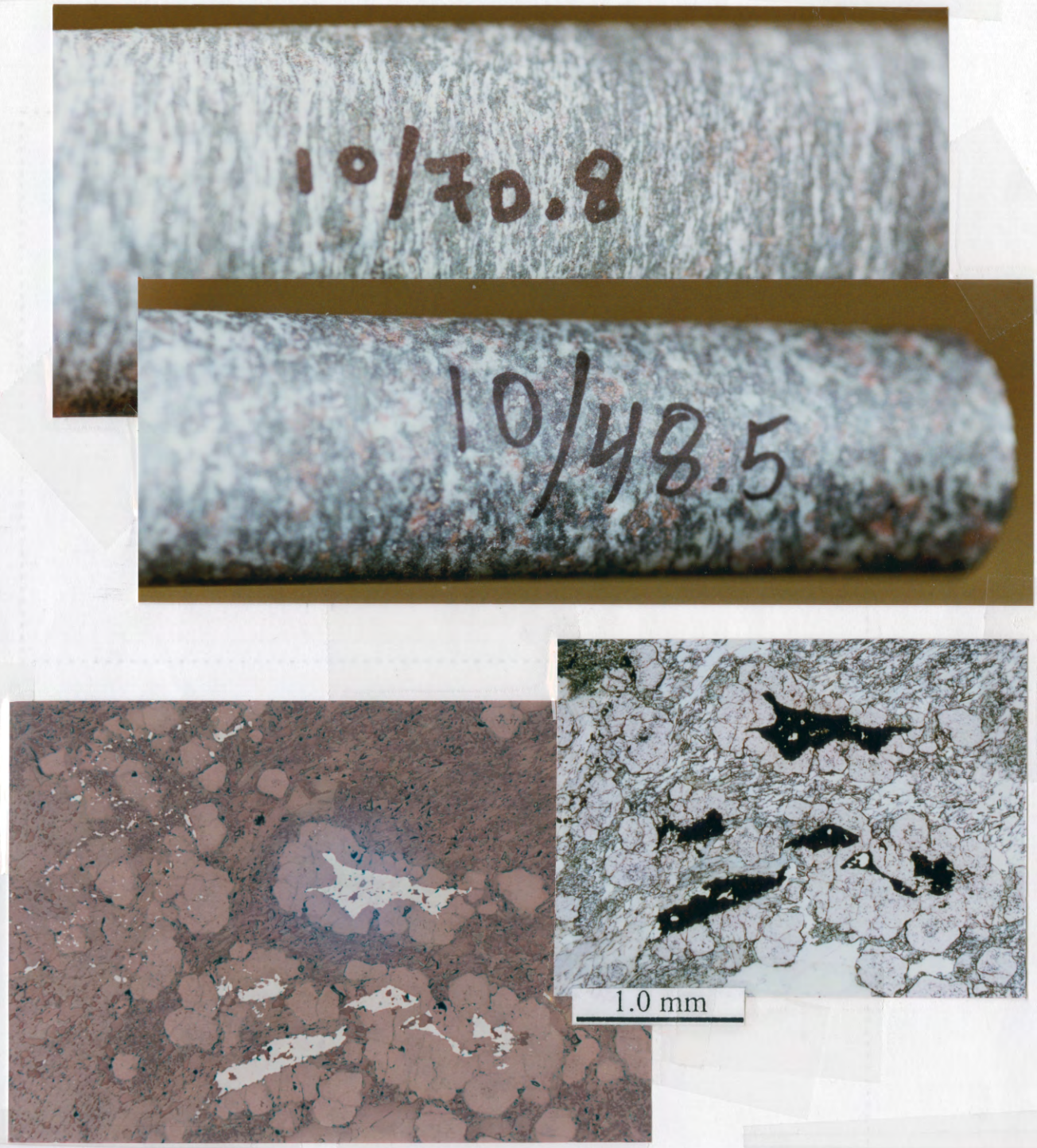

Fig. 16: Photographs of core and thin-section of leucogabbroic eclogite. Upper photo: representative, slightly sheared leucogabbroic eclogite from Dh10 at 70.8 m. Upper central photo: Massive leucogabbroic eclogite with preserved gabbroic texture from Dh10 at 48.5 m. Photo at lower right: microphotograph (thin section 10/46.9; reflected light) of rutile (black) in leucogabbroic eclogite. Garnet corona (around rutile) and fine-grained areas of clinozoisite + phengite + quartz + amphibole + omphacite after magmatic plagioclase are typical of partly recrystallized gabbroic textures. Photograph at lower left: same rutile grains (light gray; reflected light) as in the previous photo. The light gray patches in the left part of the photo are fine-grained rutile. Rutile in leucogabbroic eclogite normally occurs as fairly large grains or aggregates of grains and as scattered (dusty) grains as shown on this photograph. In retrograded leucogabbroic eclogites the fine-grained oxide dust is usually magnetite.

Fig. 17: Some retrograded eclogite varieties. Upper photo: core-sample of amphibolite/hornblendite with quartz vein from Dh10 at 255.7 m. Central photo: core-sample of slightly retrograded eclogite with coarse-grained garnets from Dh10 at 173.8 m. The light green areas consist mainly of diopside + plagioclase symplectites after omphacite and minor amphibole. In this kind of rock, the rutile is often partly altered to ilmenite and occurs as rutile/ilmenite exsolutions. Lower photo: core-sample of a strongly retrograded rock with retrograde coronas of amphibole + plagioclase (± epidote?) around the garnet crystals and amphibolitized matrix. At this stage of retrogression, rutile is more or less totally altered to ilmenite and occasionally also to titanite.

Fig. 18: Typical amphibolite unit rocks; upper photo: gray gneiss (dioritic) with amphibolite bands from Dh9 at 24.3 m. Lower photo: strongly amphibolitized eclogite with numerous mm- to cm-thick bands, often intensely folded, of a leucocratic gneiss.

Fig. 19: Sharp contact between a patchy amphibolite (left part of the core-sample) and massive ferrogabbroic eclogite (right). The eclogite is fresh and foliated with the foliation more or less parallel to the amphibolite contact.

Eclogite-facies texture and mineralogy: Texture is variable and reflects increasing degree of recrystallization with increased deformation, and eclogite rocks vary from coronite to pseudomorphic eclogite to foliated eclogite. Although ghost magmatic texture (or pseudomorphic texture) is common, especially in leucogabbroic eclogites, the mineralogy is eclogitic. The most characteristic features are fine-grained domains of clinozoisite + white mica ± plagioclase after the magmatic plagioclase and the heterogeneous distribution of garnet inherited from the coronas. However, no true coronite with relicts of pre-eclogitic minerals has been recorded. The recrystallization of the mafic eclogites is generally more advanced, but honeycomb texture may occasionally be seen. Recrystallized eclogites are granular and generally very fine-grained with average garnet size ≤ 0.5 mm. Fine grain size is largely the result of strong shear deformation, as indicated by strings of oxides parallel to the mylonitic eclogitic foliation. Omphacite porphyroblasts up to several cm long are found locally within mylonitic and folded leucogabbroic eclogites. Together with "late" amphibole porphyroblasts, these textures and mineral assemblages evidence several episodes of deformation and recrystallization under eclogite-facies conditions.

Besides garnet and omphacite, quartz is found in variable amounts in most of the studied eclogites. Abundant hydrous and volatile-bearing eclogite-facies minerals characterize these eclogites. Pale blue-green amphibole is nearly always present, often as a dominant mineral. Clinozoisite and white mica (phengite) characterize leucogabbroic eclogites and are common as minor constituents in many ferrogabbroic ones. Carbonate may be a major constituent, either as disseminated grains or as segregations together with quartz, white mica, rutile or apatite. Apatite and pyrite are a common accessories. Chalchopyrite occurs in trace amounts.

Retrogression: Many eclogites are unaltered or show only a trace of retrogression limited to incipient symplectitic breakdown of omphacite rims. Minor to extensive retrogression corresponds to the progressive development of kelyphite around garnet and symplectitic breakdown of omphacite and white mica. Eclogite-facies amphibole remains stable but re-equilibrates at the rim. Kelyphite may be composed of green-blue amphibole ± plagioclase ± magnetite, or less frequently by intergrowths of epidote + amphibole. Omphacite breaks down to diopside + plagioclase or more commonly to amphibole + plagioclase ± magnetite symplectites, and phengite to biotite + plagioclase ± epidote. The coronitic retrogression can be pervasive or limited to areas adjacent to late fractures.

Late fractures and veins contain green fibrose amphibole (actinolitic), plagioclase, epidote, often carbonate, and occasionally, chlorite. This indicates crystallization formation under epidote-amphibolite facies to greenschist facies conditions. The infiltrating fluid induces static retrogression of the wall-rock, as described above, and the local transformation of rutile to ilmenite, and rarely, to titanite.

Ti minerals: Because complete eclogitization took place even in undeformed samples, the Ti oxide in all these eclogitic rocks is rutile. Rutile grains are commonly < 0.5 mm, and seldom up to 1 mm (small clusters). Minor retrogression can lead up to 10% (in volume Ilm/Ilm+Rut) transformation of rutile to ilmenite; replacement occurs generally along cracks. This is often related to the presence of late fractures. Extensive retrogression leading to complete amphibolitization corresponds to Ilm/Ilm+Rut from ca. 20% to more than 95%, with ilmenite coronas progressively replacing rutile. Titanite is found in few samples and generally only in trace amounts. It may form coronas around rutile/ilmenite grains or subhedral crystals within late fractures.

6. Analytical results

6.1. X-Met TiO_2 and Fe_2O_3 analyses along the cores: TiO_2-and Fe_2O_3-analyses of cores by a portable XRF-instrument (Outokumpu X-Met 880) were done in the field by DuPont geologists Eric Ahrenberg and Magnus Garson, Oddvin Hansen from Fjord Blokk, and at NGU's core storage at Løkken by Gunnar Fossflaten and others from NGU. The complete analytical results are given in Appendix 9 (standard corelog printout from the project's PC-database «EngLog.mdb»). A core-log summary is given in Tables 4 to 14, and the TiO_2-variation along the cores is shown in Figs. 2 to 11 and in Appendix 1.

6.2. Major- and trace-element analyses

A number of core-sections were selected for major and trace element analyses, and S-analyses. Some selected elements are reported in Table 14, and average content of the various elements for the different rock-types is given in Table 15, while the complete analytical results are given in Appendix 2. These analytical data will be further discusssed in a later report dealing specifically with the geology of the Engebøfjell eclogite deposit.

Table 14: Core-sections analyzed for major and trace elements - a summary. See Appendix 2 for the complete analytical data. Average values for the different rock-types are given in Table 15.

Anal. no.	*Sample*	*Rock*	*% S (Leco)*	*% py (DTA)*	*% qtz (DTA)*	*% SiO_2 (XRF)*	*% Fe_2O_3 (XRF)*	*% TiO_2 (XRF)*	*% Rutile*	*% Rutile vs. TiO_2*	*% TiO_2# X-Met*	*TiO_2 (xrf) - TiO_2 (X-Met)*
1	1/20-30	AU				56.41	9.54	0.94	0.57	60.6 %	0.70[r]	0.24
2	1/65-66	LE	0.14	0.49	4	46.24	16.12	1.81	1.75	96.7 %	1.23[r]	0.58
3	1/101-103	FE	0.13			45.65	17.60	3.49	3.33	95.4 %	4.06[r]	-0.57
4	1/126-127	FE	0.14			45.26	17.95	3.71	3.46	93.3 %	3.53[r]	0.18
5	1/160-170	AU				57.45	10.59	1.41	1.02	72.3 %	0.68[r]	0.73
6	2/95-105	AU				52.12	13.04	1.73	1.51	87.3 %	1.15[r]	0.58
7	2/115-116	FE	0.15			44.59	18.17	4.90	4.75	96.9 %	3.83[r]	1.07
8	2/150-155	FE	0.24	0.65	3	44.64	19.94	3.63	3.47	95.6 %	3.14[r]	0.49
9	2/165-170	FE	0.18			44.56	18.02	5.05	4.96	98.3 %	4.30[r]	0.75
10	2/200-205	FE	0.12			42.59	18.31	3.52	3.29	93.5 %	3.05[r]	0.47
11	2/260-270	AU				56.69	10.11	1.38	1.08	78.3 %	0.97[r]	0.41
12	3/15-20	LE	0.05			51.10	9.74	0.88	0.85	97.1 %	0.61[r]	0.27
13	3/60-65	LE	0.35	0.17	6	51.03	9.54	0.83	0.80	96.5 %	0.45[r]	0.38
14	3/80-85	G				82.77	1.23	0.17	0.16	94.5 %		
15	3/110-111	LE	0.12			50.10	10.23	0.85	0.81	95.0 %	0.48[r]	0.37
16	3/135-136	LE	0.15	0.47	4	47.77	13.95	2.02	1.99	98.4 %	1.63[r]	0.39
17	3/159-160	FE	0.17			43.76	17.89	5.08	5.02	98.8 %	4.58[r]	0.50
18	4/36-40	LE	0.20			45.05	17.67	2.59	2.45	94.6 %	1.50[c]	1.09
19	4/75-77	FE	0.13			43.12	17.98	5.09	4.98	97.8 %	5.28[c]	-0.19
20	4/97-98	FE	0.19			44.68	17.28	4.44	4.38	98.6 %	5.78[c]	-1.34
21	4/120-121	FE	0.20			43.09	20.53	5.05	4.33	85.7 %	5.15[c]	-0.10
22	4/130-131	FE	0.31			44.01	19.73	4.46	4.30	96.4 %	4.58[c]	-0.12
23	4/106-108	FE	0.18	0.58	6	46.37	16.13	2.99	2.92	97.8 %	3.18[c]	-0.19
24	4/151-152	FE	0.07			45.51	17.49	4.41	4.25	96.4 %	4.35[c]	0.06

[#] X-Met analysed on round (r) vs. cut (c) core surface by DuPont's X-Met, 30 sec. counting time.
AU: amphibolite unit rocks; FE: ferrogabbroic eclogite; LE: leucogabbroic eclogite; G: quartz-rich gneiss

Table 15: Average major- and trace-elements for characteristic Engebøfjell rock-types. The complete analyses are given in Appendix 2. A detailed interpretation of the geochemical data will be given in a separate report on the geology of the Engebøfjell eclogite.

	Amphibolite unit rocks	Leucogabbroic eclogite	Ferrogabbroic eclogite
No. of anal.	4	6	13
Major elements (%), XRF-analyses:			
SiO_2	55,67	48,55	44,45
Al_2O_3	14,06	16,77	13,16
Fe_2O_3	10,82	12,88	18,23
TiO_2	1,37	1,50	4,29
MgO	4,60	6,41	5,47
CaO	6,31	9,07	9,87
Na_2O	3,29	2,73	2,28
K_2O	1,56	0,53	0,32
MnO	0,16	0,15	0,22
P_2O_5	0,33	0,12	0,44
LOI	1,08	1,15	0,29
Sum	99,22	99,83	99,03
Other analyses:			
Rutile	1,05	1,44	4,11
Rut/TiO_2	0,75	0,96	0,96
% S (Leco SC-444)		0,17	0,17
% pyrite (DTA)		0,38	0,56
Trace-elements (XRF-anal.):			
Y	50,25	19,17	25,92
Zr	216,25	56,67	58,15
Nb	9,00	<5,00	<1,38
Sr	181,75	281,33	185,08
Rb	37,00	14,33	3,15
Ba	514,00	196,00	103,92
Cu	39,25	49,00	32,54
Zn	124,25	100,67	143,92
Sc	22,75	30,17	46,15
V	154,50	315,33	354,15
Ni	72,75	67,17	16,23
Cr	133,00	173,00	45,23
Co	30,75	50,67	58,62
Rare Earth elements (ICP-analyses):			
Y	49,08	20,03	28,74
La	38,03	9,48	10,45
Ce	87,35	20,03	24,48
Pr	10,90	3,50	3,73
Nd	37,73	11,03	14,54
Sm	9,05	3,22	4,45
Eu	2,33	1,15	1,71
Gd	7,88	1,92	3,59
Tb	1,70	0,45	0,95
Dy	8,20	3,13	4,75
Ho	1,85	0,68	1,03
Er	3,43	1,05	1,45
Tm	0,65	0,22	0,32
Yb	4,18	1,87	2,56
Lu	1,05	0,50	0,66

6.3. The reliability of the X-Met TiO_2-analyses

The X-Met analyses, with one analysis pr. 0.25m along the cores, give a good indication of the TiO_2 and Fe_2O_3 variations along the core, but do not give accurate correct analytical values. The instrument was calibrated on pulverized samples, and the analyses reported here have been done on solid core, either on the curved core surface or cut (sawed) surface, and systematic errors are likely to occur.

Fig. 20 is a scattergram plot comparing XRF laboratory analyses with the average X-Met TiO_2-analyses of the same core sections (the individual X-Met analyses are plotted in Fig. 21). In this plot two groups of TiO_2-values are identified; one with less than 3% TiO_2 (the leucogabbroic and transitional eclogites) and the other with > 3% TiO_2 (the ferrogabbroic eclogites). For the first group, the X-Met TiO_2-values are distinctly lower than the laboratory XRF analyses. For the ferrogabbroic groupe the X-Met analyses are reasonably similar to the XRF-analyses.

However, as shown in Table 14, some of these data derive from X-Met analyses on round core surface, and others on cut surfaces. There is a tendency for the X-Met analyses on round core surfaces to give slightly lower values than the XRF-analyses, while the X-Met analyses on cut core tend to be slightly higher than XRF-data. These X-Met analyses were done with DuPont's X-Met.

Table 15: Comparison of different X-Met analyses on the same core-samples. Each analytical value is an average of 3 individual analyses. Based on these data NGU's X-Met give an average 0.28% TiO_2 (3 - 1) higher values than DuPont's X-Met on cut core surface. NGU's X-Met gives an average TiO_2 value 0.46% higher than on cut core surface than on round core surface.

	DuPont's X-Met (15 sec.)		NGU's X-Met (15 sec.)		NGU's X-Met (15 sec.)	
Sample	Cut surface % TiO_2	Cut surface % Fe_2O_3	Cut surface % TiO_2	Cut surface % Fe_2O_3	Round surface % TiO_2	Round surface % Fe_2O_3
4/030.0	1.6	9.0	2.3	8.4	2.0	8.1
4/035.9	2.7	15.6	2.4	13.7	2.0	14.2
4/026.9	1.5	12.9	2.0	13.0	2.1	13.3
4/024.1	3.2	16.6	3.4	15.3	2.6	15.5
4/054.0	2.8	15.7	3.0	16.7	2.6	14.9
4/159.7	2.8	17.0	3.1	16.6	2.6	14.0
4/09.9	3.7	17.9	3.7	17.0	2.7	16.3
4/064.9	3.1	17.2	3.3	17.0	2.9	15.6
4/137.9	3.2	24.7	3.6	20.7	3.0	17.2
4/037.9	3.5	17.4	4.0	17.9	3.1	17.3
4/044.1	3.4	17.7	4.0	17.2	3.1	14.4
4/016.9	3.7	16.2	3.7	20.6	3.4	18.0
4/069.9	5.0	16.7	4.3	16.6	3.4	15.6
4/059.8	3.7	19.3	3.8	19.3	3.5	18.5
4/125.2	3.5	16.6	3.4	15.9	3.5	13.5
4/074.9	2.5	15.6	2.6	15.4	3.6	14.4
4/151.9	4.1	15.2	4.7	14.7	3.6	14.3
4/098.9	4.2	15.5	4.3	15.5	3.7	14.2
4/110.4	4.0	17.1	4.4	16.6	3.8	15.1
4/113.9	4.8	16.2	4.8	15.3	4.4	13.1
4/070.8	5.7	18.2	6.5	15.1	4.5	12.8
4/140.9	4.3	18.0	4.7	17.3	4.5	16.2
4/069.7	6.1	17.3	6.2	16.8	5.2	14.2
4/073.8	5.8	15.9	6.2	15.7	5.5	14.1
4/079,9	4.7	27.4	6.1	26.3	7.7	20.3
	3.74 [1]	17.08 [2]	4.02 [3]	16.58 [4]	3.56 [5]	15.00 [6]

To investigate these differences in more detail, a number of core samples were analysed on both round and cut surfaces using NGU's X-Met. The results are plotted in Fig. 22. This figure clearly shows that X-Met analyses on cut (sawed) core surface tend to give higher TiO_2-values than the corresponding analyses on round core surface.

Table 15 is a comparison of different X-Met analyses on the same samples showing that NGU's X-Met gives distinctly higher TiO_2-values than analyses by DuPont's X-Met. This is due to the fact that the instruments were calibrated with different standard sets.

In summary:

X-Met analyses directly on cores must be used with great care considering that X-Met analyses on cut cores give distinctly higher TiO_2-values than analyses on round, outer core surfaces. The X-Met analytical results are very sensitive to the instrument's calibration. DuPont's X-Met with its calibration used until now (all X-Met analyses of Dh1 to Dh8) give fairly reliable results for the ferrogabbroic eclogite with $TiO_2 > 3\%$, while NGU's X-Met with its present calibration (the X-Met work on Dh9 to Dh10) give TiO_2-values that are too high. For future work the two X-Met instruments available for this project must be calibrated identically using the same set of calibration standards, and the X-Met results must be systematically compared with reference laboratory XRF analyses of the respective core sections.

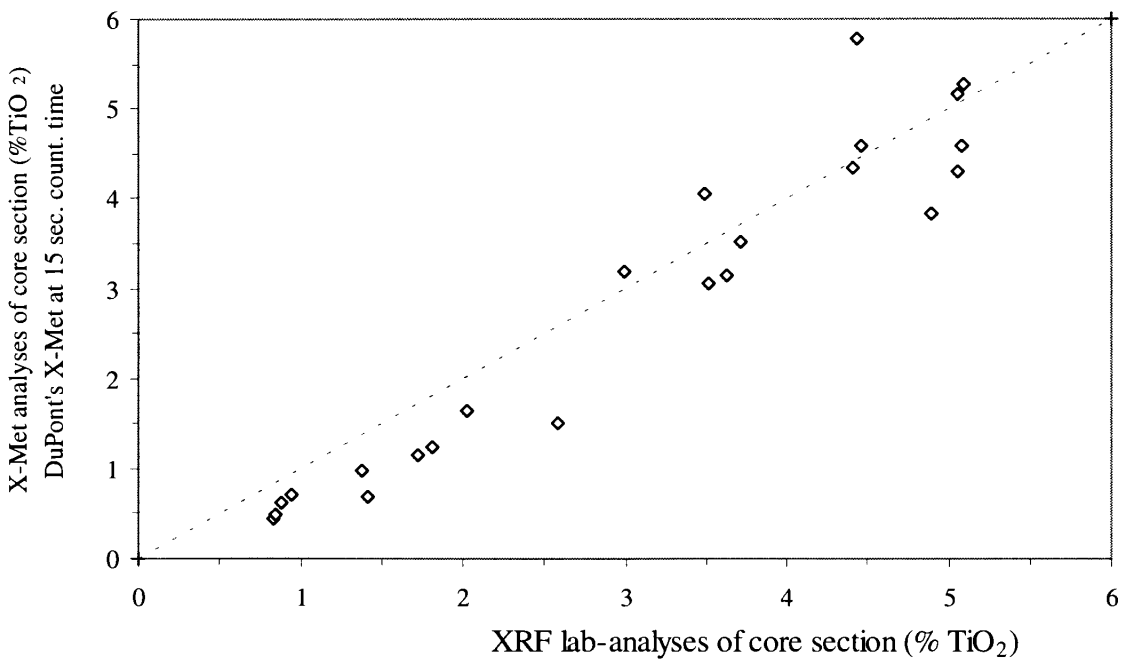

Fig. 20: TiO_2 analyses (average values) on core by DuPont's X-Met (30 sec. count. time) vs. laboratory XRF-analyses of the respective core sections. See Fig. 21 and Appendix 3 for further details.

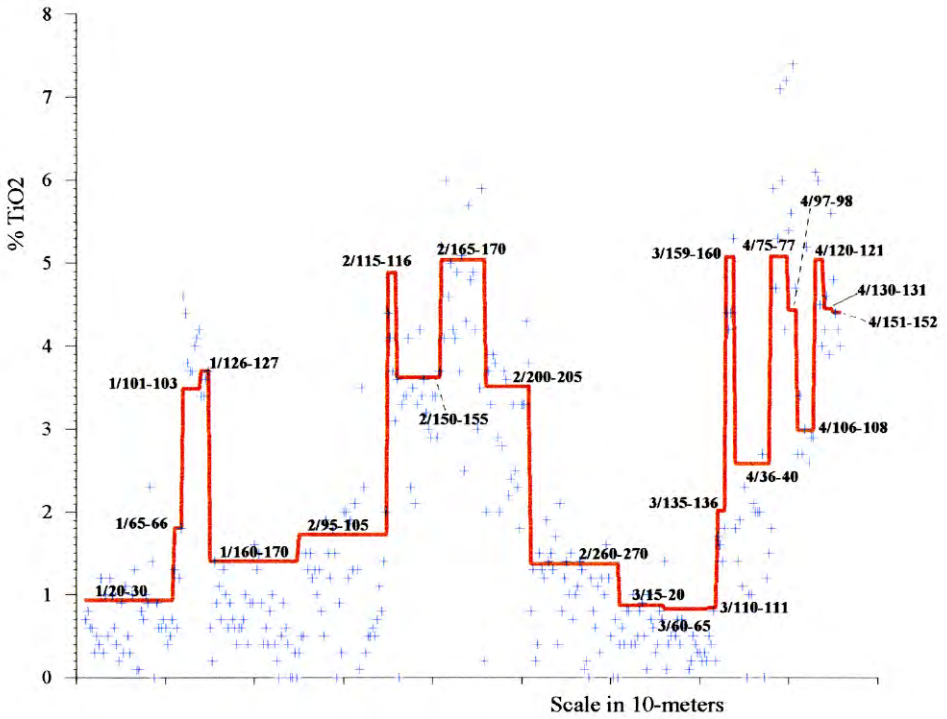

Fig. 21: Comparison of X-Met analyses of cores from Engebøfjellet (crosses) and XRF laboratory analyses (solid line) of the respective core sections.

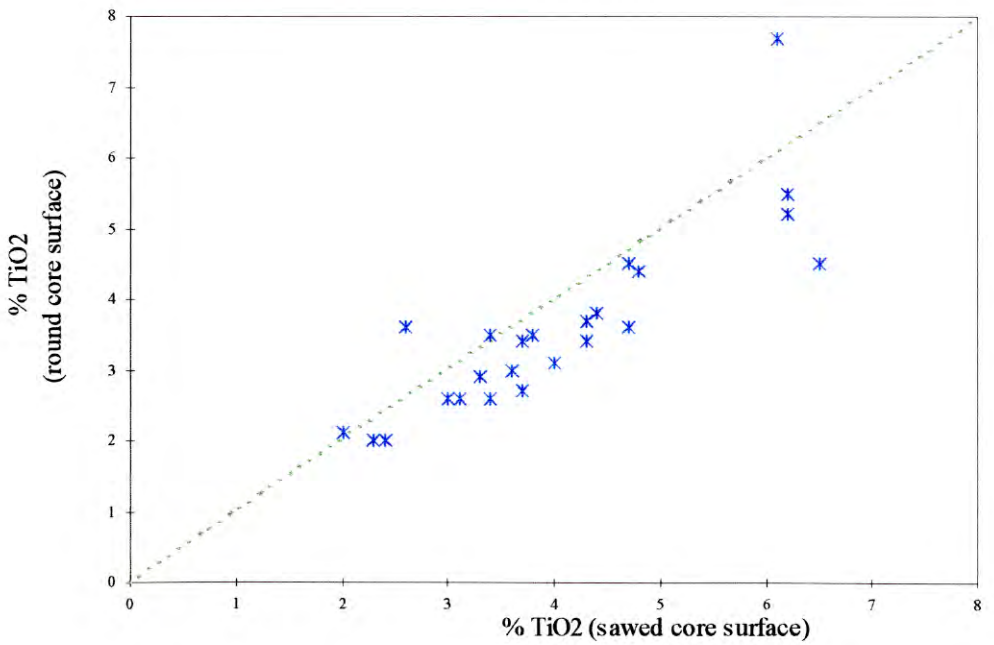

Fig. 22: TiO_2-analyses on cut (sawed) core surface vs. round core surface by NGU's X-Met. Each plotted value is an average of 3 individual analyses (15 sec. counting time). See Appendix 3 for further analytical details.

6.4. Petrophysical data

Specific gravity: Precise knowledge of the variations in specific gravity at Engebøfjellet is particularly important for the interpretations of the gravity work (see Mauring et al. 1997). As shown in Table 16 (see also Appendix 1), the ferrogabbroic eclogite is the heaviest rock at Engebøfjellet, averaging 3.45 g/cm^3 though the peak in the ferrogabbroic specific gravity, distribution (Fig. 23) is at 3.55 g/cm^3. The ferrogabbroic samples with lower specific gravity than 3.3 are retrograded, and those below 3.0 g/cm^3 are heavily retrograded. The leucogabbroic eclogite (average 3.26 g/cm^3) shows two peaks in the distribution diagram, at 3.15 and 3.40 g/cm^3, respectively. The lower peak is representative for the characteristic leucocratic eclogite in the western and northwestern parts of Engebøfjellet, this variety often shows relics of a gabbroic texture. The peak at 3.4 g/cm^3 is representative for the so-called transitional eclogite intermediate between the previous leucogabbroic eclogite and the ferrogabbroic eclogite. The variations between these eclogites are usually gradational. The transitional eclogite variety has not been mapped; it is included in the leucogabbroic unit on the geologic map (Fig. 2 and Appendix 5) and in the geological vertical profiles (Figs. 3 to 12). The leucogabbroic eclogite samples with specific gravity < 3.05 g/cm^3 are retrograded (amphibolitized).

The other rocks in Table 16 are amphibolite unit rocks: amphibolitic eclogite (3.19 g/cm^3), amphibolite (2.92 g/cm^3), gneiss with amphibolitic inclusions (2.86 g/cm^3) and gneiss (2.72 g/cm^3). Average specific gravity for the amphibolite unit (mixture of amphibolite, eclogite and gray gneiss) is approx. 3.0 g/cm^3.

Table 16: Petrophysical parameters (average values) and corresponding analytical data based on X-Met analyses. See Appendix 7 for the complete analytical data.

Rock	n	Sp. gravity (g/cm^3)	Magn. susc. (SI-units)	TiO_2	Fe_2O_3
Ferrogabbroic ecl.	169	3.45	0.00501	4.39	17.06
Leucog. and trans. ecl.	96	3.26	0.00925	1.85	13.96
Leucogabbroic ecl		3.1-3.2			
Transitional ecl.		3.2-3.4			
Amphibolitic ecl.	6	3.19	0.00278	2.18	12.17
Amphibolite	48	2.92	0.00480	1.15	9.47
Gneiss	5	2.72	0.00006	0.21	1.17
Gneiss/amph.ecl.	11	2.86	0.00549	0.85	7.86

The TiO_2 - Fe_2O_3 and TiO_2 - specific gravity plots in Fig. 24 show similar trends indicating that specific gravity largely is proportional to the iron-content (garnet-content) in the eclogite. This is also shown in Fig. 25.

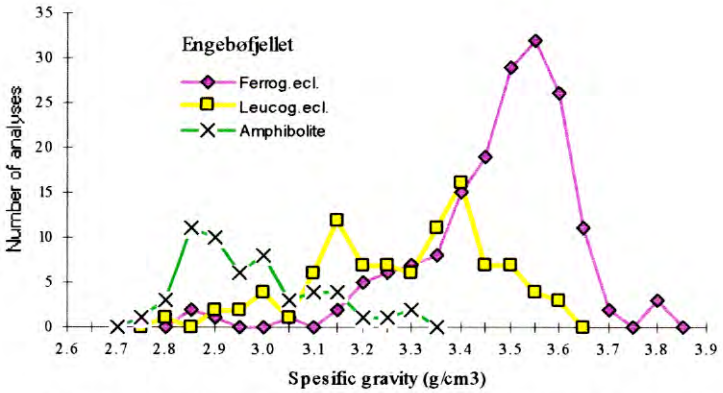

Fig. 23: Distribution of specific gravity (weight) for eclogite, leucogabbroic eclogite (incl. transitional eclogite) and amphibolite unit rocks, all from Dh1 to Dh5.

Magnetic susceptibility: Average values of magnetic susceptibility for the respective rock types are shown in Table 16. The magnetic susceptibilities of the mafic rocks are controlled dominatly by the degree of retrogression and by initial iron-content, i.e. garnet-content. Titanium do not contribute to the susceptibility; the apparent correlation between high magnetic susceptibility and titanium in unretrograded eclogite is due to the association titanium has with iron in the original rock. The magnetic samples have secondary magnetite formed during the retrogression of the rock; in most cases this magnetite occurs along the thin amphibolitic veins similar to those shown in Fig. 19. It is also found as minute crystals within symplectites after omphacite or in kelyphitic coronas around garnets. This is illustrated in Fig. 24; the *line of unretrograded eclogite* (Fig. 24 a,b) indicates that magnetic susceptibility increases gradually with specific gravity and TiO_2. And at increasing retrogression, progressively more secondary magnetite is formed, giving the rock a distinct magnetic susceptibility. Fig. 26 is a histogram showing the magnetic susceptibility distribution. The high-magnetic samples are all strongly retrograded.

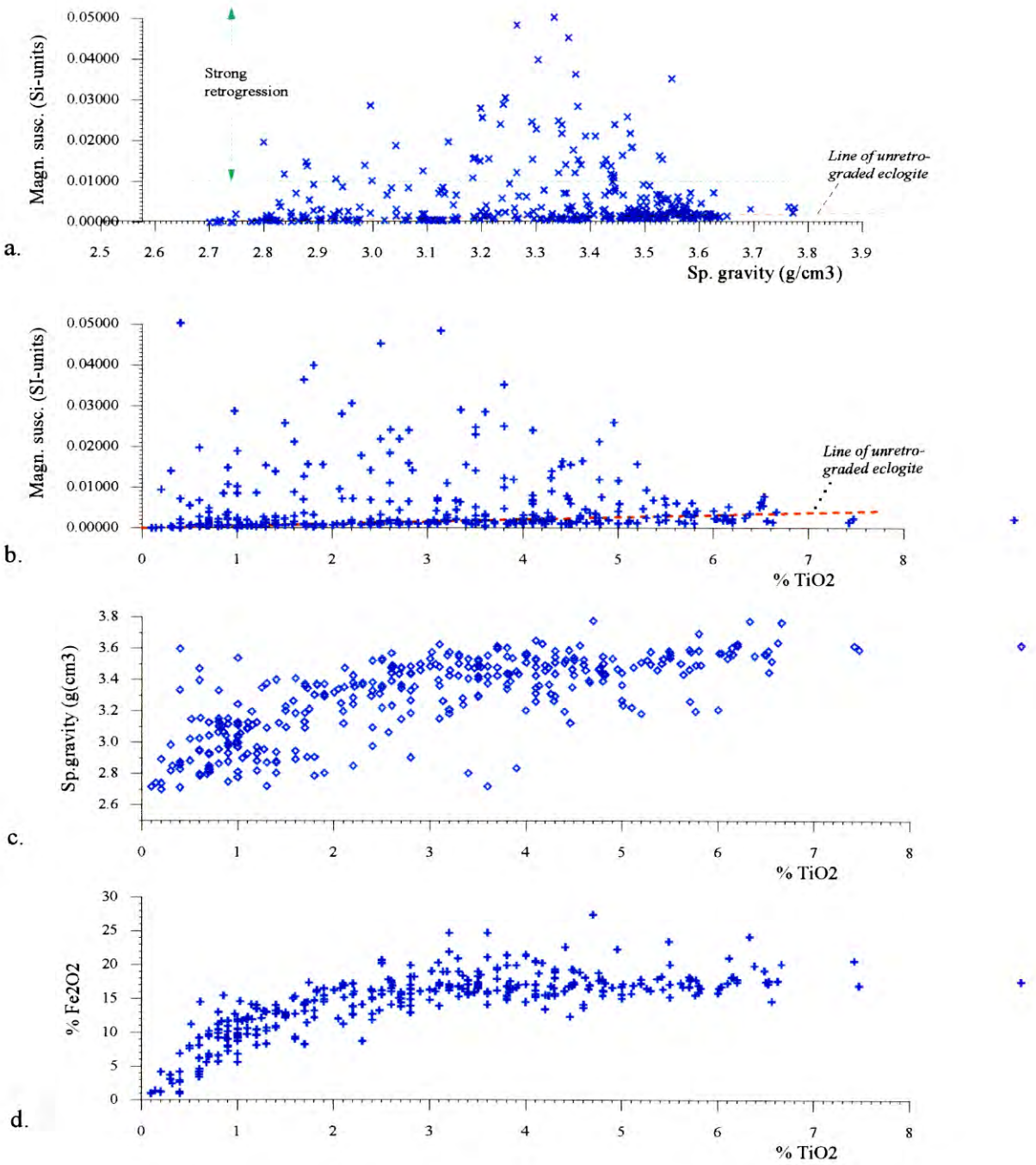

Fig. 24: Scattergram plots: (a) specific gravity vs. magnetic susceptibility, (b) % TiO_2 vs. magnetic susceptibility, (c) % TiO_2 vs. specific gravity, and (d) % TiO_2 vs. % Fe_2O_3. The high-magnetic character of some high density eclogites (<3 g/cm^3) is caused by secondary magnetite along retrogressive cracks in the eclogite; thus altogether, a relatively minor portion of these samples retrograded.

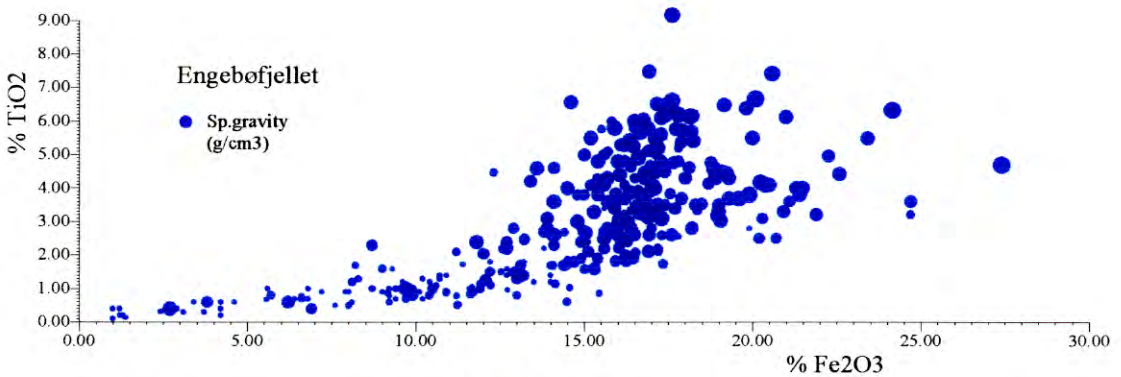

Fig.25: Scattergram plot of Fe_2O_3 vs. TiO_2 with the symbol size indicating the relative variation in specific gravity.

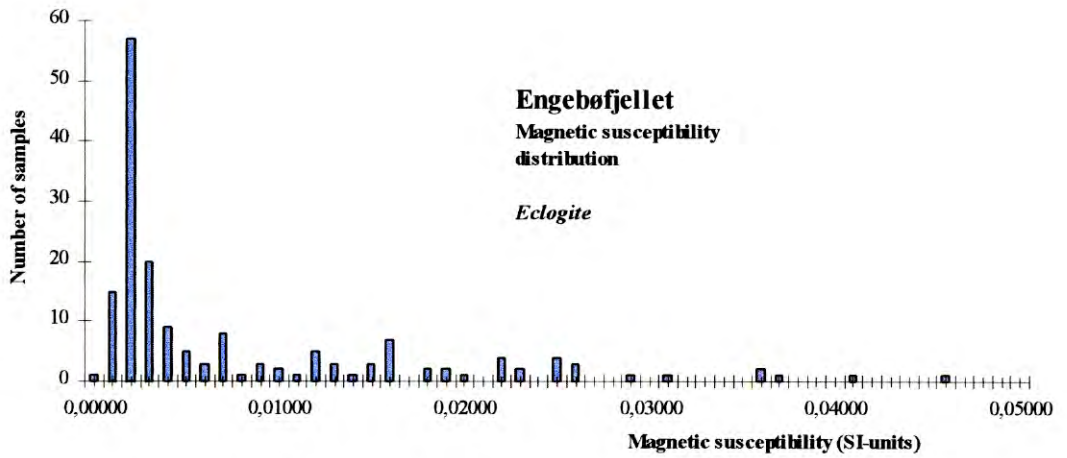

Fig. 26: Histogram showing the distribution of magnetic susceptibility for eclogite from Engebøfjellet.

7. Summary and conclusion

The complexity of the Engebøfjell rutile deposit is a consequence of a long and complex geologic history including (a) primary variations in the original Proterozoic (not dated) mafic intrusion, (b) pre-eclogitic metamorphism and deformation, (c) extensive Caledonian metamorphism and deformation under which the gabbro to eclogite transformation took place, and (d) retrograde alteration of the eclogite associated with amphibolite facies and, locally, greenshist facies deformation and metamorphism. The present geological map shows some of the complexity of the deposit; the details of this, however, will be discussed in a later report.

In the present investigation priority has been given to:

The ***TiO_2 distribution*** in the deposit, i.e. to outline the ferrogabbroic eclogite and investigate its TiO_2-content in all parts. All the drilling and most of the surface investigations have been aimed at this chemical mapping.

Analyses. The cores have rutinely been analysed by the X-Met portable XRF-instrument in order to map the TiO_2 and Fe_2O_3 distribution along the cores, as well as to investigate the Engebøfjell eclogite on the surface. However, it is clear that the two X-Mets that have been used, one owned by DuPont and the other by NGU, show slightly different results caused by different calibrations. NGU's X-Met shows consistantly high TiO_2 -values compared to laboratory XRF analyses. The X-Met analyses of Dh1, Dh2 and Dh3 (up to 160 m) that were done by DuPont's X-Met, are probably slightly too low, while the similar X-Met analyses done on cut cores (Dh3 from 160m, Dh4, Dh5, Dh6, Dh7 and Dh8), are believed to be reasonably correct relative to the XRF analyses

Retrograde alteration. One characteristic feature of the Engebøfjell eclogite is that 90-95% of the titanium is in rutile, though locally rutile is altered to ilmenite and occasionally to titanite along mm-thick cracks or veins where the eclogite is significantly retrogressed (amphibolitized). However, the overall pattern is that retrogression of the Engebøfjell eclogite is relatively small, and the rutile/ilmenite ratio is very high (> 9:1). Retrogression is associated with increased magnetic susceptibility; therefore investigation of the magnetic suscetibility along the cores is also an investigation of the degree of retrogression. In highly-magnetic eclogite (magn. susc. > 0.01) alteration of rutile to ilmenite or titanite can be expected.

The density (specific gravity) of the eclogite is a significant factor especially for Fjord Blokk's production of sea-wall blocks. In general the eclogite with the highest TiO_2-content, which is also the Fe_2O_3- and garnet-richest, is the heaviest. Knowledge of density variations within the deposit and its surroundings is essential for reliable interpetation of the gravimetric data in regard to continuation of the ferrogabbroic eclogite ore at depth.

In the future drilling-related investigation at Engebøfjellet the following priorities should be made:

- In order to have sufficient analytical control XRF lab-analyses of 10m-sections, for example one 10m-section pr. 100m core, should be done and differences vs. the corresponding X-Met analyses used as a basis for corrections.
- The same samples should be analysed by the «rutile analytical procedure», i.e. TiO_2 (rutile) = TiO_2 (xrf) - TiO_2 (icp) to define the rutile/ilmenite ratio for the respective core-sections. This will give a quantitative measure of the effect of retrogression on the rutile/TiO_2 ratio.
- Systematic measurements of magnetic susceptibility as an indirect method in mapping the degree of retrogrogresssion and thus localizing those parts of the deposit where significant rutile alteration might have happened.

8. References

Tokle, A.T. (1996): Avviksmåling kjerneborhull. Prosjekt 183, 13-14.11.97, NGU.

Korneliussen, A. 1979 a: Rutil i eklogitter, Sunnfjord. NGU rapport 1717/1, 24 s. + 7 bilag.

Korneliussen, A. 1980 a: Tunge bergarter, Sunnfjord. NGU rapport 1717/2, 7 s. + bilag.

Korneliussen, A. 1980 b: Rutil i eklogittiske bergarter i Sunnfjord, Sogn og Fjordane. NGU rapport 1717/5, 27 s. + 2 bilag.

Korneliussen, A. 1996: Core-drilling at Engebøfjellet 1995/96; Dh1 to Dh5. NGU report no. 96.062, 155 p.

Korneliussen, A. and Foslie, G. 1985: Rutile-bearing eclogites in the Sunnfjord region of Western Norway. NGU Bull. 402, 65-71.

Korneliussen, A. og Furuhaug, L. 1991: Engebøfjellet og Fureviknipa rutilforekomster, Naustdal og Førde, Sogn og Fjordane. NGU rapport 91.171, 17 s. + 2 bilag.

Mauring, E. 1996: Interpretation of a gravity profile across the Engebøfjell rutile-bearing eclogite deposit. NGU report no. 96.061, 14 p.

Mauring, E., Gellein, J. and Korneliussen, A. 1997: Interpretation of two gravity profiles across the Engebøfjell rutile-bearing eclogite deposit. NGU report no. 97.002, 21 p.

Appendix 1: Miscellaneous scattergram plots showing TiO_2, Fe_2O_3, density and magn. susc. relations.

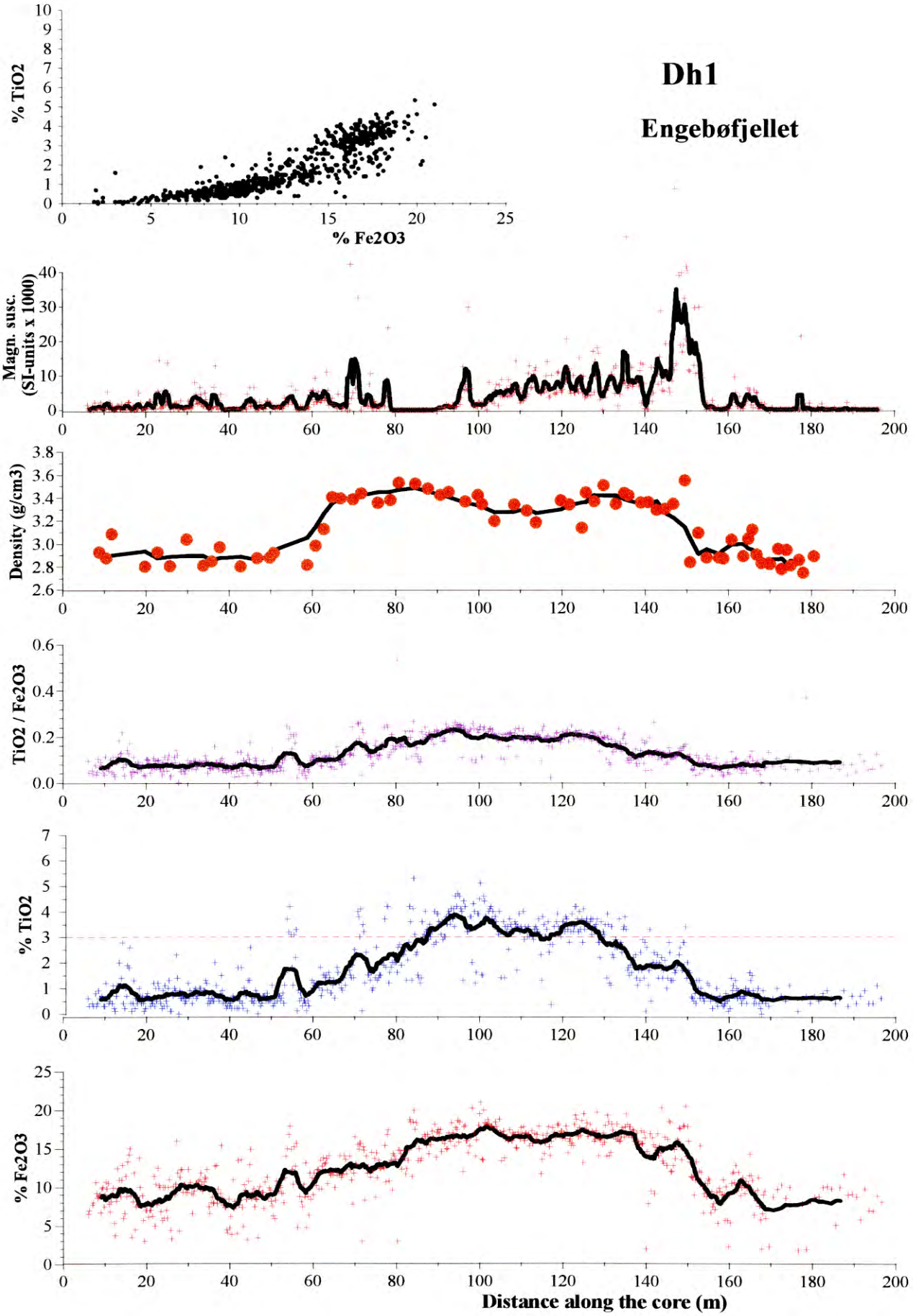
Dh1
Engebøfjellet
% TiO2
% Fe2O3
Magn. susc. (SI-units x 1000)
Density (g/cm3)
TiO2 / Fe2O3
% TiO2
% Fe2O3
Distance along the core (m)

dhmutil.grf

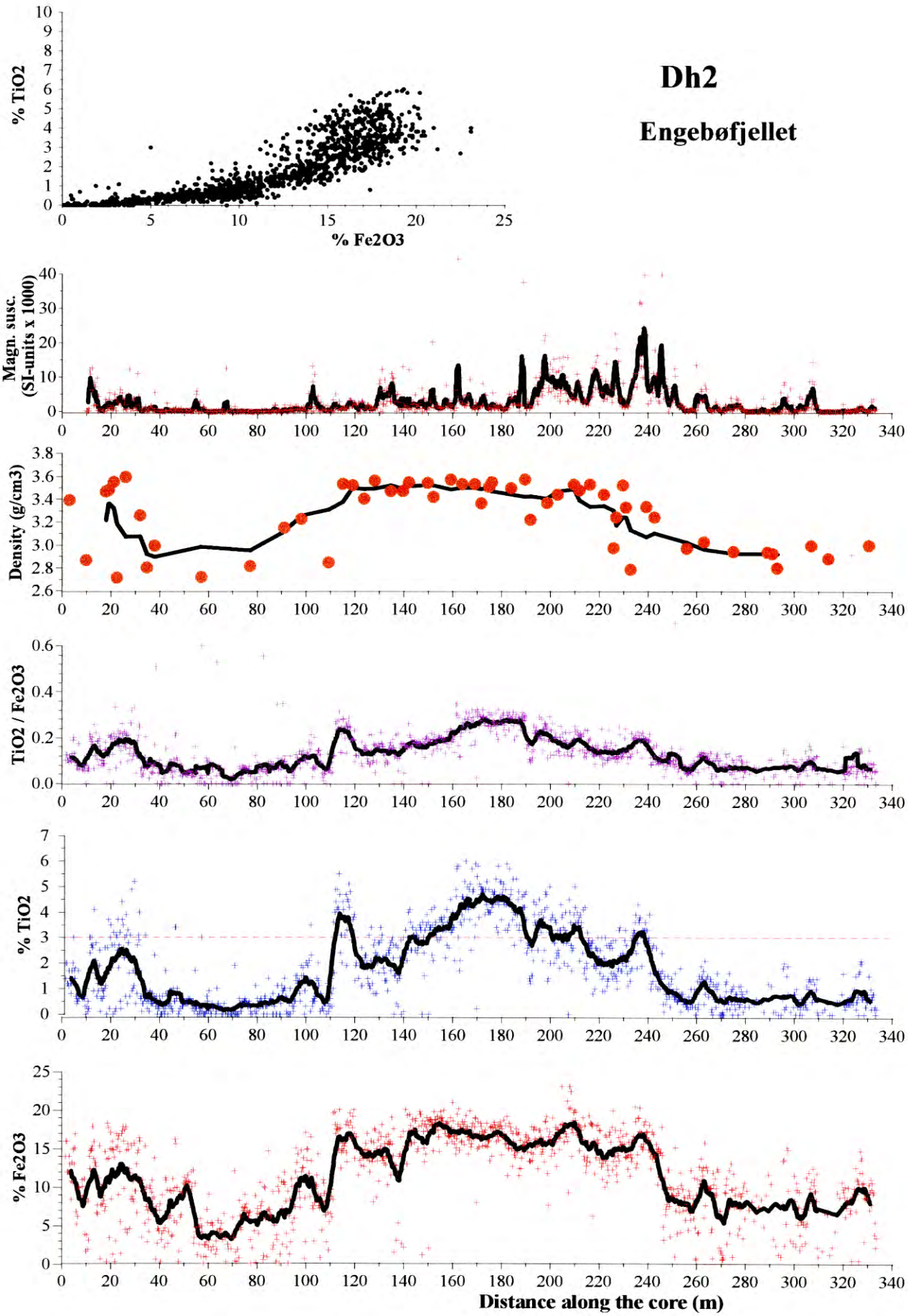
Dh2
Engebøfjellet
% TiO2
% Fe2O3
Magn. susc. (SI-units x 1000)
Density (g/cm3)
TiO2 / Fe2O3
% TiO2
% Fe2O3
Distance along the core (m)

dhmutil.grf

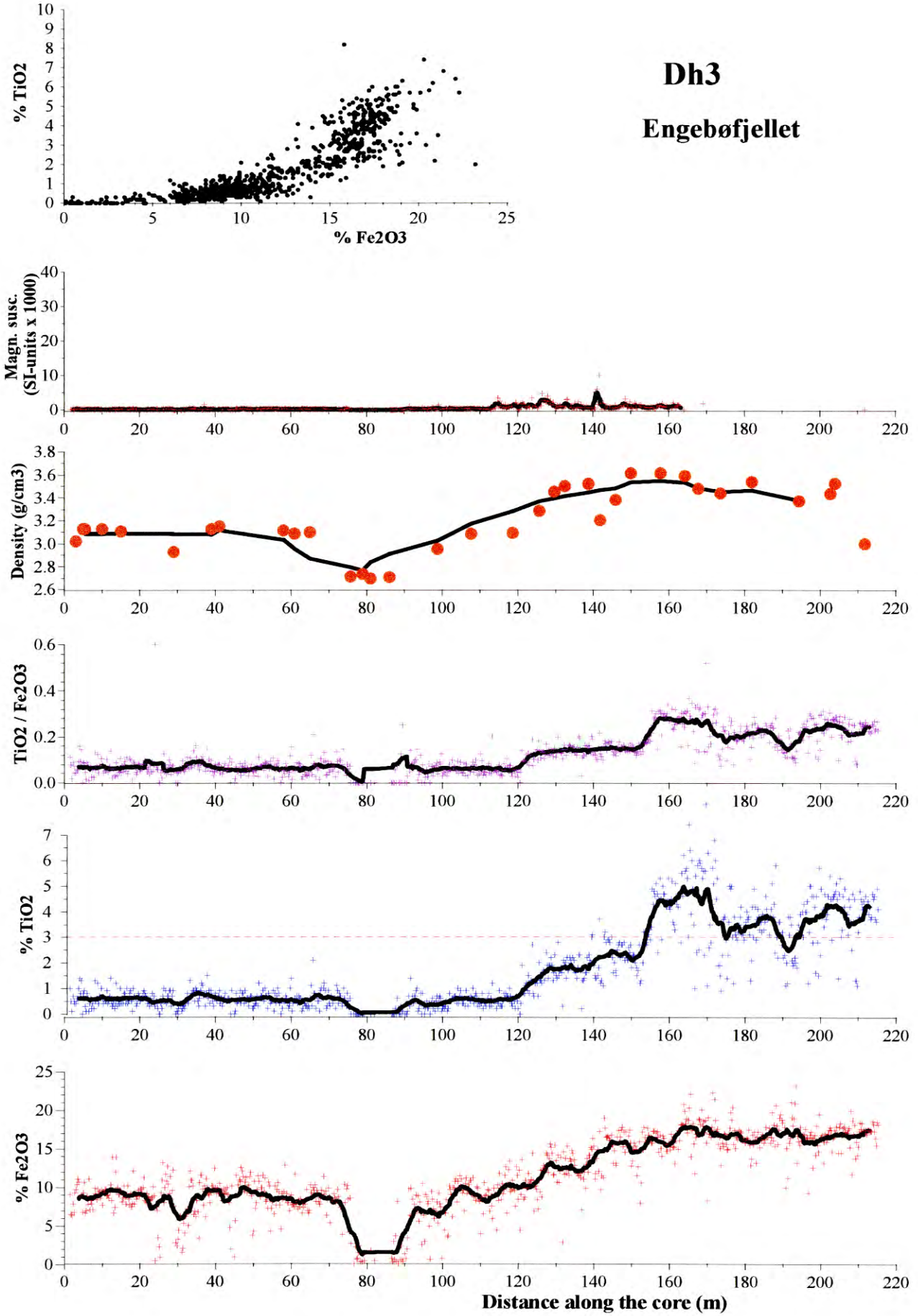
Dh3
Engebøfjellet
% TiO2
% Fe2O3
Magn. susc. (SI-units x 1000)
Density (g/cm3)
TiO2 / Fe2O3
% TiO2
% Fe2O3
Distance along the core (m)

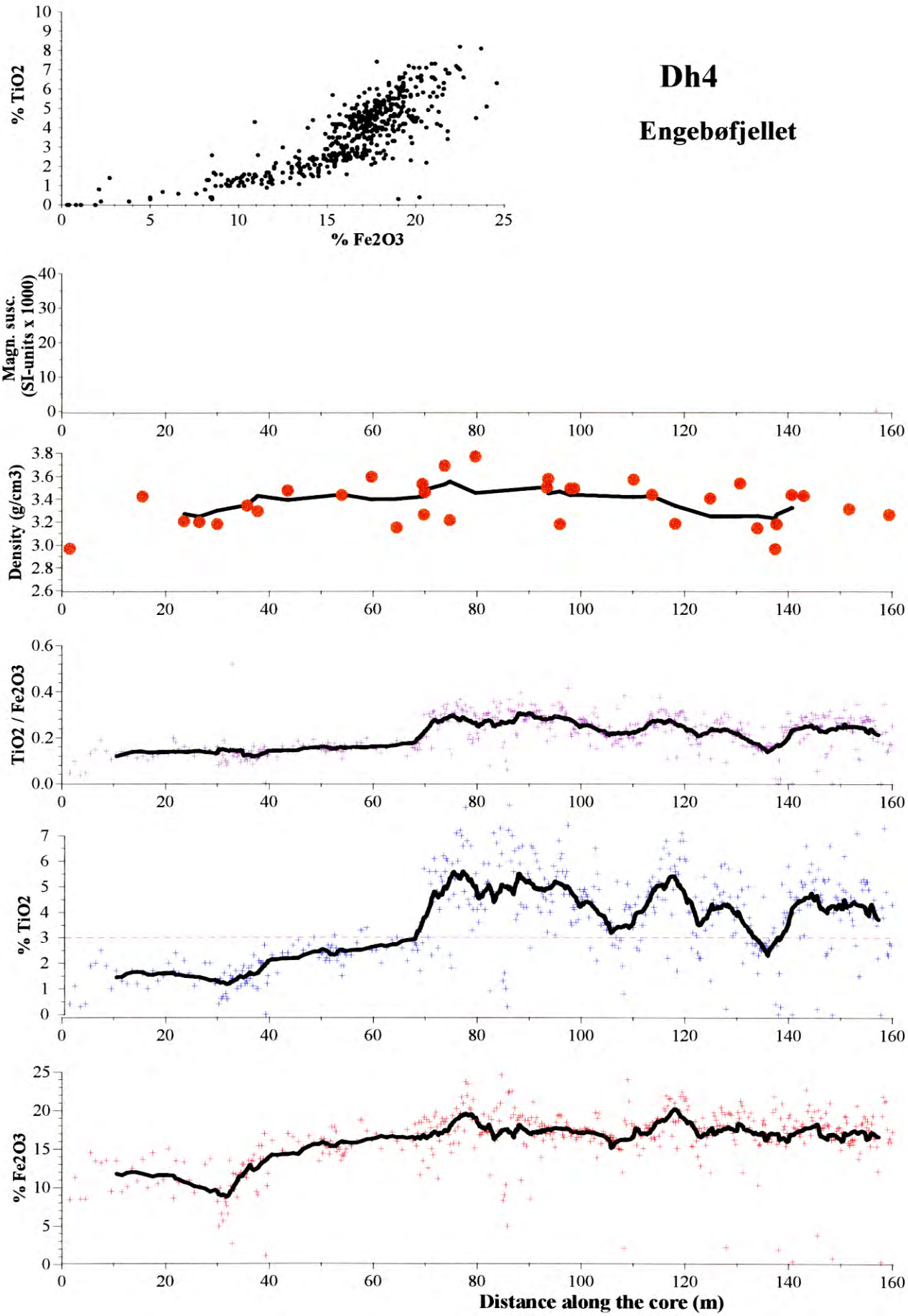
Dh4
Engebøfjellet
% TiO2
% Fe2O3
Magn. susc. (SI-units x 1000)
Density (g/cm3)
TiO2 / Fe2O3
% TiO2
% Fe2O3
Distance along the core (m)

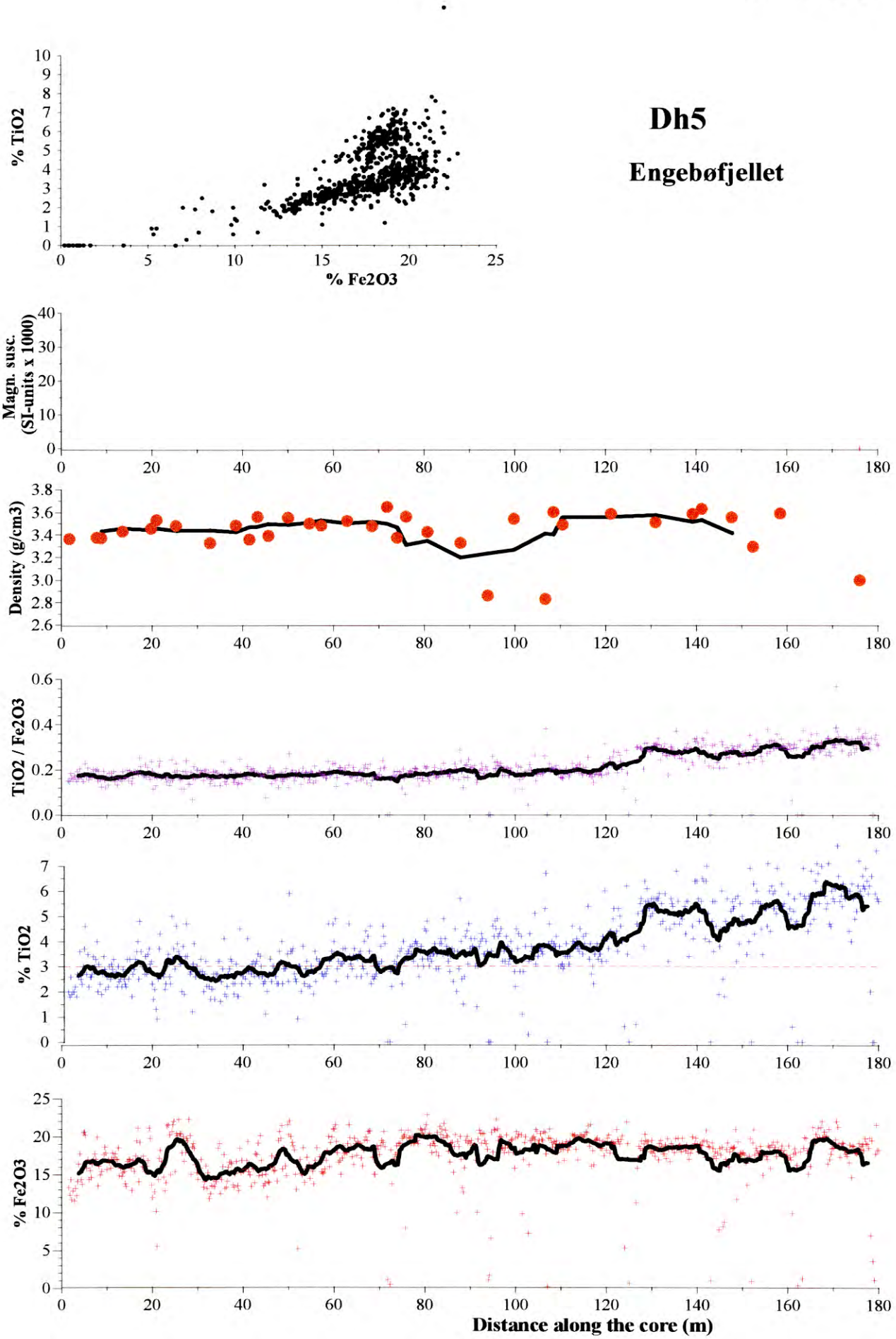
Dh5
Engebøfjellet
% TiO2
% Fe2O3
Magn. susc. (SI-units x 1000)
Density (g/cm3)
TiO2 / Fe2O3
% TiO2
% Fe2O3
Distance along the core (m)

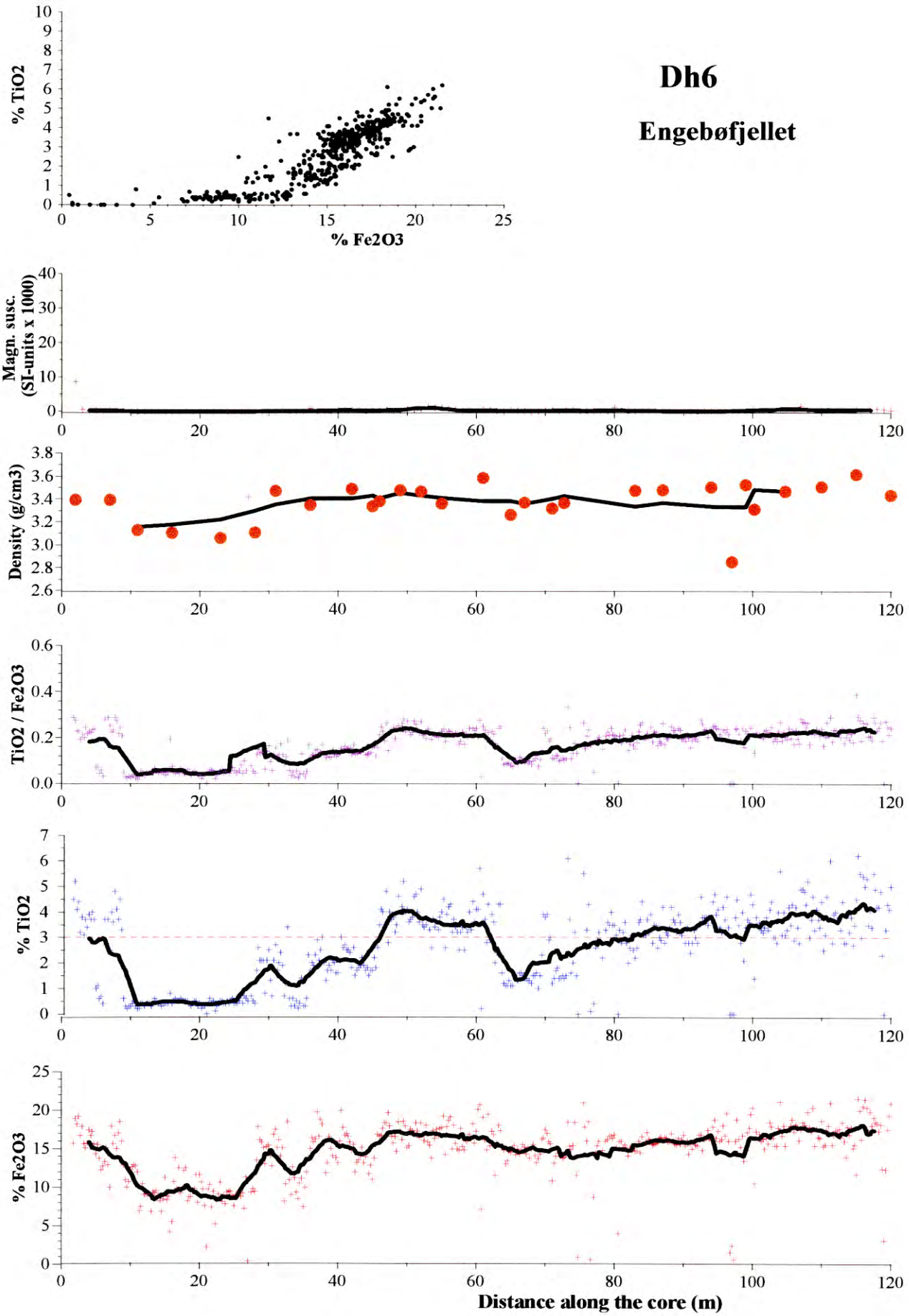
Dh6
Engebøfjellet
% TiO2
% Fe2O3
Magn. susc. (SI-units x 1000)
Density (g/cm3)
TiO2 / Fe2O3
% TiO2
% Fe2O3
Distance along the core (m)

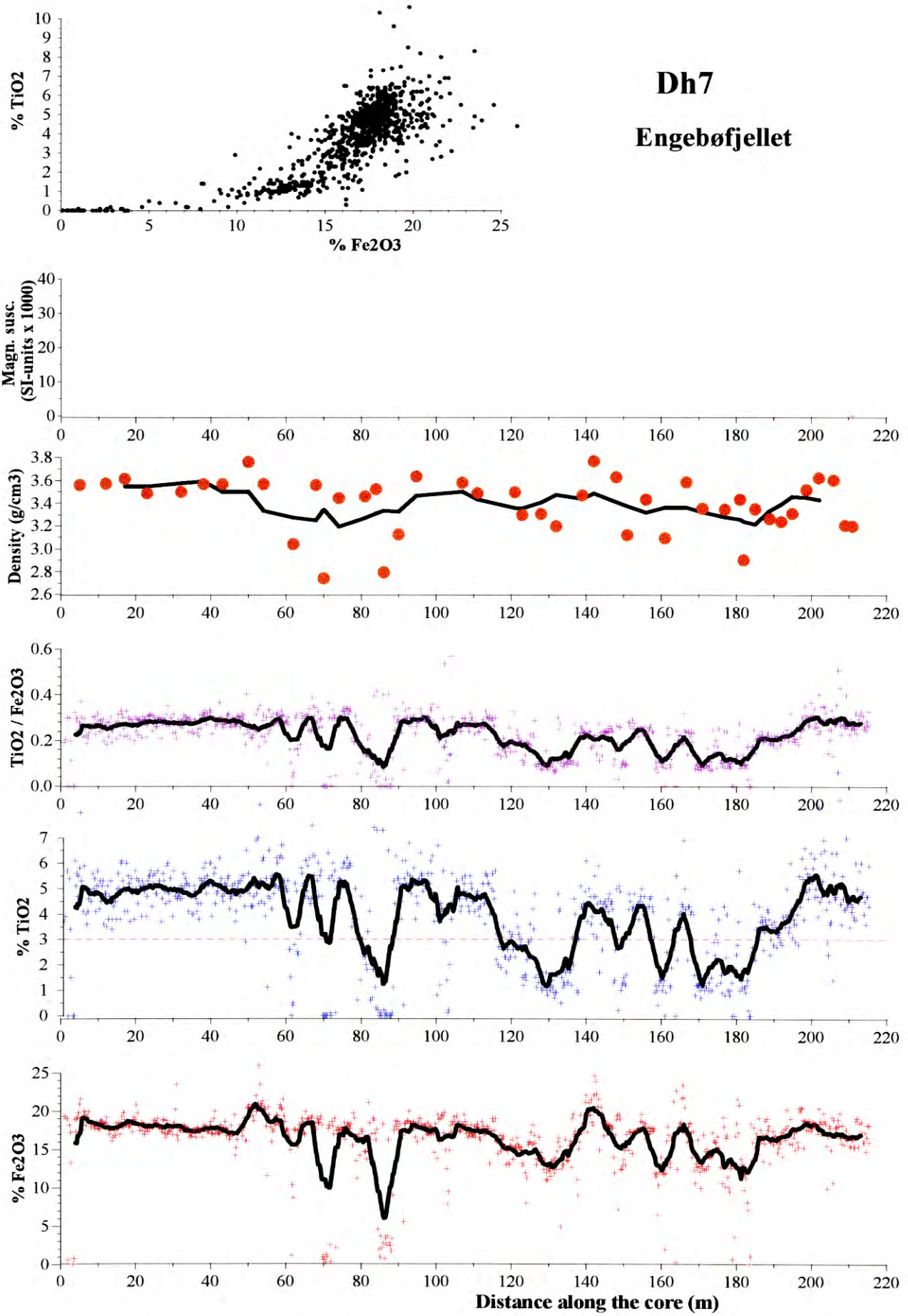
Dh7
Engebøfjellet
% TiO2
% Fe2O3
Magn. susc. (SI-units x 1000)
Density (g/cm3)
TiO2 / Fe2O3
% TiO2
% Fe2O3
Distance along the core (m)

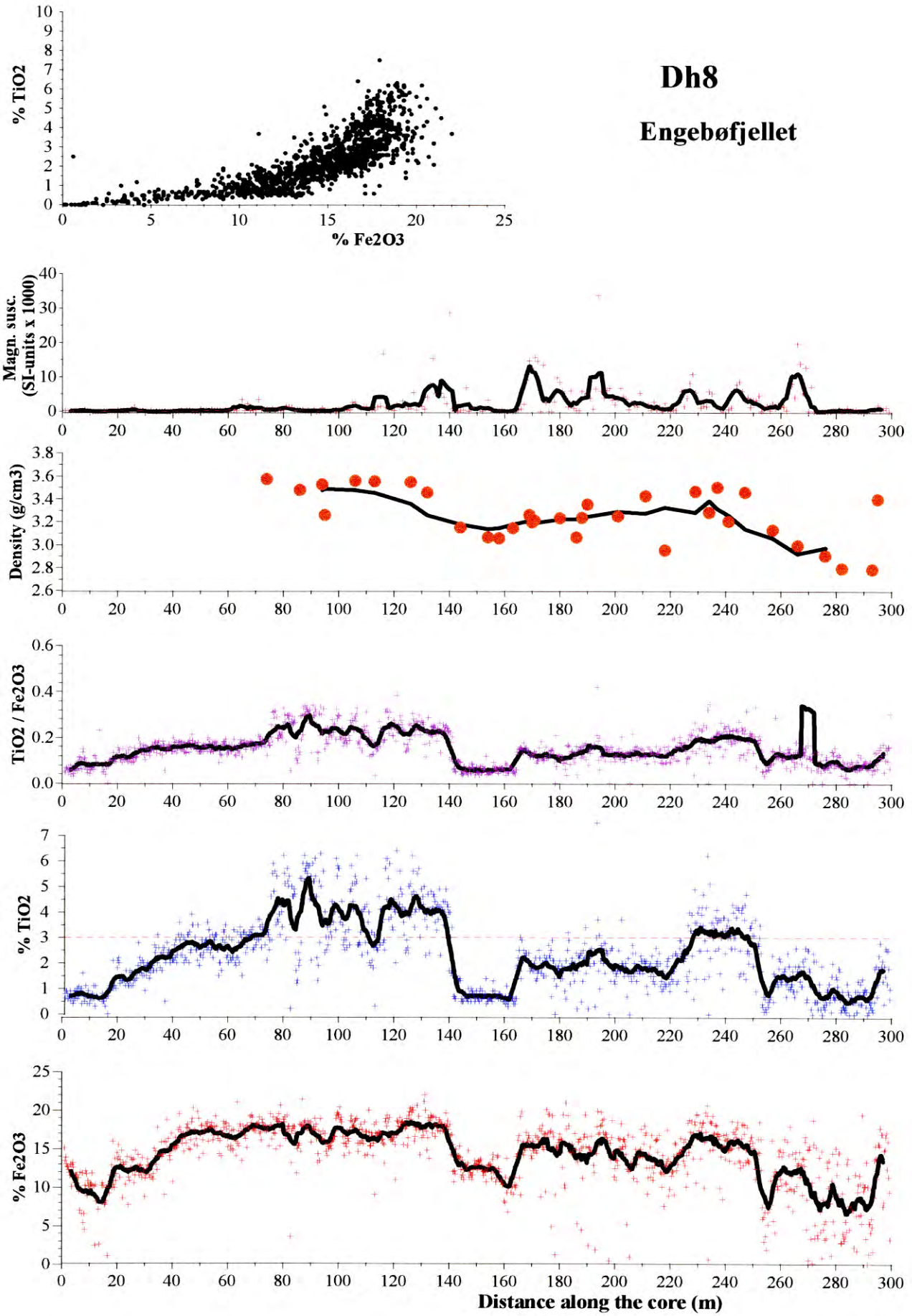
Dh8
Engebøfjellet
% TiO2
% Fe2O3
Magn. susc. (SI-units x 1000)
Density (g/cm3)
TiO2 / Fe2O3
% TiO2
% Fe2O3
Distance along the core (m)

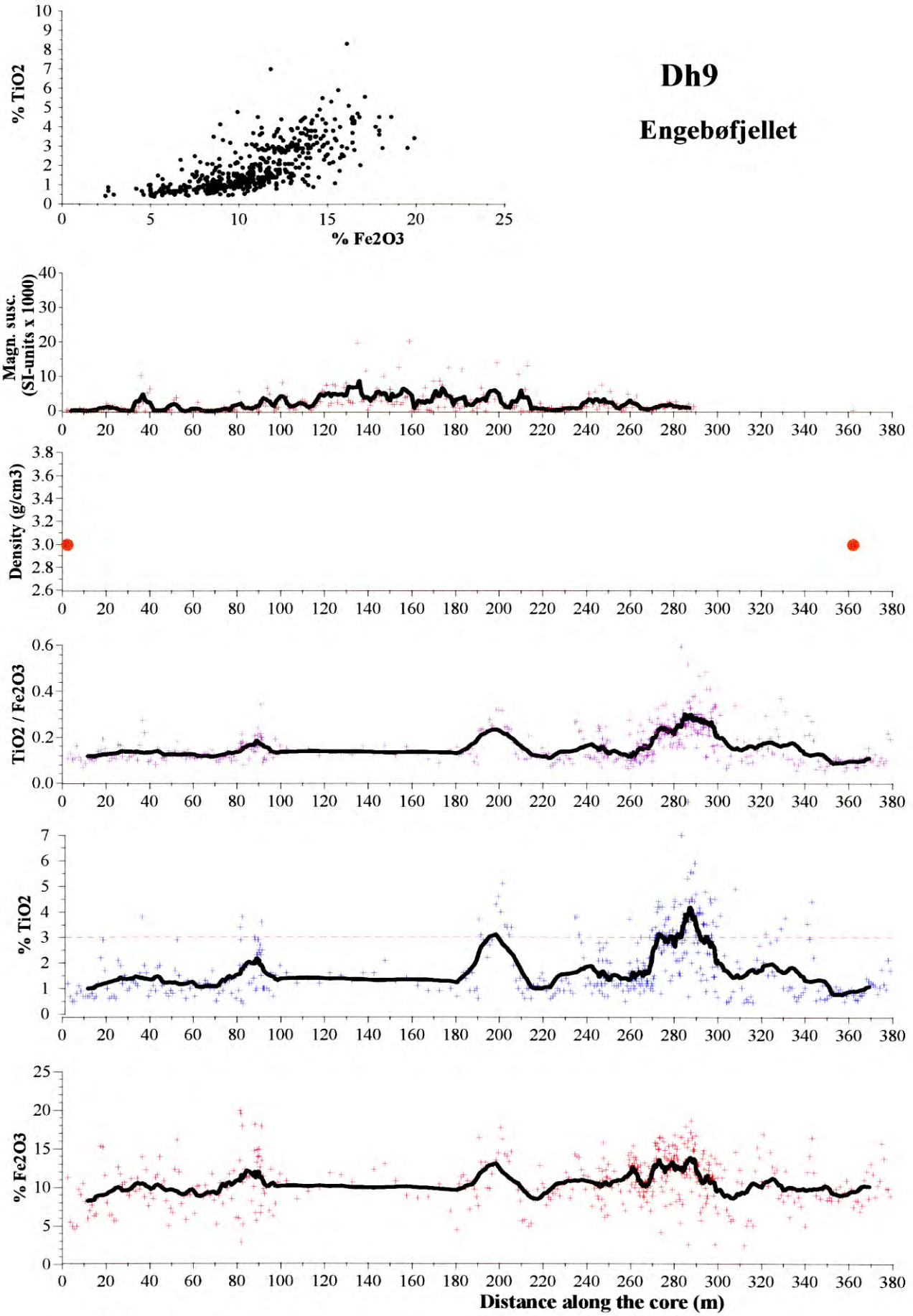
Dh9
Engebøfjellet
% TiO2
% Fe2O3
Magn. susc. (SI-units x 1000)
Density (g/cm3)
TiO2 / Fe2O3
% TiO2
% Fe2O3
Distance along the core (m)

dhmutil.grf

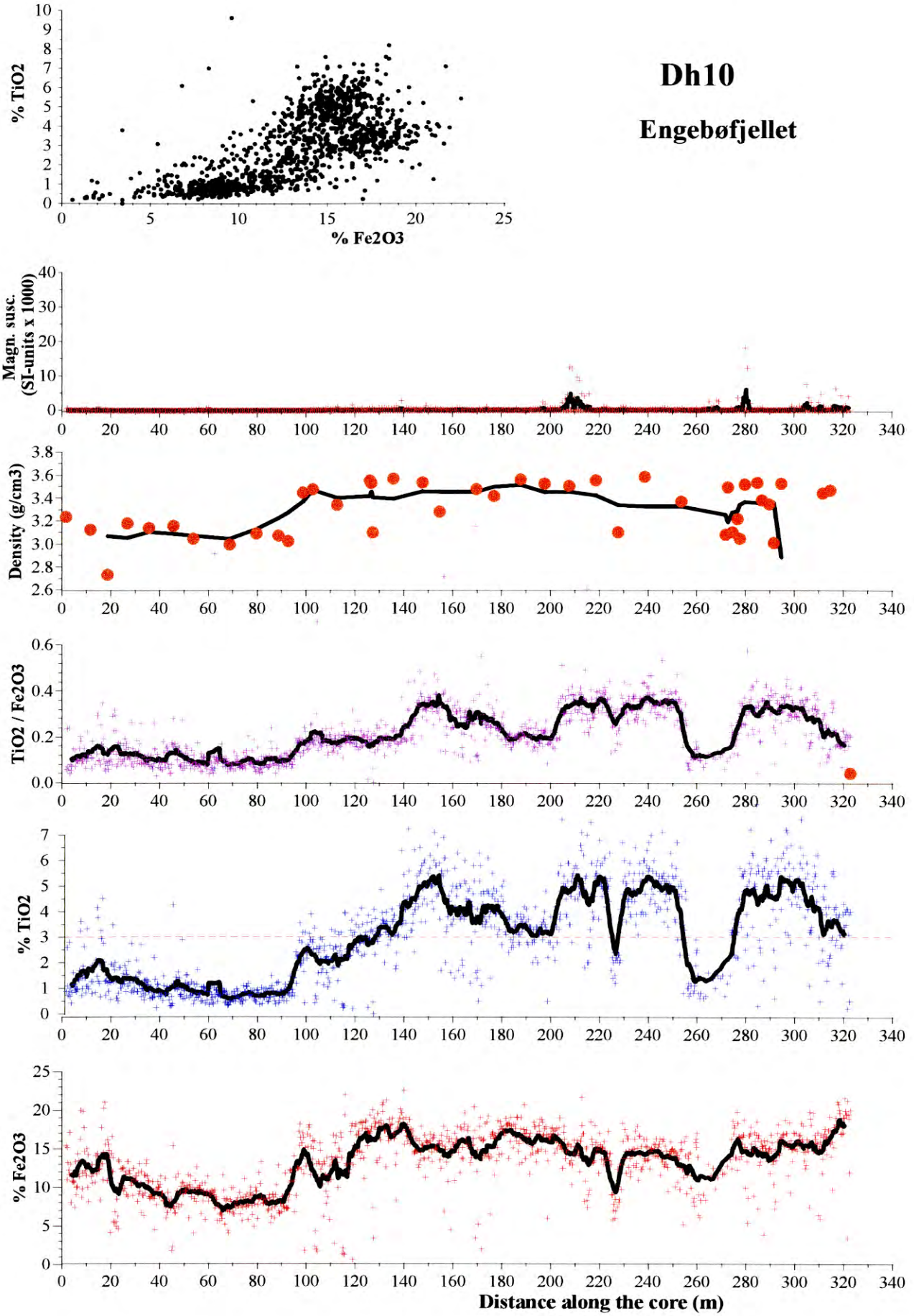
Dh10
Engebøfjellet
% TiO2
% Fe2O3
Magn. susc. (SI-units x 1000)
Density (g/cm3)
TiO2 / Fe2O3
% TiO2
% Fe2O3
Distance along the core (m)

Appendix 2: Petrophysical data, core-samples, Engebøfjellet

Dh	Sample	Rock	Retro-gression	Sp. gravity (g/cm3)	Magnetic susceptibility	Rema-nence	TiO2 (n=3)	Fe2O3 (n=3)
1	1/019.9	amphibolite	minor	2.805	0.00163	96.83	3.40	15.60
1	1/022.9	amphibolite	significant	2.932	0.01077	385.83	0.90	7.20
1	1/025.9	amphibolite	minor	2.809	0.00102	14.48	0.70	6.80
1	1/029.9	amphibolite	minor	3.043	0.00164	33.57	0.70	6.60
1	1/033.9	amphibolite	minor	2.813	0.00182	86.66	0.70	9.40
1	1/035.9	amphibolite	minor	2.850	0.00244	46.45	0.70	6.70
1	1/037.9	amphibolite	distinct	2.976	0.00386	223.18	0.90	7.90
1	1/042.9	amphibolite	minor	2.804	0.00095	40.12	1.40	10.90
1	1/046.9	amphibolite	minor	2.876	0.00121	22.45	0.40	4.20
1	1/049.9	amphibolite	distinct	2.883	0.00554	97.72	0.50	7.60
1	1/050.9	amphibolite	minor	2.923	0.00119	24.04	0.70	9.40
1	1/058.9	amphibolite	minor	2.817	0.00061	15.29	1.20	10.40
1	1/060.9	amphibolite	significant	2.985	0.01406	254.15	0.30	3.10
1	1/062.9	leucog. ecl.	distinct	3.128	0.00863	68.60	1.20	8.10
1	1/064.9	leucog. ecl.	significant	3.409	0.02119	312.91	1.60	15.30
1	1/066.9	leucog. ecl.	minor	3.399	0.00293	46.71	1.40	13.20
1	1/069.9	ferrog. ecl.	significant	3.391	0.02128	697.34	4.80	17.80
1	1/071.9	ferrog. ecl.	significant	3.443	0.01161	275.25	5.00	15.00
1	1/075.9	leucog. ecl.	distinct	3.358	0.00365	76.71	1.70	13.10
1	1/078.9	leucog. ecl.	significant	3.383	0.01423	397.14	2.40	12.70
1	1/08.9	amphibolite	minor	2.930	0.00113	77.00	0.70	6.60
1	1/080.9	ferrog. ecl.	minor	3.535	0.00146	27.95	3.00	14.80
1	1/084.9	leucog. ecl.	minor	3.525	0.00164	53.43	2.50	16.20
1	1/087.9	ferrog. ecl.	minor	3.481	0.00122	28.72	3.10	13.90
1	1/090.9	leucog. ecl.	minor	3.427	0.00122	19.88	2.20	12.70
1	1/092.9	ferrog. ecl.	minor	3.456	0.00142	14.08	4.20	13.40
1	1/096.9	ferrog. ecl.	significant	3.371	0.01228	569.19	3.80	15.00
1	1/099.9	ferrog. ecl.	distinct	3.426	0.00681	28.38	4.10	15.60
1	1/10.9	amphibolite	significant	2.877	0.01490	160.61	0.90	9.00
1	1/10.9	amphibolite	significant	2.877	0.01490	160.61	0.90	10.10
1	1/100.9	ferrog. ecl.	minor	3.347	0.00121	0.00	4.10	15.30
1	1/103.9	ferrog. ecl.	significant	3.197	0.01512	60.88	4.40	16.00
1	1/108.9	ferrog. ecl.	significant	3.341	0.01225	193.03	3.80	14.80
1	1/11.9	amphibolite	minor	3.091	0.00204	119.93	1.30	8.30
1	1/111.9	ferrog. ecl.	significant	3.292	0.02481	439.22	3.50	16.50
1	1/113.9	leucog. ecl.	significant	3.187	0.01592	121.35	2.80	14.90
1	1/119.8	leucog. ecl.	significant	3.377	0.01539	299.27	1.30	13.00
1	1/121.9	ferrog. ecl.	significant	3.341	0.02503	337.12	3.80	16.80
1	1/124.9	amphibolite	significant	3.138	0.01984	457.13		
1	1/125.9	ferrog. ecl.	distinct	3.445	0.00847	157.09		
1	1/127.9	leucog. ecl.	significant	3.368	0.01785	197.24	2.30	8.70
1	1/130.1	ferrog. ecl.	distinct	3.509	0.00908	144.40	4.30	15.70
1	1/133.1	ferrog. ecl.	significant	3.347	0.02406	374.80	4.10	17.10
1	1/135.1	leucog. ecl.	significant	3.444	0.02405	425.30	2.80	18.20
1	1/136.1	ferrog. ecl.	significant	3.423	0.01413	248.02	3.50	19.00
1	1/139.1	leucog. ecl.	significant	3.359	0.04535	1073.85	2.50	20.70
1	1/140.9	leucog. ecl.	distinct	3.362	0.00335	119.82	2.50	16.20
1	1/142.9	leucog. ecl.	significant	3.293	0.01560	212.56	1.90	14.90
1	1/144.9	leucog. ecl.	significant	3.303	0.04003	778.40	1.80	14.70
1	1/146.9	leucog. ecl.	significant	3.347	0.02190	221.56	2.50	20.20
1	1/149.9	ferrog. ecl.	significant	3.549	0.03523	630.75	3.80	21.40
1	1/150.9	ferrog. ecl.	significant	2.837	0.01194	37.91	3.90	19.90
1	1/152.9	amphibolite	significant	3.092	0.01269	155.41	1.70	8.20
1	1/154.9	amphibolite	significant	2.879	0.01391	390.70	1.40	12.70
1	1/157.9	amphibolite	minor	2.877	0.00121	19.65	1.40	14.00
1	1/158.9	amphibolite	minor	2.871	0.00127	22.75	1.30	10.20
1	1/160.9	amphibolite	distinct	3.034	0.00853	124.34	1.00	9.40
1	1/163.9	amphibolite	minor	2.891	0.00294	56.51	1.60	12.70
1	1/164.9	amphibolite	significant	3.042	0.01899	277.82	1.00	8.70
1	1/165.7	amph. eclogite	minor	3.121	0.00722	79.27	2.10	11.20
1	1/166.9	amphibolite	distinct	2.905	0.00324	47.01	1.80	12.20
1	1/168.1	amphibolite	distinct	2.831	0.00394	160.93	0.70	10.20
1	1/169.9	amphibolite	distinct	2.828	0.00491	57.47	0.70	6.40
1	1/170.0	amphibolite	minor	2.824	0.00061	20.38	0.70	6.80
1	1/172.0	amphibolite	minor	2.953	0.00075	0.00	0.60	4.20

Db	Sample	Rock	Retro-gression	Sp. gravity (g/cm3)	Magnetic susceptibility	Rema-nence	TiO2 (n=3)	Fe2O3 (n=3)
1	1/173.0	amphibolite	minor	2.777	0.00013	20.74	1.00	11.60
1	1/174.1	amphibolite	minor	2.945	0.00071	0.00	0.60	3.40
1	1/175.0	gneiss/amph.		2.811	0.00058	17.44	1.00	9.20
1	1/177.1	gneiss/amph.		2.859	0.00724	31.41	0.40	1.20
1	1/178.1	gneiss/amph.		2.748	0.00207	31.95	0.90	8.00
1	1/180.9	gneiss/amph.		2.891	0.00943	0.00	0.20	4.20
2	2/003.0	leucog. ecl.	minor	3.396	0.00106	20.35	0.60	3.80
2	2/009.9	amphibolite	minor	2.872	0.00187	17.55	1.40	10.70
2	2/018.1	leucog. ecl.	minor	3.472	0.00280	65.78	0.60	6.20
2	2/019.1	ferrog. ecl.	distinct	3.481	0.00332	175.55	4.10	15.30
2	2/021.3	ferrog. ecl.	distinct	3.555	0.00338	127.46	3.60	14.10
2	2/026.0	leucog. ecl.	minor	3.598	0.00210	46.42	0.40	2.70
2	2/032.0	amph. eclogite	minor	3.261	0.00163	20.00	4.10	16.20
2	2/034.9	amphibolite	minor	2.804	0.00051	167.60	1.90	14.50
2	2/038.0	amphibolite	significant	2.998	0.01030	15.71	1.00	6.80
2	2/047.6	amphibolite	minor	2.719	0.00054	0.00	3.60	16.00
2	2/057.0	gneiss/amph.		2.721	0.00037	23.23	1.30	10.70
2	2/077.0	gneiss/amph.		2.819	0.00043	0.00	0.30	3.70
2	2/091.0	amph. eclogite	minor	3.152	0.00141	35.14	0.80	5.70
2	2/098.0	amph. eclogite	minor	3.230	0.00229	86.42	1.50	12.20
2	2/109.4	amphibolite	minor	2.850	0.00157	12.08	2.20	13.80
2	2/115.0	leucog. ecl.	minor	3.538	0.00205	66.00	1.00	9.70
2	2/119.0	ferrog. ecl.	minor	3.527	0.00298	90.10	4.60	13.60
2	2/123.8	ferrog. ecl.	minor	3.406	0.00198	68.52	3.40	15.90
2	2/128.0	leucog. ecl.	minor	3.568	0.00198	22.99	2.60	14.10
2	2/134.9	leucog. ecl.	significant	3.473	0.02187	774.38	2.70	15.90
2	2/139.5	leucog. ecl.	significant	3.475	0.01839	604.27	2.60	16.00
2	2/142.2	ferrog. ecl.	distinct	3.549	0.00447	138.01	3.30	16.80
2	2/142.3	ferrog. ecl.	distinct	3.626	0.00729	167.03	3.10	17.30
2	2/149.9	ferrog. ecl.	minor	3.545	0.00235	101.91	4.30	18.90
2	2/152.0	ferrog. ecl.	minor	3.423	0.00293	105.41	3.60	15.70
2	2/159.2	ferrog. ecl.	distinct	3.576	0.00329	99.62	3.20	17.10
2	2/164.2	ferrog. ecl.	distinct	3.533	0.00598	435.20	4.10	17.00
2	2/169.0	ferrog. ecl.	minor	3.533	0.00190	25.40	4.90	16.60
2	2/171.9	ferrog. ecl.	distinct	3.366	0.00410	140.53	5.00	15.60
2	2/175.0	ferrog. ecl.	minor	3.511	0.00213	39.88	4.00	14.50
2	2/176.0	ferrog. ecl.	minor	3.549	0.00255	101.22	4.80	15.40
2	2/184.0	ferrog. ecl.	distinct	3.497	0.00935	141.95	5.30	16.10
2	2/189.9	ferrog. ecl.	distinct	3.574	0.00328	97.24	5.50	15.20
2	2/192.0	ferrog. ecl.	minor	3.223	0.00127	17.00	5.10	15.70
2	2/198.9	leucog. ecl.	significant	3.372	0.03643	1196.16	1.70	14.40
2	2/203.0	ferrog. ecl.	significant	3.440	0.01002	225.65	3.80	15.40
2	2/209.9	ferrog. ecl.	distinct	3.530	0.00513	108.86	3.50	16.90
2	2/212.0	leucog. ecl.	significant	3.477	0.01857	509.90	2.60	16.50
2	2/216.6	ferrog. ecl.	significant	3.532	0.01560	428.02	3.40	17.10
2	2/222.0	leucog. ecl.	significant	3.443	0.01107	786.78	2.60	17.60
2	2/226.0	leucog. ecl.	minor	2.976	0.00087	20.79	2.40	16.00
2	2/227.0	leucog. ecl.	minor	3.243	0.00256	71.59	1.00	10.50
2	2/229.8	leucog. ecl.	distinct	3.522	0.00694	173.31	2.40	11.80
2	2/229.9	leucog. ecl.	minor	2.904	0.00094	0.00	2.80	19.90
2	2/231.0	leucog. ecl.	minor	3.330	0.00227	35.53	0.80	9.90
2	2/233.2	leucog. ecl.	minor	2.786	0.00024	22.38	1.80	13.20
2	2/239.4	leucog. ecl.	significant	3.333	0.05035	1139.28	0.40	6.90
2	2/242.9	leucog. ecl.	significant	3.243	0.03066	1424.65	2.20	17.20
2	2/256.0	amphibolite	minor	2.970	0.00079	0.00	1.20	14.00
2	2/263.0	gneiss/amph.ecl.		3.026	0.00682	144.55	0.60	9.20
2	2/275.0	gneiss/amph.ecl.		2.944	0.00887	205.11	1.60	9.30
2	2/289.0	gneiss/amph.ecl.		2.938	0.00270	58.50	1.40	13.20
2	2/291.0	gneiss/amph.ecl.		2.928	0.00206	33.49	1.10	9.70
2	2/293.0	gneiss/amph.ecl.		2.799	0.01978	199.62	0.60	8.10
2	2/307.0	amphibolite	minor	2.995	0.00239	28.62	0.90	10.10
2	2/314.0	amphibolite	minor	2.881	0.00045	0.00	1.20	9.60
3	3/015.6	leucog. ecl.	minor	3.110	0.00057	0.00	1.00	9.90
3	3/029.0	leucog. ecl.	minor	2.929	0.00046	10.20	1.20	13.50
3	3/03.0	leucog. ecl.	minor	3.021	0.00054	0.00	0.50	8.00
3	3/039.0	leucog. ecl.	minor	3.128	0.00056	0.00	0.70	9.70
3	3/041.0	leucog. ecl.	minor	3.153	0.00064	0.00	0.90	10.90
3	3/05.0	amphibolite	minor	3.128	0.00044	34.24		
3	3/058.0	leucog. ecl.	minor	3.118	0.00071	11.39	0.90	11.70
3	3/061.0	leucog. ecl.	minor	3.090	0.00080	69.65	1.10	10.60

Db	Sample	Rock	Retro-gression	Sp. gravity (g/cm3)	Magnetic susceptibility	Rema-nence	TiO2 (n=3)	Fe2O3 (n=3)
3	3/065.0	leucog. ecl.	minor	3.102	0.00061	0.00	0.80	10.40
3	3/075.9	gneiss	variable	2.716	0.00002	14.49	0.10	1.00
3	3/079.1	gneiss		2.739	0.00009	11.38	0.20	1.30
3	3/081.1	gneiss		2.700	0.00009	25.58	0.20	1.20
3	3/086.0	gneiss		2.712	0.00005	0.00	0.40	1.00
3	3/098.9	amphibolite	minor	2.956	0.00053	23.50	0.80	9.20
3	3/107.9	amphibolite	minor	3.085	0.00063	30.22	1.10	11.90
3	3/11.0	leucog. ecl.	minor	3.129	0.00055	12.87	0.80	13.00
3	3/118.9	amph. eclogite	minor	3.095	0.00220	40.82	2.40	15.10
3	3/125.9	amph. eclogite	minor	3.284	0.00192	44.62	2.20	12.60
3	3/129.9	ferrog. ecl.	minor	3.454	0.00171	127.37	3.90	16.60
3	3/132.5	leucog. ecl.	minor	3.501	0.00112	32.82	2.90	16.00
3	3/138.9	ferrog. ecl.	minor	3.521	0.00104	43.34	3.50	17.20
3	3/141.8	ferrog. ecl.	minor	3.208	0.00252	96.56	3.20	16.20
3	3/146.0	leucog. ecl.	minor	3.381	0.00167	90.38	2.20	15.60
3	3/150.1	ferrog. ecl.	minor	3.613	0.00120	187.37	3.70	19.60
3	3/157.8	ferrog. ecl.	minor	3.616	0.00219	70.70	6.20	17.40
3	3/164.5	ferrog. ecl.	minor	3.591	0.00229	126.41	7.47	16.94
3	3/164.5	ferrog. ecl.	minor	3.591	0.00229	126.41	7.47	16.94
3	3/173.9	ferrog. ecl.	minor	3.437	0.00121	27.62	3.92	16.97
3	3/182.0	ferrog. ecl.	minor	3.539	0.00138	37.22	3.86	16.36
3	3/194.5	ferrog. ecl.	minor	3.370	0.00190	89.55	4.24	15.45
3	3/202.9	ferrog. ecl.	distinct	3.434	0.00764	352.56	4.83	17.28
3	3/204.0	ferrog. ecl.	distinct	3.523	0.00477	266.55	5.26	16.46
3	3/5.9	leucog. ecl.	minor	3.128	0.00044	34.24	1.00	11.90
4	4/016.9	ferrog. ecl.	minor	3.425	0.00149	43.65	3.70	16.20
4	4/024.1	ferrog. ecl.	minor	3.211	0.00167	48.27	3.20	16.60
4	4/026.9	leucog. ecl.	significant	3.201	0.02576	164.18	1.50	12.90
4	4/030.0	leucog. ecl.	minor	3.185	0.00157	74.07	1.60	9.00
4	4/035.9	leucog. ecl.	minor	3.346	0.00140	71.54	2.70	15.60
4	4/037.9	ferrog. ecl.	significant	3.300	0.02296	739.56	3.50	17.40
4	4/044.1	ferrog. ecl.	minor	3.480	0.00121	24.75	3.40	17.70
4	4/054.0	leucog. ecl.	minor	3.438	0.00094	24.99	2.80	15.70
4	4/059.8	ferrog. ecl.	minor	3.597	0.00148	24.57	3.70	19.30
4	4/064.9	ferrog. ecl.	distinct	3.153	0.00676	98.41	3.10	17.20
4	4/069.7	ferrog. ecl.	minor	3.533	0.00190	55.56	6.10	17.30
4	4/069.9	ferrog. ecl.	minor	3.267	0.00109	31.50	5.00	16.70
4	4/070.8	ferrog. ecl.	minor	3.463	0.00122	24.51	5.70	18.20
4	4/073.8	ferrog. ecl.	distinct	3.694	0.00335	81.38	5.80	15.90
4	4/074.9	leucog. ecl.	minor	3.220	0.00085	37.01	2.50	15.60
4	4/079,9	ferrog. ecl.	distinct	3.775	0.00378	0.00	4.70	27.40
4	4/09.9	ferrog. ecl.	minor	3.477	0.00123	42.45	3.70	17.90
4	4/093.7	ferrog. ecl.	distinct	3.503	0.00427	227.42		
4	4/093.8	ferrog. ecl.	minor	3.578	0.00252	36.54	5.30	16.20
4	4/096.1	ferrog. ecl.	significant	3.184	0.01574	44.30	5.20	17.80
4	4/098.1	ferrog. ecl.	minor	3.496	0.00230	51.61	4.60	14.10
4	4/098.9	ferrog. ecl.	minor	3.493	0.00178	26.81	4.20	15.50
4	4/110.4	ferrog. ecl.	minor	3.569	0.00112	0.00	4.00	17.10
4	4/113.9	ferrog. ecl.	significant	3.437	0.01195	271.68	4.80	16.20
4	4/118.4	leucog. ecl.	minor	3.187	0.00094	21.32	1.70	14.00
4	4/125.2	ferrog. ecl.	minor	3.405	0.00212	25.48	3.50	16.60
4	4/130.8	ferrog. ecl.	distinct	3.537	0.00576	188.43	5.50	20.00
4	4/134.0	leucog. ecl.	distinct	3.148	0.00440	75.22	2.70	14.40
4	4/137.7	leucog. ecl.	significant	2.968	0.14264	5687.70	2.50	18.70
4	4/137.9	ferrog. ecl.	significant	3.183	0.01104	1833.23	3.20	24.70
4	4/140.9	ferrog. ecl.	significant	3.437	0.01397	653.77	4.30	18.00
4	4/143.1	ferrog. ecl.	significant	3.428	0.01555	414.09	4.50	17.40
4	4/151.9	ferrog. ecl.	distinct	3.314	0.00805	441.61	4.10	15.20
4	4/159.7	leucog. ecl.	distinct	3.268	0.00654	267.61	2.80	17.00
4	4/2.1	leucog. ecl.	minor	2.971	0.00000	34.08	1.00	5.60
5	5/001.9	ferrog. ecl.	minor	3.366	0.00081	34.64	2.70	13.80
5	5/007.9	ferrog. ecl.	minor	3.379	0.00085	29.46	2.30	14.10
5	5/008.8	ferrog. ecl.	minor	3.373	0.00087	37.22	1.90	15.40
5	5/013.7	ferrog. ecl.	minor	3.435	0.00101	44.07	2.80	13.90
5	5/019.8	ferrog. ecl.	minor	3.459	0.00119	33.35	2.90	16.10
5	5/021.1	ferrog. ecl.	minor	3.534	0.00101	30.03	2.50	15.60
5	5/025.3	ferrog. ecl.	minor	3.484	0.00191	47.72	3.60	24.70
5	5/032.9	ferrog. ecl.	minor	3.329	0.00140	21.10	2.40	14.90
5	5/038.5	ferrog. ecl.	minor	3.485	0.00150	38.12	2.80	16.40
5	5/041.7	ferrog. ecl.	minor	3.362	0.00099	0.00	3.10	16.90

Dh	Sample	Rock	Retro-gression	Sp. gravity (g/cm3)	Magnetic susceptibility	Rema-nence	TiO2 (n=3)	Fe2O3 (n=3)
5	5/043.3	ferrog. ecl.	minor	3.561	0.00220	56.32	3.30	19.00
5	5/045.9	ferrog. ecl.	distinct	3.392	0.00650	86.76	2.60	16.50
5	5/050.2	ferrog. ecl.	distinct	3.555	0.00319	35.89	4.00	21.50
5	5/054.9	ferrog. ecl.	minor	3.502	0.00213	68.99	3.30	15.30
5	5/057.4	ferrog. ecl.	minor	3.485	0.00101	23.92	3.00	16.30
5	5/063.0	ferrog. ecl.	distinct	3.528	0.00699	168.14	4.10	20.50
5	5/068.7	ferrog. ecl.	minor	3.478	0.00104	0.00	2.70	15.00
5	5/070.9	ferrog. ecl.	minor	3.651	0.00170	0.00	4.10	20.40
5	5/074.2	ferrog. ecl.	significant	3.376	0.02854	795.65	3.60	21.10
5	5/076.2	ferrog. ecl.	minor	3.560	0.00237	49.38	4.00	21.30
5	5/080.8	ferrog. ecl.	distinct	3.426	0.00326	25.71	3.20	21.90
5	5/088.2	ferrog. ecl.	minor	3.330	0.00099	24.10	2.80	12.90
5	5/094.2	ferrog. ecl.	minor	2.863	0.00045	19.72	0.80	6.60
5	5/099.9	ferrog. ecl.	distinct	3.542	0.00602	233.62	4.50	19.10
5	5/106.9	ferrog. ecl.	minor	2.830	0.00016	0.00	0.40	2.90
5	5/108.5	ferrog. ecl.	distinct	3.603	0.00484	241.67	3.80	19.90
5	5/110.7	ferrog. ecl.	distinct	3.489	0.00306	54.42	3.50	18.30
5	5/121.4	ferrog. ecl.	minor	3.584	0.00180	66.30	4.30	19.30
5	5/131.0	ferrog. ecl.	minor	3.510	0.00123	0.00	5.20	17.20
5	5/139.4	ferrog. ecl.	minor	3.585	0.00118	23.98	5.80	16.90
5	5/141.4	ferrog. ecl.	minor	3.629	0.00139	39.84	6.20	17.80
5	5/147.8	ferrog. ecl.	minor	3.554	0.00199	76.94	5.50	17.10
5	5/152.5	ferrog. ecl.	minor	3.295	0.00275	107.14	4.30	15.40
5	5/158.5	ferrog. ecl.	minor	3.590	0.00131	25.25	5.70	16.70
6	6/002.0	ferrog. ecl.	distinct	3.394	0.00457	306.47	4.65	16.38
6	6/007.0	ferrog. ecl.	minor	3.392	0.00113	34.37	3.84	17.55
6	6/011.0	leucog. ecl.	minor	3.128	0.00056	41.14	1.11	12.22
6	6/016.0	leucog. ecl.	minor	3.104	0.00058	47.29	0.83	11.62
6	6/023.0	leucog. ecl.	minor	3.063	0.00057	167.21	0.79	11.21
6	6/028.0	leucog. ecl.	minor	3.111	0.00059	0.00	1.15	11.92
6	6/031.2	leucog. ecl.	minor	3.475	0.00092	18.48	2.11	16.91
6	6/036.0	leucog. ecl.	minor	3.352	0.00084	0.00	2.11	15.12
6	6/042.2	leucog. ecl.	minor	3.490	0.00118	37.74	2.61	16.93
6	6/045.1	leucog. ecl.	minor	3.340	0.00100	0.00	2.05	12.01
6	6/046.1	ferrog. ecl.	minor	3.384	0.00123	42.59	4.67	16.96
6	6/049.0	ferrog. ecl.	minor	3.477	0.00177	33.28	5.12	16.91
6	6/052.0	ferrog. ecl.	minor	3.465	0.00167	74.65	4.76	18.76
6	6/055.0	ferrog. ecl.	minor	3.363	0.00289	110.96	4.13	18.69
6	6/061.0	ferrog. ecl.	minor	3.588	0.00103	29.40	4.45	16.81
6	6/065.0	leucog. ecl.	minor	3.264	0.00089	24.04	1.58	15.02
6	6/067.0	leucog. ecl.	minor	3.371	0.00076	0.00	1.82	15.93
6	6/071.0	leucog. ecl.	minor	3.319	0.00078	18.05	2.00	16.23
6	6/072.9	leucog. ecl.	minor	3.365	0.00084	30.41	1.83	16.25
6	6/083.0	ferrog. ecl.	minor	3.474	0.00096	20.45	3.46	15.89
6	6/087.9	ferrog. ecl.	minor	3.476	0.00105	0.00	4.23	15.45
6	6/094.0	ferrog. ecl.	minor	3.503	0.00107	0.00	4.81	16.00
6	6/097.2	leucog. ecl.	minor	2.851	0.00017	21.51	0.32	2.42
6	6/099.0	ferrog. ecl.	minor	3.523	0.00118	0.00	4.51	17.12
6	6/100.3	leucog. ecl.	minor	3.309	0.00096	0.00	2.47	13.22
6	6/104.9	ferrog. ecl.	minor	3.466	0.00112	0.00	4.48	16.82
6	6/110.0	ferrog. ecl.	minor	3.508	0.00107	28.63	4.40	16.06
6	6/115.0	ferrog. ecl.	minor	3.615	0.00143	19.92	7.42	20.59
6	6/120.9	ferrog. ecl.	minor	3.436	0.00105	0.00	3.83	15.94
6	6/125.0	leucog. ecl.	minor	3.345	0.00082	0.00	1.73	14.45
7	7/005.0	ferrog. ecl.	distinct	3.563	0.00513	306.72	6.49	19.16
7	7/012.0	ferrog. ecl.	distinct	3.575	0.00418	180.03	5.72	17.91
7	7/017.0	ferrog. ecl.	minor	3.619	0.00149	45.25	4.56	18.86
7	7/023.0	ferrog. ecl.	distinct	3.492	0.00618	324.25	5.77	17.72
7	7/032.0	ferrog. ecl.	distinct	3.503	0.00610	101.30	5.61	17.27
7	7/038.0	ferrog. ecl.	minor	3.569	0.00236	38.08	6.01	16.50
7	7/043.0	ferrog. ecl.	minor	3.570	0.00231	74.39	6.04	16.76
7	7/050.0	ferrog. ecl.	distinct	3.764	0.00401	154.58	6.66	20.09
7	7/054.0	ferrog. ecl.	distinct	3.570	0.00311	116.79	6.12	21.00
7	7/062.0	ferrog. ecl.	distinct	3.043	0.00333	23.85	0.88	9.16
7	7/068.0	ferrog. ecl.	distinct	3.560	0.00636	247.53	6.50	17.46
7	7/070.1	gneiss		2.742	0.00007	26.25	0.14	1.37
7	7/074.0	ferrog. ecl.	distinct	3.445	0.00777	295.76	6.53	17.59
7	7/081.0	ferrog. ecl.	minor	3.461	0.00181	55.17	3.21	16.74
7	7/084.2	ferrog. ecl.	significant	3.527	0.01641	620.96	4.41	22.58
7	7/090.0	ferrog. ecl.	distinct	3.125	0.00789	305.45	4.46	12.31

Dh	Sample	Rock	Retro-gression	Sp. gravity (g/cm3)	Magnetic susceptibility	Rema-nence	TiO2 (n=3)	Fe2O3 (n=3)
7	7/095.0	ferrog. ecl.	minor	3.637	0.00144	26.14	6.62	17.61
7	7/107.0	ferrog. ecl.	distinct	3.582	0.00551	66.39	6.52	17.17
7	7/111.0	ferrog. ecl.	distinct	3.491	0.00426	117.17	5.82	16.51
7	7/121.0	ferrog. ecl.	minor	3.499	0.00191	31.71	3.06	16.02
7	7/123.0	ferrog. ecl.	minor	3.296	0.00103	0.00	2.39	16.30
7	7/128.0	leucog. ecl.	minor	3.307	0.00094	0.00	1.90	16.46
7	7/132.0	leucog. ecl.	minor	3.197	0.00082	0.00	1.14	14.14
7	7/139.1	ferrog. ecl.	distinct	3.470	0.00354	91.28	4.76	17.66
7	7/142.0	ferrog. ecl.	minor	3.772	0.00248	52.49	6.33	24.16
7	7/148.0	ferrog. ecl.	minor	3.629	0.00185	27.62	4.17	20.23
7	7/151.0	ferrog. ecl.	minor	3.123	0.00070	22.78	1.43	13.11
7	7/156.0	ferrog. ecl.	minor	3.433	0.00171	51.88	5.64	16.67
7	7/161.0	leucog. ecl.	minor	3.096	0.00071	0.00	1.50	12.52
7	7/166.0	ferrog. ecl.	distinct	3.584	0.00730	382.09	5.49	23.42
7	7/171.0	leucog. ecl.	distinct	3.355	0.00728	250.00	2.21	16.03
7	7/177.0	leucog. ecl.	minor	3.347	0.00081	26.74	1.25	12.07
7	7/181.0	leucog. ecl.	minor	3.436	0.00189	39.36	2.68	15.06
7	7/182.0	leucog. ecl.	minor	2.900	0.00061	44.07	1.05	11.67
7	7/185.0	ferrog. ecl.	distinct	3.351	0.00716	241.67	4.48	19.27
7	7/189.0	ferrog. ecl.	significant	3.264	0.01232	357.19	4.29	16.51
7	7/191.0	ferrog. ecl.	distinct	3.237	0.00597	334.82	5.01	17.14
7	7/195.0	ferrog. ecl.	distinct	3.309	0.00375	109.08	4.26	16.80
7	7/199.0	ferrog. ecl.	minor	3.518	0.00178	32.29	6.56	14.60
7	7/202.0	ferrog. ecl.	minor	3.620	0.00225	64.38	9.16	17.62
7	7/206.0	ferrog. ecl.	minor	3.603	0.00192	0.00	6.14	18.15
7	7/209.0	ferrog. ecl.	distinct	3.208	0.00426	83.17	6.00	15.81
7	7/211.0	ferrog. ecl.	minor	3.198	0.00277	62.99	5.76	15.52
8	8/074.0	ferrog. ecl.	minor	3.577	0.00128	24.70	3.02	19.06
8	8/086.0	leucog. ecl.	minor	3.481	0.00145	32.44	3.53	18.49
8	8/094.0	ferrog. ecl.	minor	3.532	0.00146	51.79	5.43	16.34
8	8/095.0	ferrog. ecl.	distinct	3.260	0.00353	66.71	5.71	17.69
8	8/106.0	ferrog. ecl.	distinct	3.562	0.00521	135.02	6.16	18.22
8	8/113.0	leucog. ecl.	minor	3.557	0.00199	33.28	3.18	18.95
8	8/126.0	ferrog. ecl.	distinct	3.550	0.00354	122.39	6.38	19.82
8	8/132.0	ferrog. ecl.	significant	3.459	0.01649	979.83	4.62	18.11
8	8/144.2	leucog. ecl.	minor	3.155	0.00098	20.49	0.61	14.48
8	8/154.0	leucog. ecl.	distinct	3.065	0.00851	542.28	0.85	15.45
8	8/158.0	leucog. ecl.	minor	3.058	0.00069	0.00	1.03	14.57
8	8/163.0	leucog. ecl.	minor	3.147	0.00068	0.00	0.52	11.23
8	8/169.0	leucog. ecl.	significant	3.264	0.04849	961.50	3.14	18.94
8	8/170.0	leucog. ecl.	significant	3.198	0.02807	226.07	2.10	17.21
8	8/170.9	leucog. ecl.	significant	3.213	0.01567	395.86	1.74	17.34
8	8/180.0	leucog. ecl.	significant	3.234	0.02419	775.33	2.61	17.31
8	8/186.0	leucog. ecl.	minor	3.065	0.00171	73.07	2.57	17.79
8	8/188.0	leucog. ecl.	significant	3.239	0.02900	1099.23	3.34	18.36
8	8/190.0	leucog. ecl.	significant	3.354	0.01421	496.45	2.84	18.21
8	8/201.0	leucog. ecl.	distinct	3.251	0.00957	329.39	2.07	16.52
8	8/211.0	leucog. ecl.	distinct	3.426	0.00678	435.19	3.29	20.93
8	8/218.0	leucog. ecl.	minor	2.955	0.00281	27.55	1.27	13.13
8	8/229.0	ferrog. ecl.	significant	3.468	0.02597	1242.23	4.95	22.26
8	8/234.0	leucog. ecl.	distinct	3.282	0.00641	272.72	3.34	16.43
8	8/237.0	ferrog. ecl.	minor	3.503	0.00281	70.60	5.42	18.24
8	8/241.0	ferrog. ecl.	minor	3.205	0.00159	49.36	4.00	14.47
8	8/247.0	ferrog. ecl.	distinct	3.460	0.00686	210.43	5.37	17.88
8	8/257.0	amphibolite	distinct	3.131	0.00702	489.16	1.70	14.07
8	8/266.0	amphibolite	significant	2.995	0.02872	1135.76	0.97	12.72
8	8/276.0	amphibolite	minor	2.905	0.00049	0.00	1.72	11.39
8	8/282.0	amphibolite	minor	2.796	0.00059	46.19	0.68	5.56
8	8/293.0	amphibolite	minor	2.788	0.00040	36.45	0.60	4.60
8	8/295.0	leucog. ecl.	distinct	3.398	0.00428	113.42	3.09	20.29

Table 3: Major and trace element analyses of core samples

Anal. #	*Sample*	*Rock*	*SiO2*	*Al2O3*	*Fe2O3*	*TiO2*	*MgO*	*CaO*	*Na2O*	*K2O*	*MnO*	*P2O5*	*LOI*	*Sum*	*TiO2*	*% Rutile*	*Rut/TiO2*	*% S* (Leco SC-444)	*Y*	*Zr*	*Nb*
			xrf	*xrf*	*xrf*	*xrf*	*xrf*	*xrf*	*xrf*	*xrf*	*xrf*	*xrf*	*xrf*	*xrf*	*icp*	*calculated*			*xrf*	*xrf*	*xrf*
1	1/20-30	amph. unit	56.41	13.74	9.54	0.94	5.41	6.38	3.41	1.56	0.14	0.35	1.30	99.17	0.37	0.57	60.6 %		45	183	10
2	1/65-66	leucogab. ecl.	46.24	15.04	16.12	1.81	6.01	9.57	2.77	0.91	0.18	0.23	0.96	99.83	0.06	1.75	96.7 %	0.14	39	119	-5
3	1/101-103	ferrog. ecl.	45.65	13.47	17.60	3.49	4.70	9.40	2.57	0.52	0.23	1.54	0.12	99.29	0.16	3.33	95.4 %	0.13	48	82	8
4	1/126-127	ferrog. ecl.	45.26	13.00	17.95	3.71	4.65	9.55	2.37	0.56	0.23	1.75	0.38	99.42	0.25	3.46	93.3 %	0.14	49	83	-5
5	1/160-170	amph. unit	57.45	13.12	10.59	1.41	3.98	6.43	3.05	1.52	0.16	0.46	1.38	99.54	0.39	1.02	72.3 %		54	210	9
6	2/95-105	amph. unit	52.12	14.09	13.04	1.73	5.42	6.77	3.54	1.24	0.17	0.22	0.78	99.12	0.22	1.51	87.3 %		40	164	6
7	2/115-116	ferrog. ecl.	44.59	13.67	18.17	4.90	5.49	9.94	2.54	0.27	0.21	0.10	-0.01	99.89	0.15	4.75	96.9 %	0.15	23	77	-5
8	2/150-155	ferrog. ecl.	44.64	12.85	19.94	3.63	6.14	10.01	2.26	0.25	0.21	0.11	0.01	100.06	0.16	3.47	95.6 %	0.24	22	58	-5
9	2/165-170	ferrog. ecl.	44.56	13.15	18.02	5.05	5.22	9.76	2.30	0.40	0.21	0.15	0.01	98.83	0.09	4.96	98.3 %	0.18	26	79	-5
10	2/200-205	ferrog. ecl.	42.59	13.38	18.31	3.52	4.30	9.50	2.23	0.52	0.25	1.51	0.10	96.22	0.23	3.29	93.5 %	0.12	48	66	6
11	2/260-270	amph. unit	56.69	15.27	10.11	1.38	3.59	5.67	3.17	1.91	0.16	0.27	0.85	99.05	0.30	1.08	78.3 %		62	308	11
12	3/15-20	leucogab. ecl.	51.10	17.60	9.74	0.88	7.35	8.22	2.47	0.42	0.14	0.11	1.70	99.75	0.03	0.85	97.1 %	0.05	17	56	-5
13	3/60-65	leucogab. ecl.	51.03	18.42	9.54	0.83	6.93	8.48	2.79	0.56	0.14	0.11	1.69	100.51	0.03	0.80	96.5 %	0.35	15	41	-5
14	3/80-85	gneiss	82.77	8.77	1.23	0.17	0.68	1.47	1.28	1.35	0.01	0.02	0.98	98.75	0.01	0.16	94.5 %		18	561	-5
15	3/110-111	leucogab. ecl.	50.10	17.40	10.23	0.85	7.61	8.07	2.96	0.70	0.15	0.12	1.85	100.03	0.04	0.81	95.0 %	0.12	16	54	-5
16	3/135-136	leucogab. ecl.	47.77	16.93	13.95	2.02	4.57	10.19	2.64	0.31	0.13	0.08	0.52	99.10	0.03	1.99	98.4 %	0.15	11	44	-5
17	3/159-160	ferrog. ecl.	43.76	13.53	17.89	5.08	5.78	10.23	2.25	0.21	0.20	0.07	0.21	99.22	0.06	5.02	98.8 %	0.17	11	37	-5
18	4/36-40	leucogab. ecl.	45.05	15.22	17.67	2.59	5.96	9.88	2.72	0.27	0.18	0.06	0.17	99.77	0.14	2.45	94.6 %	0.20	17	26	-5
19	4/75-77	ferrog. ecl.	43.12	13.99	17.98	5.09	5.36	9.81	2.11	0.43	0.21	0.08	0.95	99.13	0.11	4.98	97.8 %	0.13	16	44	-5
20	4/97-98	ferrog. ecl.	44.68	13.37	17.28	4.44	5.85	10.35	2.26	0.13	0.21	0.08	0.18	98.82	0.06	4.38	98.6 %	0.19	19	37	-5
21	4/120-121	ferrog. ecl.	43.09	11.29	20.53	5.05	6.55	10.10	1.82	0.08	0.26	0.08	0.26	99.11	0.72	4.33	85.7 %	0.20	20	50	-5
22	4/130-131	ferrog. ecl.	44.01	11.78	19.73	4.46	6.22	9.87	2.13	0.18	0.25	0.09	0.22	98.95	0.16	4.30	96.4 %	0.31	20	48	6
23	4/106-108	ferrog. ecl.	46.37	13.49	16.13	2.99	5.96	10.27	2.25	0.22	0.22	0.08	0.84	98.83	0.07	2.92	97.8 %	0.18	18	38	-5
24	4/151-152	ferrog. ecl.	45.51	14.15	17.49	4.41	4.94	9.47	2.51	0.33	0.21	0.11	0.44	99.57	0.16	4.25	96.4 %	0.07	17	57	7

Sr	*Rb*	*Ba*	*Cu*	*Zn*	*Pb*	*Sc*	*V*	*Ni*	*Cr*	*Ga*	*Yb*	*Co*	*Ce*	*La*	*Nd*	*Y*	*La*	*Ce*	*Pr*	*Nd*	*Sm*	*Eu*	*Gd*	*Tb*	*Dy*	*Ho*	*Er*	*Tm*	*Yb*	*Lu*
xrf	*xrf*	*xrf*	*xrf*	*xrf*	*xrf*	*xrf*	*xrf*	*xrf*	*xrf*	*xrf*	*xrf*	*xrf*	*xrf*	*xrf*	*xrf*	*xrf*	*icp*	*icp*	*icp*	*icp*	*icp*	*icp*	*icp*	*icp*	*icp*	*icp*	*icp*	*icp*	*icp*	*icp*	*icp*
202	43	388	62	143	33	20	120	102	217	21	-10	31	55	27	14	47.6	28.1	63.5	7.9	28.2	7.5	1.9	6.5	1.8	7.2	1.7	2.4	0.5	4.3	1.1
256	24	401	83	136	12	42	379	72	51	26	-10	51	51	15	-10	39.6	16.9	41.1	6.4	22.1	6.5	1.9	5.6	1.5	6.4	1.4	2.3	0.3	3.5	0.8
294	17	170	26	166	11	38	206	15	44	25	-10	43	75	20	34	49.0	19.7	49.9	6.8	29.1	8.9	3.0	8.9	1.8	8.1	1.8	2.2	0.5	3.4	0.9
288	16	174	27	165	17	30	207	11	9	26	-10	51	82	31	38	43.3	16.5	40.9	5.8	24.6	7.1	2.5	7.3	1.5	7.1	1.5	2.7	0.4	3.0	0.8
181	36	502	25	114	-10	22	144	59	125	21	-10	26	86	33	23	51.2	42.7	99.1	12.3	41.7	9.5	2.4	8.5	1.7	8.7	1.9	3.8	0.6	4.4	1.3
128	29	414	48	137	-10	27	221	77	106	25	-10	42	79	33	14	42.8	34.2	75.4	9.1	32.3	7.2	2.1	6.4	1.5	7.0	1.7	3.3	0.6	3.6	0.9
119	-5	94	29	143	-10	48	404	15	69	27	-10	58	46	10	20	28.6	9.8	21.9	3.0	12.5	3.4	1.6	2.8	0.9	4.8	1.0	1.9	0.4	2.9	0.9
135	-5	96	42	158	-10	50	597	17	48	30	-10	68	40	15	-10	25.8	8.3	16.5	2.5	10.9	3.7	1.1	2.3	0.7	4.1	0.9	0.8	0.2	2.6	0.7
139	11	123	26	135	-10	47	406	12	36	27	-10	60	44	11	24	27.8	10.1	24.0	3.3	14.0	4.6	1.7	3.1	0.8	4.3	1.1	0.8	0.5	2.5	0.5
250	14	158	28	163	-10	36	178	10	23	27	-10	48	88	16	34	59.9	22.0	56.2	8.8	35.2	9.8	3.5	10.1	2.1	9.8	2.0	3.0	0.6	4.2	0.9
216	40	752	22	103	16	22	133	53	84	24	-10	24	79	43	28	54.7	47.1	111.4	14.3	48.7	12.0	2.9	10.1	1.8	9.9	2.1	4.2	0.9	4.4	0.9
369	7	134	24	83	-10	19	130	84	261	19	-10	39	-10	-10	-10	17.1	9.3	20.5	2.8	10.9	3.0	1.1	1.3	0.2	2.5	0.6	0.8	0.2	1.6	0.6
327	14	186	37	76	12	17	128	76	280	22	-10	40	-10	-10	-10	17.0	8.3	18.7	3.0	9.9	2.8	1.2	1.5	0.2	2.7	0.5	0.8	0.2	1.6	0.4
169	40	1093	6	25	-10	-10	15	-5	24	-10	-10	-10	-10	13	-10	15.4	21.8	39.0	5.7	12.4	2.7	0.7	1.1	0.5	1.3	0.4	1.4	0.2	2.4	0.7
307	26	256	40	92	-10	25	129	87	287	17	-10	45	13	-10	-10	18.2	8.6	16.6	2.4	10.6	2.6	1.2	1.6	0.2	2.5	0.6	0.8	0.2	1.8	0.4
285	8	115	68	87	-10	34	554	56	56	25	-10	54	22	-10	-10	10.0	5.7	10.2	3.9	5.8	2.1	0.8	1.0	0.3	1.8	0.4	0.8	0.2	1.0	0.4
70	-5	84	29	128	-10	51	474	15	108	24	-10	64	38	-10	15	14.5	5.6	10.1	3.1	5.5	2.3	0.8	1.0	0.3	2.3	0.5	0.8	0.2	1.4	0.6
144	7	84	42	130	-10	44	572	28	103	25	-10	75	24	-10	-10	18.3	8.1	13.1	2.5	6.9	2.3	0.7	0.5	0.3	2.9	0.6	0.8	0.2	1.7	0.4
163	12	115	38	127	-10	49	433	19	19	25	-10	66	35	-10	-10	19.6	5.8	12.5	2.1	7.6	2.8	1.0	1.1	0.8	3.0	0.6	0.8	0.2	1.8	0.5
194	-5	53	30	125	-10	50	355	14	74	24	-10	63	25	-10	13	16.5	4.7	9.8	2.3	6.7	2.7	1.2	1.7	0.4	2.8	0.6	0.8	0.3	1.4	0.3
81	-5	37	36	149	-10	56	399	26	29	24	-10	68	49	13	16	18.2	11.6	24.4	3.6	13.3	3.9	1.4	2.8	0.8	4.8	1.0	1.6	0.2	2.9	0.7
319	-5	60	46	159	-10	52	341	24	45	25	-10	64	24	-10	-10	26.4	7.1	16.2	3.1	10.5	3.1	1.5	2.1	0.7	4.1	0.9	0.8	0.2	2.7	0.7
237	-5	77	21	122	-10	47	338	18	68	25	-10	54	16	-10	-10	22.2	5.7	15.2	1.9	7.2	2.1	1.2	1.7	0.8	3.2	0.7	1.8	0.2	2.3	0.6
117	6	110	45	131	-10	46	266	15	16	29	-10	55	42	24	17	21.8	8.9	20.6	2.2	11.9	3.5	1.7	1.8	0.7	3.3	0.8	0.8	0.2	2.2	0.5

Appendix 4: Comparison of different X-Met analyses on the same core-sections.

Sample	Rock	Sp.w.	Magn. susc	Anal. by DuPont's X-Met (15 sec.) Cut surface % TiO2	Anal. by DuPont's X-Met (15 sec.) Cut surface % Fe2O3	Anal. by NGU's X-Met (15 sec.) Cut surface % TiO2	Anal. by NGU's X-Met (15 sec.) Cut surface % Fe2O3	Anal. by NGU's X-Met (15 sec.) Core surface % TiO2	Anal. by NGU's X-Met (15 sec.) Core surface % Fe2O3
4/030.0	eclogite	3185	0.00157	1.6	9.0	2.3	8.4	2.0	8.1
4/035.9	eclogite	3346	0.00141	2.7	15.6	2.4	13.7	2.0	14.2
4/026.9	eclogite	3201	0.02576	1.5	12.9	2.0	13.0	2.1	13.3
4/024.1	amphibolite	3211	0.00167	3.2	16.6	3.4	15.3	2.6	15.5
4/054.0	eclogite	3438	0.00094	2.8	15.7	3.0	16.7	2.6	14.9
4/159.7	eclogite	3268	0.00654	2.8	17.0	3.1	16.6	2.6	14.0
4/09.9	eclogite	3477	0.00123	3.7	17.9	3.7	17.0	2.7	16.3
4/064.9	eclogite	3153	0.00676	3.1	17.2	3.3	17.0	2.9	15.6
4/137.9	eclogite	3183	0.01104	3.2	24.7	3.6	20.7	3.0	17.2
4/037.9	eclogite	3300	0.02296	3.5	17.4	4.0	17.9	3.1	17.3
4/044.1	eclogite	3480	0.00121	3.4	17.7	4.0	17.2	3.1	14.4
4/016.9	eclogite	3425	0.00149	3.7	16.2	3.7	20.6	3.4	18.0
4/069.9	eclogite	3267	0.00109	5.0	16.7	4.3	16.6	3.4	15.6
4/059.8	eclogite	3597	0.00148	3.7	19.3	3.8	19.3	3.5	18.5
4/125.2	eclogite	3405	0.00212	3.5	16.6	3.4	15.9	3.5	13.5
4/074.9	eclogite	3220	0.00085	2.5	15.6	2.6	15.4	3.6	14.4
4/151.9	eclogite	3314	0.00805	4.1	15.2	4.7	14.7	3.6	14.3
4/098.9	eclogite	3493	0.00178	4.2	15.5	4.3	15.5	3.7	14.2
4/110.4	eclogite	3569	0.00112	4.0	17.1	4.4	16.6	3.8	15.1
4/113.9	eclogite	3437	0.01195	4.8	16.2	4.8	15.3	4.4	13.1
4/070.8	eclogite	3463	0.00122	5.7	18.2	6.5	15.1	4.5	12.8
4/140.9	eclogite	3437	0.01397	4.3	18.0	4.7	17.3	4.5	16.2
4/069.7	eclogite	3533	0.00191	6.1	17.3	6.2	16.8	5.2	14.2
4/073.8	eclogite	3694	0.00335	5.8	15.9	6.2	15.7	5.5	14.1
4/079,9	eclogite	3775	0.00378	4.7	27.4	6.1	26.3	7.7	20.3
		Average:		3.74 [1]	17.08 [2]	4.02 [3]	16.58 [4]	3.56 [5]	15.00 [6]

TiO_2-differences:

3 - 1: 0.28 % TiO2

3 - 5: 0.46 % TiO2

Based on these data NGU's X-Met give in average 0.28% TiO2 (7.5%) higher values than DuPont's X-Met on cut surface.

NGU's X-Met give 0.46% TiO2 higher values (12.9%) on cut surface than on round surface.

Appendix 5: Microscopy information summary.

Table 14a: Thin-section information, Engebøfjellet

Thin-section	Rock type	Gt size	Gt mode	Oxide %	Oxide size (max.)	Rut/Op (I and/or II)	Ilm / Ilm+Rut	Sphene	Retrogr.
1/66.8	leucog. ecl.	<1.5 (3)		abundant		Op I>Rut	tr.(<1-2%)	0	tr.
1/101.9	interm. ecl.	<0.5	30-35	abundant	Rut 0.5-1	Rut>>Op I	#10%	0	tr.
1/126.5	leucog. ecl.	<0.5		abundant		Ru >Op I	10 %	0	minor/tr.
1/164.2	ferrog. ecl. layer	<0.3-0.4		abundant		Op>Rut	>80%	+	extensive
"	felsic layer	<2		abundant			>80%	+	extensive
2/115.9	ferrog. ecl.	<0.3 (0.5)	30-35	abundant	Rut 0.1	Rut>>Op I	tr.	tr	tr.
2/125.9	leucog. /interm. ecl..	<0.1-0.15		minor?	Rut 0.1-0.2	Rut.Op I	<5%	0	minor
2/154.8	ferrog. ecl.	<1		abundant	Rut 0.5-1	Rut>OpI	tr.	0	none
2/169.0	ferrog. ecl.	<0.7		abundant		Rut>>OpI	<3-5%	0	tr.
2/201.8	leucog. ecl.	<0.8		abundant	Rut 0.5	Rut>Op I	# 5%	0	tr.
3/6.8	leucog. ecl.	<0.5	<10	minor		Rut>>Op I		0	tr.
3/22.1	layered leucog. ecl.	<0.3	15-20	moderate	Rut 0.2-0.3	Rut>>>Op	tr.	0	tr.
3/33.9	leucog. ecl.	<0.3 (0.7)	10-15	mod/minor		Rut.Op	# 20%	0	minor
3/37.1	amphibolite?	<8	<<5?	abundant		Op I>>Rut	# 5%	0	?
3/62.9	leucog. ecl.	<0.5	15-20	moderate		Rut>Op I	tr.	0	minor
3/65.3	coronitic leucog. ecl.	<0.5	15-20	moderate		Op I>Rut	tr.	0	tr./minor
3/76.9	"gneiss"	relict	tr.	tr.		only Rut?			extensive?
3/85.7	"gneiss"		0	tr. Rut					
3/101.9	leucog. ecl.	<0.3	10-15	abundant	Rut 0.5	Rut>Op I	5 %	0	extensive
3/110.0	leucog. ecl.	<0.5	10-15	moderate		Rut>Op I		0	min/ext.?
3/117.9	leucog. ecl.	<0.4	10-15	minor	Rut 0.2	Rut>Op I	5-10%	0	tr./minor
3/127.3	layer./interm. ecl.	<0.5 (1.2)	35-40	abund.	Rut 0.15	Rut=Op I	#10%	0	minor
3/136.6	leucog. /interm. ecl.	<0.5	20	abundant	Rut 0.5	Rut>=OpI	tr.	0	minor/tr
3/137.8	layered ecl	<0.4	25-30	moderate	Rut 0.2-0.4	Rut>Op I	5 %	0	tr.
3/146.9	ferrog. /interm. ecl.	<0.4	30-35	very abund	Rut 0.3	Rut>>Op I	tr.	0	none
3/159.8	ferrog. ecl.	<0.5	40	very abund	Rut 0.8	Rut>>OpI	<5%	0	none
3/160.9	ferrog. ecl.	<0.7	40	very abund		Rut>>Op I	tr.	0	none/tr.
4/2.0	leucog. ecl.	<0.4	10	minor	Rut 0.1	both		0	variable
4/9.1	interm. ecl.	<0.5	25-30	moderate	Rut 0.8	Rut>OpI	<5%	tr.(vein)	tr.
4/16.9	interm. ecl..	<0.5	20	moderate	Rut 0.5	Rut>>Op I	<5%	0	tr.
4/21.0	layer. leucog. ecl.	<2	30?	mod/abund		Rut>Op	30%?	tr.?	extensive
4/24.0	interm. ecl..	<0.3-0.4	15	abundant		Rut=Op	30-40%	tr.?	extensive
4/26.9	leucog. ecl.	<0.3 (0.5)	15-20	mod/minor		Rut>Op	>20%	0	extensive
4/30.0	leucog. ecl.	<0.6	10	mod/minor	Rut 0.2-0.3	Rut>Op	<5%	0	minor/tr.
4/35.9	leucog. ecl.	<0.3	20	mod/abund	Rut 0.5	Rut>Op I	5 %	0	tr.
4/37.9	ferrog. ecl.	<0.5	25-30	abundant		Rut>>Op I	10-15%	tr?	minor
4/38.9	ferrog. ecl.	<0.5 (0.15)	25-30	abundant	Rut 0.5	Rut>Op I	5 %	tr.	none *
4/44.1	interm. ecl..	<0.8	20-25	mod/abund		Rut>Op I	<5%	0?	tr.
4/54.0	layered	<0.5-0.7	25	minor		Op I>Rut		0	minor
4/59.9	ferrog. ecl.	<0.6	25-30	abundant	Rut 0.6	Rut>>Op I	<5%	0	tr./none
4/65.9	lay. amphib.		10	abundant		Op>Rut	>60-70%	+ (vein)	extensive
4/69.9	leucog. ecl.	<0.8	50	mod/abund		Rut>Op I	10-15%?	0	minor
4/72.9	ferrog. ecl./layer.	<0.7		very abund		Rut>Op	15 %	+(corona)	extensive

Thin-section	Rock type	Gt size	Gt mode	Oxide %	Oxide size (max.)	Rut/Op (I and/or II)	Ilm / Ilm+Rut	Sphene	Retrogr.
4/75.4	ferrog. ecl.	<0.5	40	very abund	Rut 0.5	Rut>Op I	<5%	0	none
4/79.9	ferrog. ecl.	<0.5	45-50	very abund		Rut>>Op I	tr.	0	none
4/81.9	amphibolite		0?	abundant		Op>>Rut	>=70%	tr.	amphibol.
4/86.0	ferrog. ecl.	<0.8	55	very abund		Rut>>Op I	<5%	0	none
4/87.9	ecl.	<0.7	25	very abund	Rut 0.5	Rut>Op I	#5%	+ (vein)	none/tr.
4/97.3	"leucog. ecl."	<0.5	45	abundant	Rut 0.3	Rut>>>Op	tr.	0	none
4/120.9	ferrog. ecl.	<0.5	20	very abund		Op I>Rut	>60%	0	tr.
4/130.3	ferrog. ecl.	<0.7	35	abundant		Op I>Rut	10 %	0	minor
4/151.5	layered	<0.7	35	moderate		Rut	<5%	0	minor
5/37.9	leucog. ecl.	<0.7	20	moderate		Op I<Rut	<5%	0	none
5/61.9	ferrog. ecl.	<0.4	30	abundant	Rut 0.5	Rut	<5%	0	none
5/134.2	ferrog. ecl.	<0.8	35-40	very abund		Rut>>Op I	<5%	0	tr.
5/170.1	ferrog. ecl.	<0.5	35	very abund	Rut 1.0	Rut>Op I	tr.	0	none

Appendix 4, continued

Thin-section	Late fract.	Carb.	Other minerals I	Texture	Comments
1/66.8	+	abundant I	Om,Am, Wmica,cZo/Ep	folded foliation (crenulation)	
1/101.9	+	tr.(incl)	Om, Am, Wmica(m),Q,Ap	granular, weak F:Om,Am,Q,mica	
1/126.5	+(carb)	abundant I	Om,Am(M), Wmica(m),Ap,Q	granular, weak orientation	
1/164.2			(Om),Am, cZo/Ep (II?),Q(m)		
"		abundant I	(Om),Q,Wmica, Ap,cZo/Ep,Zirc	strong F	Kel:Ep+Biot+Mag
2/115.9		no I	Om,Am,Wmica, Q(m)	granular tabular	foliation Om,Am,mica,Rut
2/125.9		abundant I	Om,Am,cZo, Wmica,Q	Heterog., Cpx porphyroclasts	
2/154.8	+(carb)	tr. I	Om,Am,Q,Ap	Heterog., granular not oriented	
2/169.0	+	tr (incl)	Om,Am, Wmica(m),Q,Ap	granular not oriented	see 2/154.8
2/201.8	tr.	+ I	Om,Am,Wmica, Q,Ap	tabular,F=Om,Am, mica,oxides	
3/6.8	0	+ I	Om,Am,Wmica, Zo,Q	strong F,fine-grained domains	
3/22.1	0	abundant	(sympl),Am,Zo, Wmica,Q	strong F;deformed pseudomorph.	
3/33.9	0?	+ I	Om,Am(M),Wmica,Q (tr),cZo/Ep	foliation; fine-grained areas	Om porphyrobl.:various orientations
3/37.1		0	(Am,Q,cZo,Biot,Ap)	Gt porphyrobl.; fine-grained matrix	
3/62.9	tr.(carb)	abundant I	Om?,Am,Q(M), cZo/Zo+Pl+Wmica	oriented pseud./recryst.coronitic	association carb I/Rut; Om?
3/65.3	+ (carb)	minor I	Om,Am,Zo,Wmica, Pl?,Q	pseudomorphic	Partly recryst. coronite
3/76.9			Q(50%?),(cZo/Ep, Wmica,Pl,Chl,?)		euhedral pseudomorphs=?
3/85.7			Q,Wmica,cZo/Ep, (Chl II?)	folded F:mica, cZo	eclogite-facies;euhedral pseudom.(Om?)

Thin-section	Late fract.	Carb.	Other minerals I	Texture	Comments
3/101.9	0	tr. I (incl)	Am(M),(sympl), cZo,Q,Wmica,Ap	pseudomorphic, deformed	
3/110.0		tr.	Am(M),Wmica, Q,cZo,Ep	pseudomorphic+F; see 3/65.3	
3/117.9	0		Am(M),Wmica(M), Q,cZo	F: mica	
3/127.3	thin (carb)	abundant I	Om,Am,Q, Wmica(m)	tabular granular	layers Om+Gt vs Q-,carb-rich
3/136.6	0		Cpx,Am,Wmica, Q,cZo/Ep	not oriented, "crenulation"	
3/137.8	tr. (carb)	abundant I	Om,Am,Wmica, Q,cZo	foliation; Am porphyrobl.	layers Wmica+Q- vs carb-rich
3/146.9	0	abundant I	Om,Am,Q	granular not oriented	abundant Pyr I
3/159.8		tr/minor I	Om,Am,Q, Wmica(m),Ap		
3/160.9	tr.	abundant I	Om,Am(m),Q, cZo(m/tr)	granular tabular (Rut streaks)	diffuse layering:carb-rich "schlieren"
4/2.0		+ I	(sympl),Am,cZo, Wmica(M),Q	pseudom.;strong F:mica,cZo,Q	carb+mica+Q vein?
4/9.1	+ (carb)	+ I	Om,Am,cZo(M), Wmica	mylonitic, Am porphyroblasts	layering=sheared pseudomorphic texture
4/16.9	+	no I	Om,Am,cZo/Ep, Wmica,Q	oriented,granular,Am porphyrobl.	see 5/37.9
4/21.0		abundant I	(sympl),Am(m), cZo/Ep,Wmica,Q	foliation/layering	Kel:Am+Ep+Pl
4/24.0	0	+	(sympl),Am, cZo/Ep,Q	oriented Rut,carb, cZo segreg.	
4/26.9		0	(sympl),Am, cZo/Ep(M),Wmica,Q	sheared + late ultramylonite	
4/30.0	0	incl.	Om,Am,cZo(M), Q(M),Wmica		
4/35.9	+ (carb)	no I	Om,Am(M), cZo/Ep(M),Wmica,Q	recrystallized pseudomorphic	
4/37.9	abundant	0	Om,Am,Q(m), Wmica(tr)	granular, F= Om,oxides	
4/38.9	++ (carb)	tr (incl)	Om,Am,Q(m), Wmica(m),cZo,Ap	deformed honeycomb	
4/44.1	minor	incl.	Om,Am,Wmica,cZo, Q	heterogeneous (mode)	
4/54.0	+ (carb)	major I	Om,Am(M),Wmica,Q (M),Ep	layered but not oriented	
4/59.9	tr.	tr. I	Om,Am,Wmica,Q(m), Ap	mylonitic foliation Om, mica,Rut	
4/65.9	+ (carb)	major	(sympl),cZo/Ep, Wmica,Q,Ap	layered, amphibolitized	carb + sphene (vein)
4/69.9	0	major	Wmica(M),(sympl), Am(m),Q,cZo	granular+ F:mica	
4/72.9			(sympl),Wmica, Am,Ep(II?)	layered	Kelyp. Ep+Am;sphene vs Ep
4/75.4	+ (carb)	abundant I	Om,Am,Q,Ep?, Wmica(tr.)	weak orientation (Om, oxides)	
4/79.9	0	minor I	Om,Am(m),Q(m),Ap	granular but oxide streaks	
4/81.9	+ (carb)	+ (also I?)	(sympl AmII+Pl+Ep), Ap		sphene+carb;sphene vs Ep
4/86.0	abundant	0	Om,Am	granular	similar to 4/79.9 but no Q,carb I
4/87.9	+	abundant I	Om,Am(m),Q	granular, not oriented	sphene along fractures
4/97.3	thin (carb)	major I	Q(M),Am,Om	granular, weakly oriented	Fluid incl.;Q+Carb-rich Ecl, not leucogab.
4/120.9	+(carb)	+ I	Om,Am(M),Q,Ap		abundant Pyr I + abundant Ilm (I?+II)
4/130.3	carb	abundant I	Om,Am(M),Q	foliation Om,Am,Rut	abundant Mag I

Thin-section	Late fract.	Carb.	Other minerals I	Texture	
4/151.5	+	0	Om,Am,Wmica,Q, cZo/Ep	ferrog. ecl. and mica-rich layers	
5/37.9	+ (carb)	no I	Om,Am,cZo/Ep, Wmica,Q	weak orientation; cZo segreg.	
5/61.9	tr.	0	Om,Am,Q(m),Ap	heterogranular	
5/134.2	0	minor I	Om,Am,cZo/Ep, Wmica,Q,Ap	mylonitic	
5/170.1	0	minor I	Om,Am,Q(m), cZo(m),Ap	granular,strong orientation (Rut)	carb I associated Rut

Explanations:

Rock type: mafic eclogite (or ferrogabbroic): silicates are mainly garnet, omphacite and amphibole; quartz, clinozoisite, white mica may be present in minor amounts. Light eclogite or leucogabbroic: quartz, clinozoisite, mica and amphibole are major minerals. Intermediate eclogite: mafic with notable amounts of quartz, mica, clinozoisite or carbonate.

Garnet size: maximal size in mm. Where two values are given, the first number indicates the size of the largest population, the one in brackets a minor population.

Garnet mode: visual estimates in volume%.

Oxide%: relative scale from trace (tr) to minor, moderate, abundant and very abundant. Visual estimates of the total amount of oxides (rutile, magnetite and ilmenite I and II) ans sulfides (pyrite).

Oxide size: maximal size in mm. Indicated for single rutile grains, not cluster.

Rutile/Opaque: Opaque = magnetite and ilmenite I and II. Op I is generally magnetite. Op = Op I + II.

Ilm/Ilm+Rut: visual estimates in volume%.

Sphene: not recorded = 0, present = + , as corona around rutile/ilmenite within the rock ("corona") or as subhedral crystals within late veins ("vein").

Retrogression: relative scale from none, trace, minor, extensive, very extensive. None* = no retrogression except along numerous late fractures.

Other minerals I: eclogite-facies minerals in addition to garnet, oxides and carbonate.
In brackets: minerals II (retrogressive), (Om) = symplectites after omphacite.
Abbreviations: Am (amphibole), Ap (apatite), Biot (biotite), Carb (carbonate), Chl (chlorite), cZo (clinozoisite), Ep (epidote), FK (alkali feldspar), Gt (garnet), Ilm (ilmenite), Kel (kelyphite), Mag (magnetite), Om (omphacite), Pl (plagioclase), Pyr (pyrite), Q (quartz), Rut (rutile), sympl (symplectites), Wmica (white mica: phengite ± paragonite), Zirc (zircon).
Trace = (tr), minor = (m), major = (M).

Texture: F = foliation

Geological map of the Førdefjord area

Scale 1:100.000

0 2 4 6 8 10 km

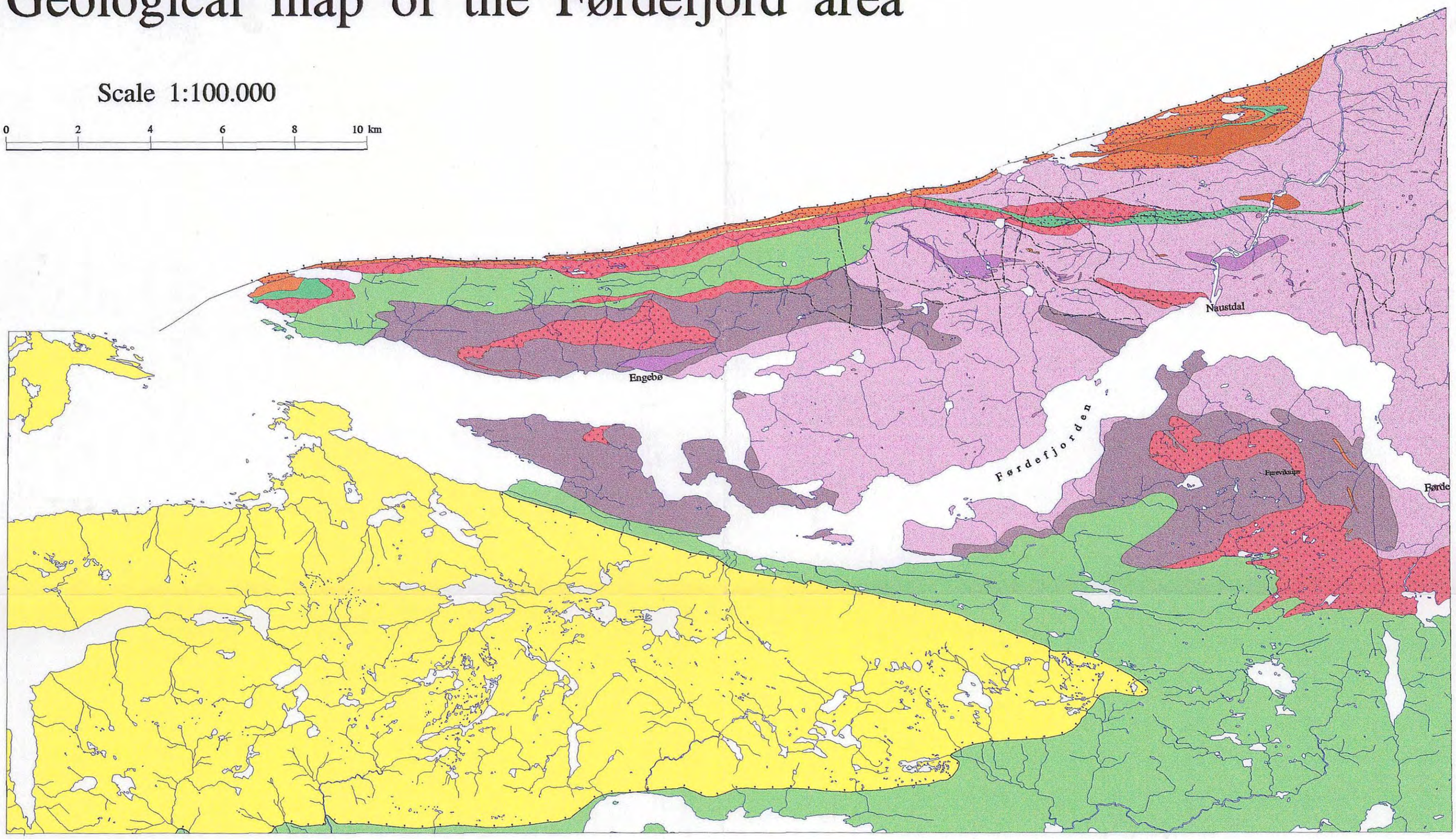

Legend

Upper plate

Undifferentiated metasedimentary, metavolcanic and intrusive rocks

The Lykkjebø Group

Ultramafic rock
Mica schist
Quartzite

The Eikefjord Group

Ultramafic rock
Meta-gabbro
Meta-anorthosite
Mylonittic gneis, in places with layers of meta-anorthosite and amphibolite

Basement

Blastomylonitic gneis
Mica schist
Quartzite
Ultramafic rock
Meta-gabbro, amfibolitt
Augengneiss
Eclogite
Anorthosite
Eclogite and grey gneis (quartz-dioritic ?) alternating
Granitic othogneis
Granitic to granodioritic gneis

GEOLOGY OF THE ENGEBØ AREA, SOGN OG FJORDANE

NGU
Norges geologiske undersøkelse

LEGEND

- 1 Ferrogabbroic eclogite
- 2 Leucogabbroic eclogite
- 3 Amphibolite unit (amphibolite, eclogite and gray gneiss)
- 4 Granitoid gneisses. undiff.

Samples

- < 1% TiO2
- 1 - 2% TiO2
- 2 - 3% TiO2
- 3 - 4% TiO2
- > 4% TiO2

- D1 fabric
- D2 fabric
- D3 and D4 fabric
- Vertical profile
- Dh-3 ⊙ Drillhole position with Dh number
- ⊞ End of gravimetric profile

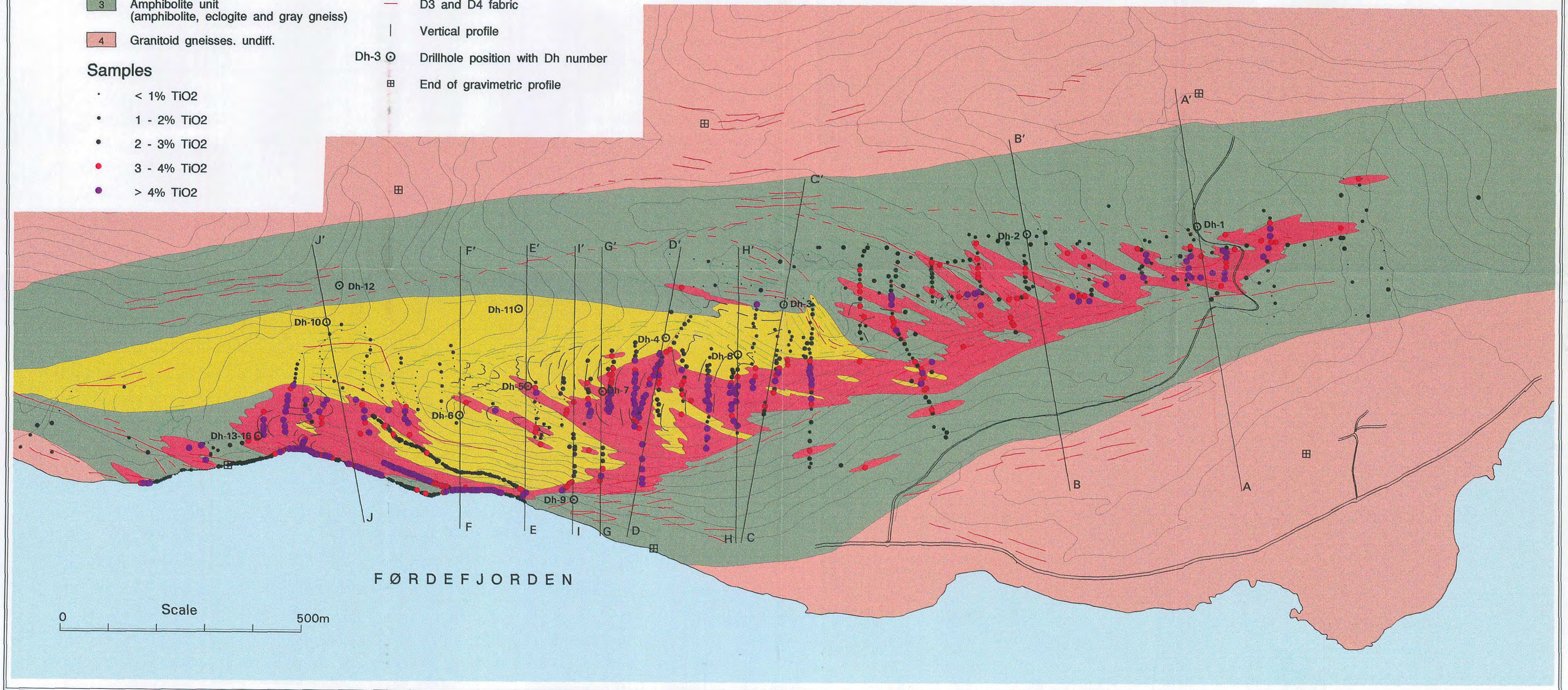

Appendix 8a:

Photographs of 10m core sections

Dh6

Photographed at NGU's core storage at Løkken

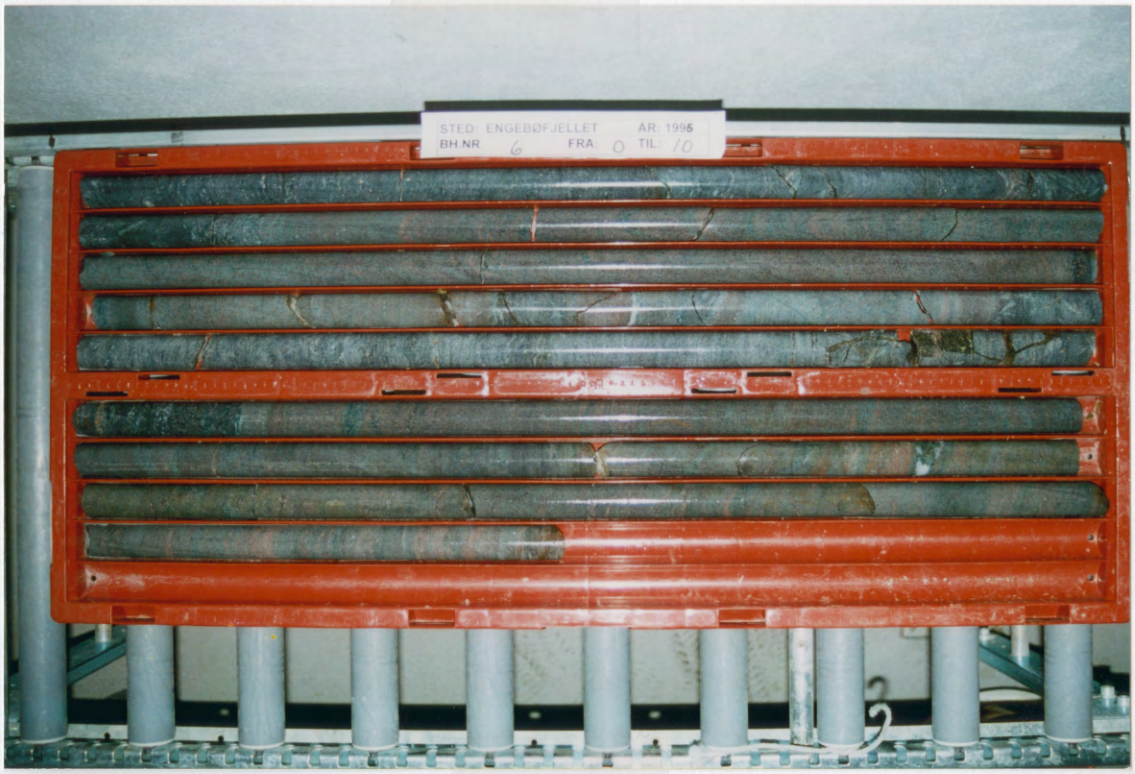
STED: ENGEBØFJELLET ÅR: 1996
BH.NR 6 FRA: 0 TIL: 10

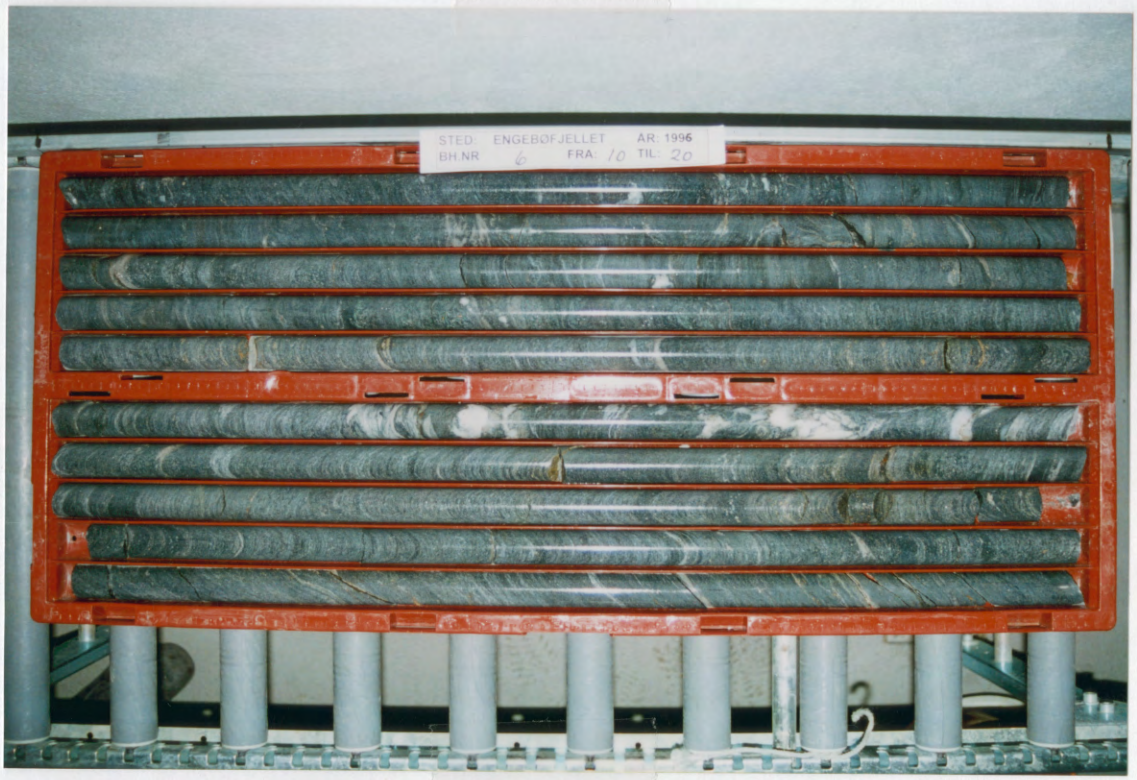
STED: ENGEBØFJELLET ÅR: 1996
BH.NR 6 FRA: 10 TIL: 20

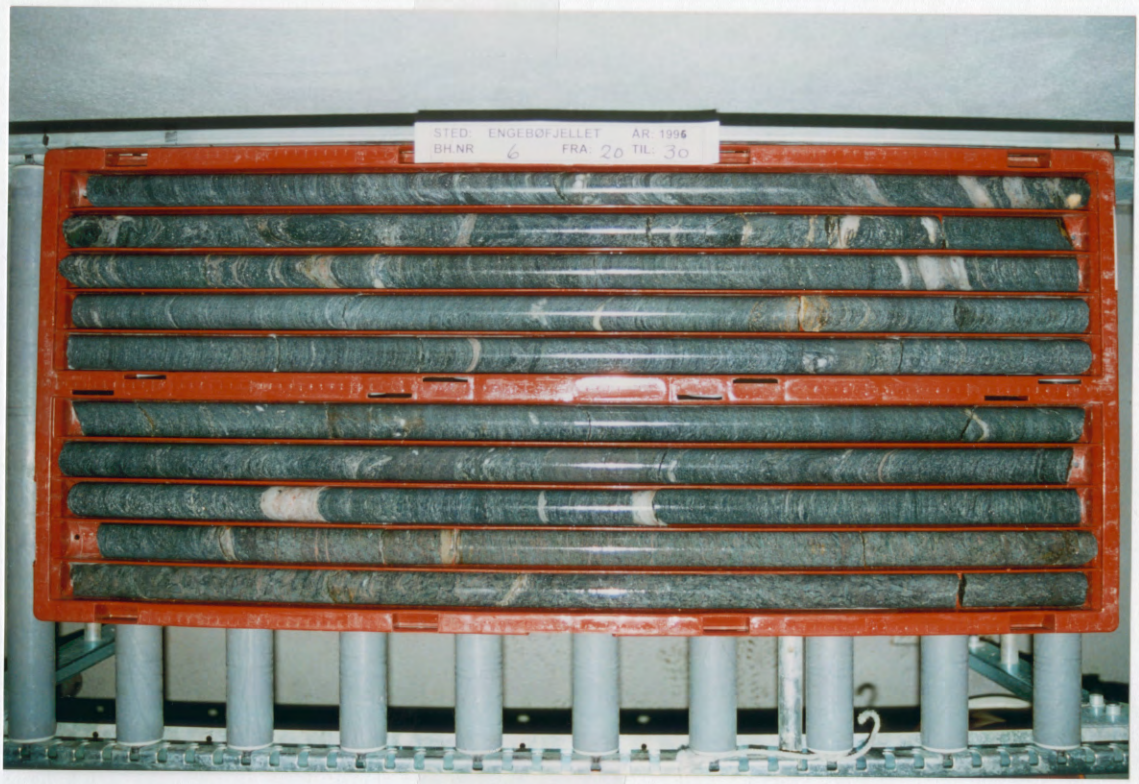
STED: ENGEBØFJELLET ÅR: 1996
BH.NR 6 FRA: 20 TIL: 30

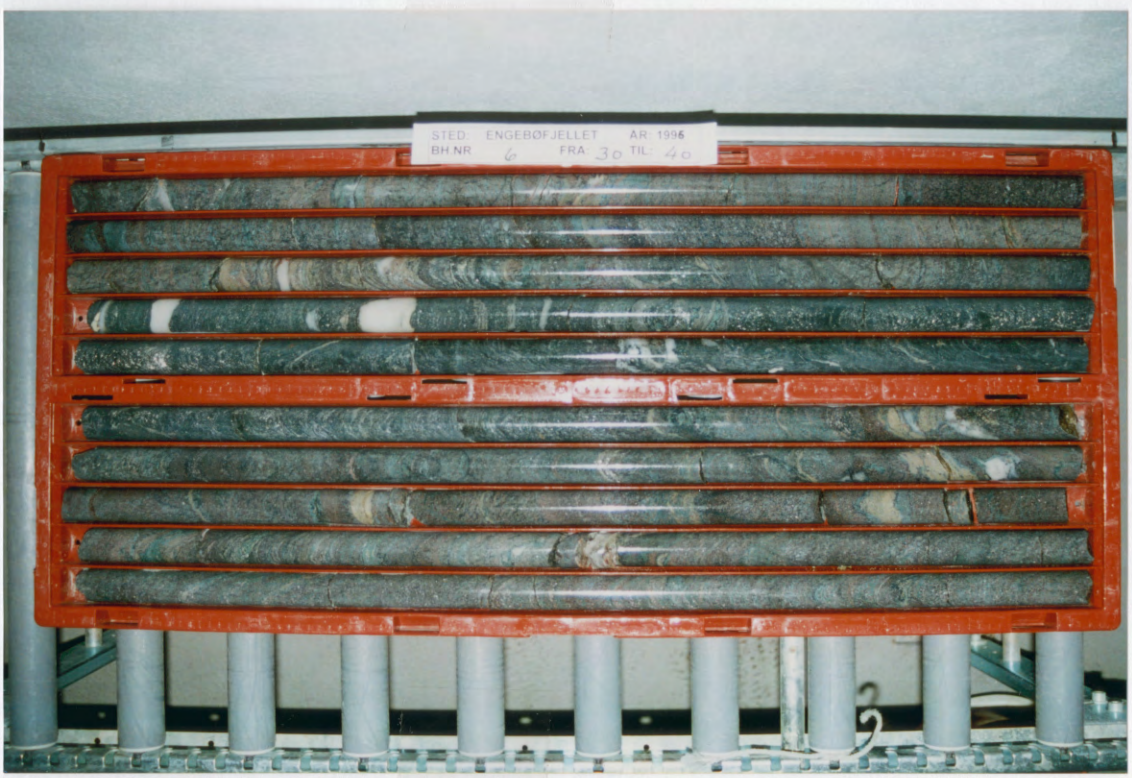
STED: ENGEBØFJELLET ÅR: 1996
BH.NR 6 FRA: 30 TIL: 40

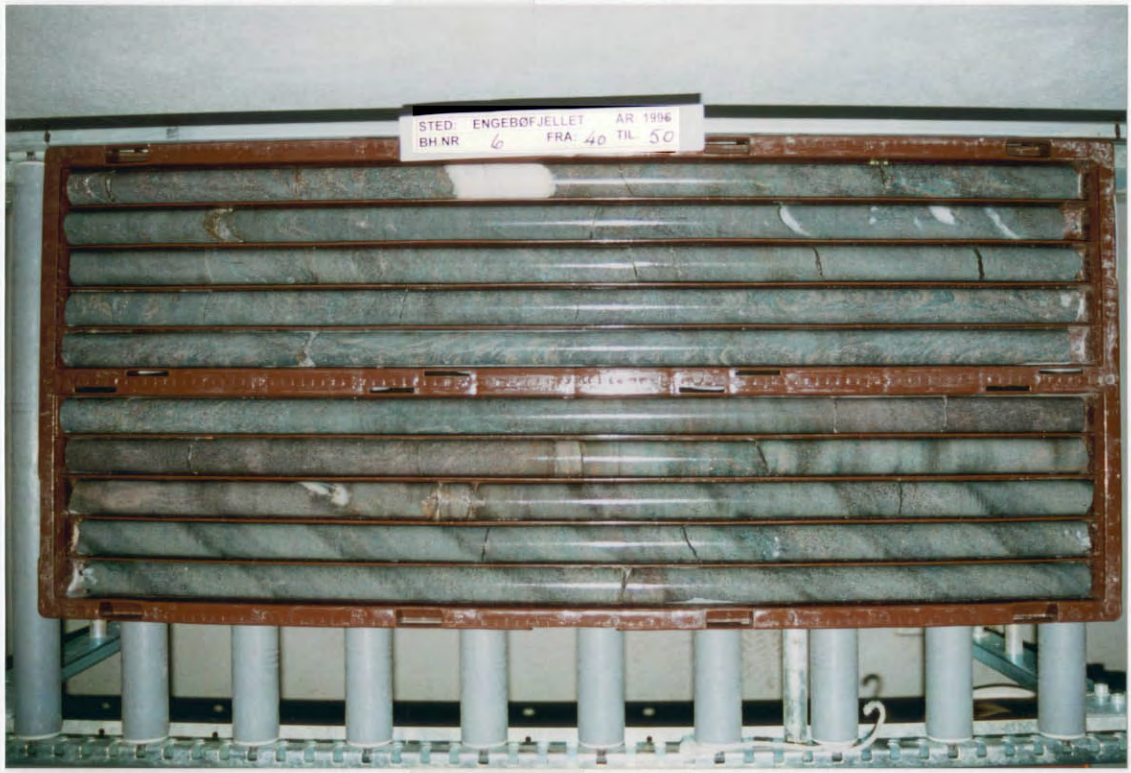
STED: ENGEBØFJELLET ÅR: 1996
BH.NR 6 FRA: 40 TIL: 50

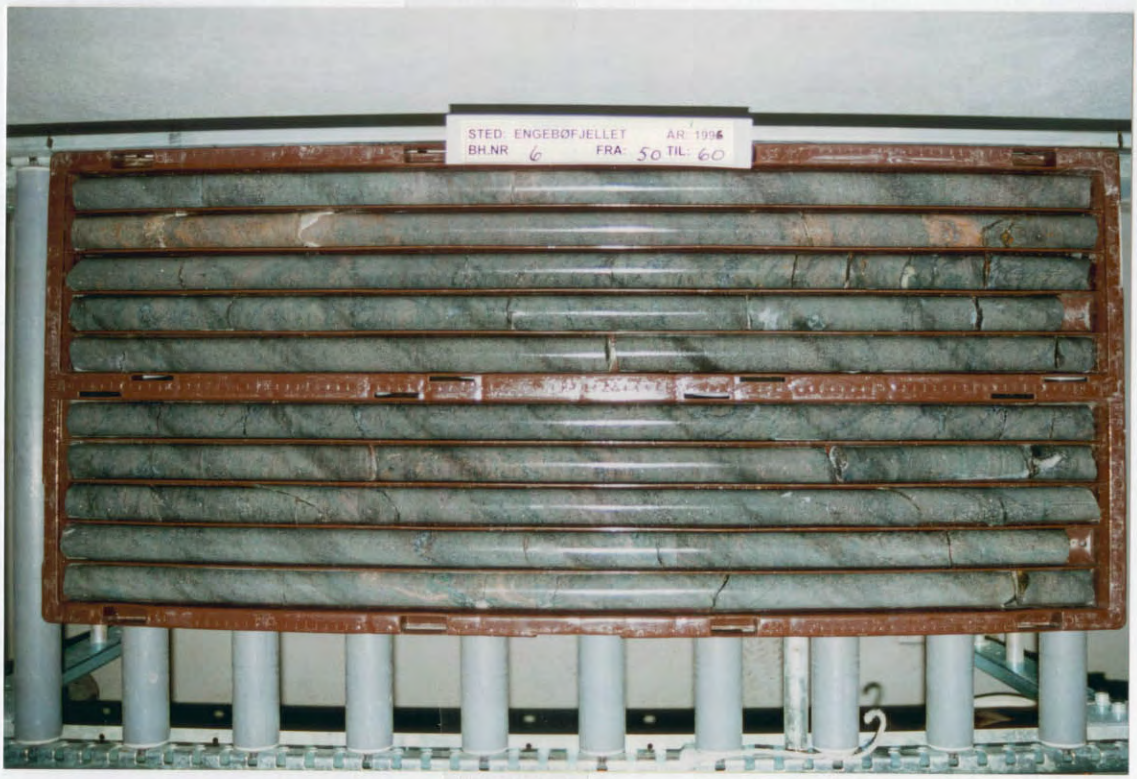
STED: ENGEBØFJELLET ÅR: 1996
BH.NR 6 FRA: 50 TIL: 60

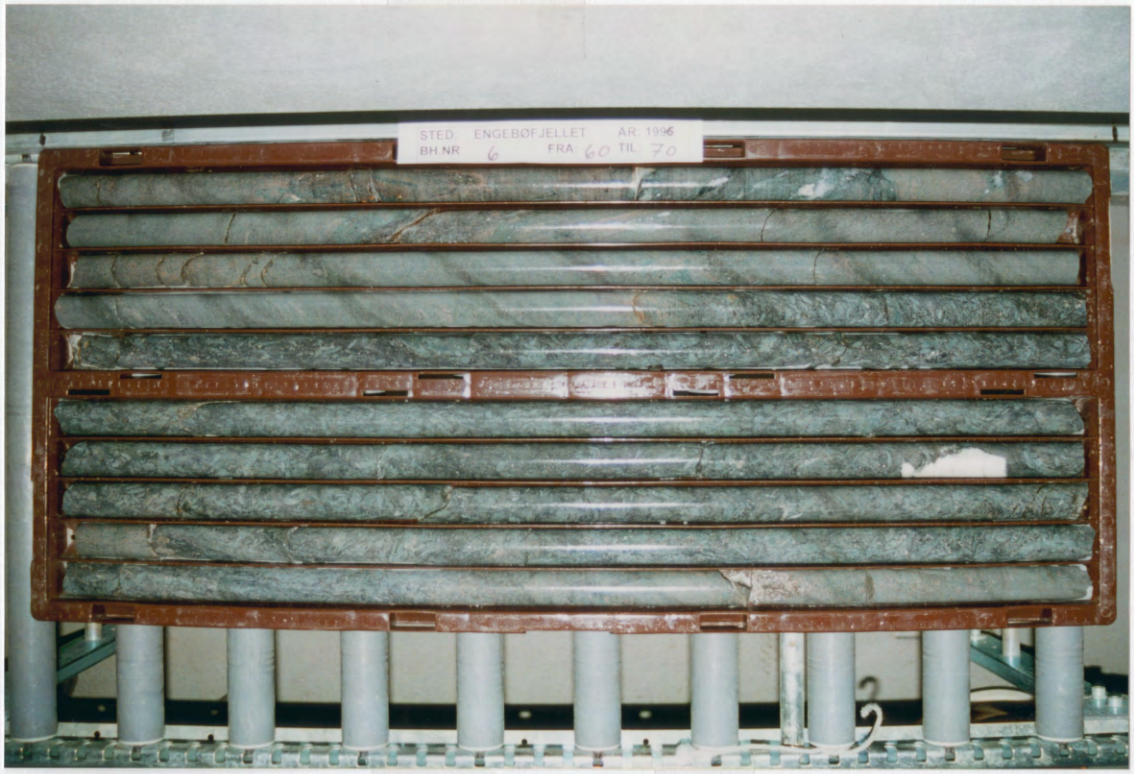
STED: ENGEBØFJELLET ÅR: 1996
BH.NR 6 FRA: 60 TIL: 70

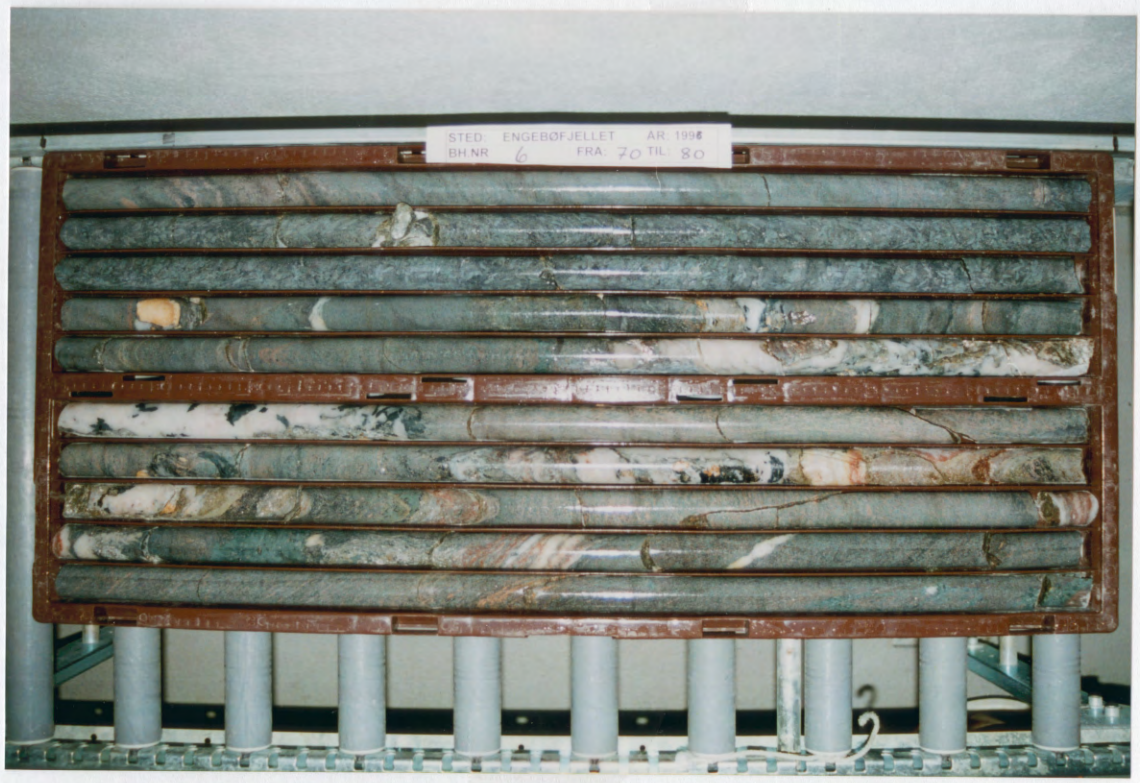
STED: ENGEBØFJELLET ÅR: 1996
BH.NR 6 FRA: 70 TIL: 80

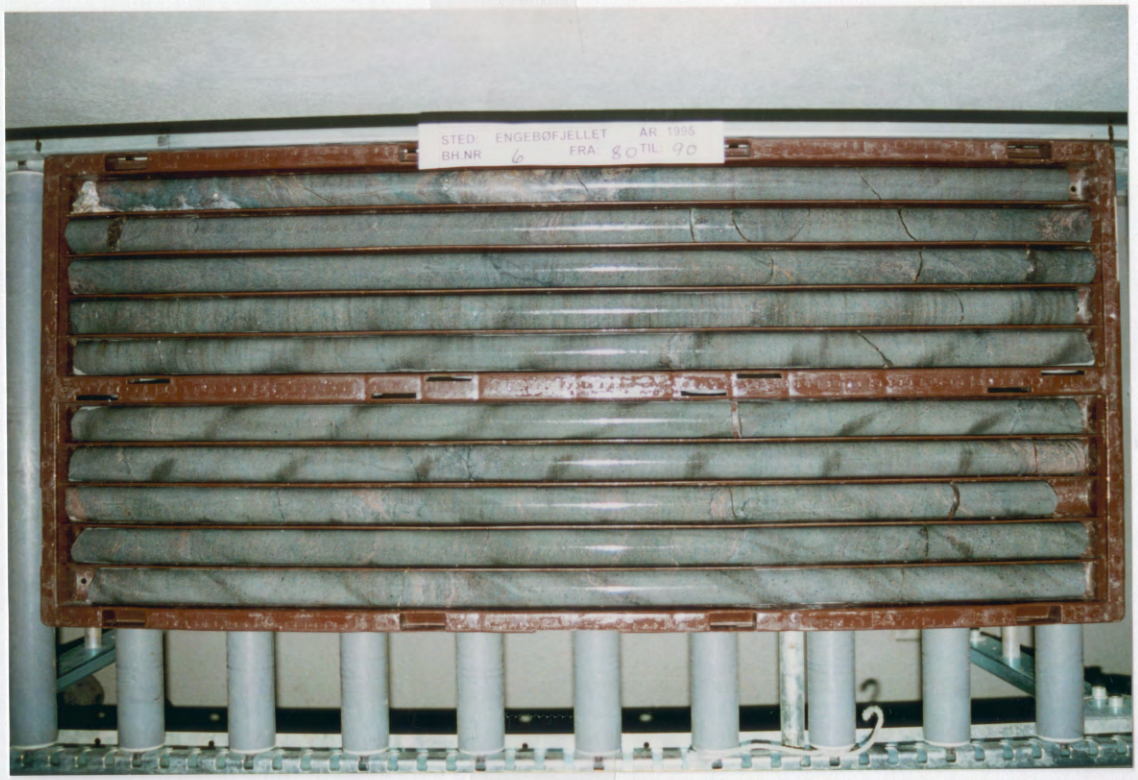
STED: ENGEBØFJELLET ÅR: 1995
BH.NR. 6 FRA: 80 TIL: 90

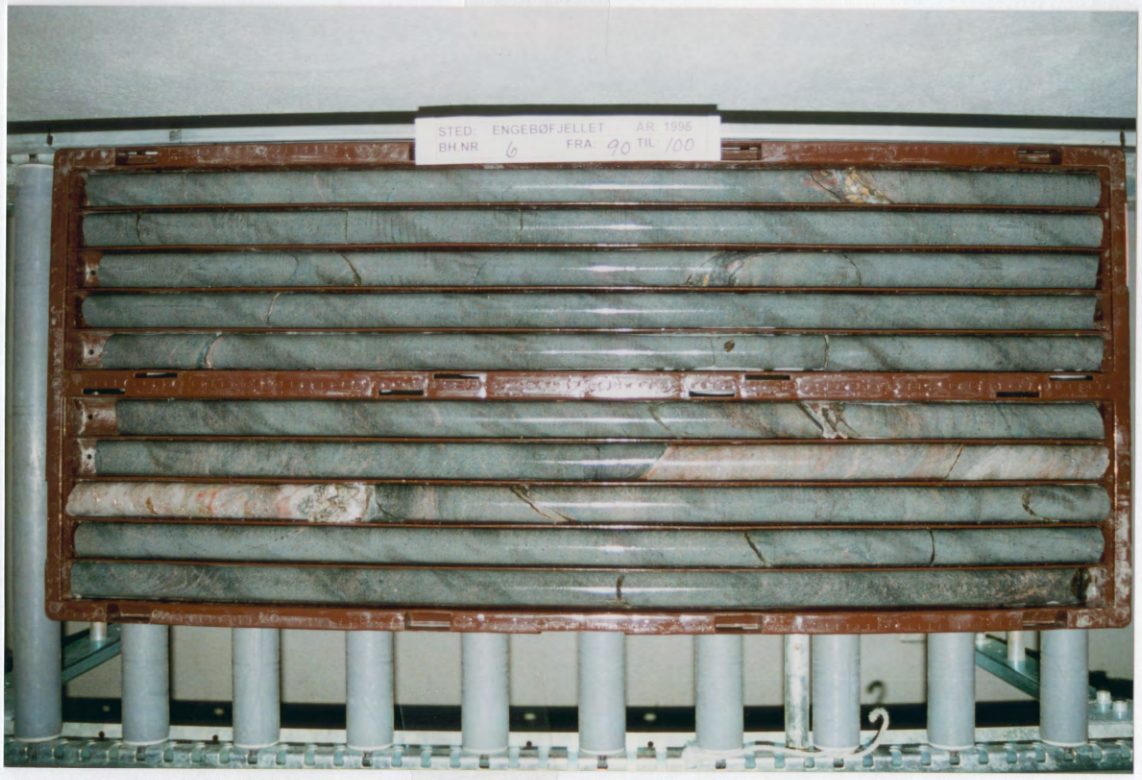
STED: ENGEBØFJELLET ÅR: 1995
BH.NR. 6 FRA: 90 TIL: 100

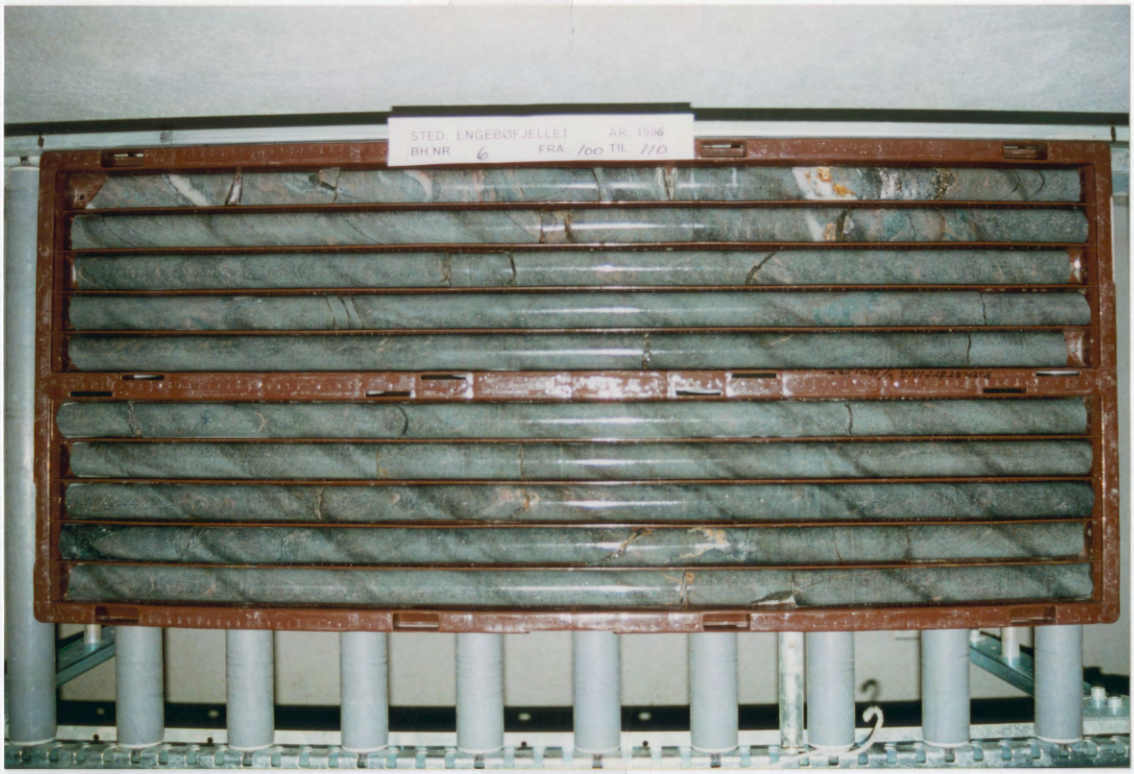
STED: ENGEBØFJELLET ÅR: 1996
BH.NR 6 FRA: 100 TIL: 110

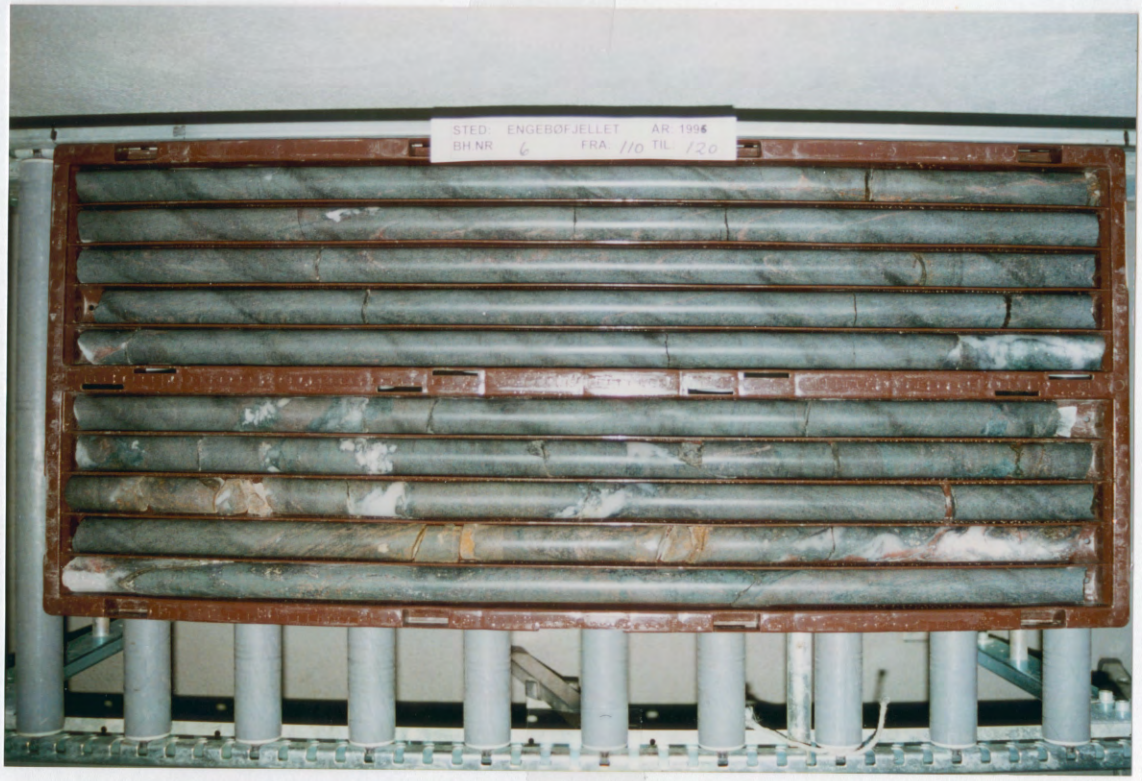
STED: ENGEBØFJELLET ÅR: 1996
BH.NR 6 FRA: 110 TIL: 120


STED: ENGEBØFJELLET ÅR: 1996
BH.NR 6 FRA 120 TIL 130


STED: ENGEBØFJELLET ÅR: 1996
BH.NR 6 FRA: 120 TIL: 130

Appendix 8b:

Photographs of 10m core sections

Dh7

Photographed at NGU's core storage at Løkken


STED: ENGEBØFJELLET AR: 1995
BH.NR 7 FRA: 0 TIL: 10

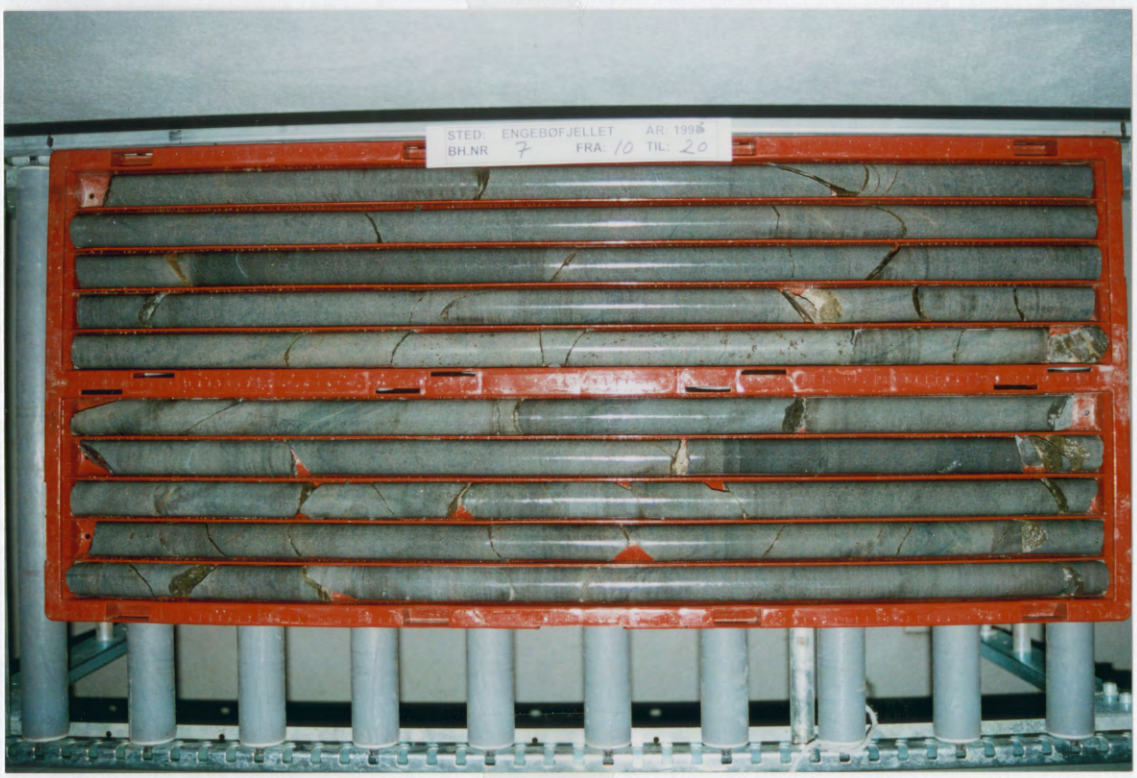
STED: ENGEBØFJELLET AR: 1995
BH.NR 7 FRA: 10 TIL: 20


STED: ENGEBØFJELLET ÅR: 1995
BH.NR 7 FRA: 20 TIL: 30

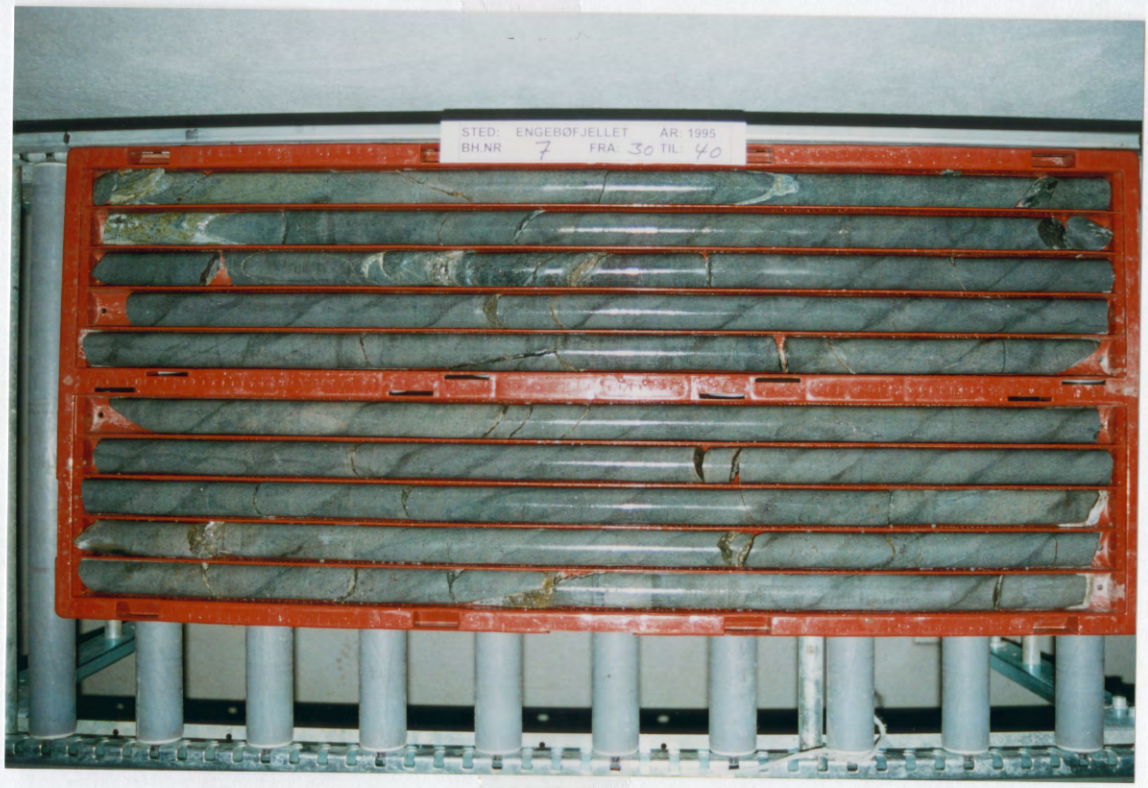
STED: ENGEBØFJELLET ÅR: 1995
BH.NR 7 FRA: 30 TIL: 40

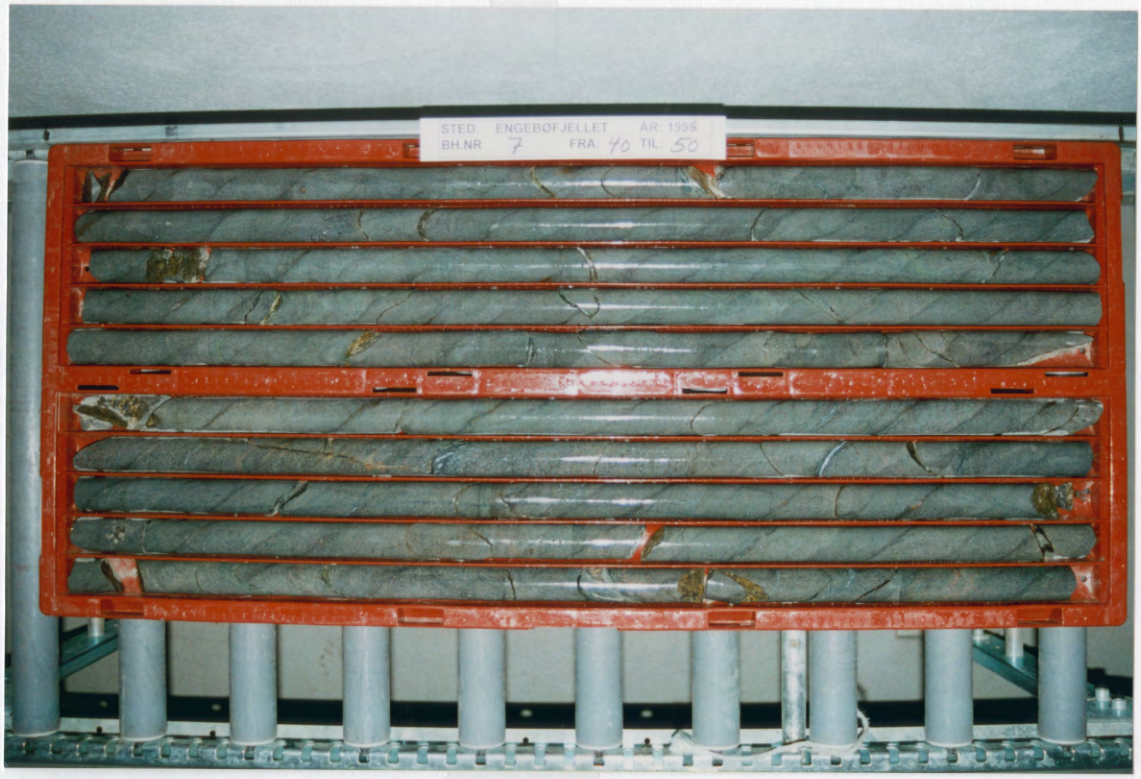
STED: ENGEBØFJELLET ÅR: 1995
BH.NR 7 FRA: 40 TIL: 50

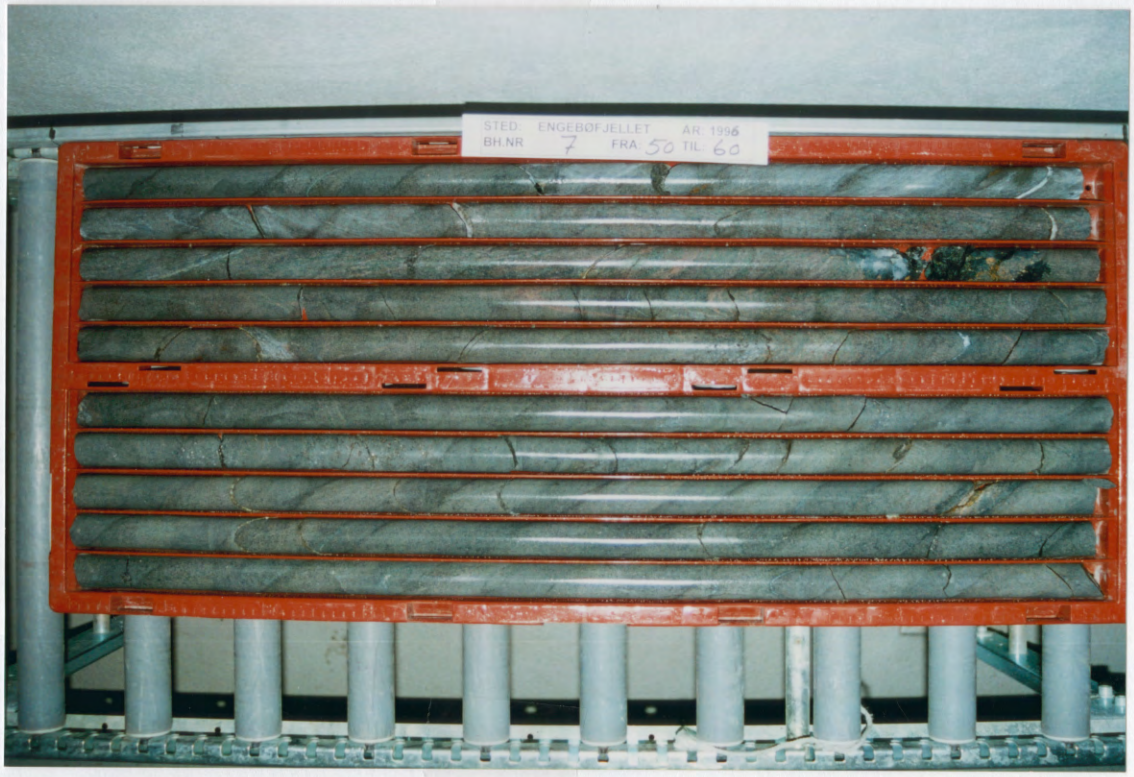
STED: ENGEBØFJELLET ÅR: 1995
BH.NR 7 FRA: 50 TIL: 60


STED: ENGEBØFJELLET ÅR: 1996
BH.NR 7 FRA: 60 TIL: 70

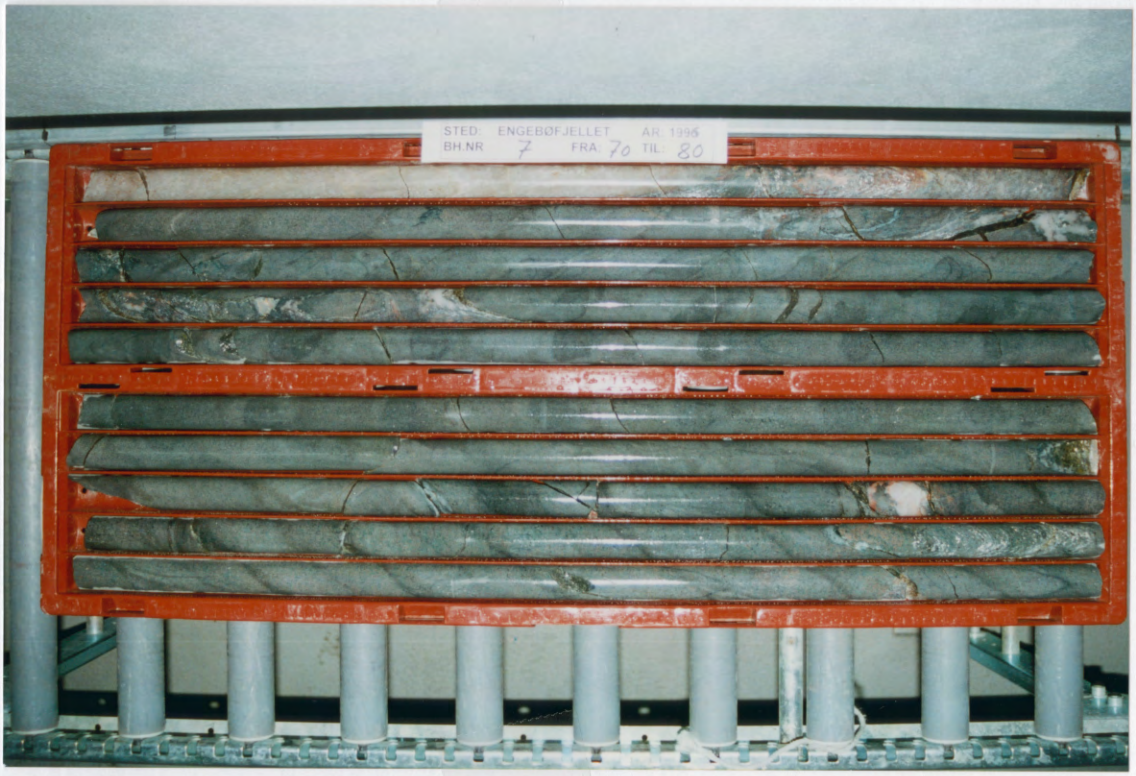
STED: ENGEBØFJELLET ÅR: 1996
BH.NR 7 FRA: 70 TIL: 80

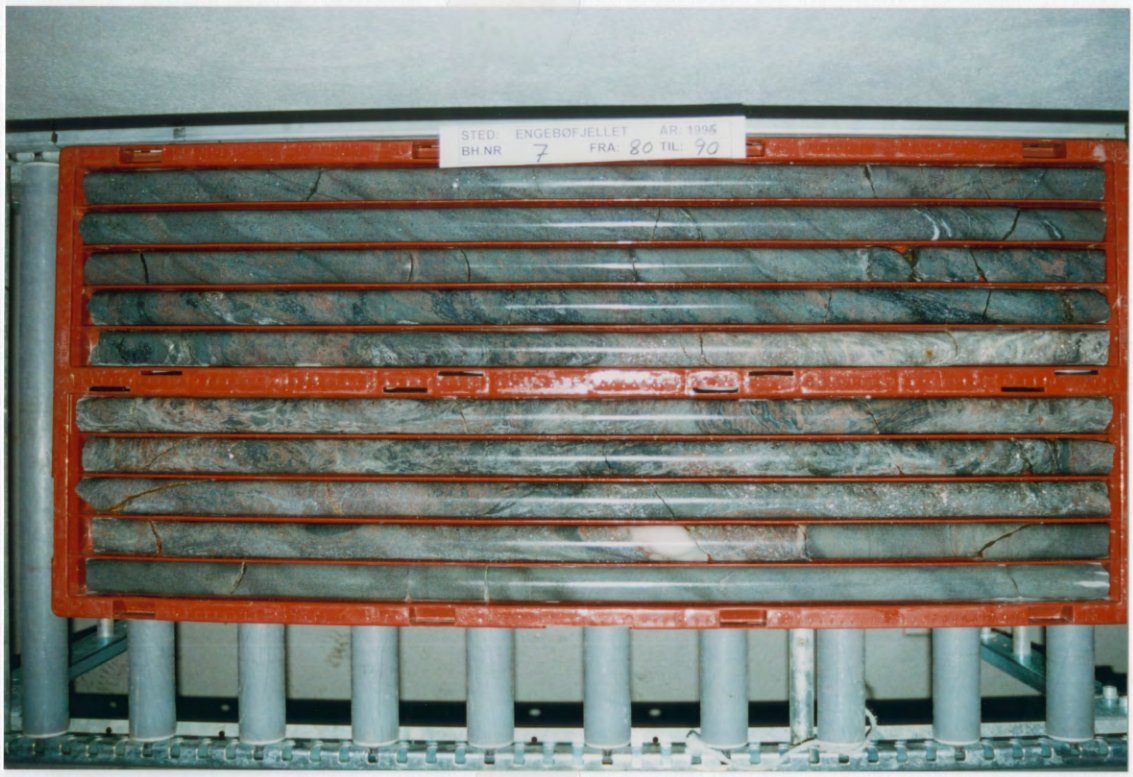
STED: ENGEBØFJELLET ÅR: 1995
BH.NR 7 FRA: 80 TIL: 90

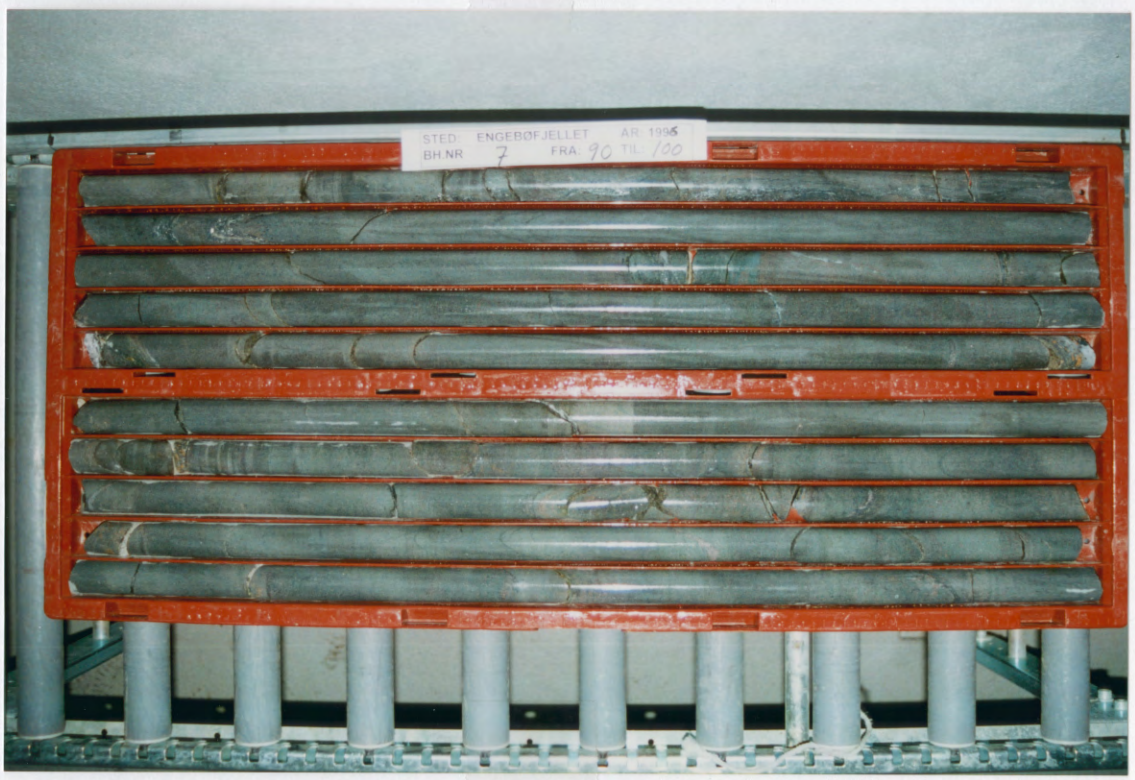
STED: ENGEBØFJELLET ÅR: 1995
BH.NR 7 FRA: 90 TIL: 100

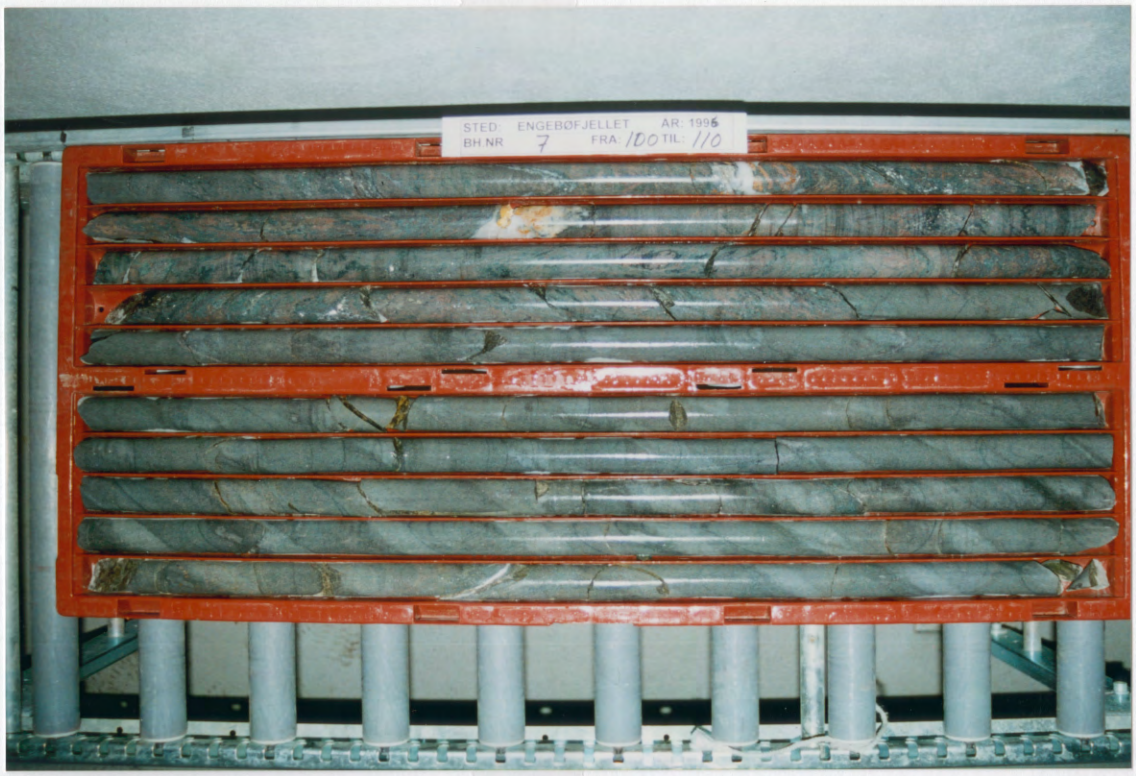
STED: ENGEBØFJELLET ÅR: 1996
BH.NR 7 FRA: 100 TIL: 110

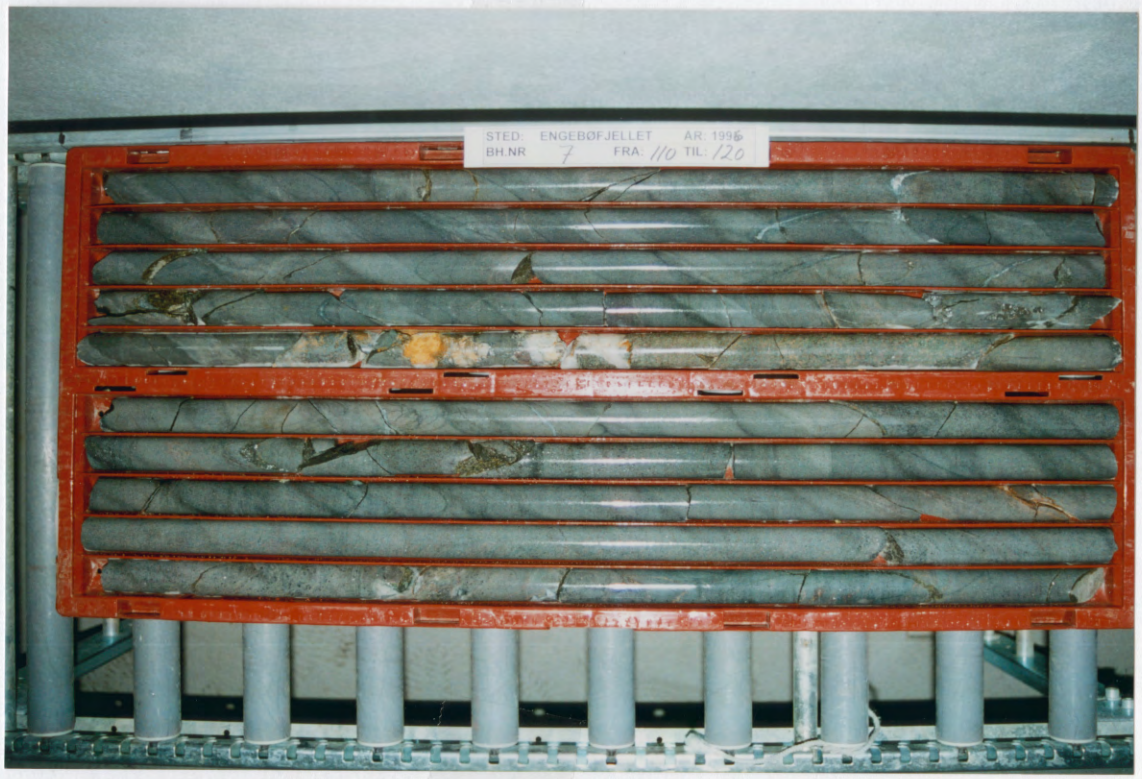
STED: ENGEBØFJELLET ÅR: 1996
BH.NR 7 FRA: 110 TIL: 120

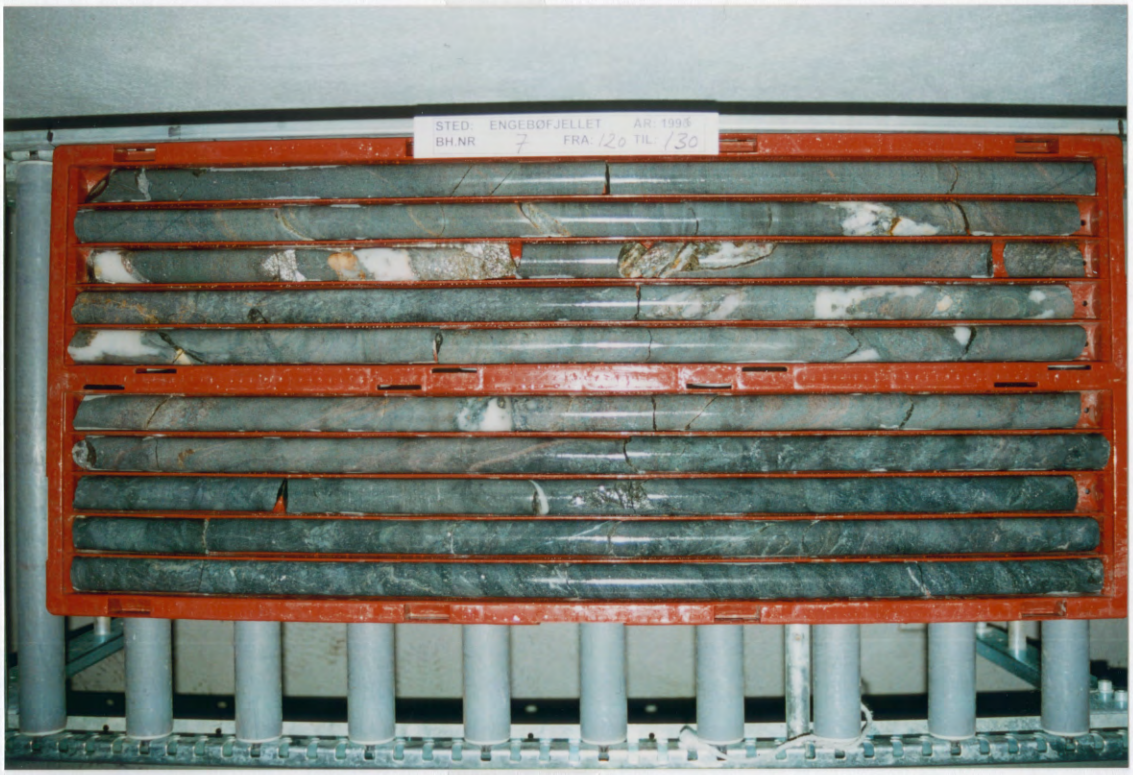
STED: ENGEBØFJELLET ÅR: 1995
BH.NR 7 FRA: 120 TIL: 130


STED: ENGEBØFJELLET ÅR: 1995
BH.NR 7 FRA: 130 TIL: 140

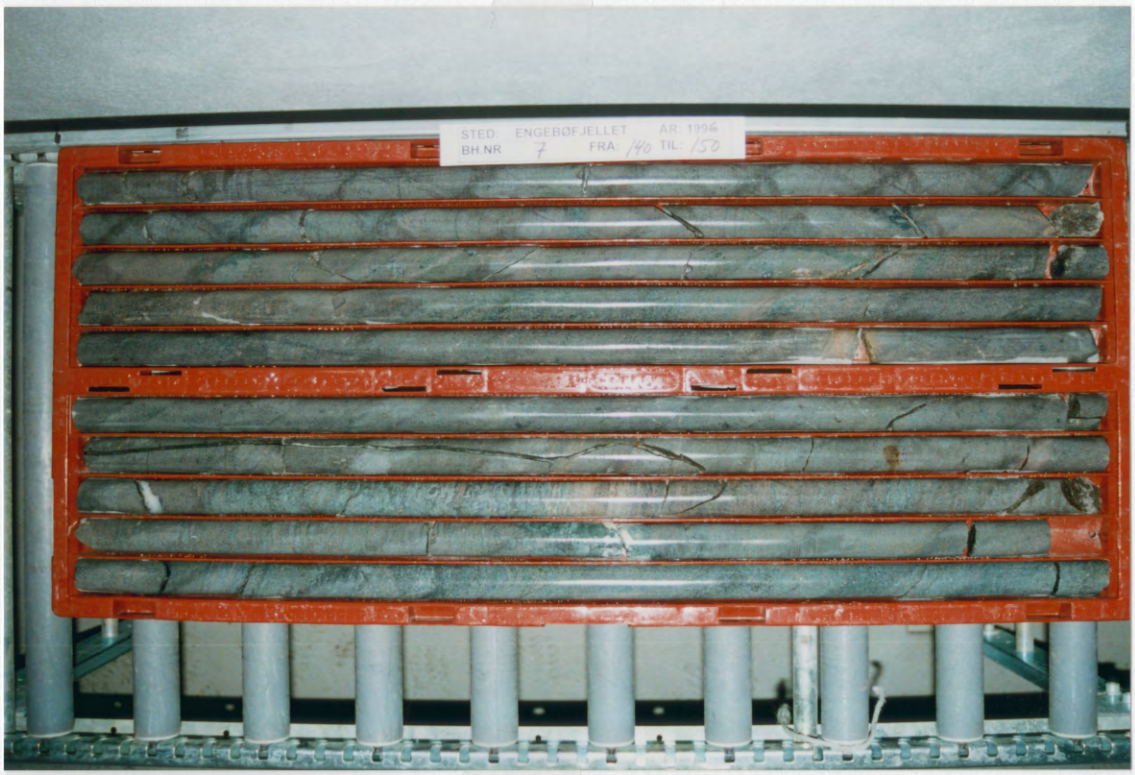
STED: ENGEBØFJELLET ÅR: 1996
BH.NR 7 FRA: 140 TIL: 150


STED: ENGEBØFJELLET ÅR: 1996
BH.NR 7 FRA: 150 TIL: 160


STED: ENGEBØFJELLET ÅR: 1995
BH.NR 7 FRA: 160 TIL: 170

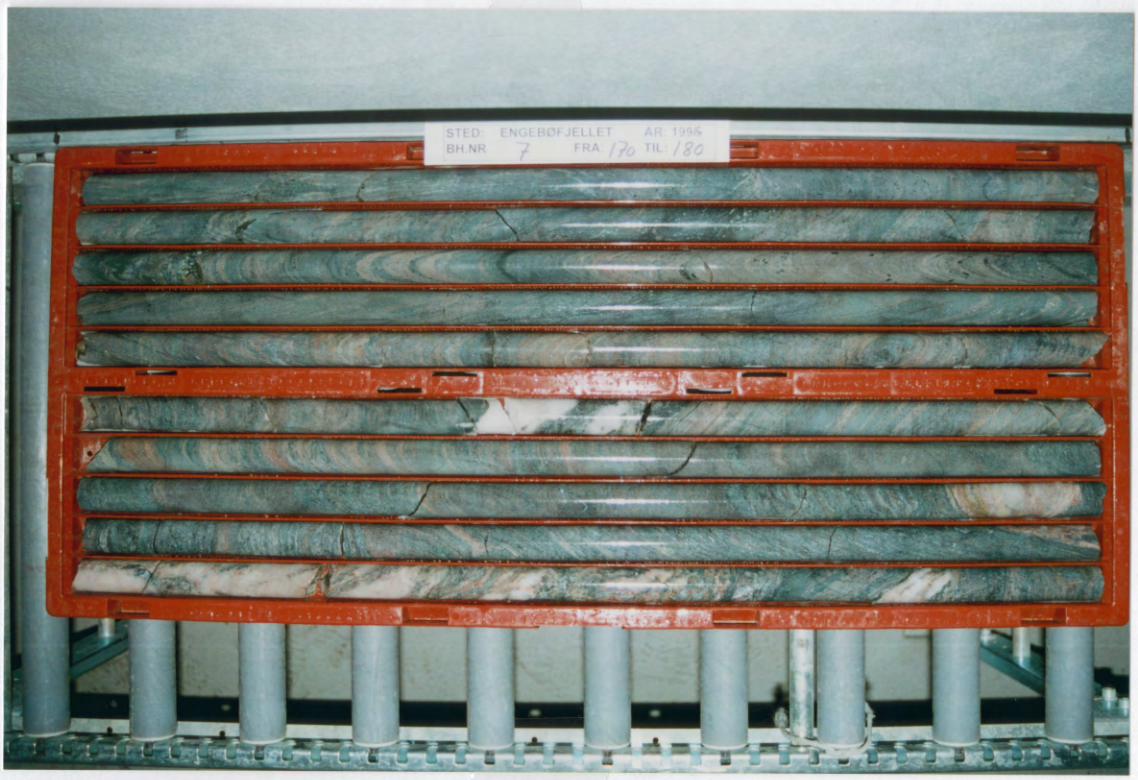
STED: ENGEBØFJELLET ÅR: 1995
BH.NR 7 FRA: 170 TIL: 180

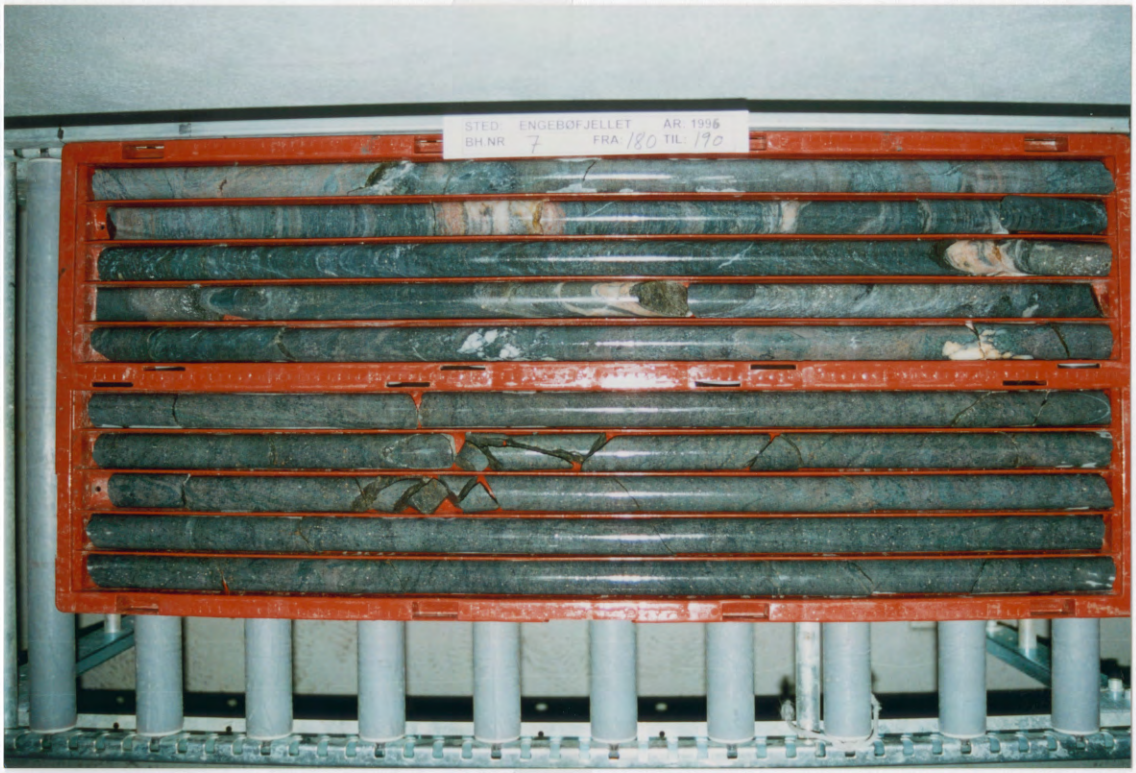
STED: ENGEBØFJELLET ÅR: 1996
BH.NR 7 FRA: 180 TIL: 190

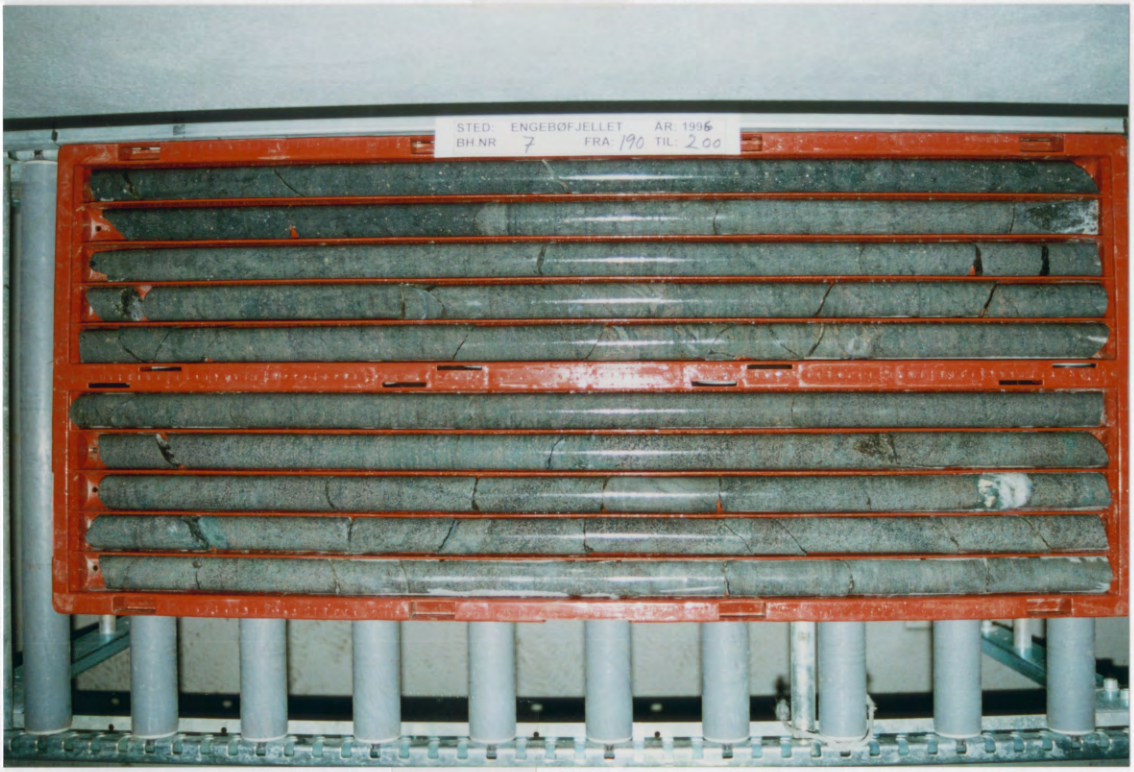
STED: ENGEBØFJELLET ÅR: 1996
BH.NR 7 FRA: 190 TIL: 200

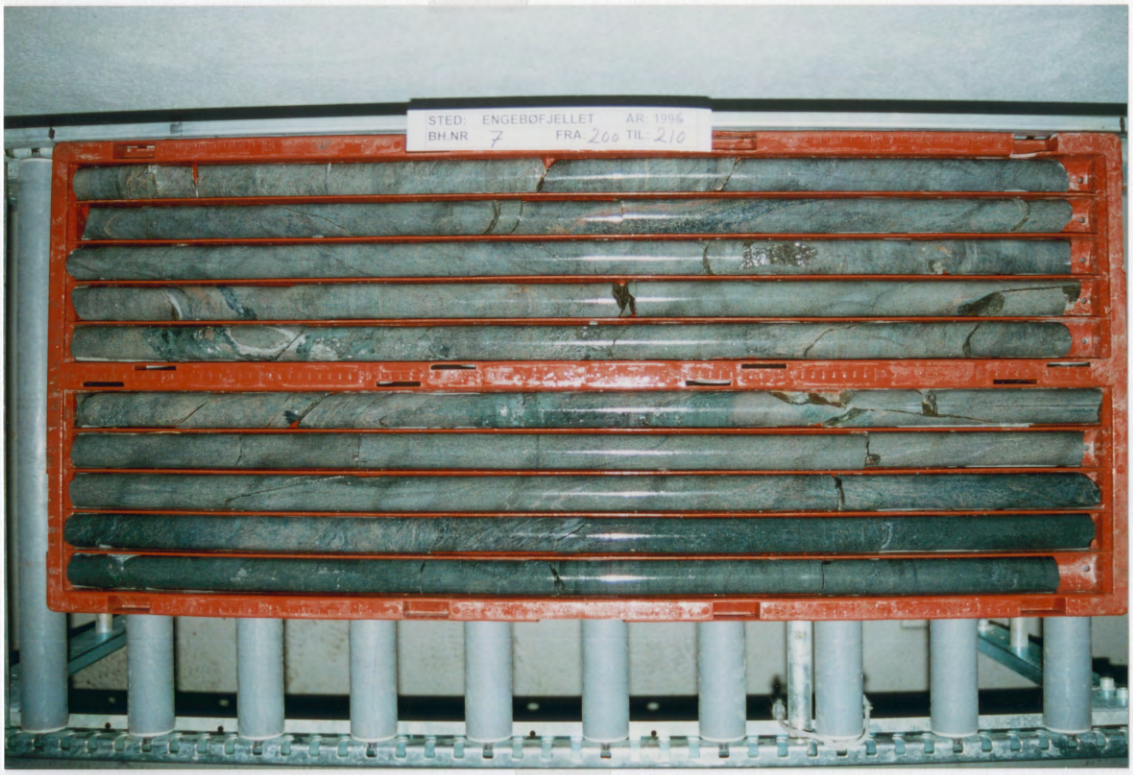
STED: ENGEBØFJELLET ÅR: 1996
BH.NR 7 FRA: 200 TIL: 210


STED: ENGEBØFJELLET ÅR: 1996
BH.NR 7 FRA: 210 TIL: 220

Appendix 8c:

Photographs of 10m core sections

Dh8

Photographed at NGU's core storage at Løkken

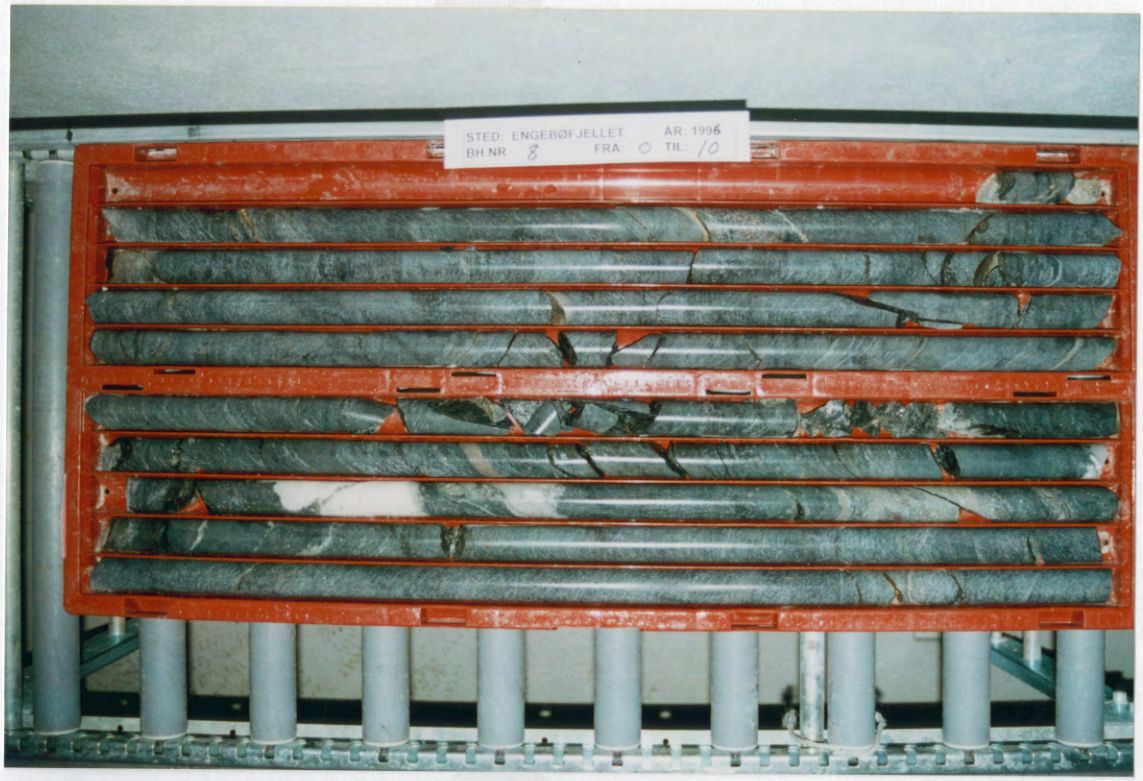
STED: ENGEBØFJELLET ÅR: 1996
BH.NR 8 FRA: 0 TIL: 10

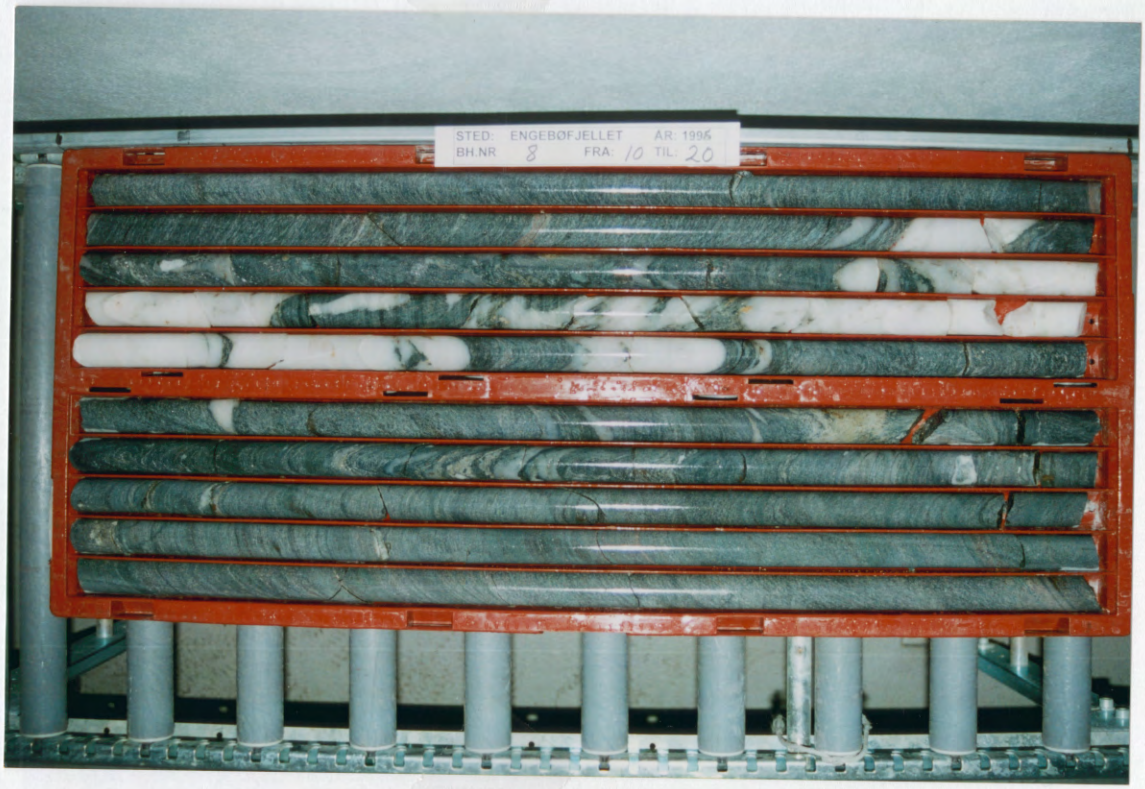
STED: ENGEBØFJELLET ÅR: 1996
BH.NR 8 FRA: 10 TIL: 20

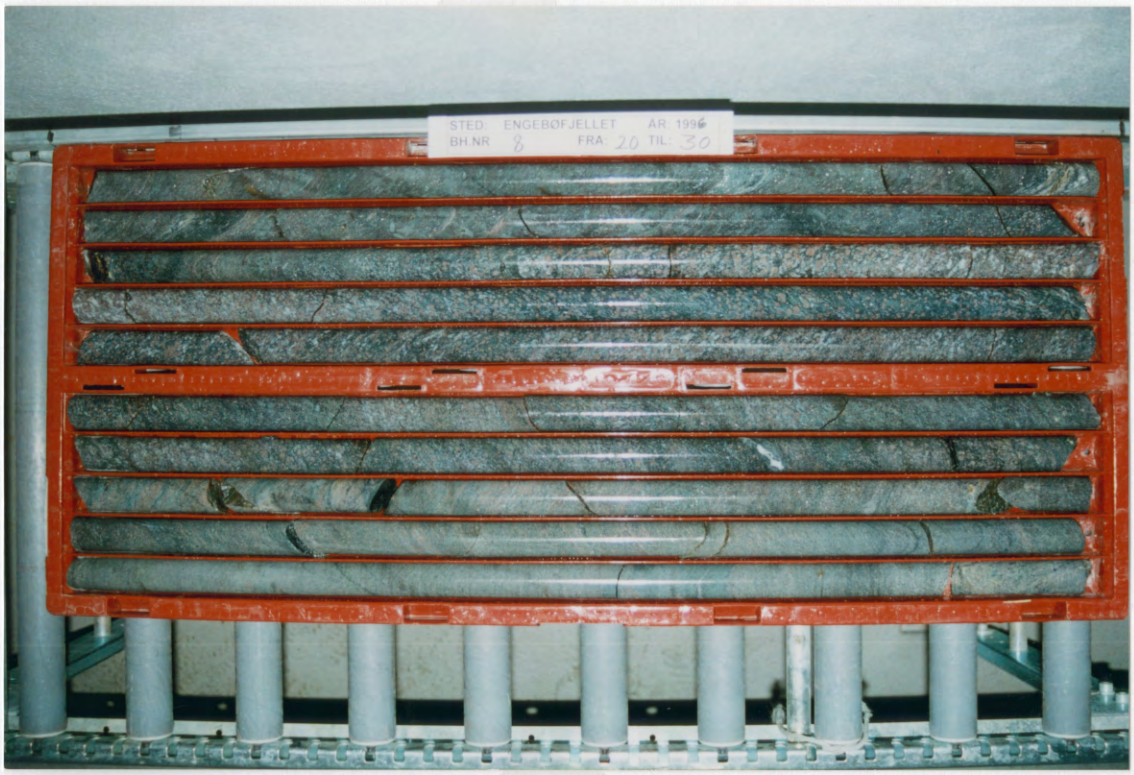
STED: ENGEBØFJELLET ÅR: 1996
BH.NR 8 FRA: 20 TIL: 30

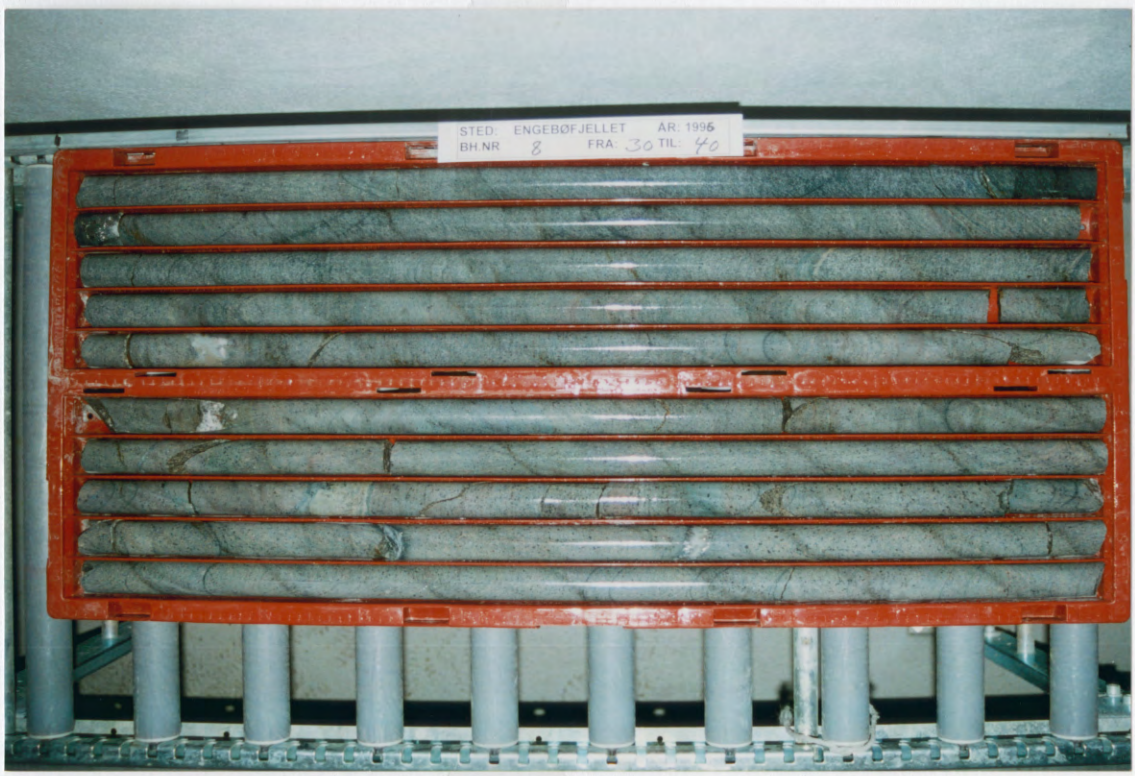
STED: ENGEBØFJELLET ÅR: 1996
BH.NR 8 FRA: 30 TIL: 40


STED: ENGEBØFJELLET ÅR: 1996
BH.NR 8 FRA: 40 TIL: 50


STED: ENGEBØFJELLET ÅR: 1996
BH.NR 8 FRA: 50 TIL: 60

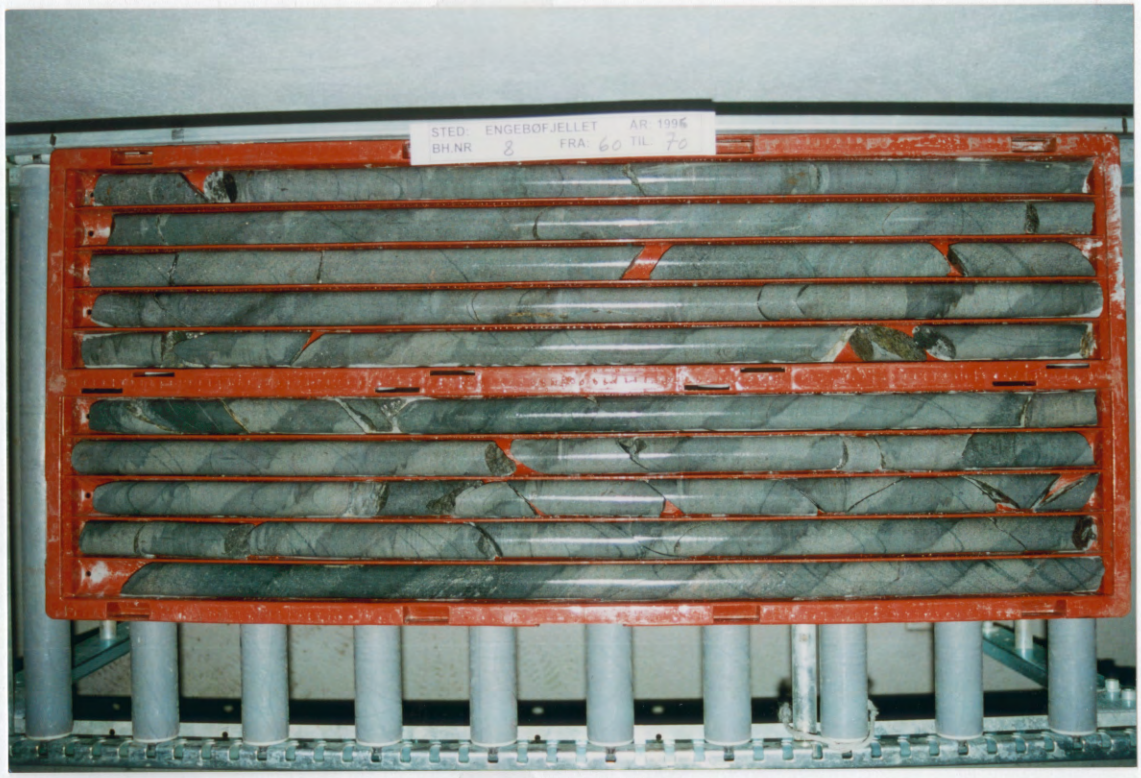
STED: ENGEBØFJELLET ÅR: 1996
BH.NR 8 FRA: 60 TIL: 70


STED: ENGEBØFJELLET ÅR: 1996
BH.NR 8 FRA: 70 TIL: 80


STED: ENGEBØFJELLET ÅR: 1996
BH.NR 8 FRA: 80 TIL: 90


STED: ENGEBØFJELLET ÅR: 1996
BH.NR 8 FRA: 90 TIL: 100

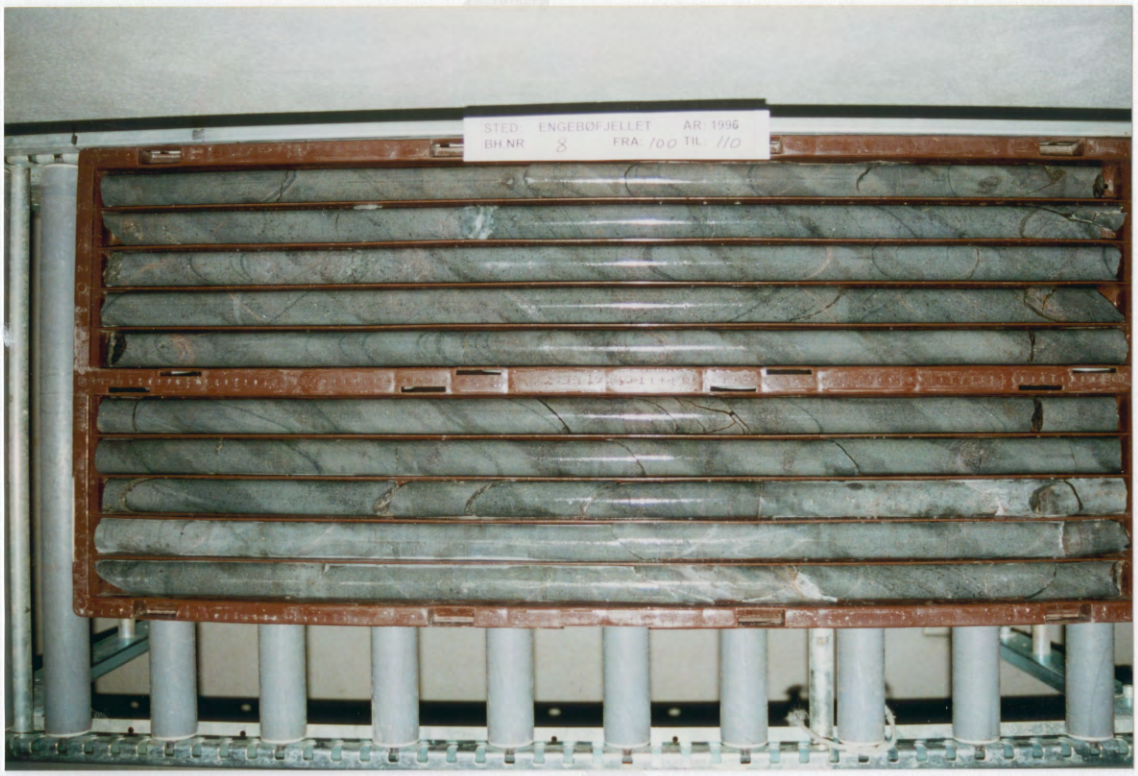
STED: ENGEBØFJELLET ÅR: 1996
BH.NR 8 FRA: 100 TIL: 110


STED: ENGEBØFJELLET ÅR: 1996
BH.NR 8 FRA: 110 TIL: 120

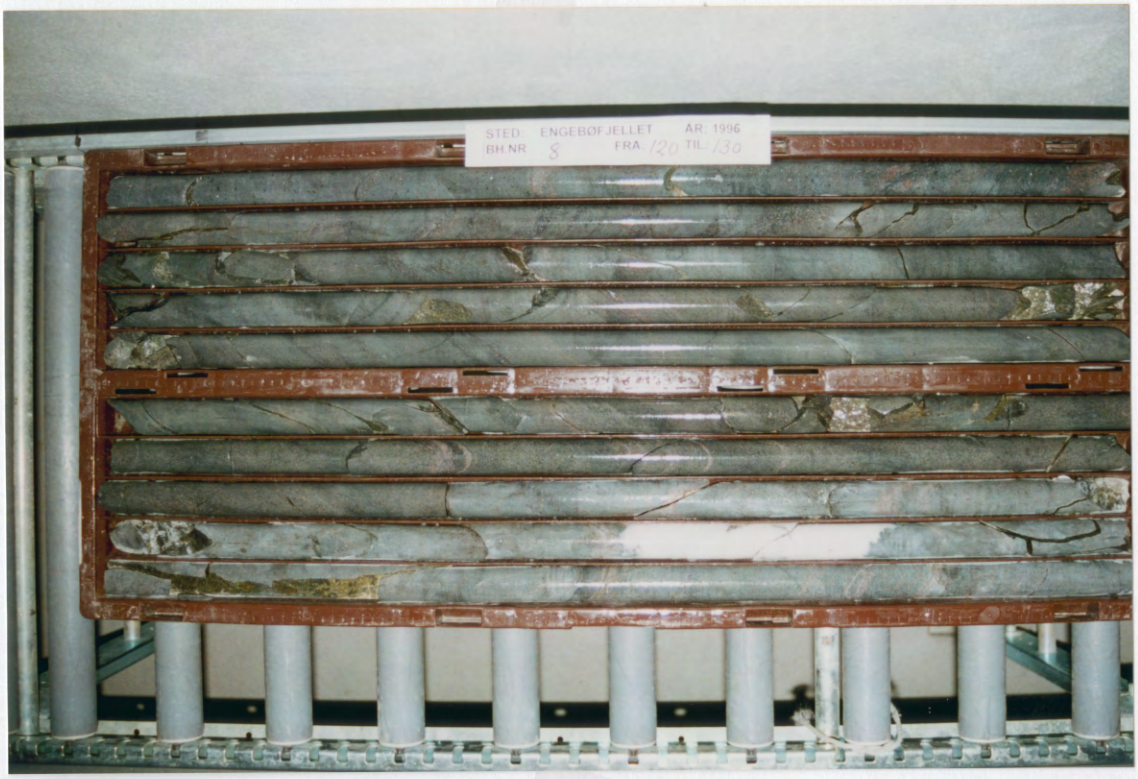
STED: ENGEBØFJELLET ÅR: 1996
BH.NR 8 FRA: 120 TIL: 130

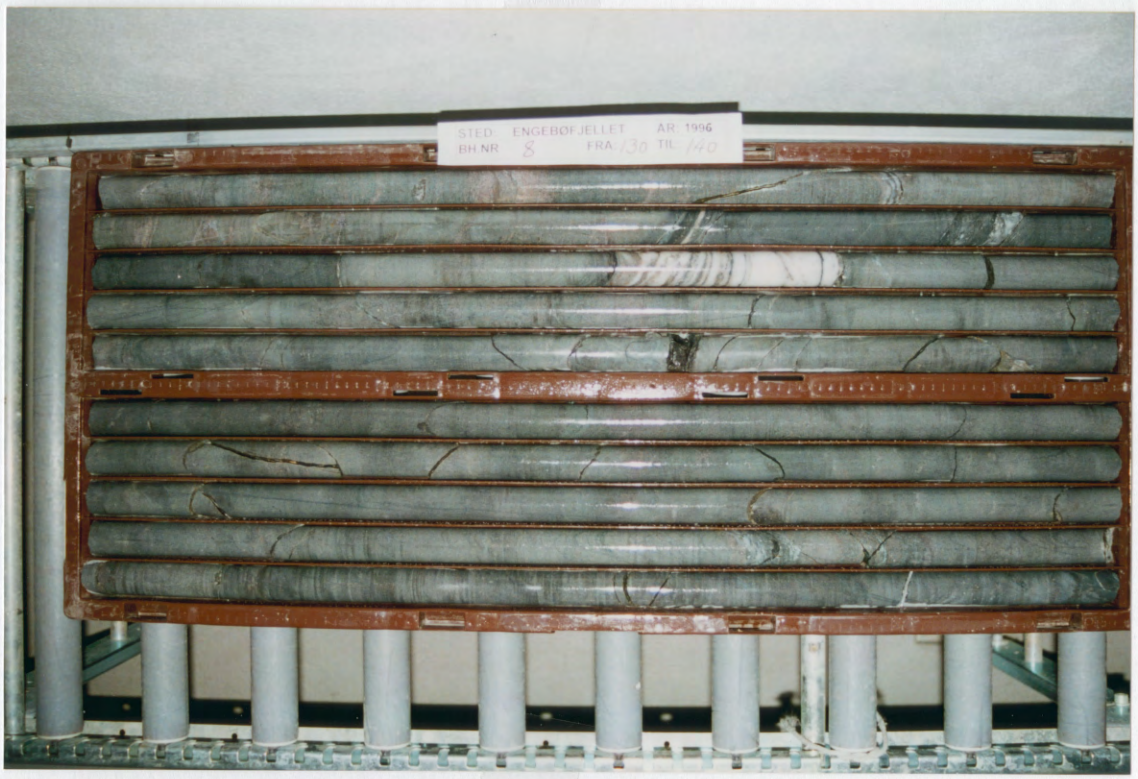
STED: ENGEBØFJELLET ÅR: 1996
BH.NR 8 FRA: 130 TIL: 140


STED: ENGEBØFJELLET AR: 1996
BH.NR 8 FRA: 140 TIL: 150


STED: ENGEBØFJELLET AR: 1996
BH.NR 8 FRA: 150 TIL: 160

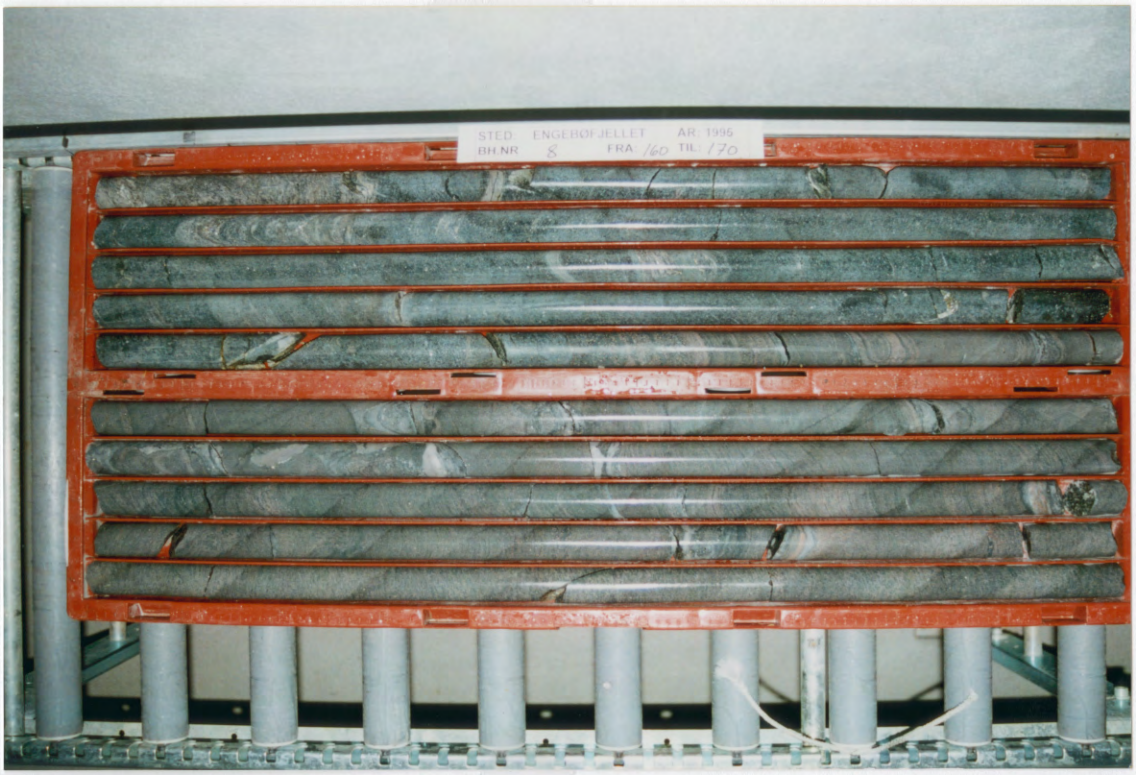
STED: ENGEBØFJELLET ÅR: 1995
BH.NR 8 FRA 160 TIL 170

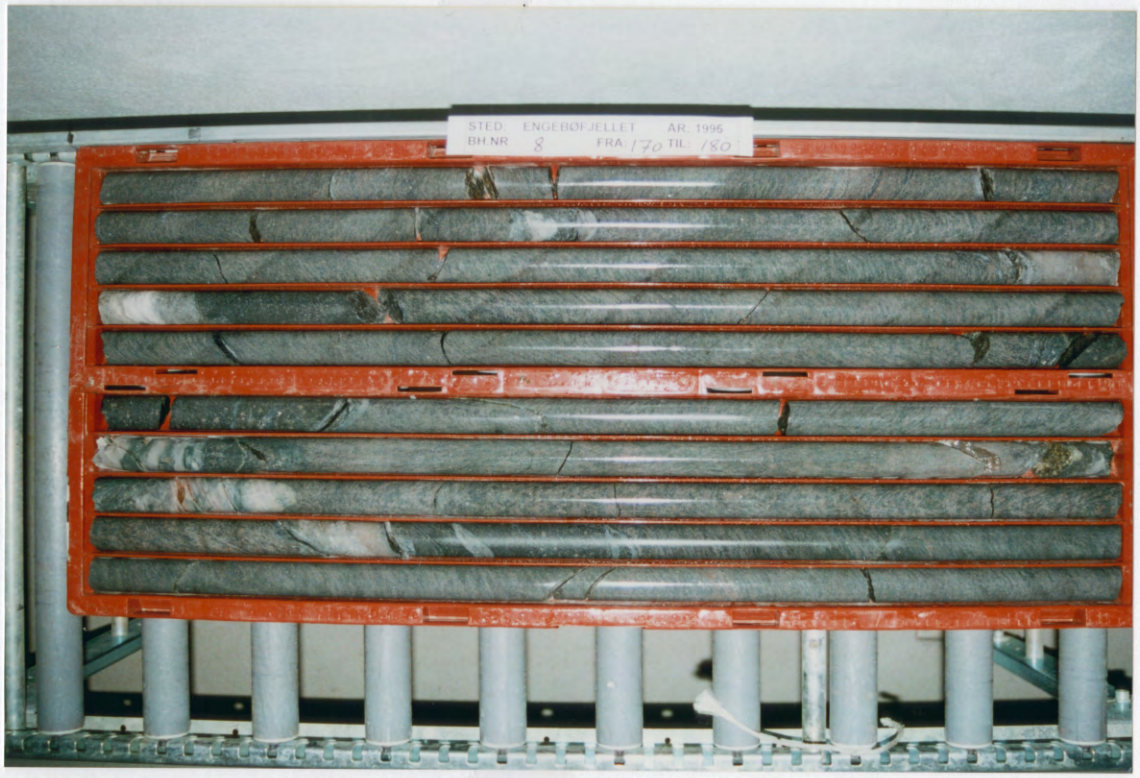
STED: ENGEBØFJELLET ÅR: 1995
BH.NR 8 FRA 170 TIL 180

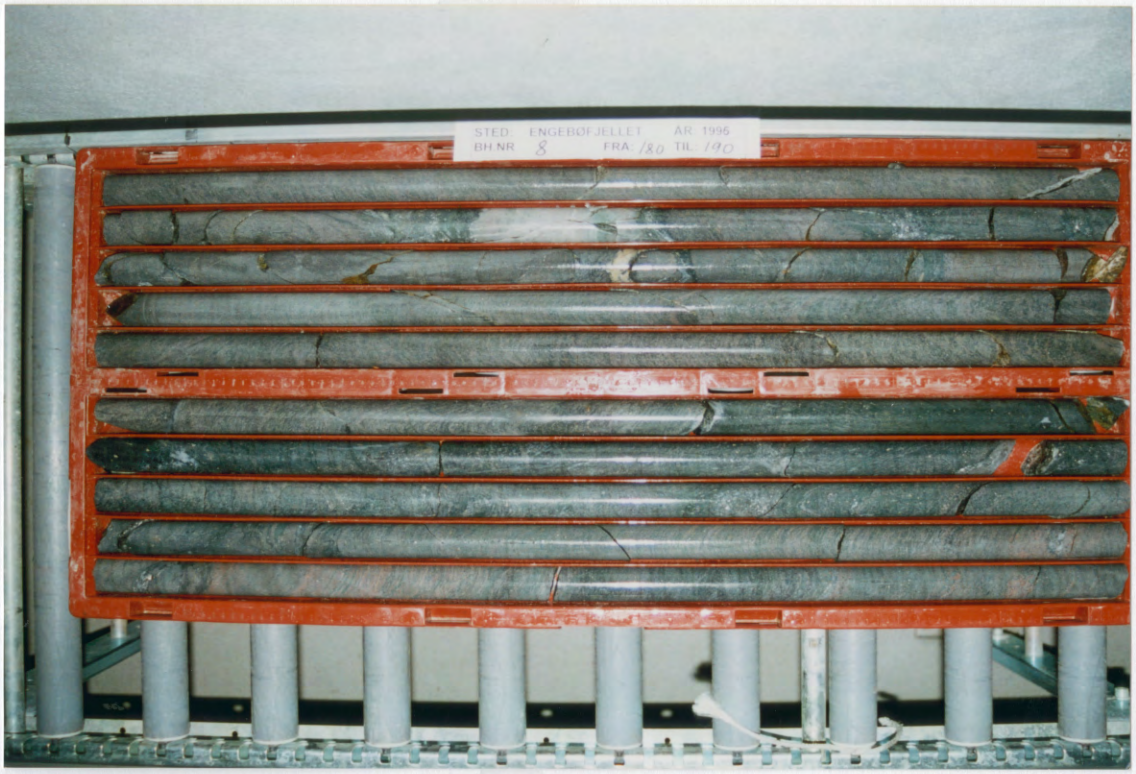
STED: ENGEBØFJELLET ÅR: 1995
BH.NR 8 FRA: 180 TIL: 190

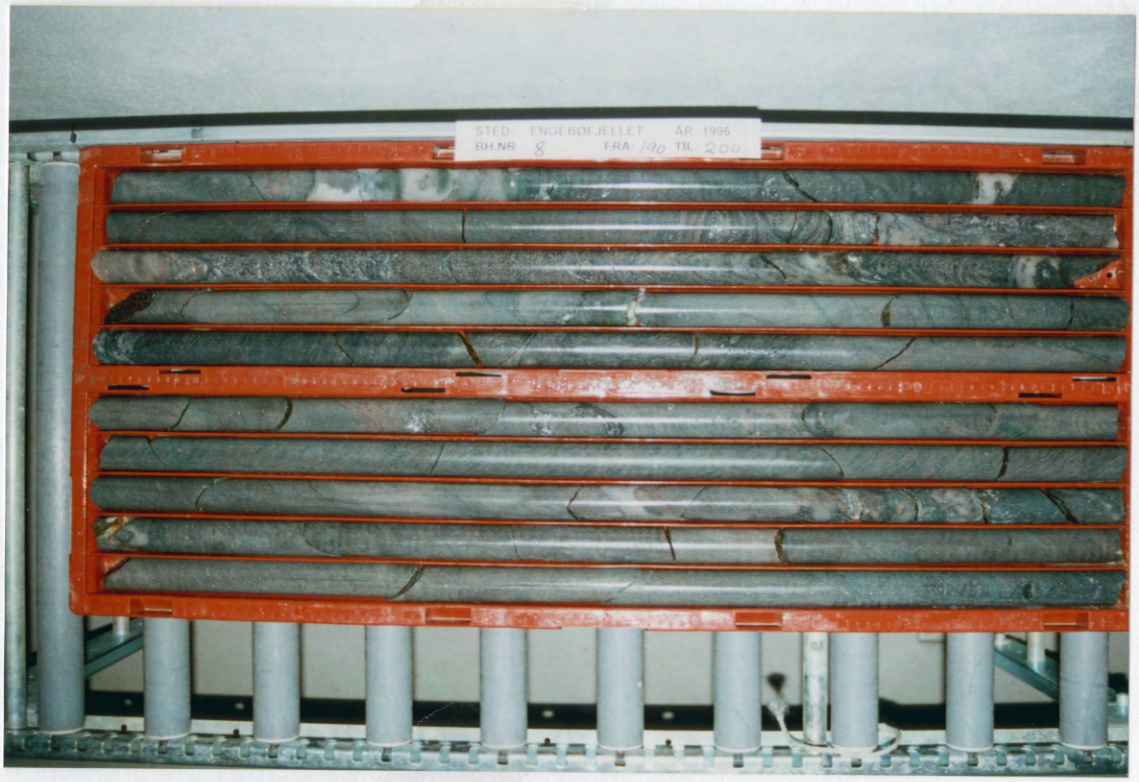
STED: ENGEBØFJELLET ÅR: 1995
BH.NR 8 FRA: 190 TIL: 200


STED: ENGEBØFJELLET ÅR: 1995
BH.NR 8 FRA 200 TIL 210


STED: ENGEBØFJELLET ÅR: 1995
BH.NR 8 FRA 210 TIL 220

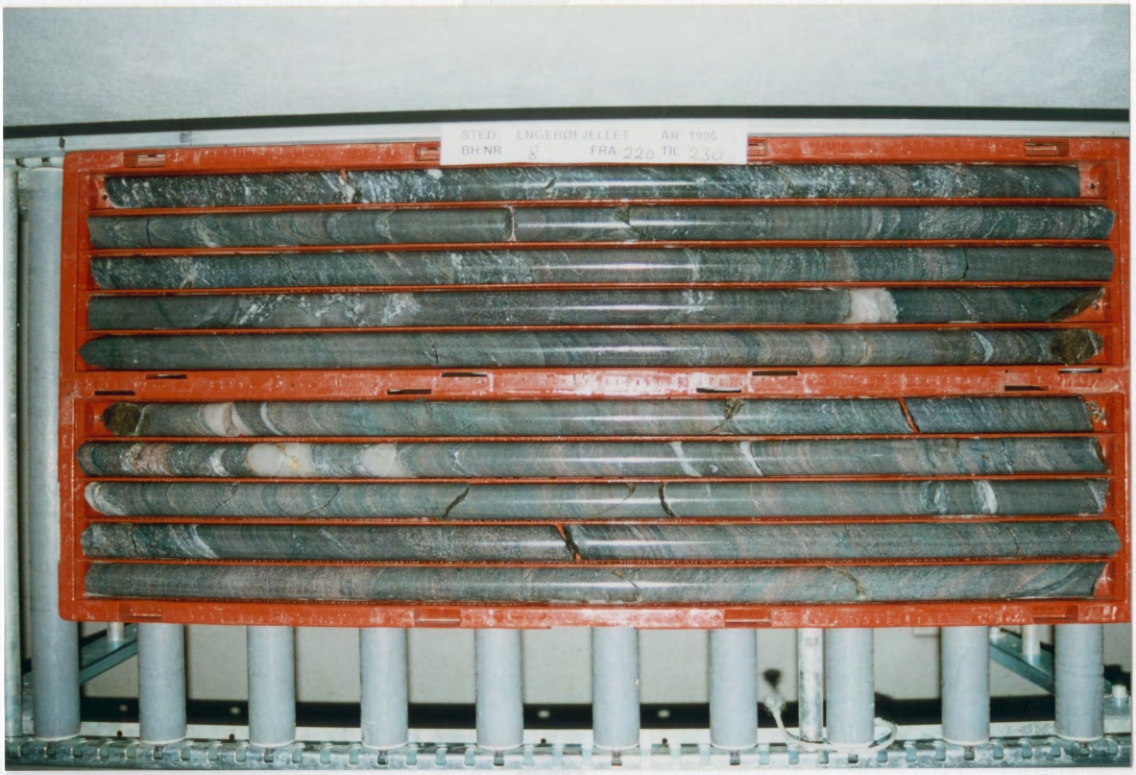
STED: ENGEBØFJELLET ÅR: 1996
BH.NR 8 FRA: 220 TIL: 230

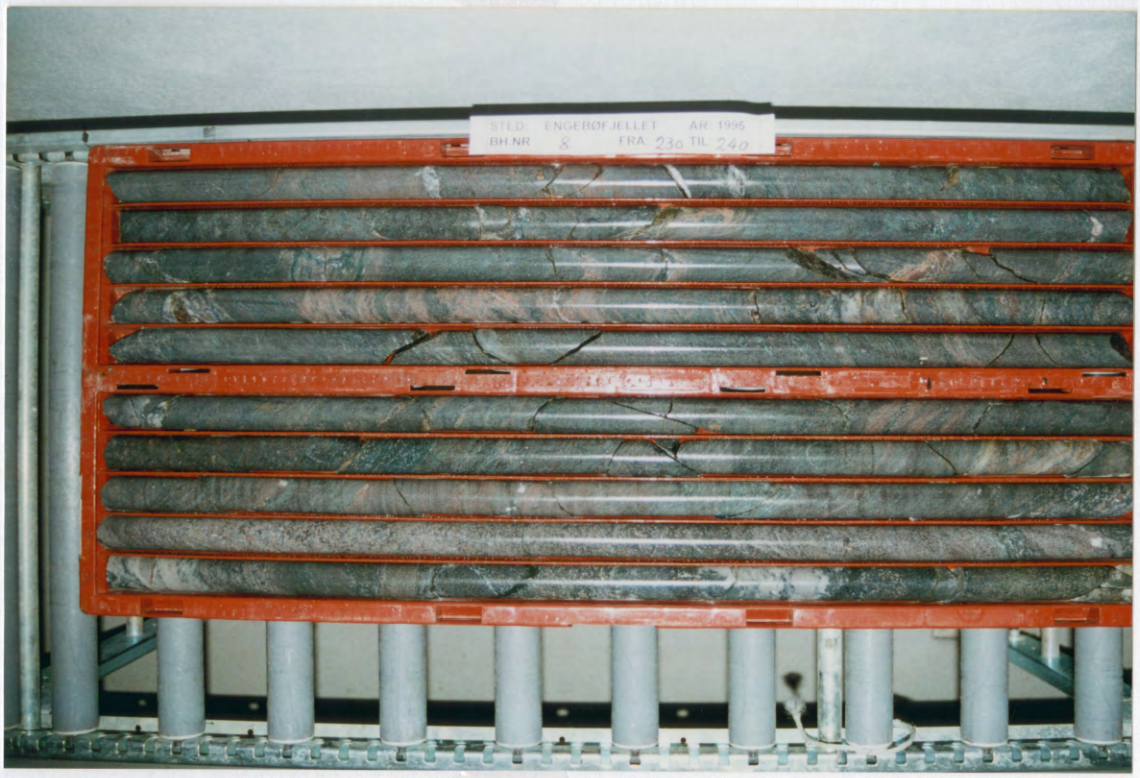
STED: ENGEBØFJELLET ÅR: 1996
BH.NR 8 FRA: 230 TIL: 240

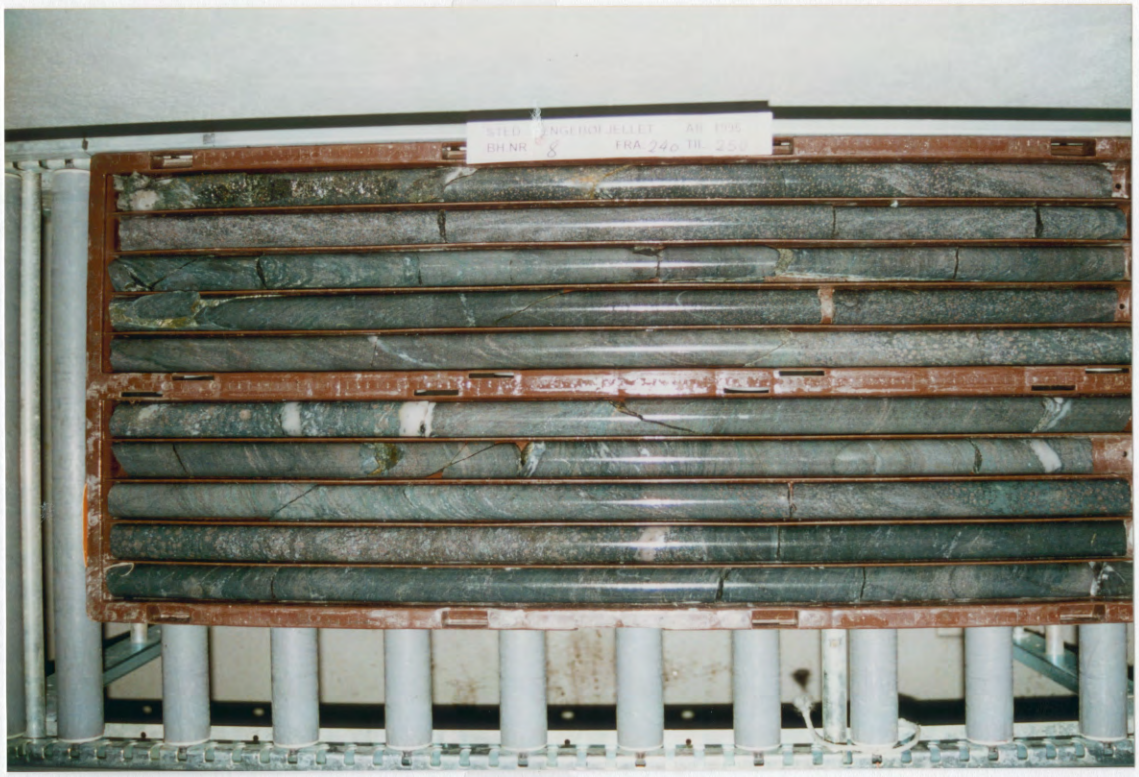
STED ENGEBØFJELLET ÅR 1995
BH NR 8 FRA 246 TIL 248


STED ENGEBØFJELLET ÅR 1995
BH NR 8 FRA 250 TIL 252

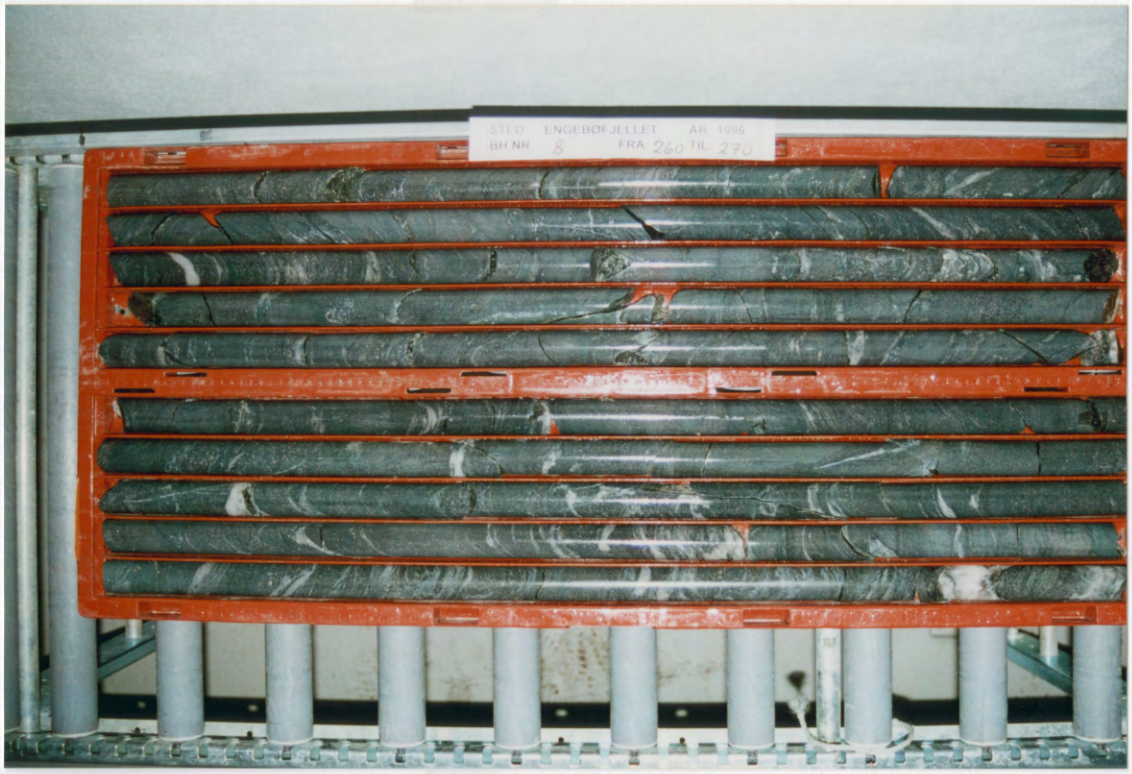
STED ENGEBØFJELLET ÅR 1995
BH.NR 8 FRA 260 TIL 270

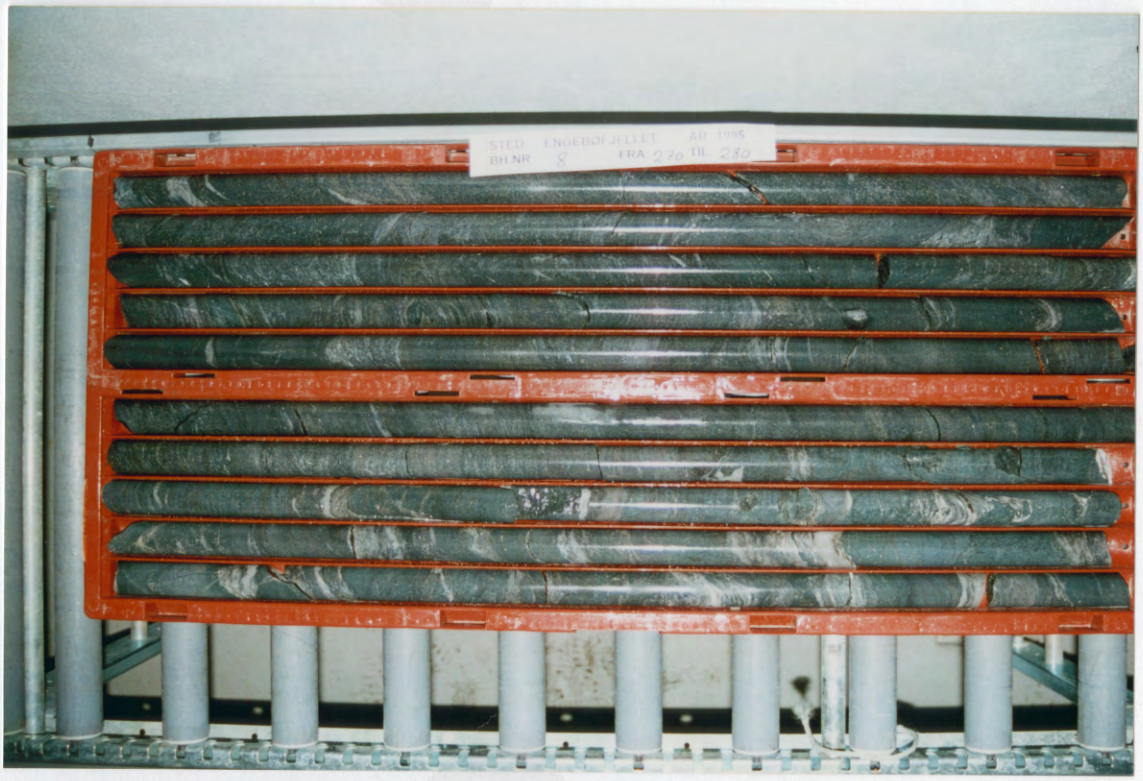
STED ENGEBØFJELLET ÅR 1995
BH.NR 8 FRA 270 TIL 280

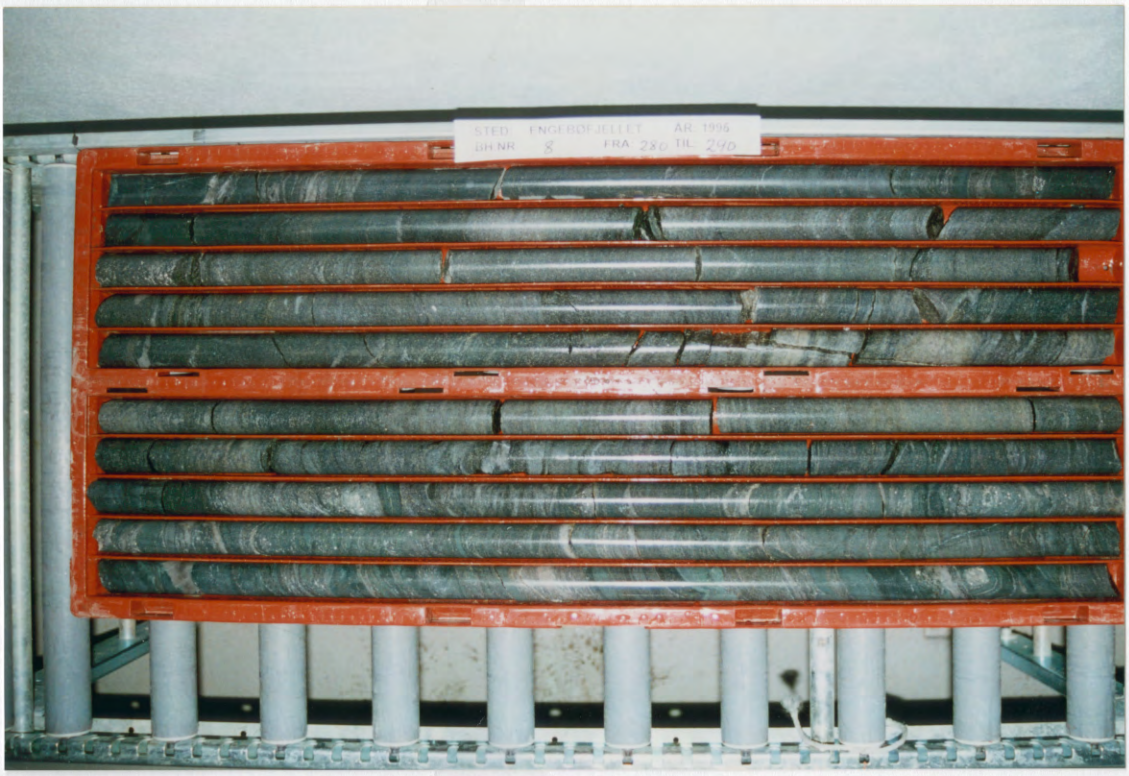
STED: ENGEBØFJELLET ÅR: 1996
BH.NR 8 FRA 280 TIL 290

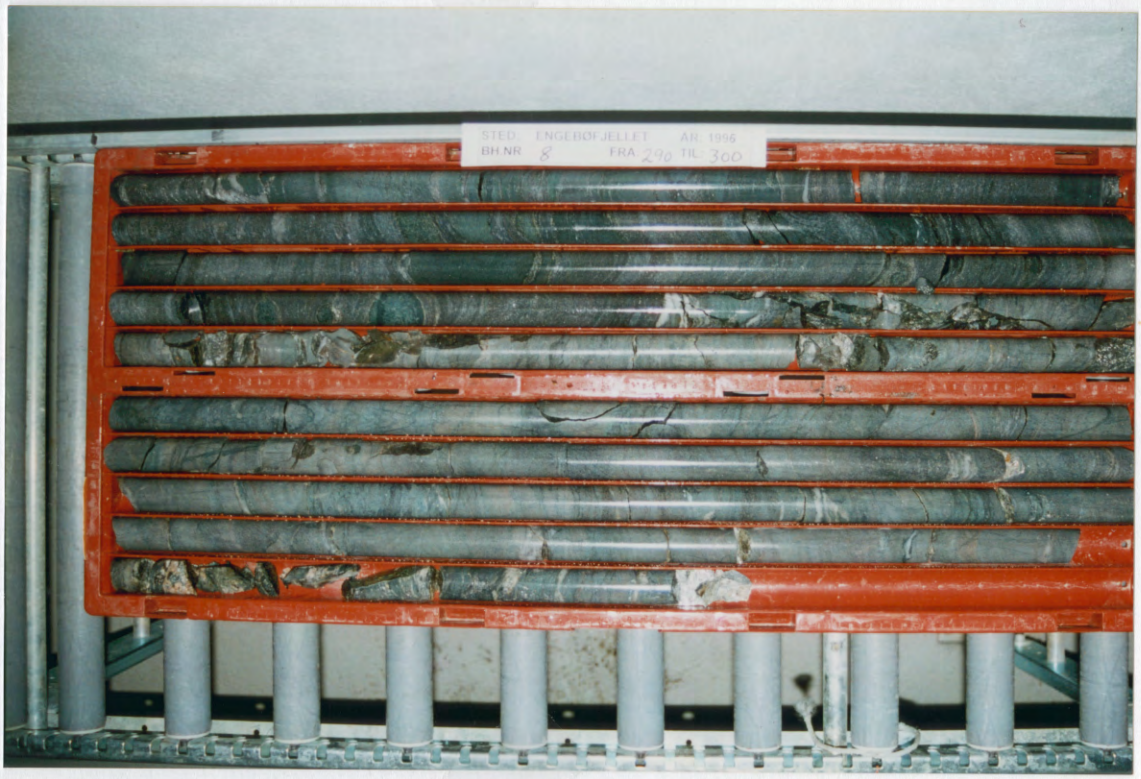
STED: ENGEBØFJELLET ÅR: 1996
BH.NR 8 FRA 290 TIL 300

Appendix 8d:

Photographs of 10m core sections

Dh9

Photographed at NGU's core storage at Løkken

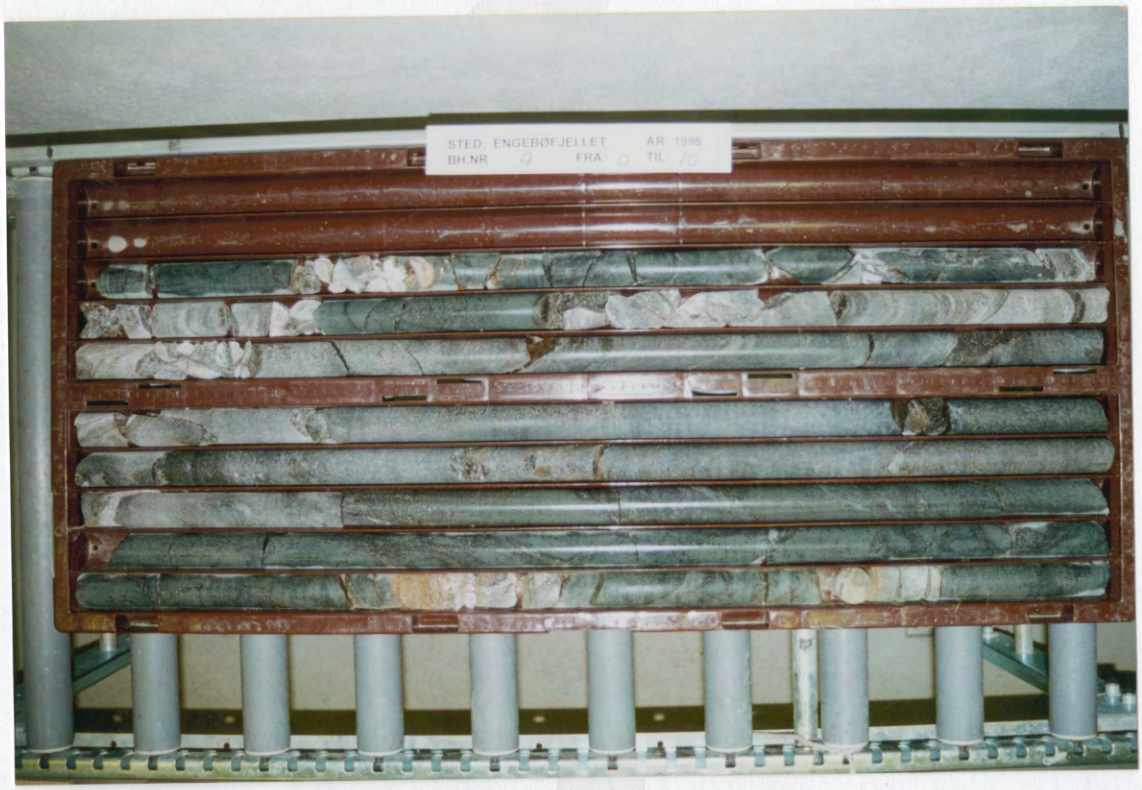
STED: ENGEBØFJELLET ÅR: 1995
BH.NR. 9 FRA: 0 TIL: 10

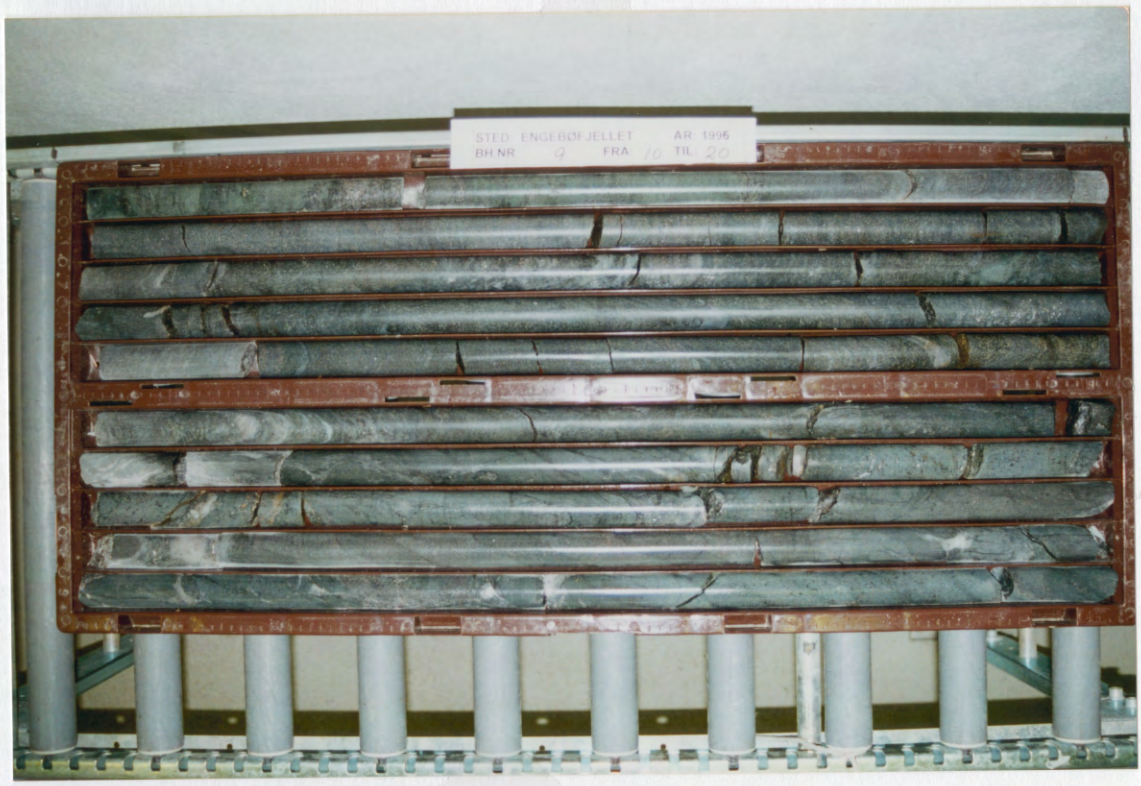
STED: ENGEBØFJELLET ÅR: 1995
BH.NR. 9 FRA: 10 TIL: 20

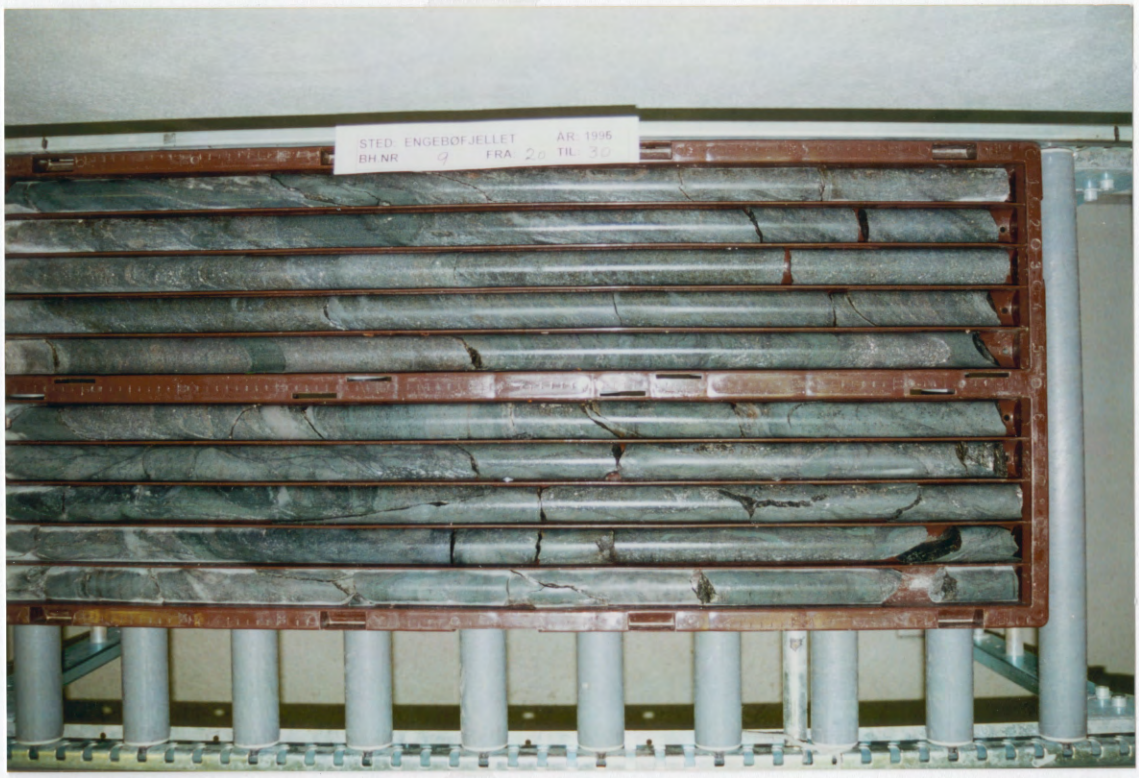
STED: ENGEBØFJELLET ÅR: 1995
BH.NR 9 FRA: 20 TIL: 30

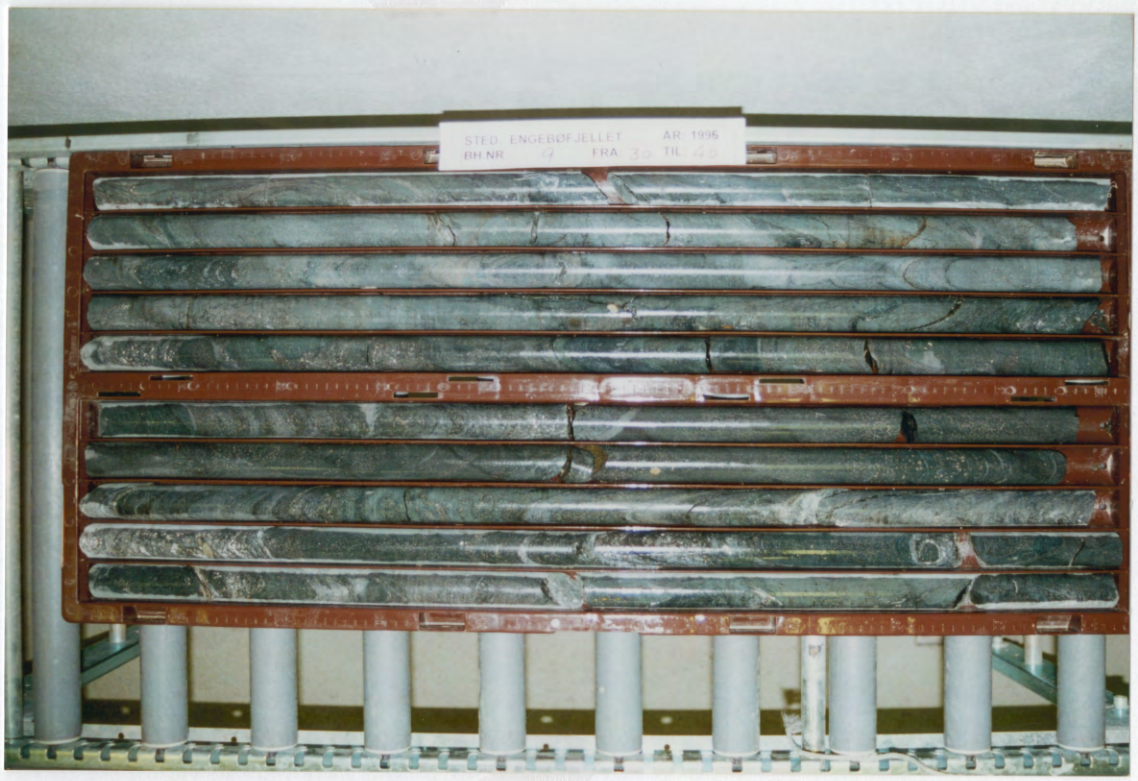
STED: ENGEBØFJELLET ÅR: 1995
BH.NR 9 FRA: 30 TIL: 40

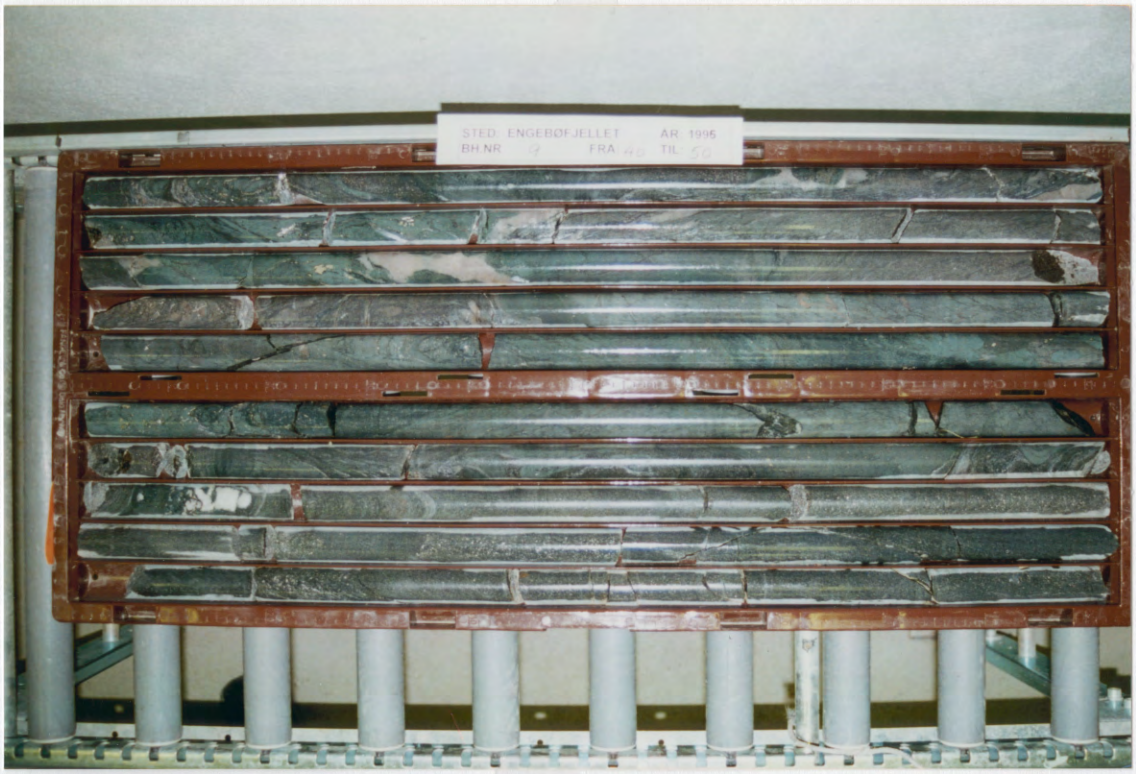
STED: ENGEBØFJELLET ÅR: 1995
BH.NR 4 FRA: 40 TIL: 50

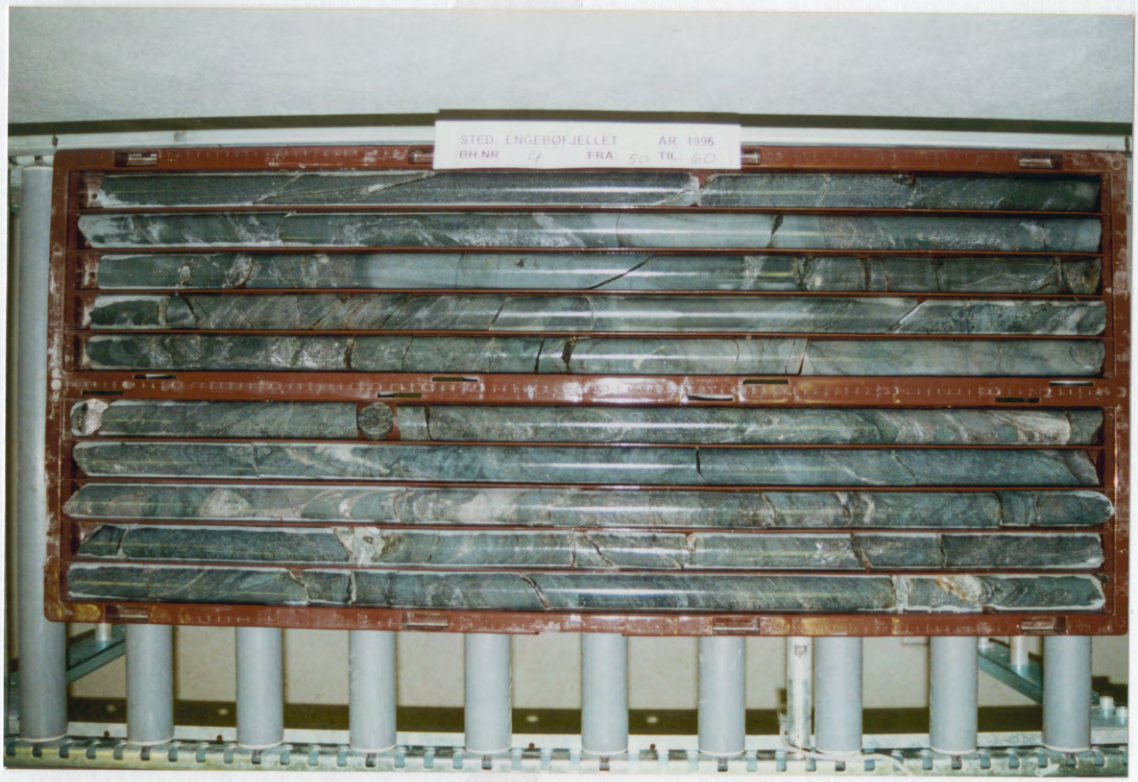
STED: ENGEBØFJELLET ÅR: 1995
BH.NR 4 FRA: 50 TIL: 60

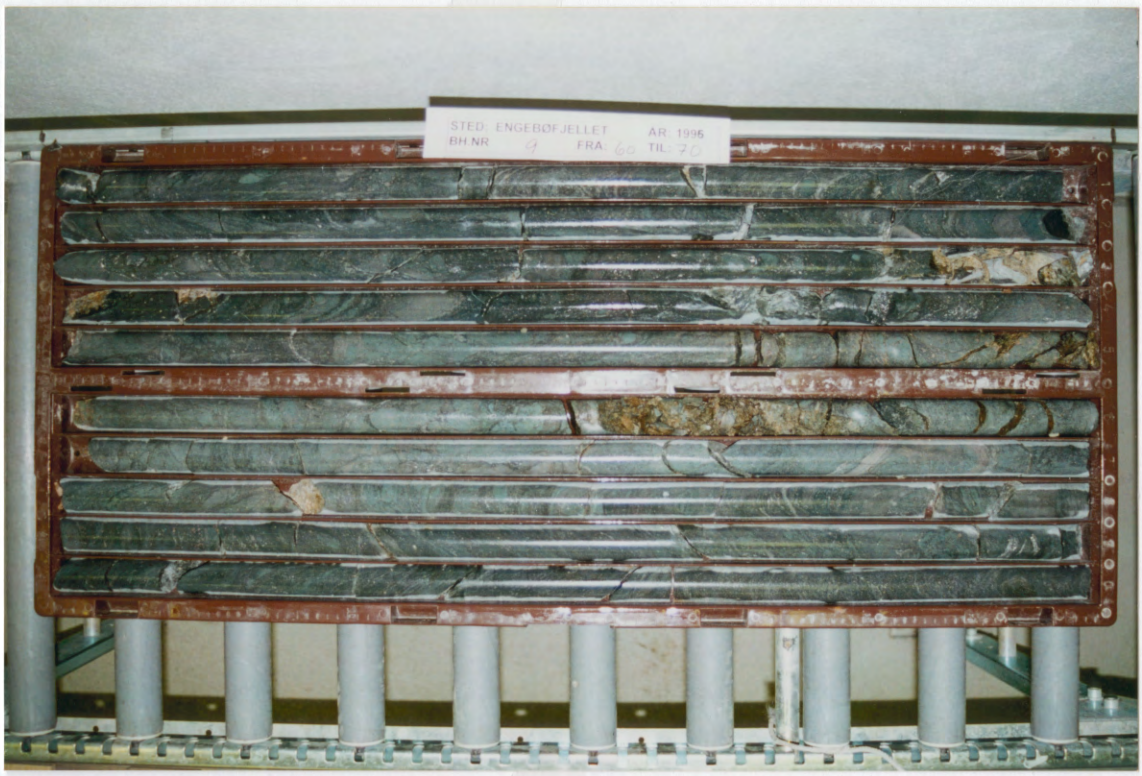
STED: ENGEBØFJELLET ÅR: 1996
BH.NR 9 FRA: 60 TIL: 70

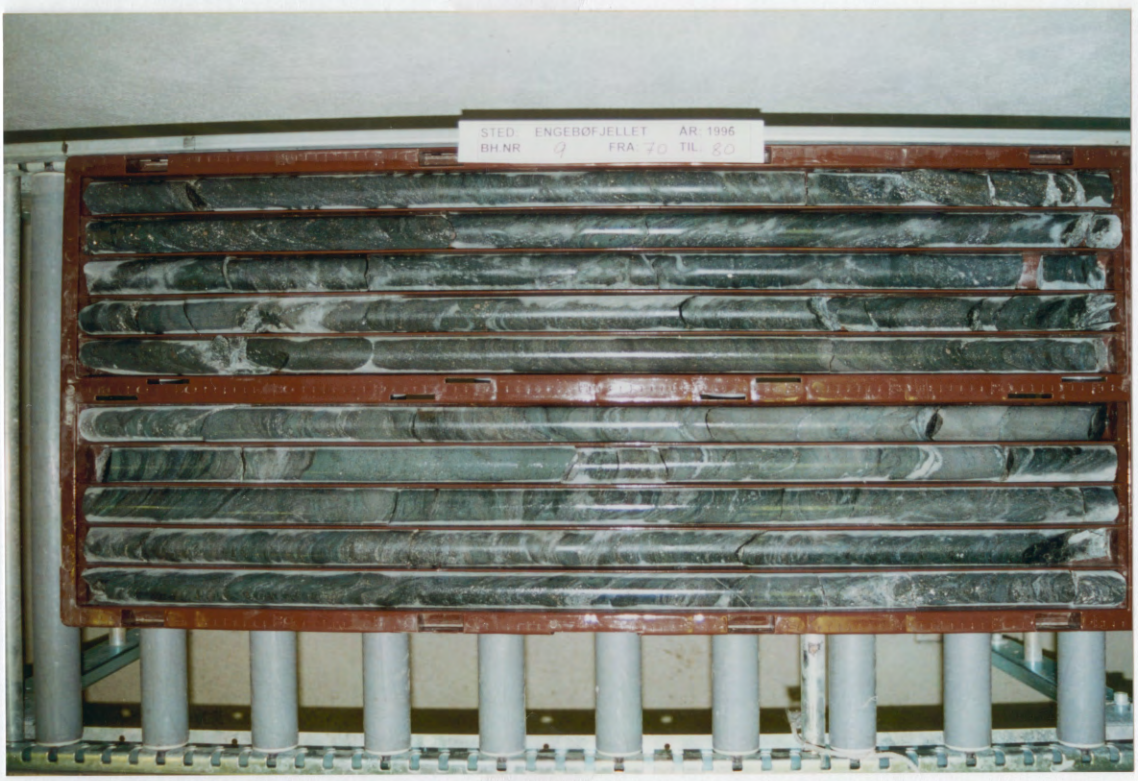
STED: ENGEBØFJELLET ÅR: 1996
BH.NR 9 FRA: 70 TIL: 80

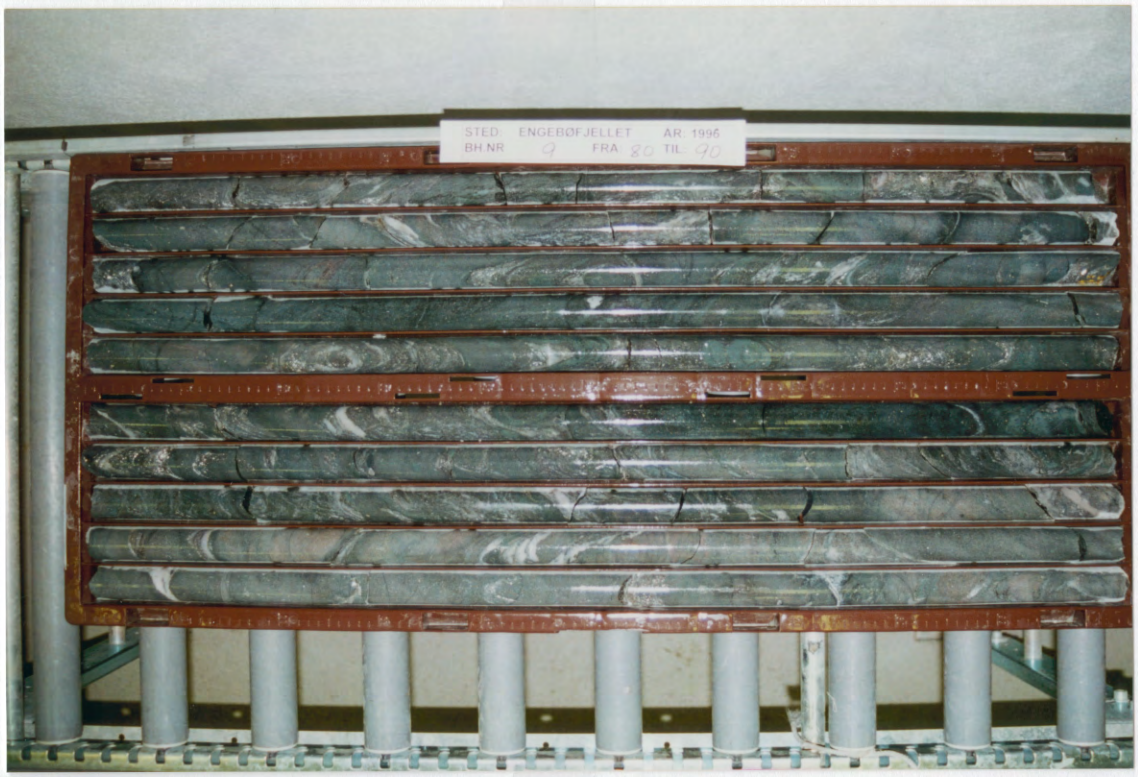
STED: ENGEBØFJELLET ÅR: 1996
BH.NR 9 FRA: 80 TIL: 90

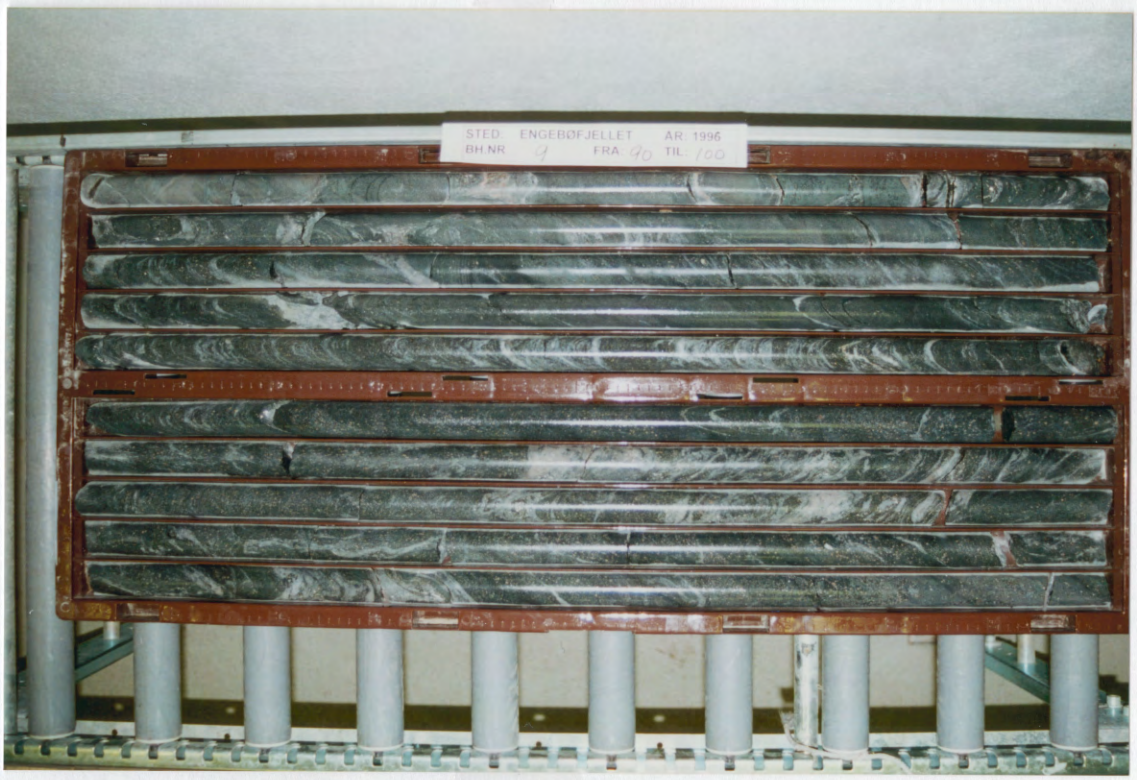
STED: ENGEBØFJELLET ÅR: 1996
BH.NR 9 FRA: 90 TIL: 100

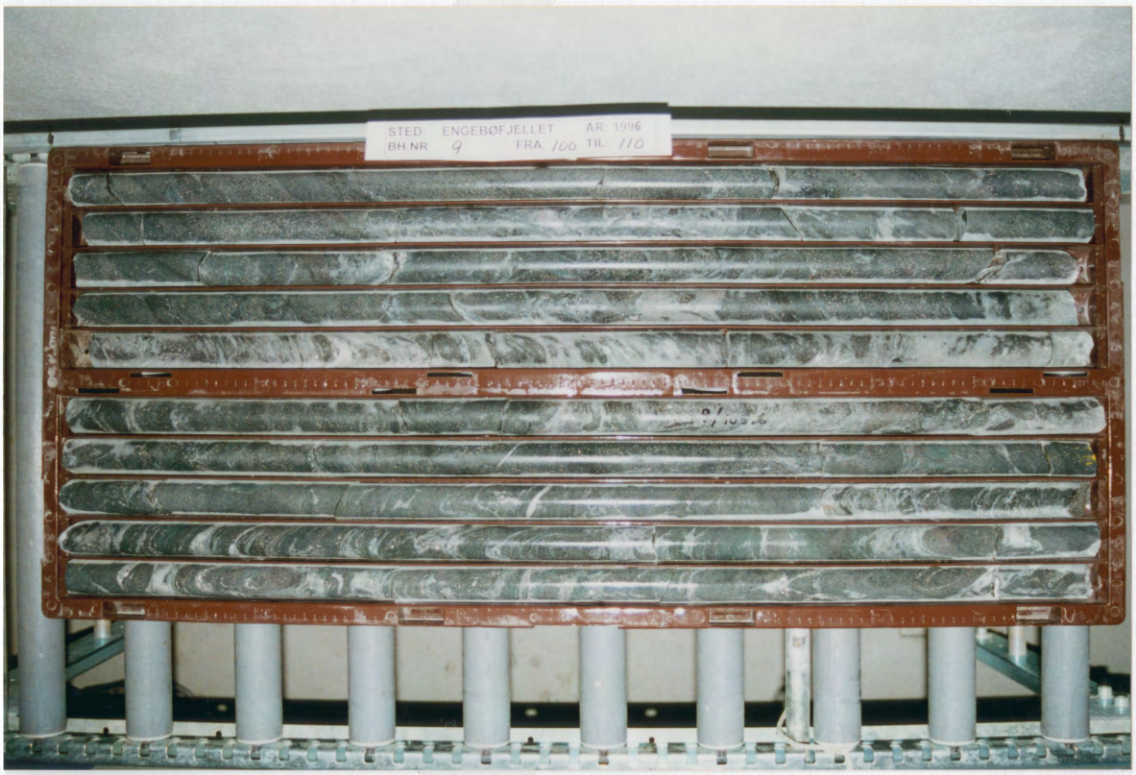
STED: ENGEBØFJELLET ÅR: 1996
BH.NR 9 FRA: 100 TIL: 110

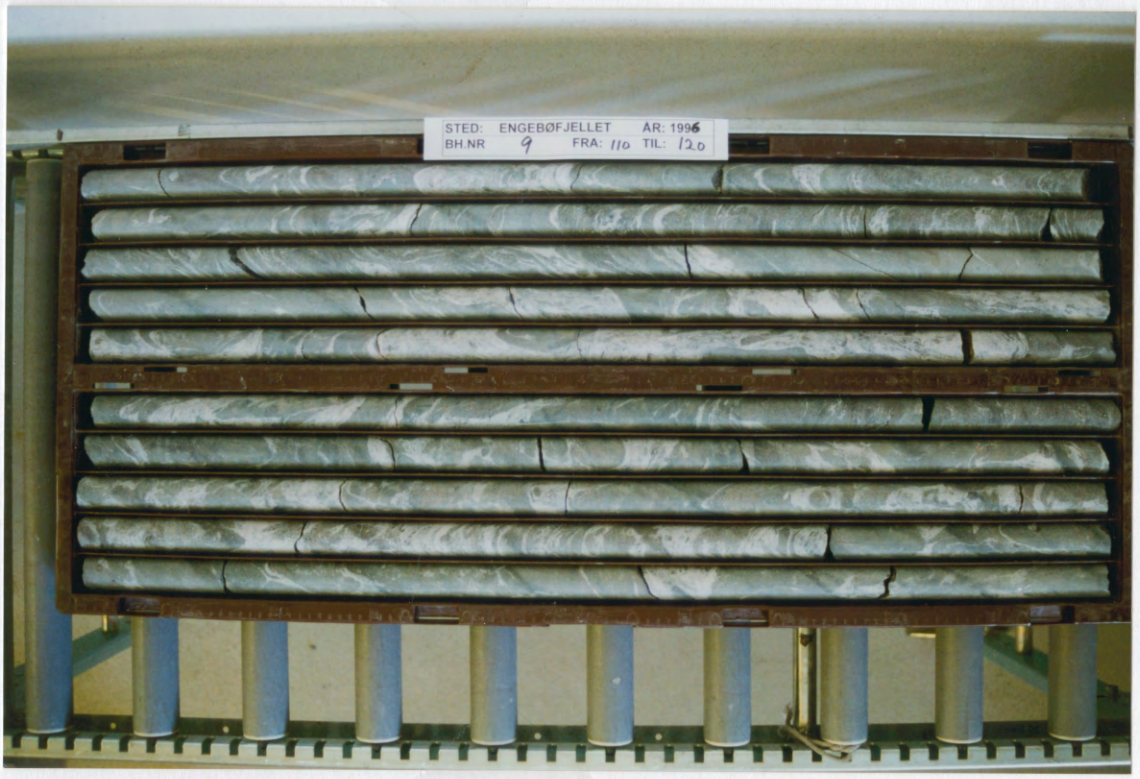
STED: ENGEBØFJELLET ÅR: 1996
BH.NR 9 FRA: 110 TIL: 120

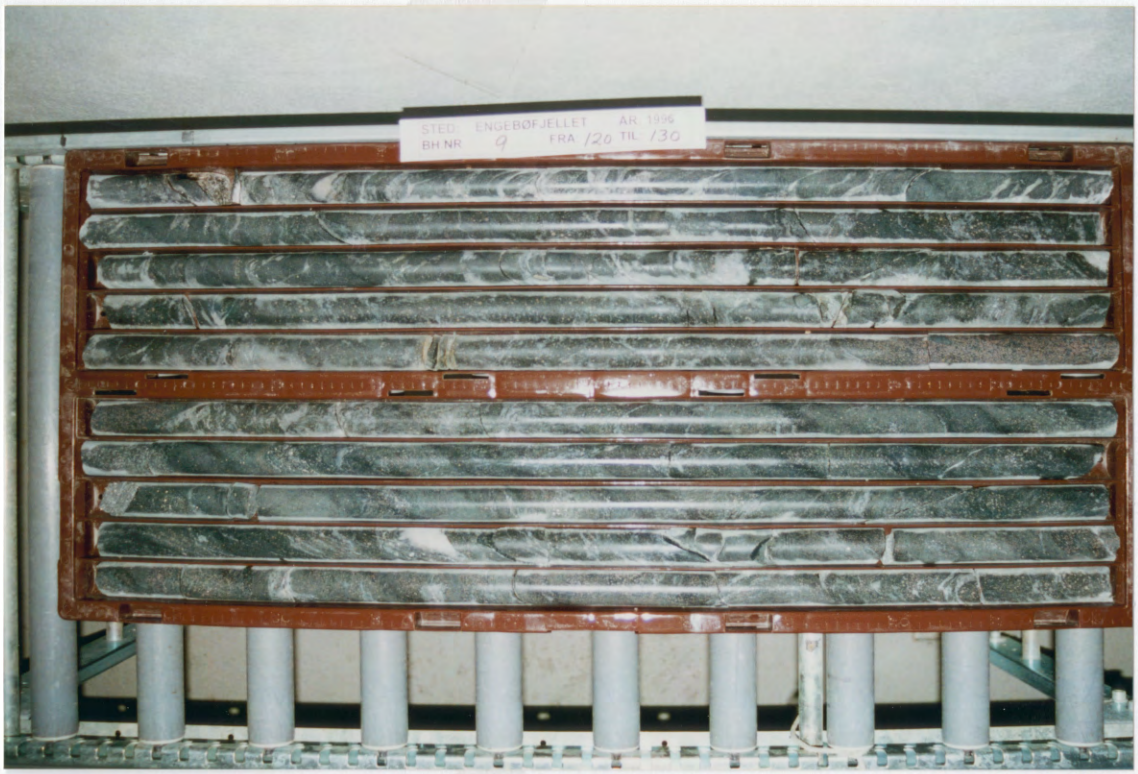
STED ENGEBØFJELLET ÅR 1996
BH NR 9 FRA 120 TIL 130

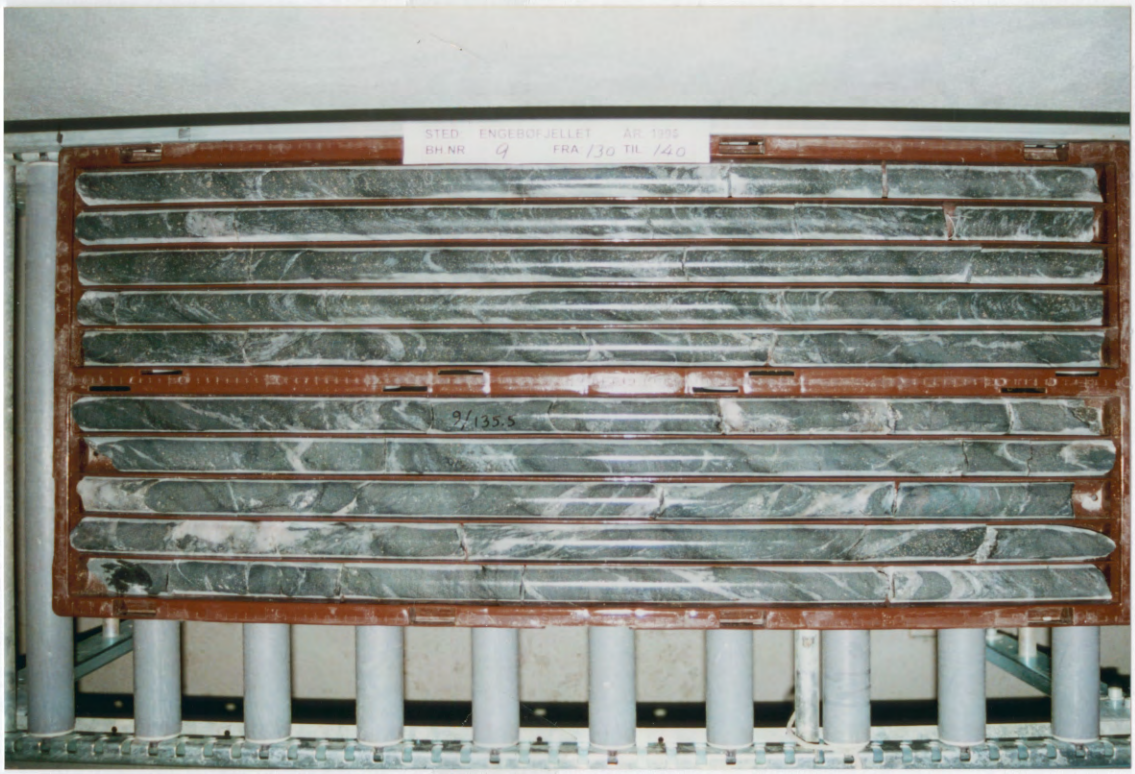
STED ENGEBØFJELLET ÅR 1996
BH NR 9 FRA 130 TIL 140
9/135.5


STED ENGEBØFJELLET ÅR 199
BH.NR 9 FRA 140 TIL 150


STED ENGEBØFJELLET ÅR 1996
BH.NR 9 FRA 150 TIL 160

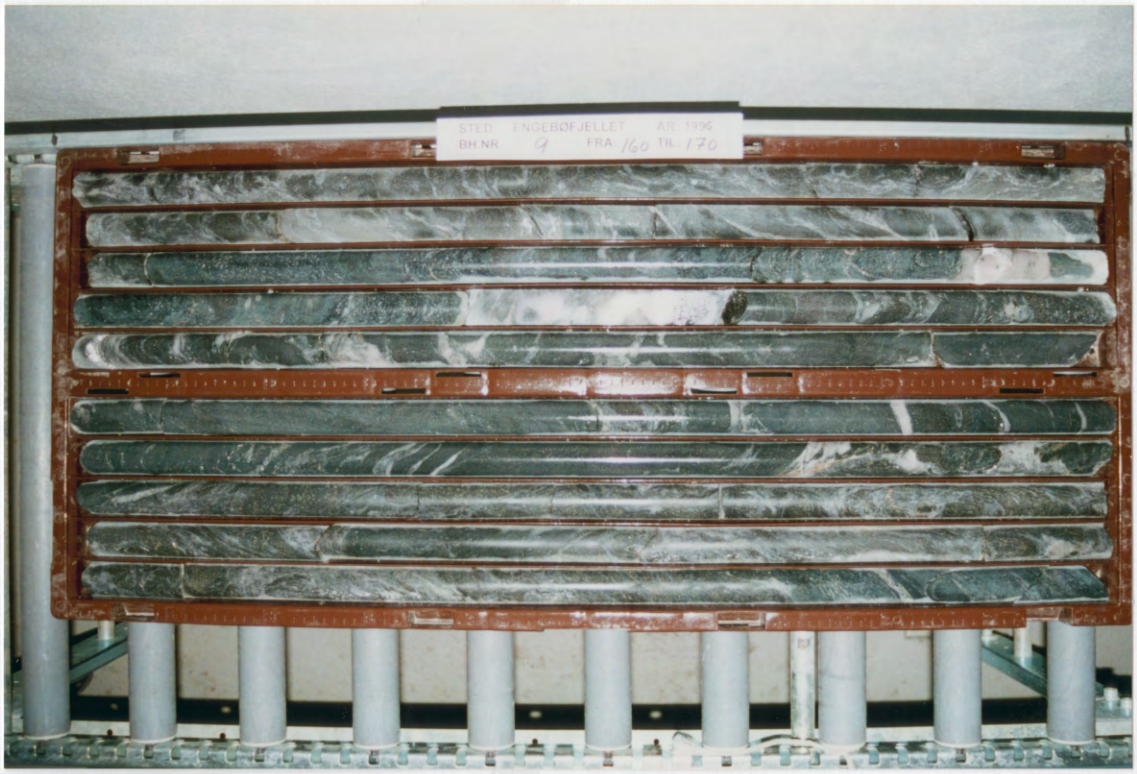
STED: ENGEBØFJELLET ÅR: 1996
BH.NR 9 FRA: 160 TIL: 170

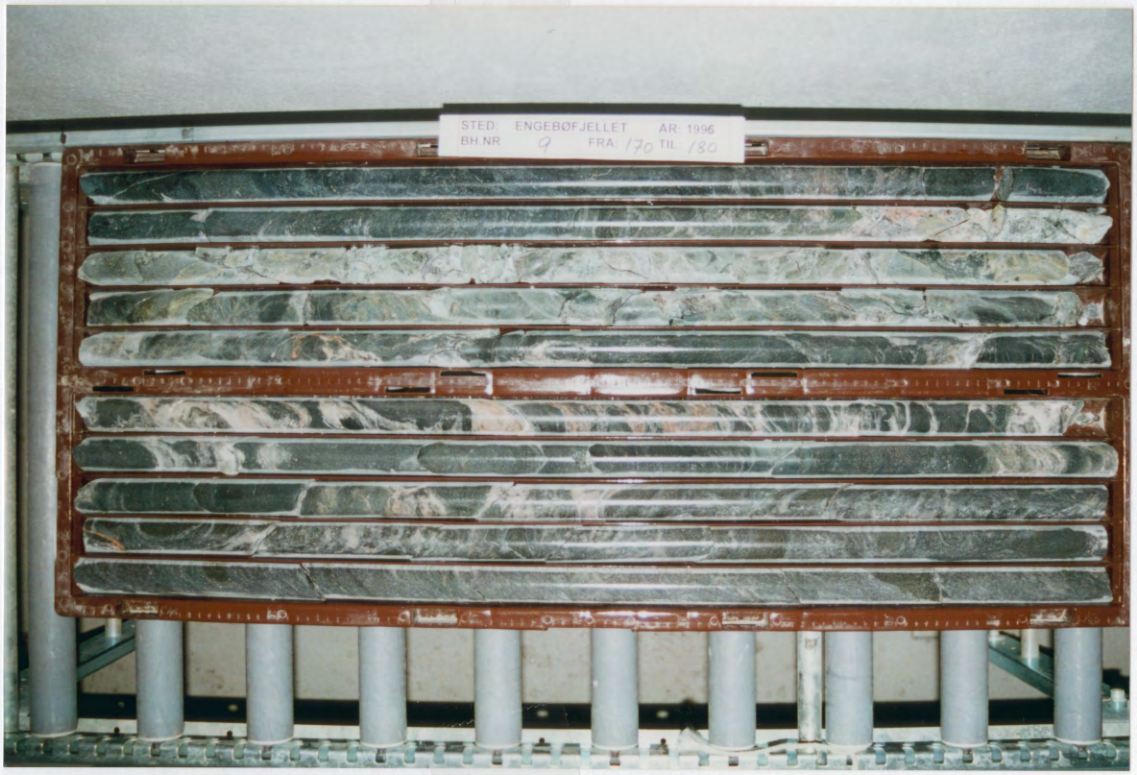
STED: ENGEBØFJELLET ÅR: 1996
BH.NR 9 FRA: 170 TIL: 180

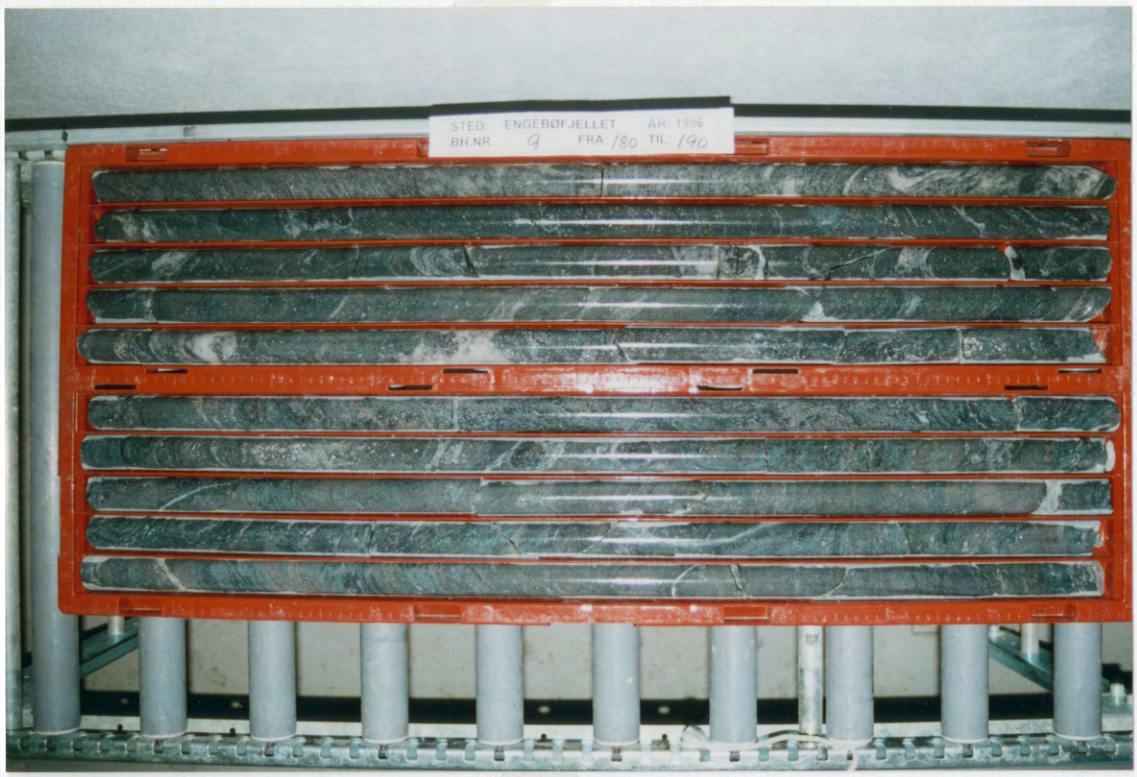
STED: ENGEBØFJELLET ÅR: 1996
BH.NR 9 FRA: 180 TIL: 190

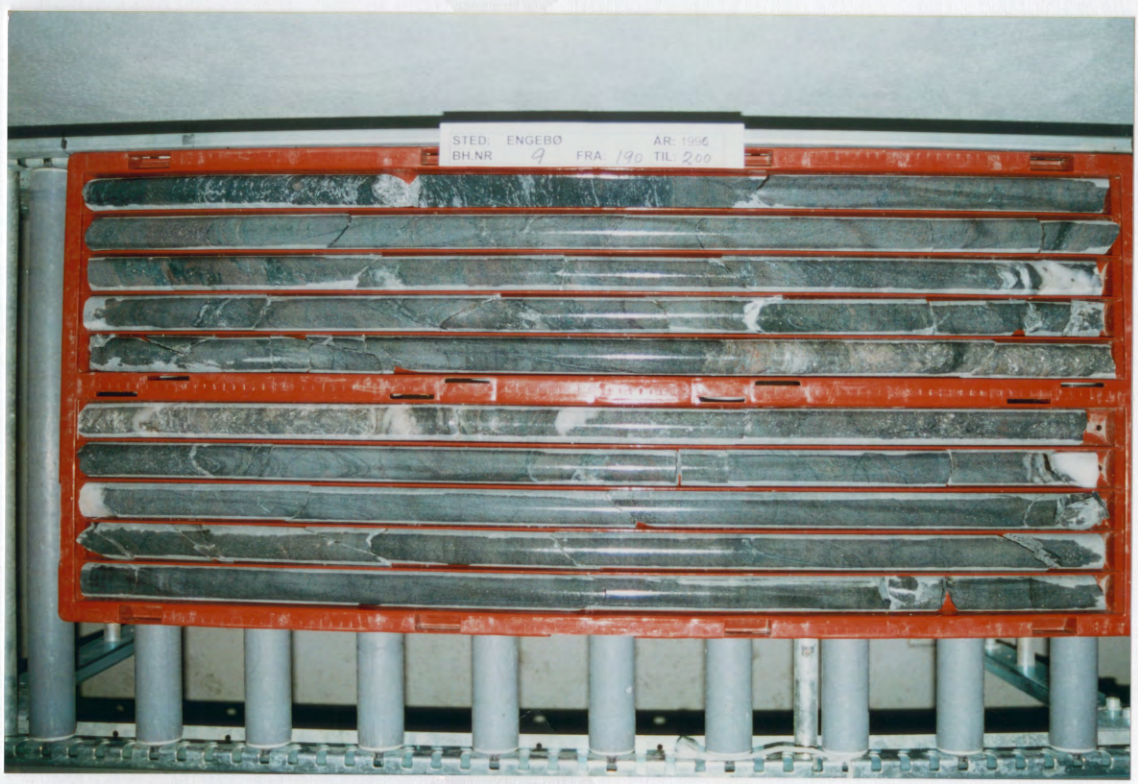
STED: ENGEBØ ÅR: 1996
BH.NR 9 FRA: 190 TIL: 200


STED: ENGEBØ ÅR: 1996
BH.NR 9 FRA: 200 TIL: 210

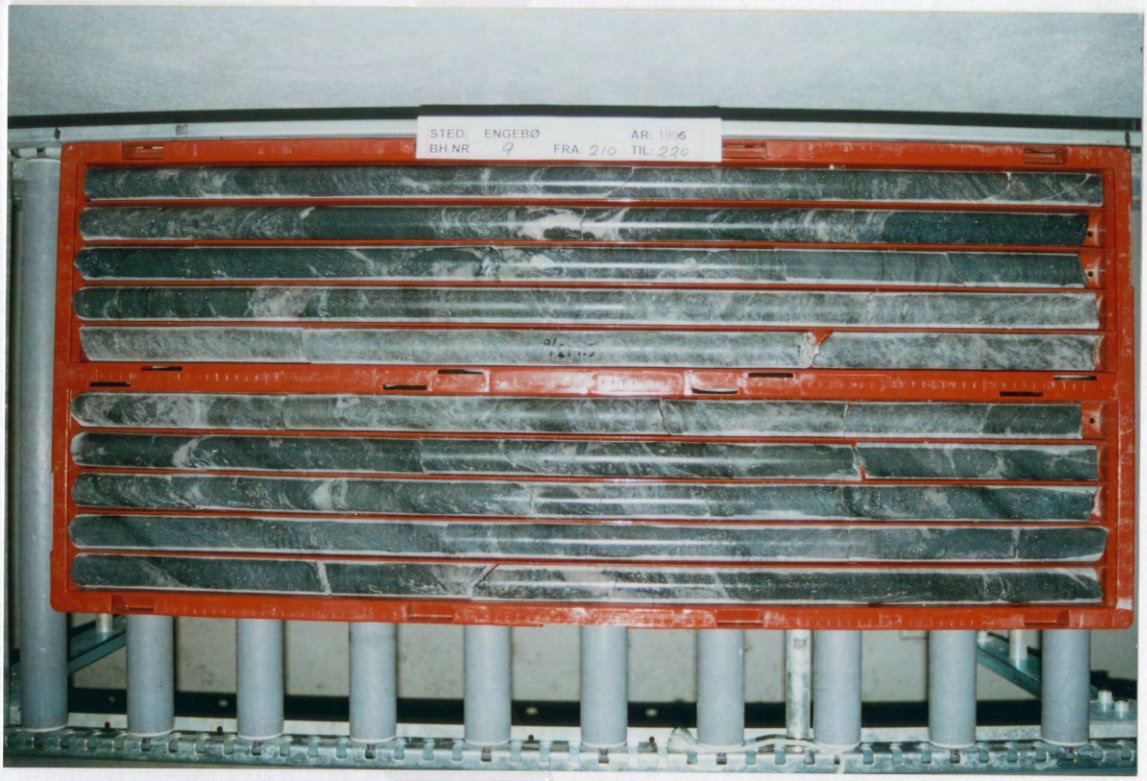
STED: ENGEBØ ÅR: 1996
BH.NR 9 FRA: 210 TIL: 220

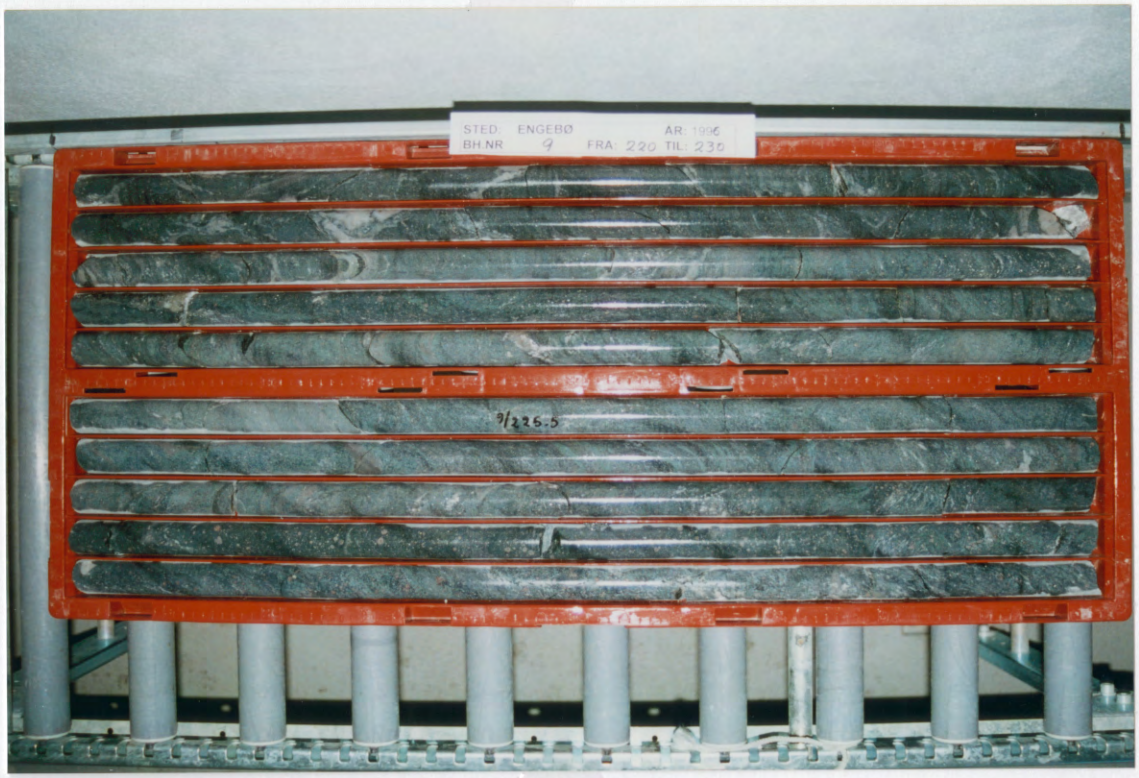
STED: ENGEBØ ÅR: 1996
BH.NR 9 FRA: 220 TIL: 230
9/225.5

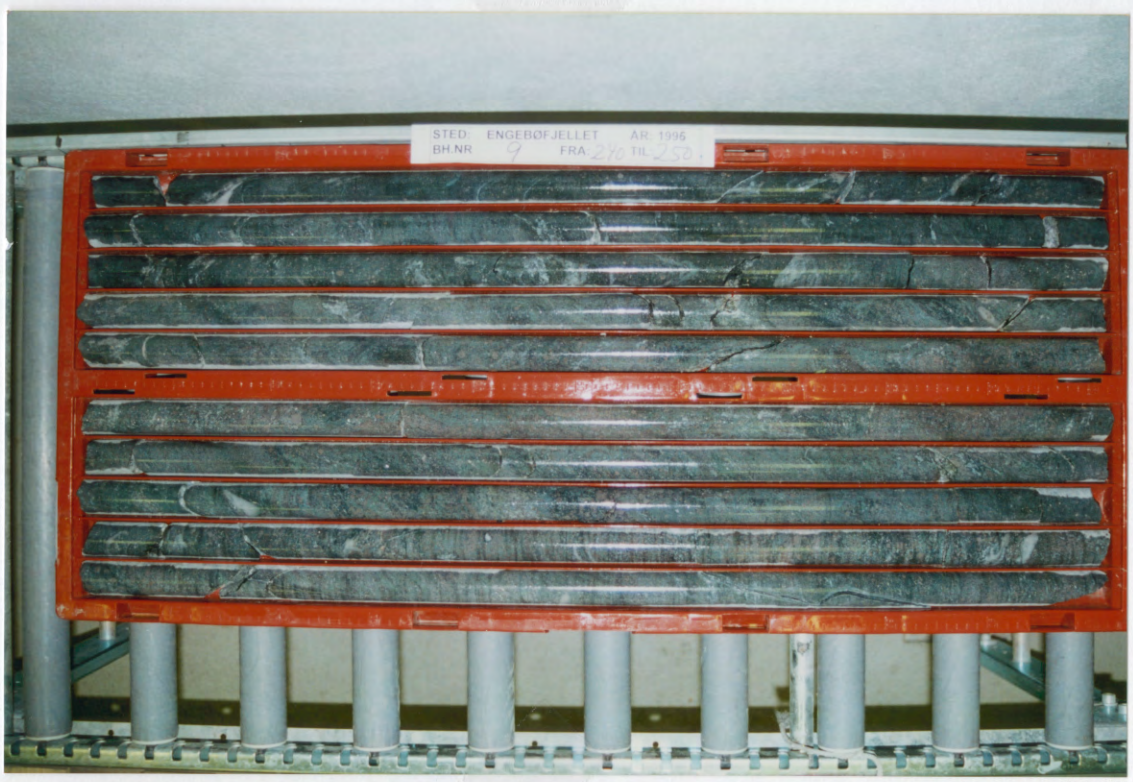
STED: ENGEBØFJELLET ÅR: 1996
BH.NR 9 FRA: 240 TIL: 250

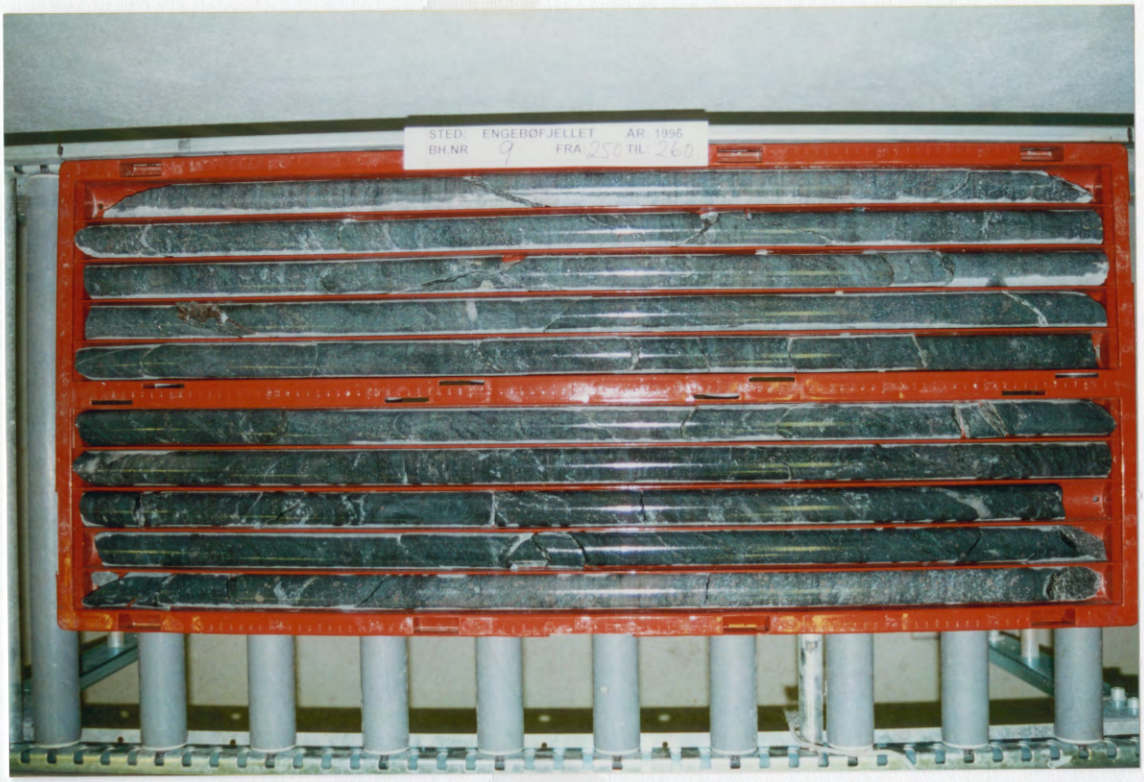
STED: ENGEBØFJELLET ÅR: 1996
BH.NR 9 FRA 250 TIL 260

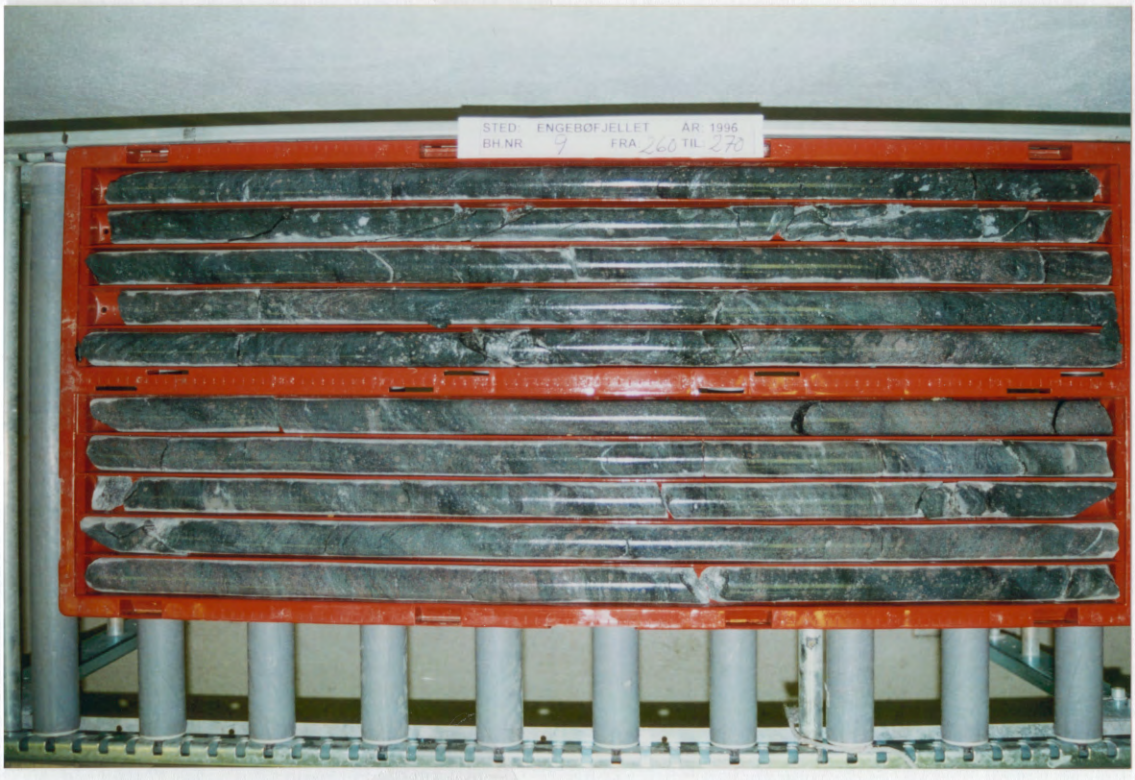
STED: ENGEBØFJELLET ÅR: 1996
BH.NR 9 FRA 260 TIL 270

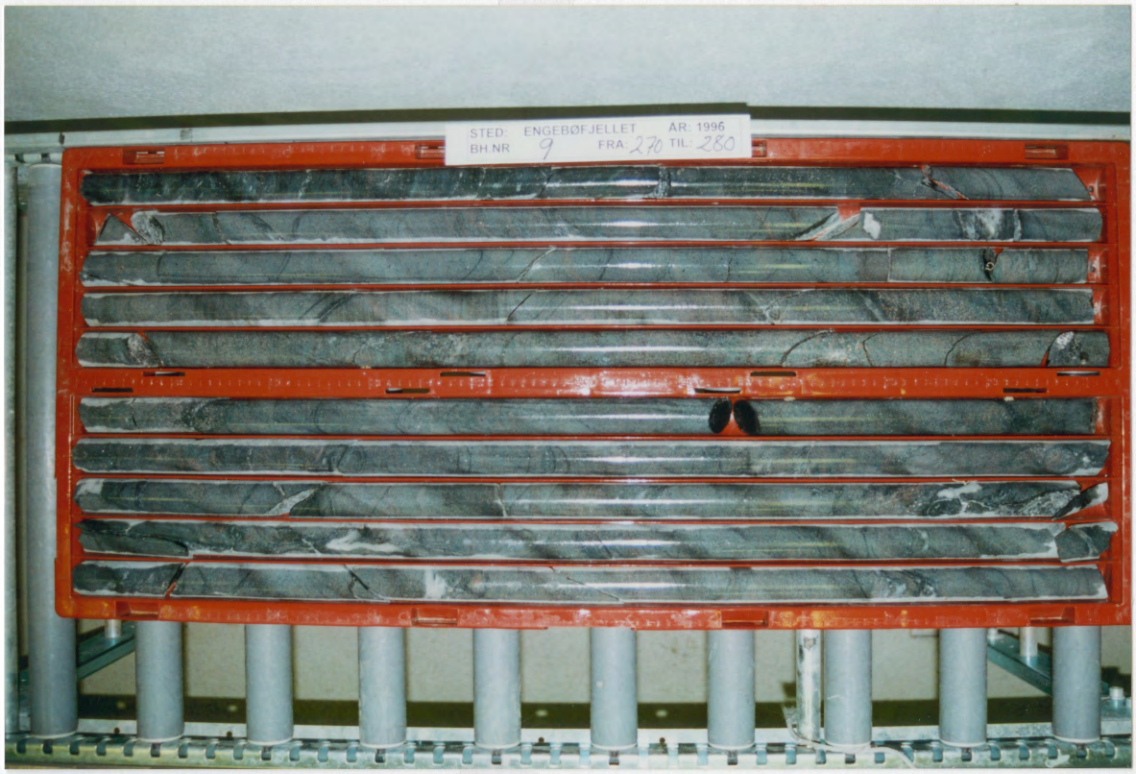
STED: ENGEBØFJELLET ÅR: 1996
BH.NR 9 FRA: 270 TIL: 280

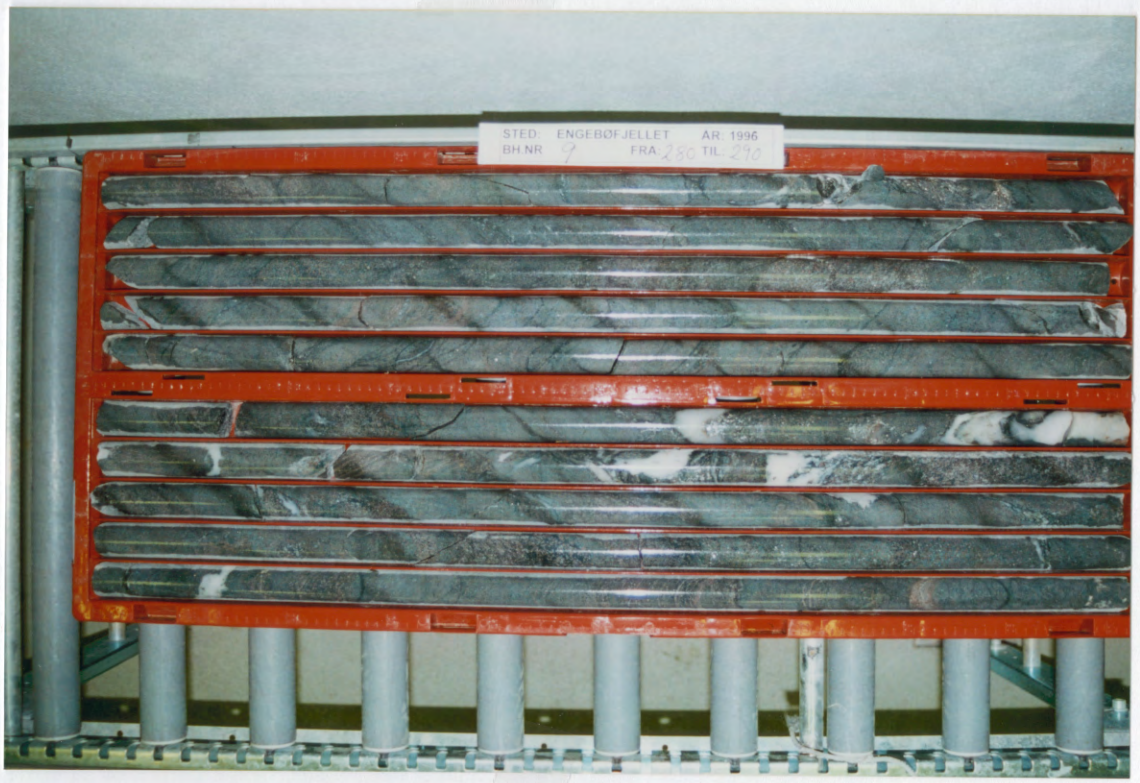
STED: ENGEBØFJELLET ÅR: 1996
BH.NR 9 FRA: 280 TIL: 290

Appendix 8e:

Photographs of 10m core sections

Dh10

Photographed at NGU's core storage at Løkken

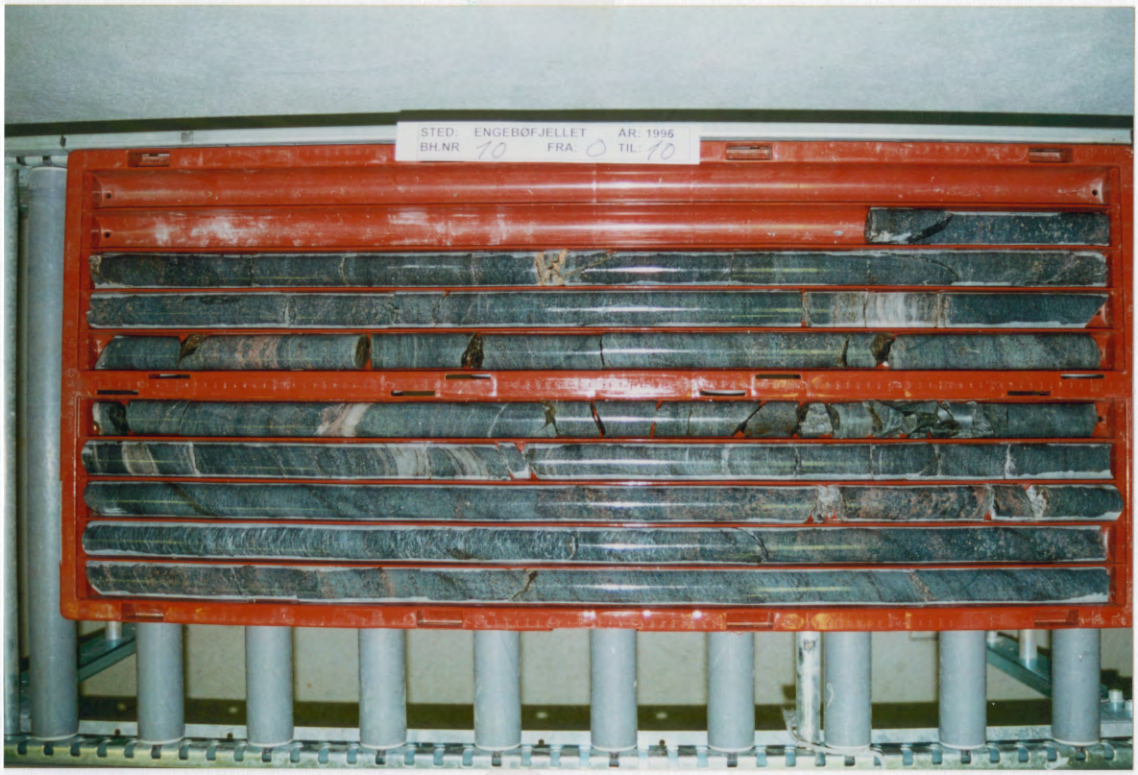
STED: ENGEBØFJELLET ÅR: 1996
BH.NR 10 FRA: 0 TIL: 10

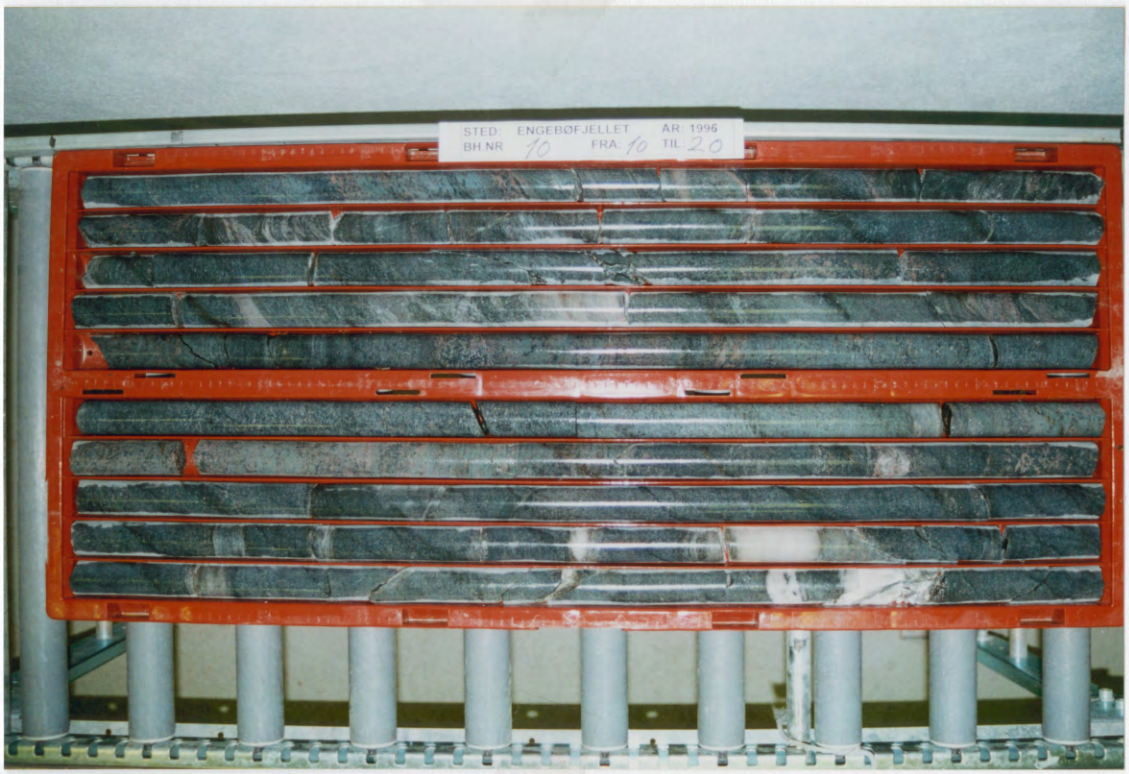
STED: ENGEBØFJELLET ÅR: 1996
BH.NR 10 FRA: 10 TIL: 20

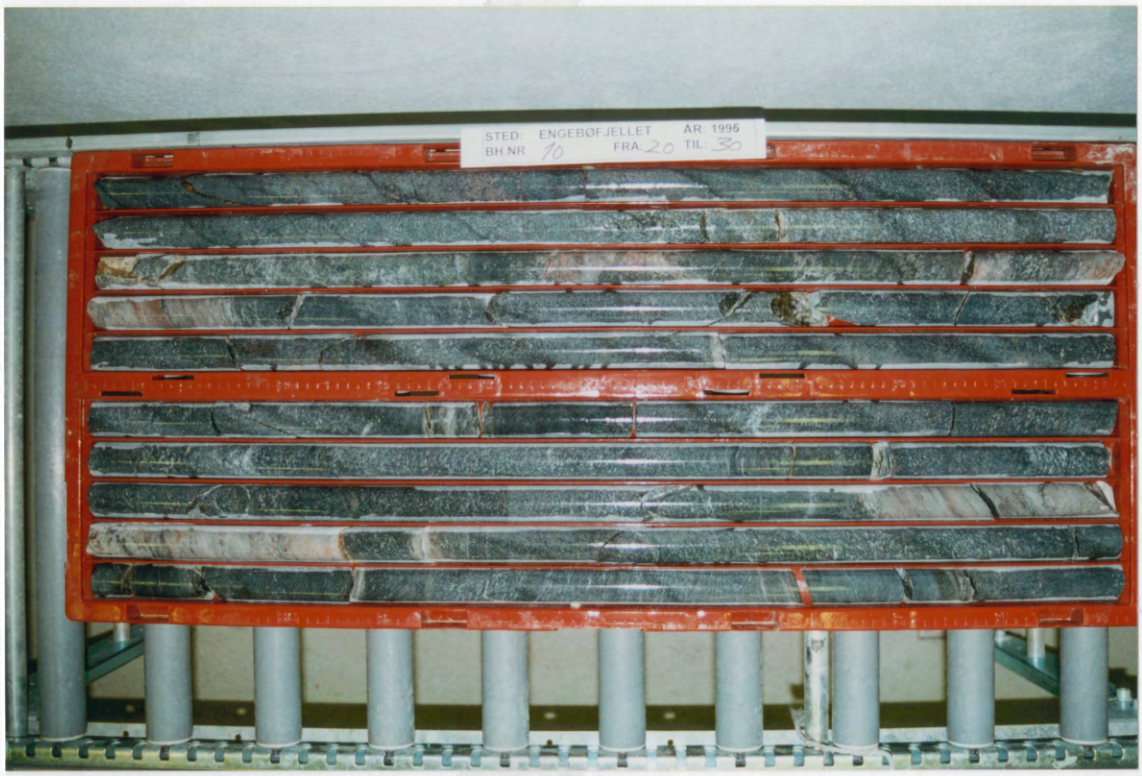
STED: ENGEBØFJELLET ÅR: 1995
BH.NR 10 FRA: 20 TIL: 30

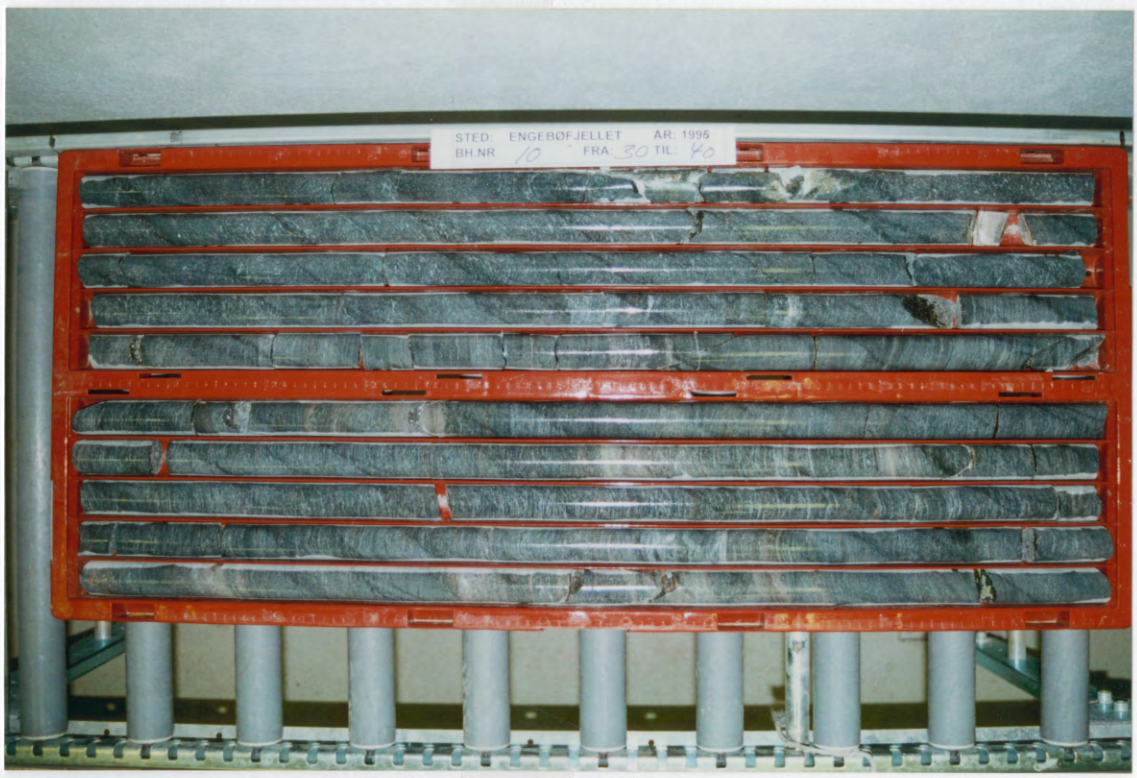
STED: ENGEBØFJELLET ÅR: 1995
BH.NR 10 FRA: 30 TIL: 40

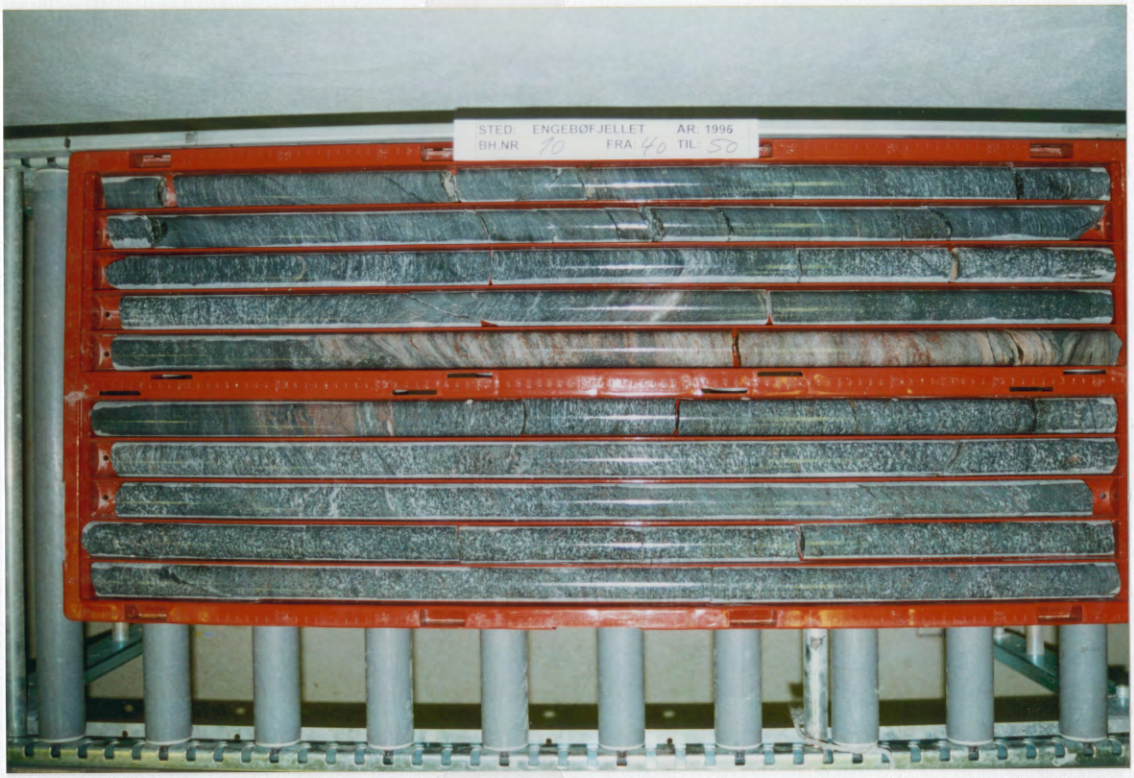
STED: ENGEBØFJELLET AR: 1996
BH.NR 10 FRA: 40 TIL: 50

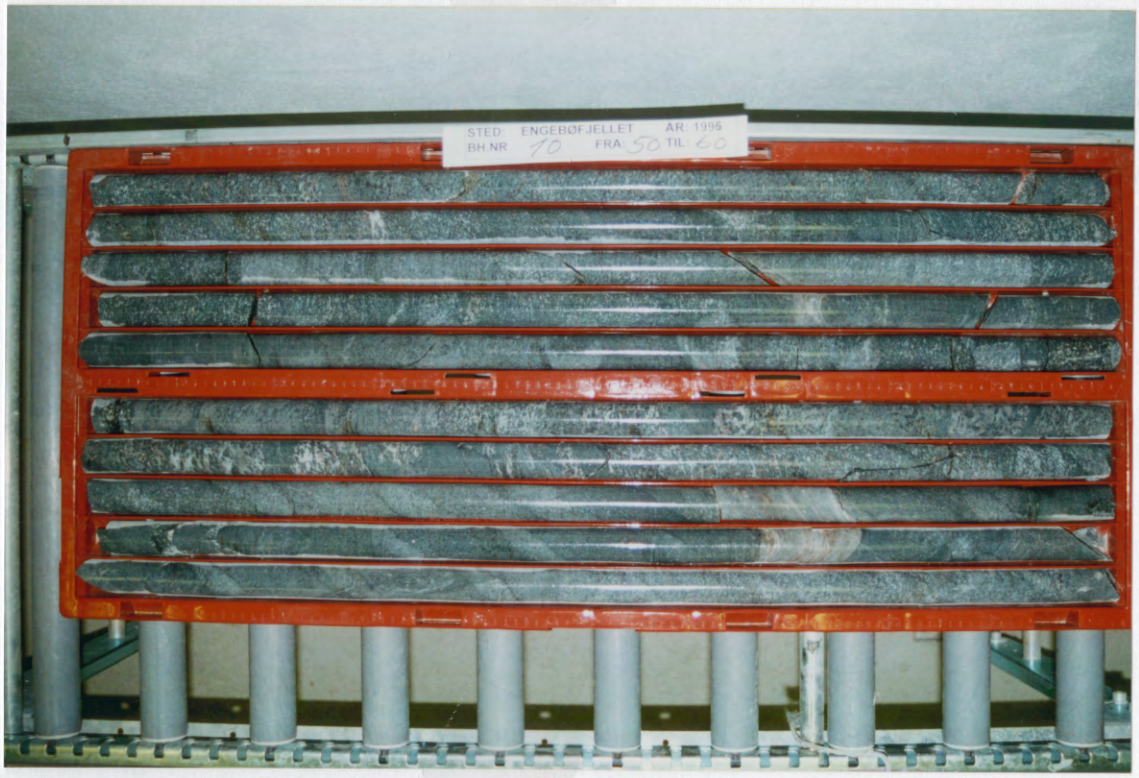
STED: ENGEBØFJELLET AR: 1996
BH.NR 10 FRA: 50 TIL: 60

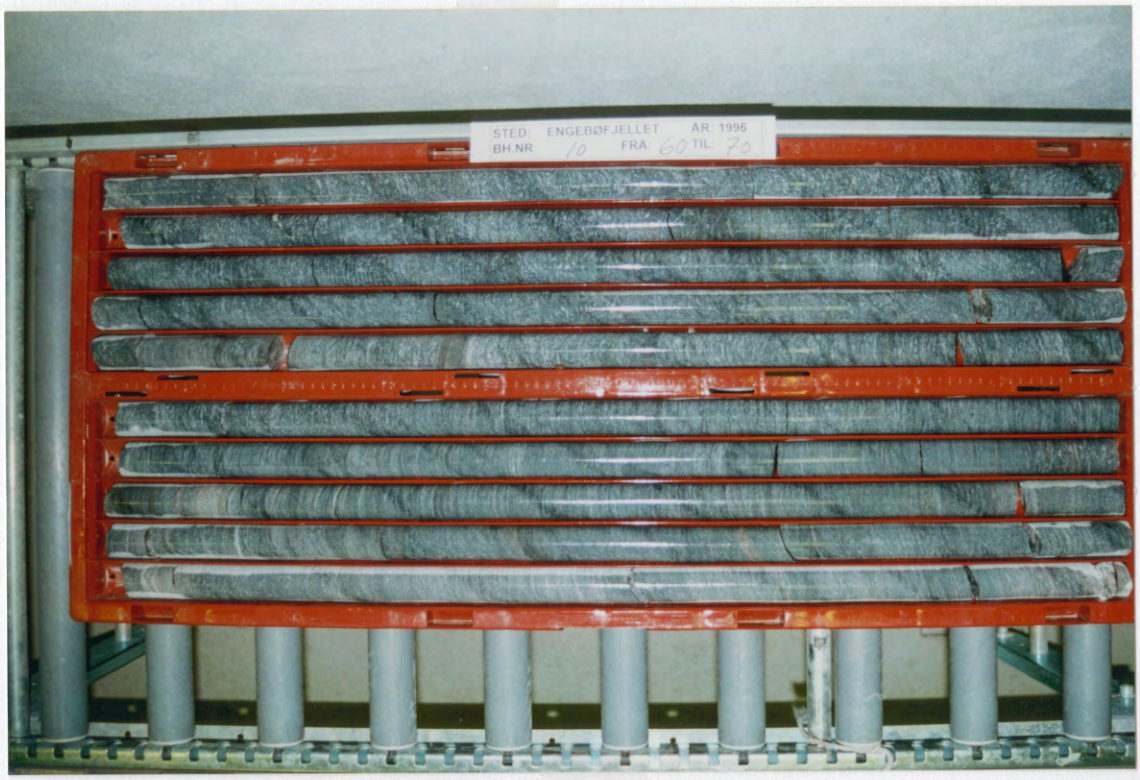
STED: ENGEBØFJELLET ÅR: 1995
BH.NR 10 FRA: 60 TIL: 70

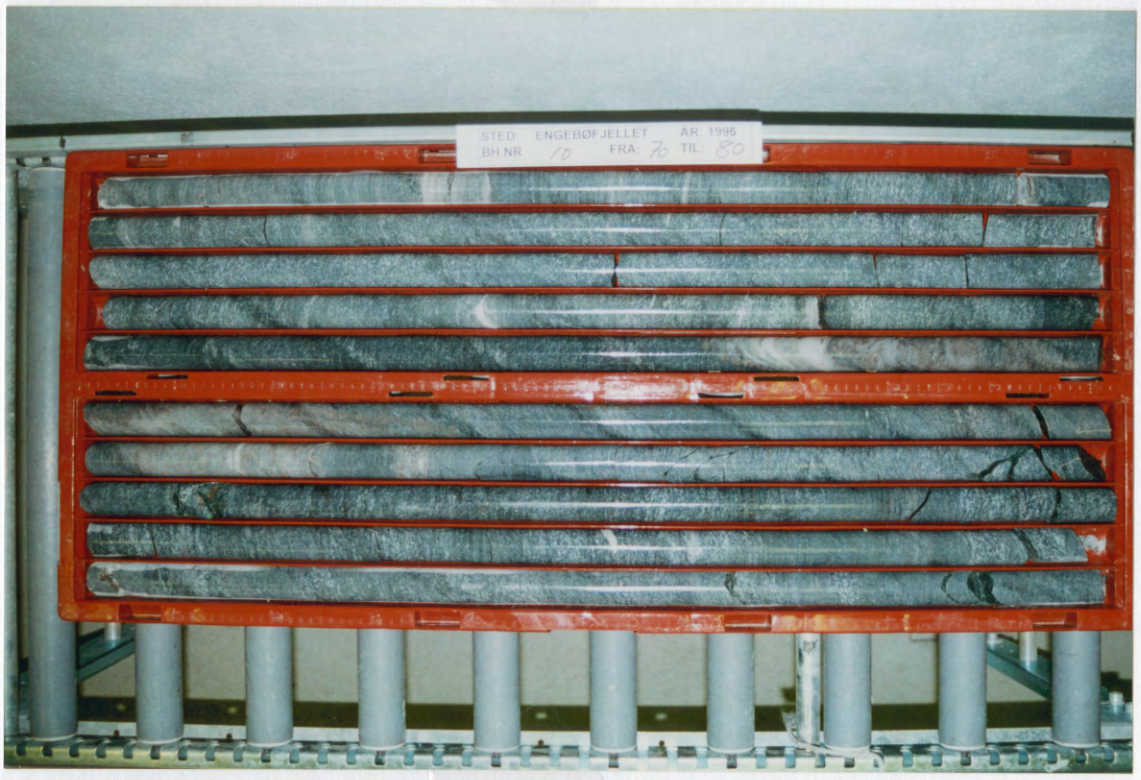
STED: ENGEBØFJELLET ÅR: 1995
BH.NR 10 FRA: 70 TIL: 80

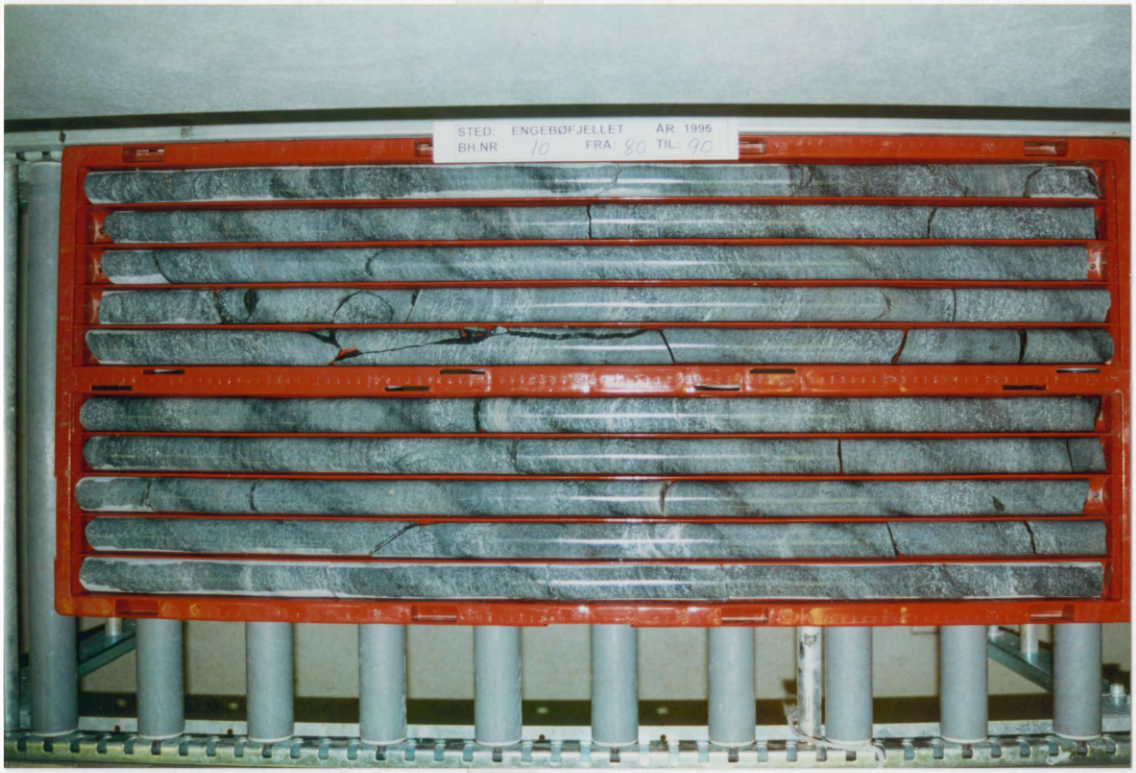
STED: ENGEBØFJELLET ÅR: 1995
BH.NR 10 FRA: 80 TIL: 90

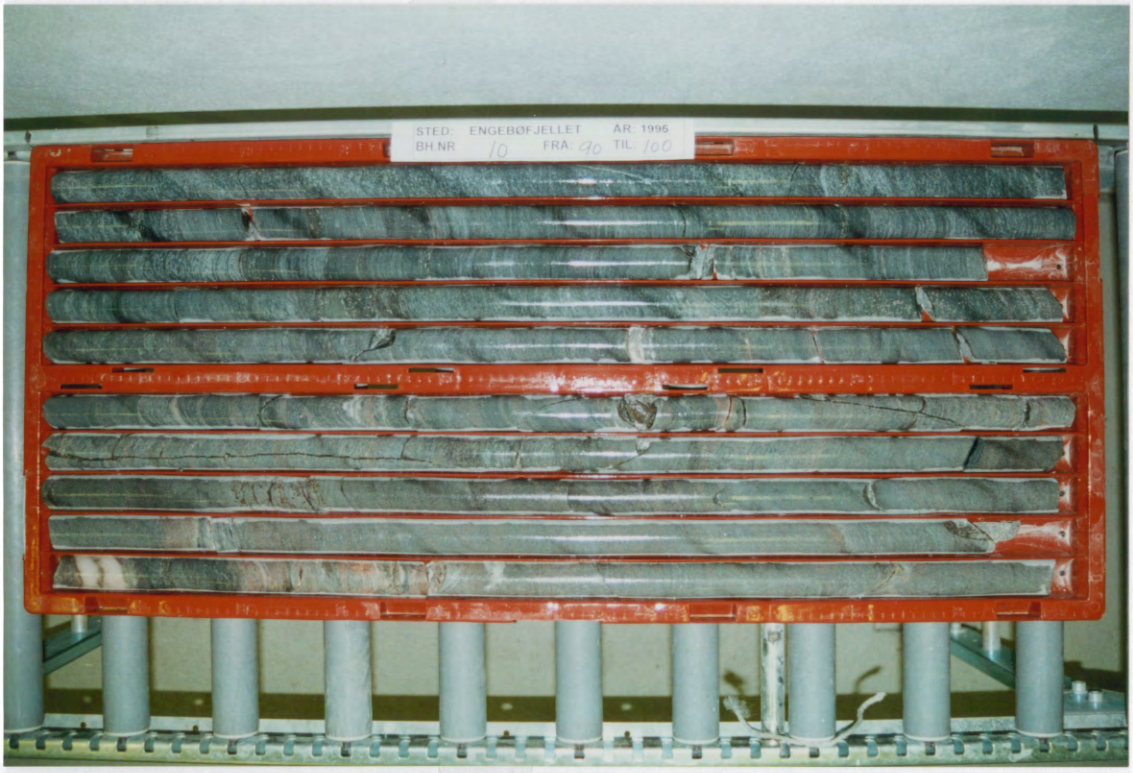
STED: ENGEBØFJELLET ÅR: 1995
BH.NR 10 FRA: 90 TIL: 100

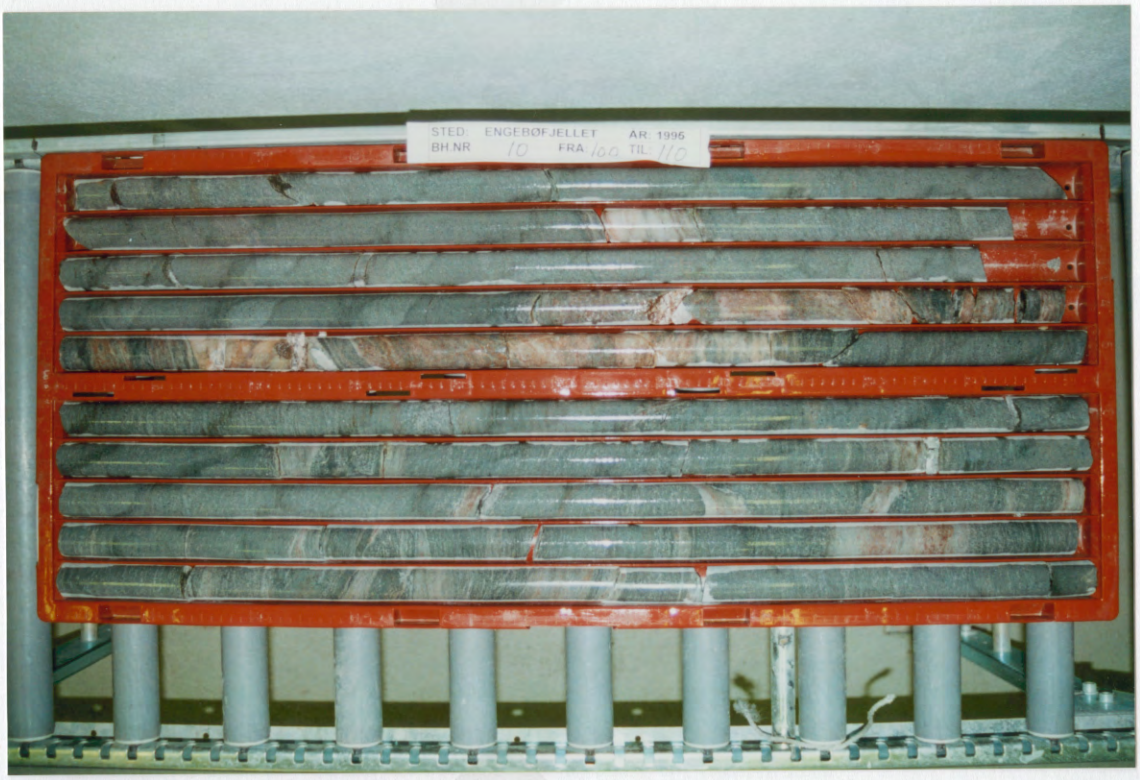
STED: ENGEBØFJELLET ÅR: 1996
BH.NR 10 FRA: 100 TIL: 110

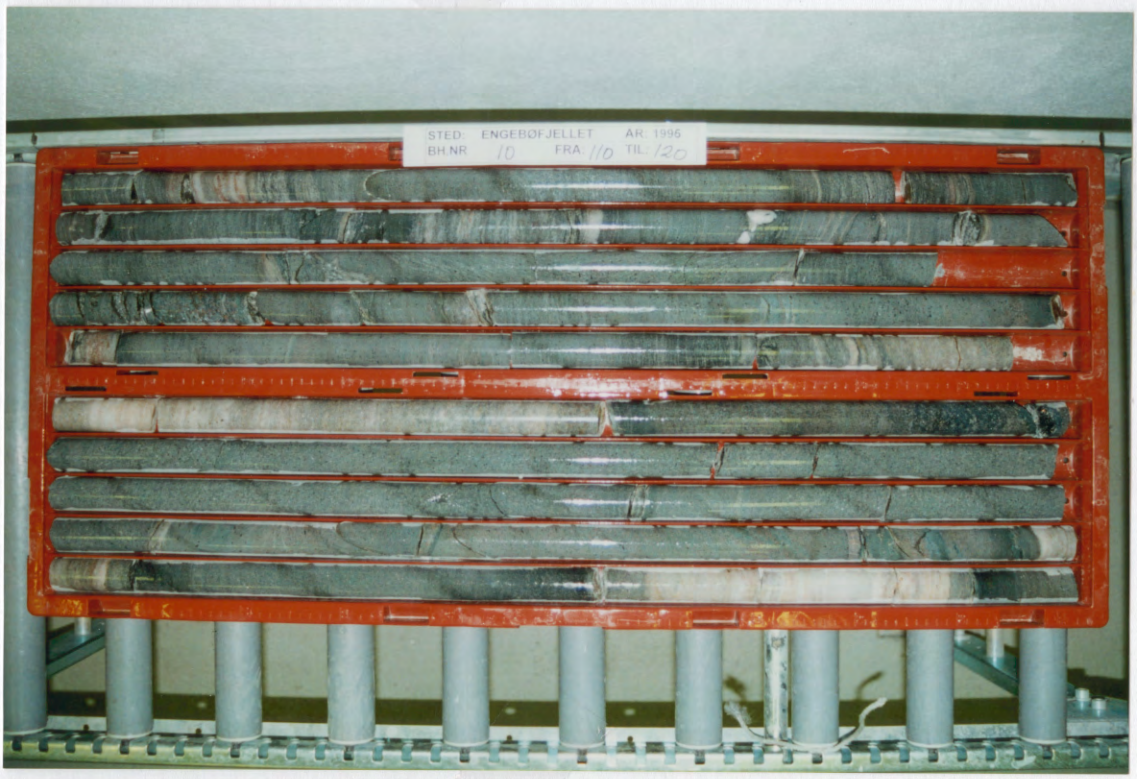
STED: ENGEBØFJELLET ÅR: 1996
BH.NR 10 FRA: 110 TIL: 120


STED: ENGEBØFJELLET ÅR: 1995
BH.NR 16 FRA: 120 TIL: 130

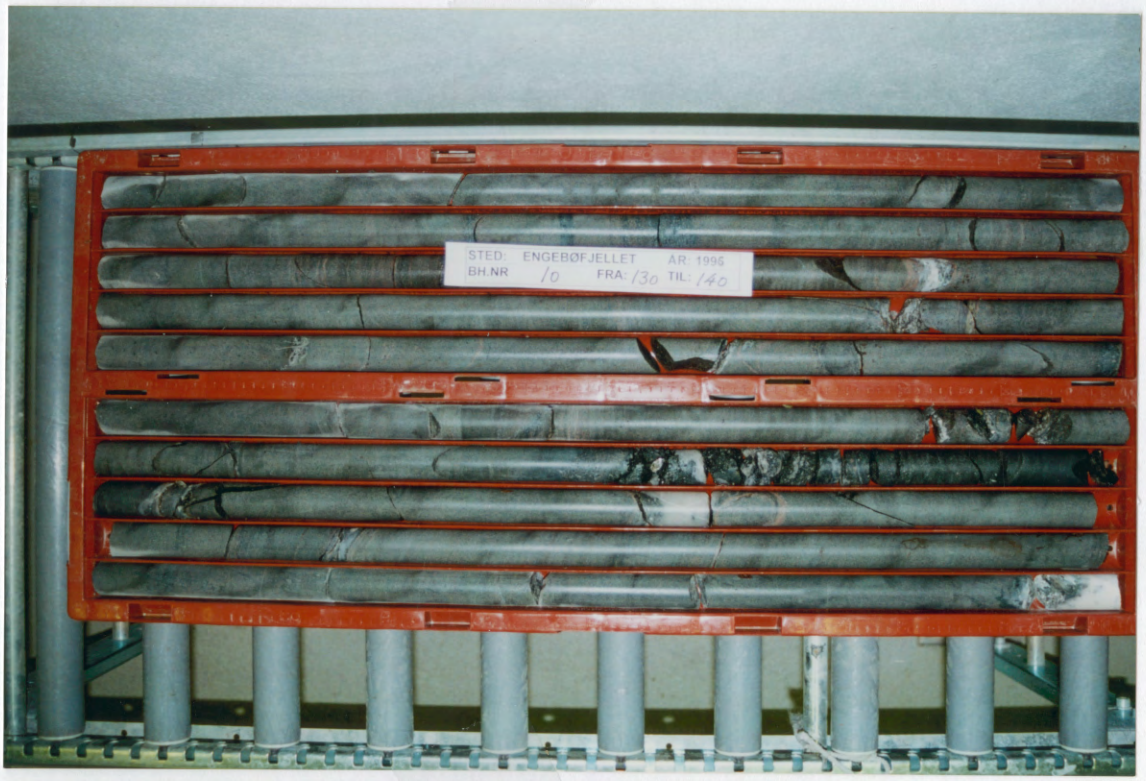
STED: ENGEBØFJELLET ÅR: 1995
BH.NR 10 FRA: 130 TIL: 140

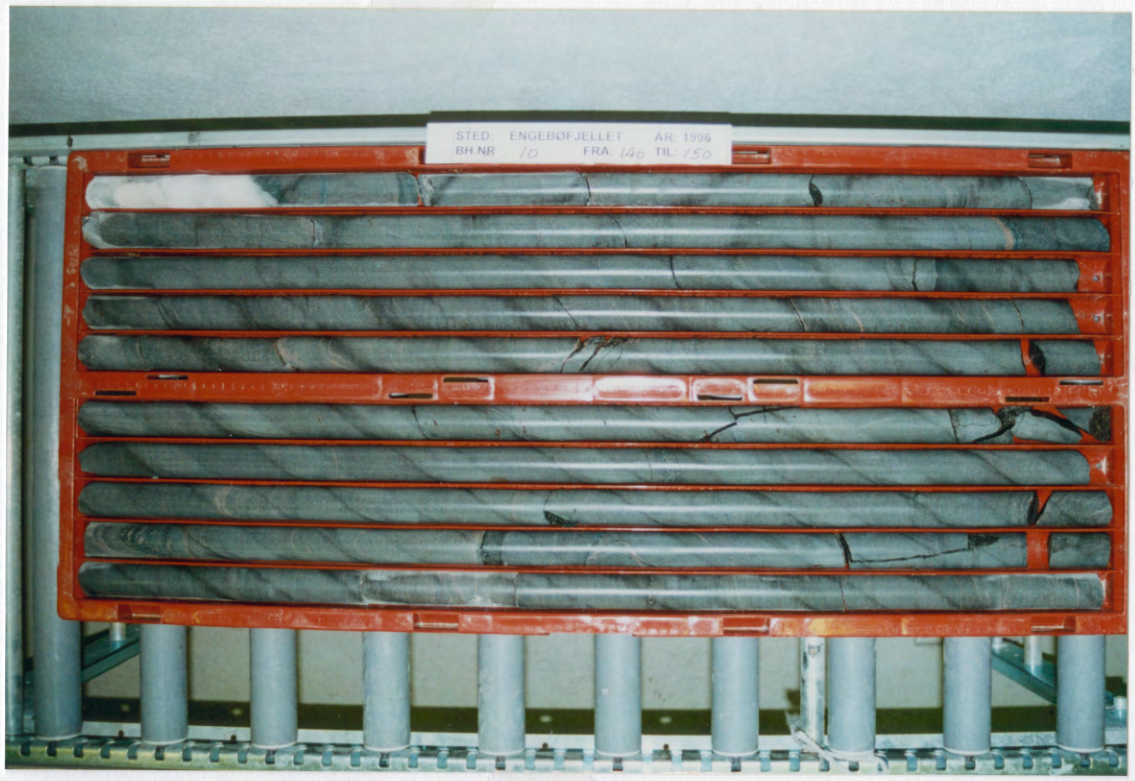
STED: ENGEBØFJELLET ÅR: 1996
BH.NR 10 FRA: 140 TIL: 150

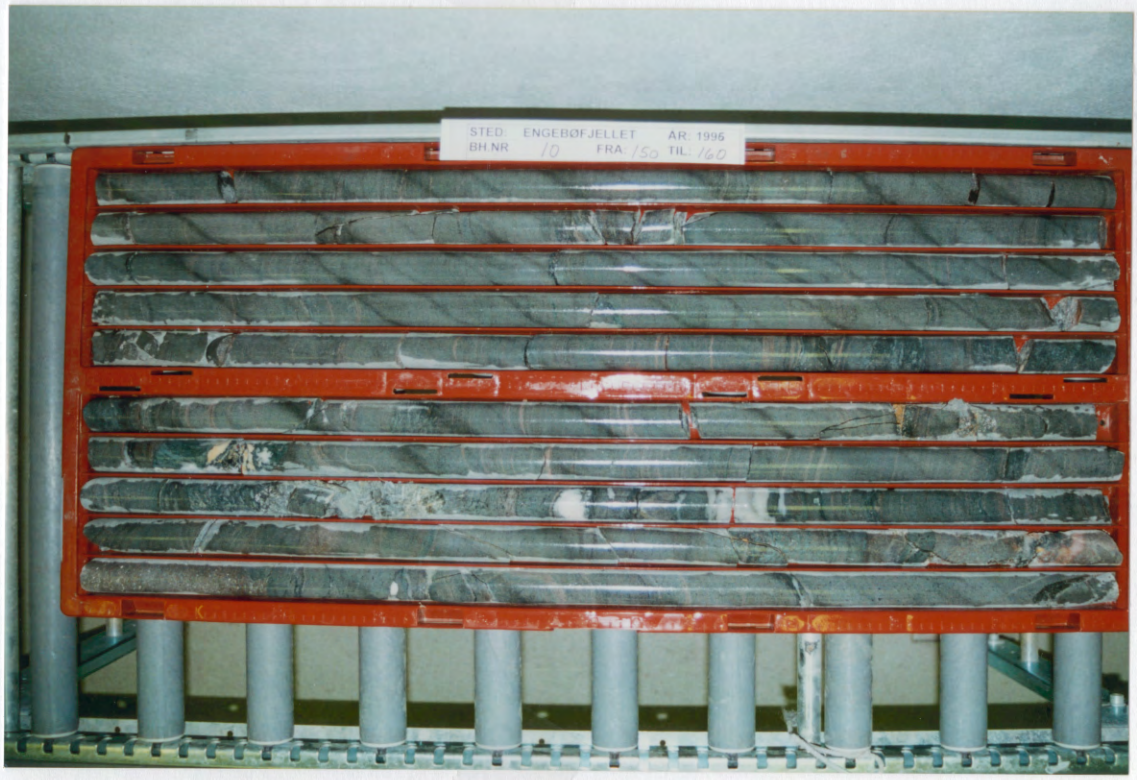
STED: ENGEBØFJELLET ÅR: 1996
BH.NR 10 FRA: 150 TIL: 160

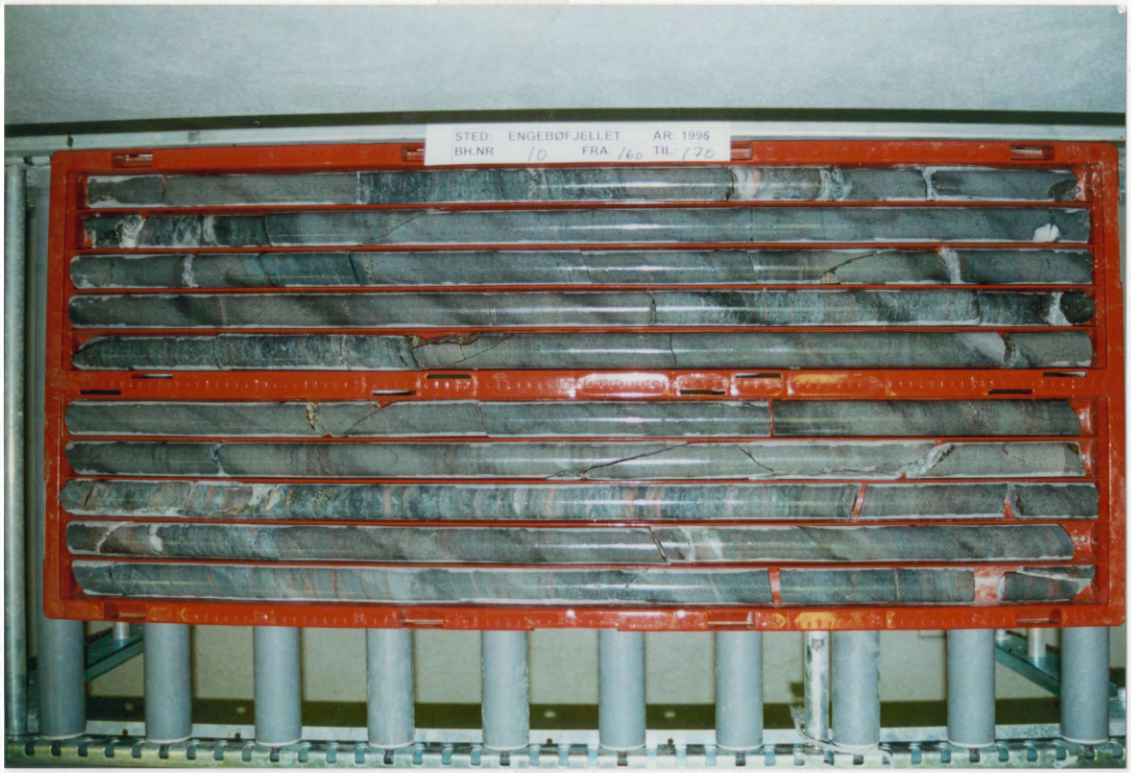
STED: ENGEBØFJELLET ÅR: 1996
BH.NR 10 FRA: 160 TIL: 170

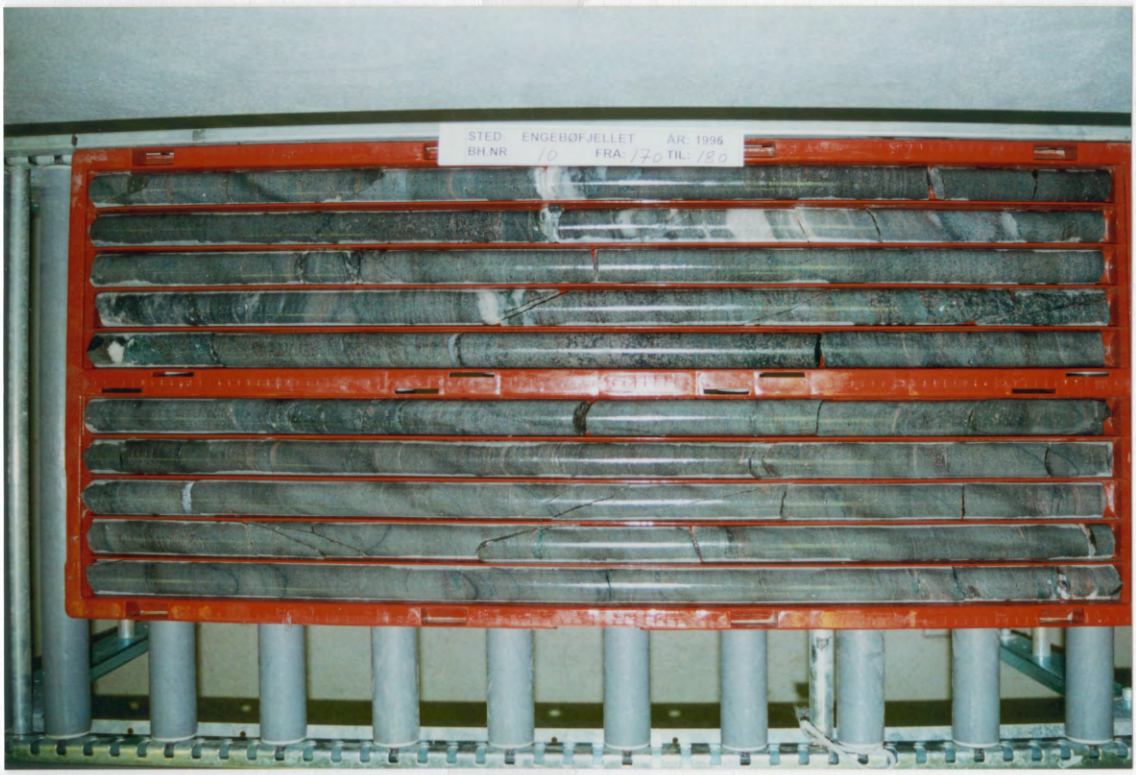
STED: ENGEBØFJELLET ÅR: 1996
BH.NR 10 FRA: 170 TIL: 180

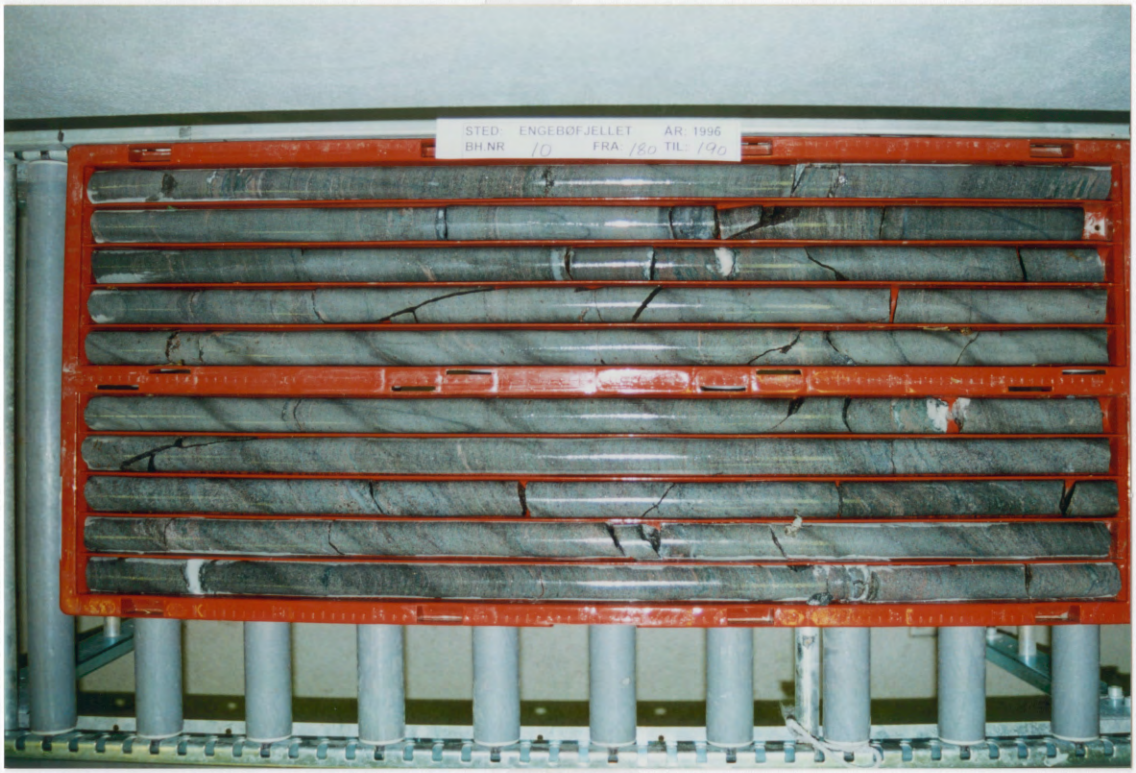
STED: ENGEBØFJELLET ÅR: 1996
BH.NR 10 FRA: 180 TIL: 190

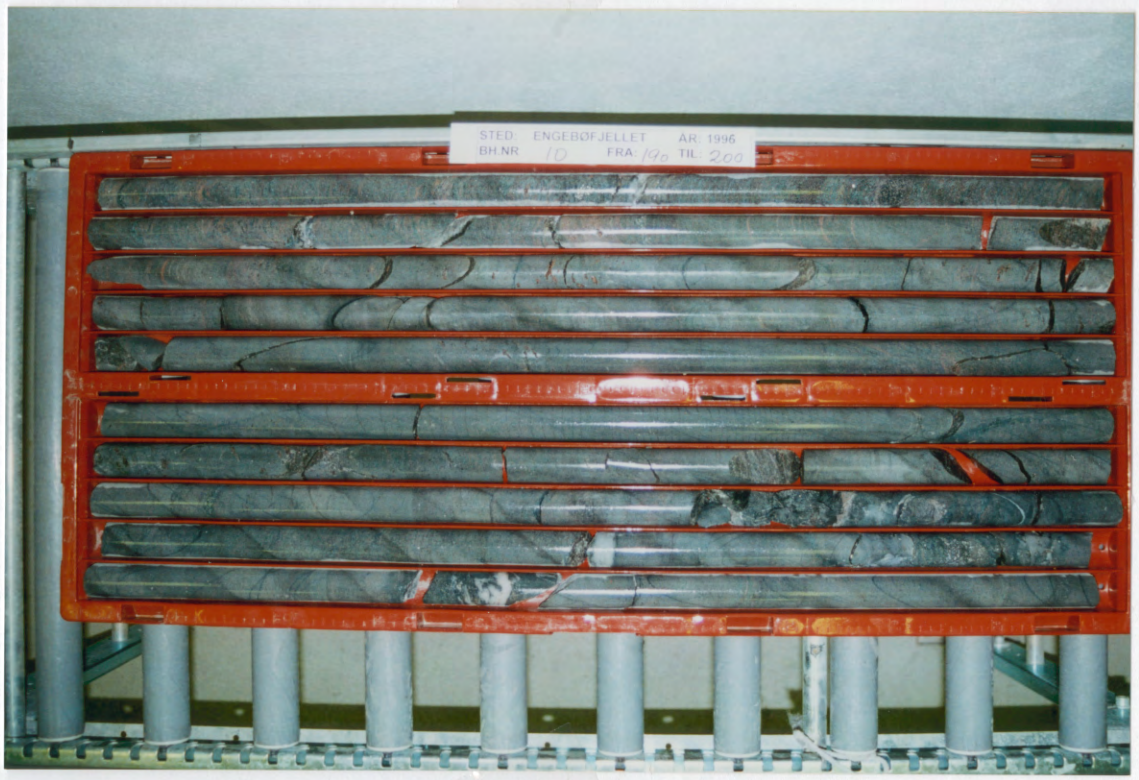
STED: ENGEBØFJELLET ÅR: 1996
BH.NR 10 FRA: 190 TIL: 200

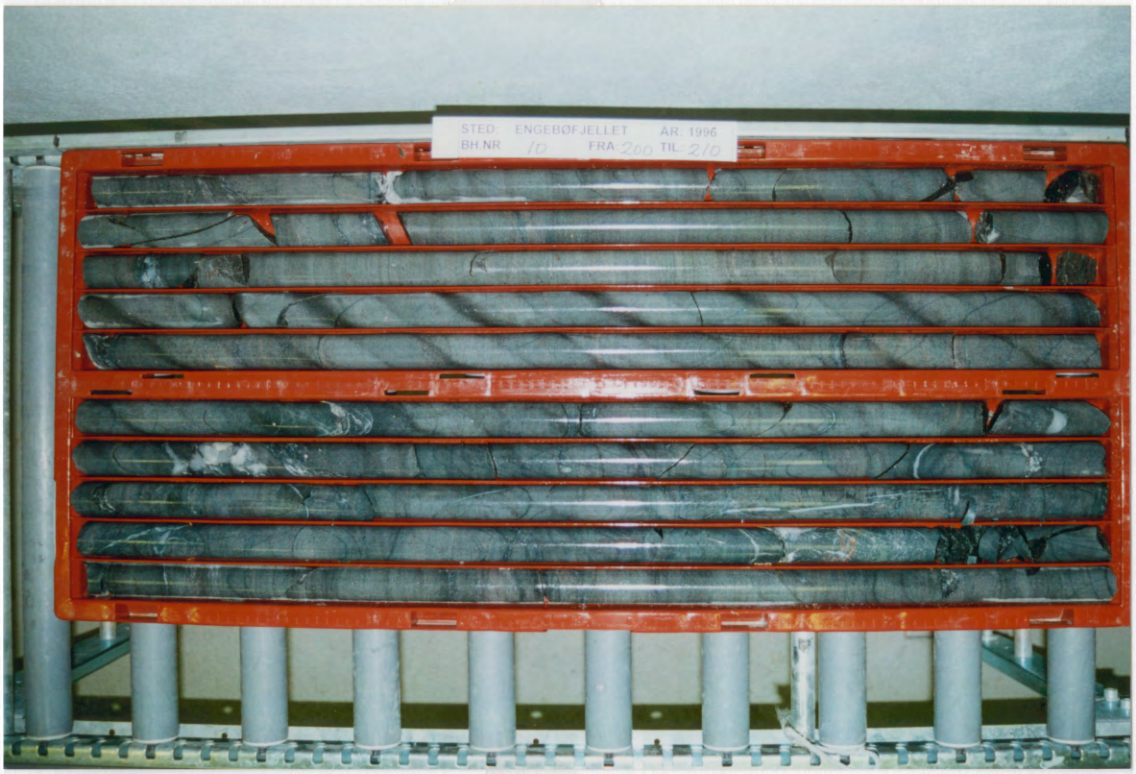
STED: ENGEBØFJELLET ÅR: 1996
BH.NR 10 FRA: 200 TIL: 210

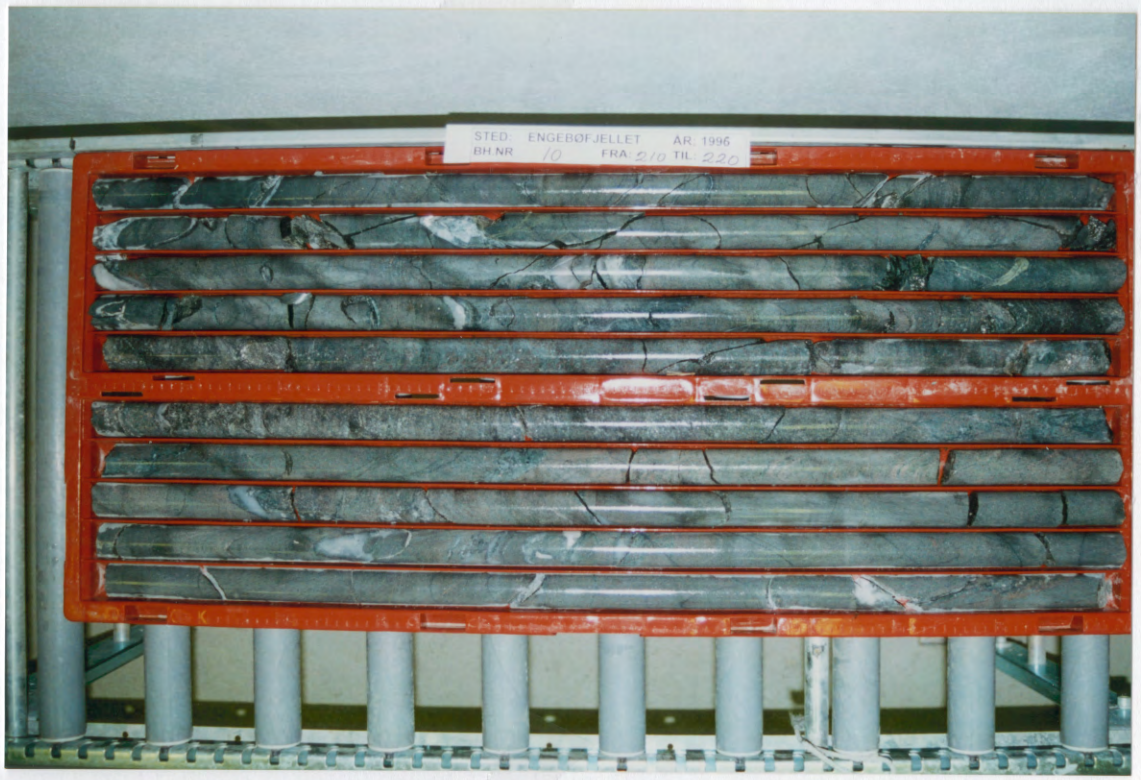
STED: ENGEBØFJELLET ÅR: 1996
BH.NR 10 FRA: 210 TIL: 220

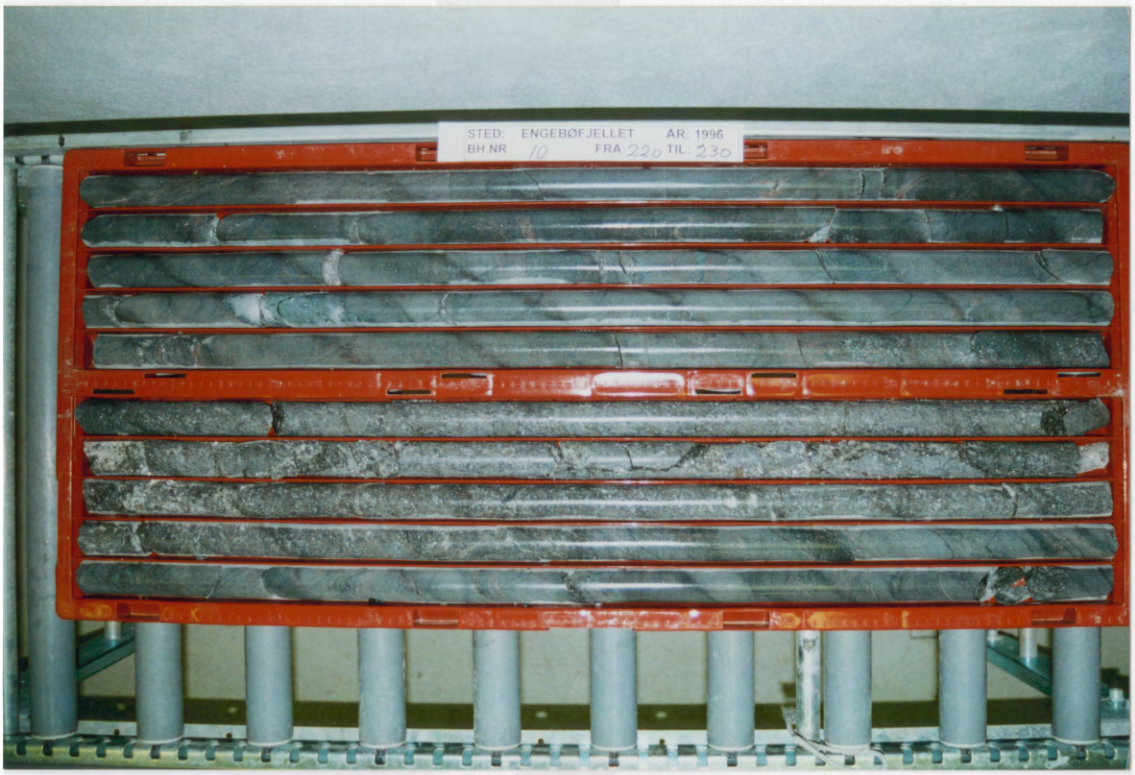
STED: ENGEBØFJELLET ÅR: 1996
BH.NR 10 FRA: 220 TIL: 230

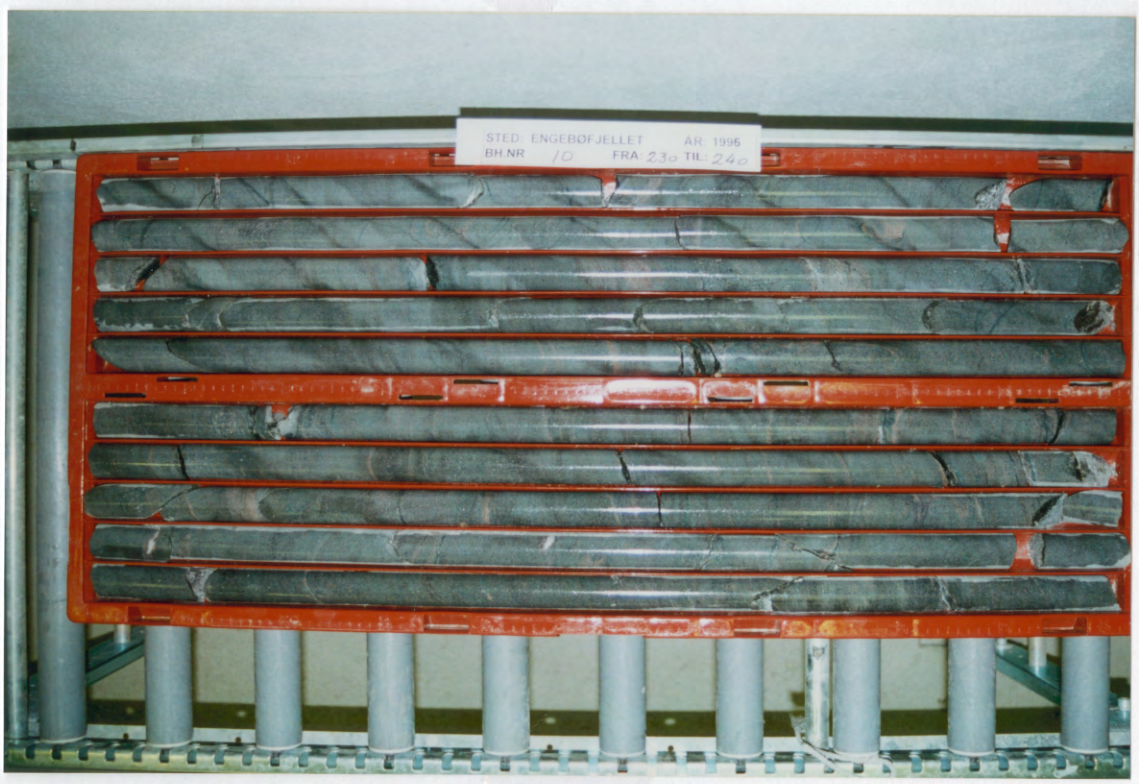
STED: ENGEBØFJELLET ÅR: 1996
BH.NR 10 FRA: 230 TIL: 240

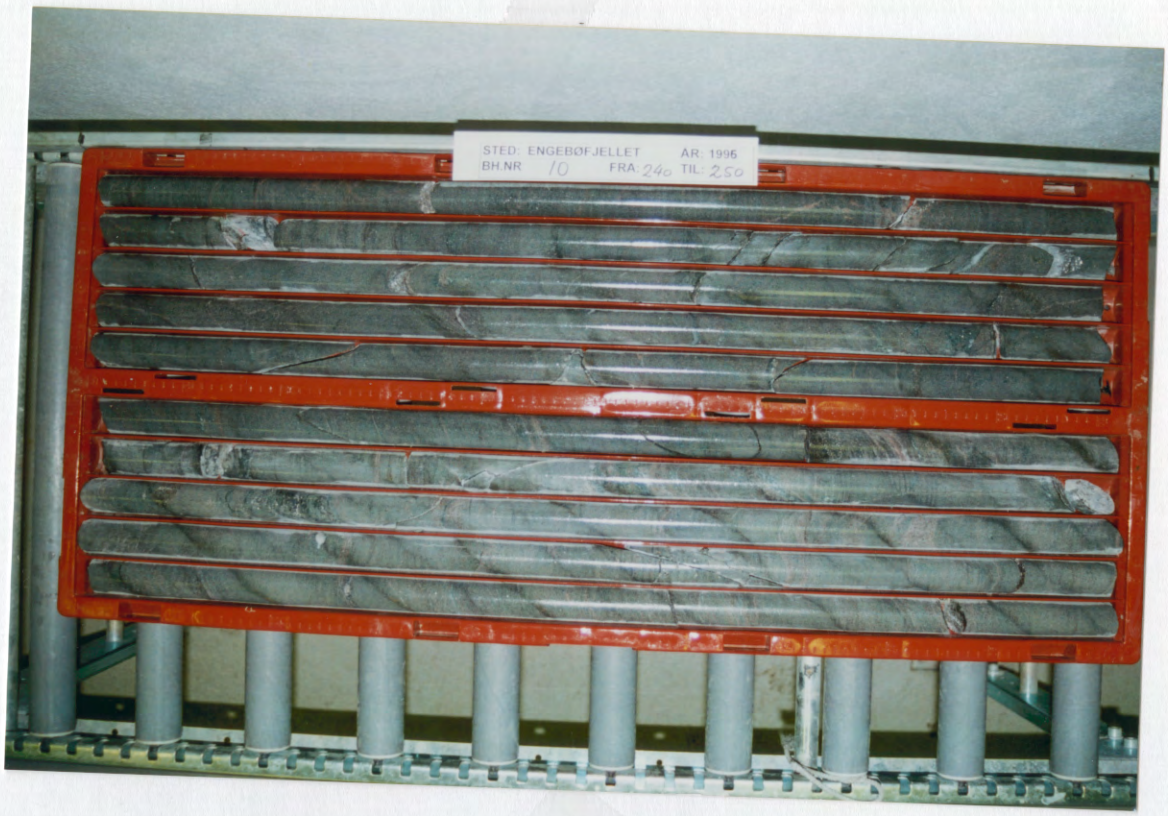
STED: ENGEBØFJELLET ÅR: 1996
BH.NR 10 FRA: 240 TIL: 250

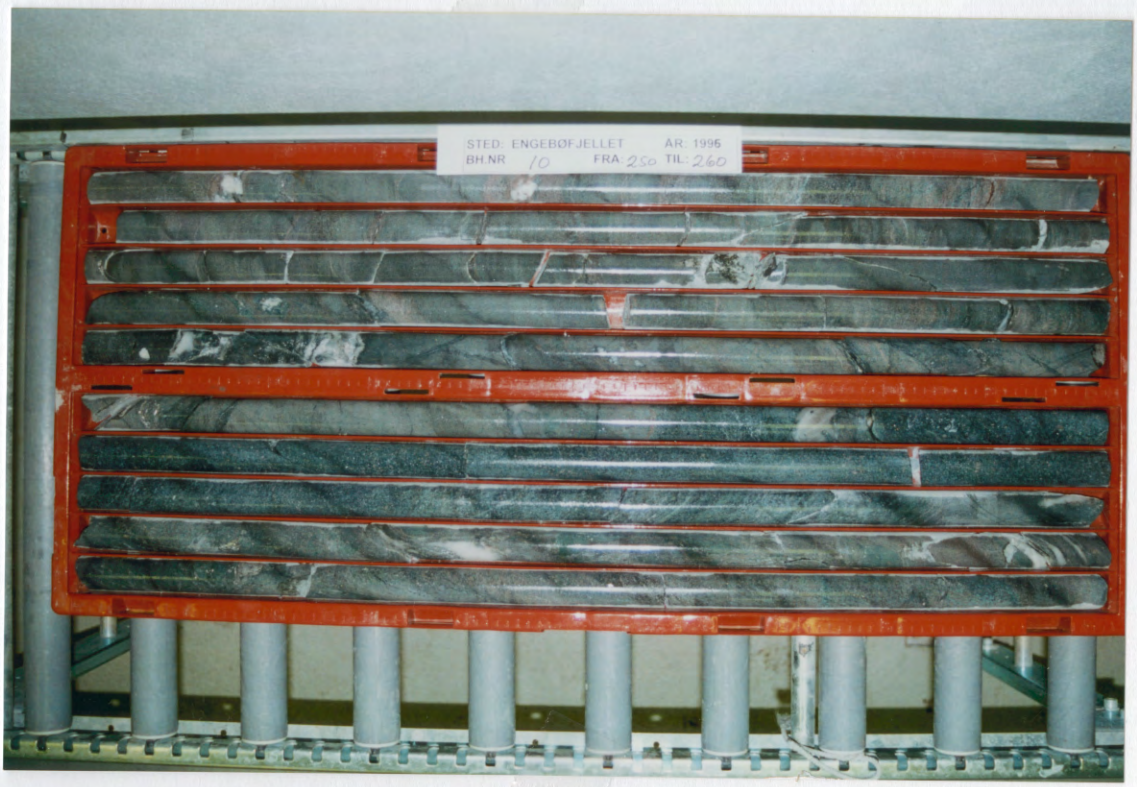
STED: ENGEBØFJELLET ÅR: 1996
BH.NR 10 FRA: 250 TIL: 260

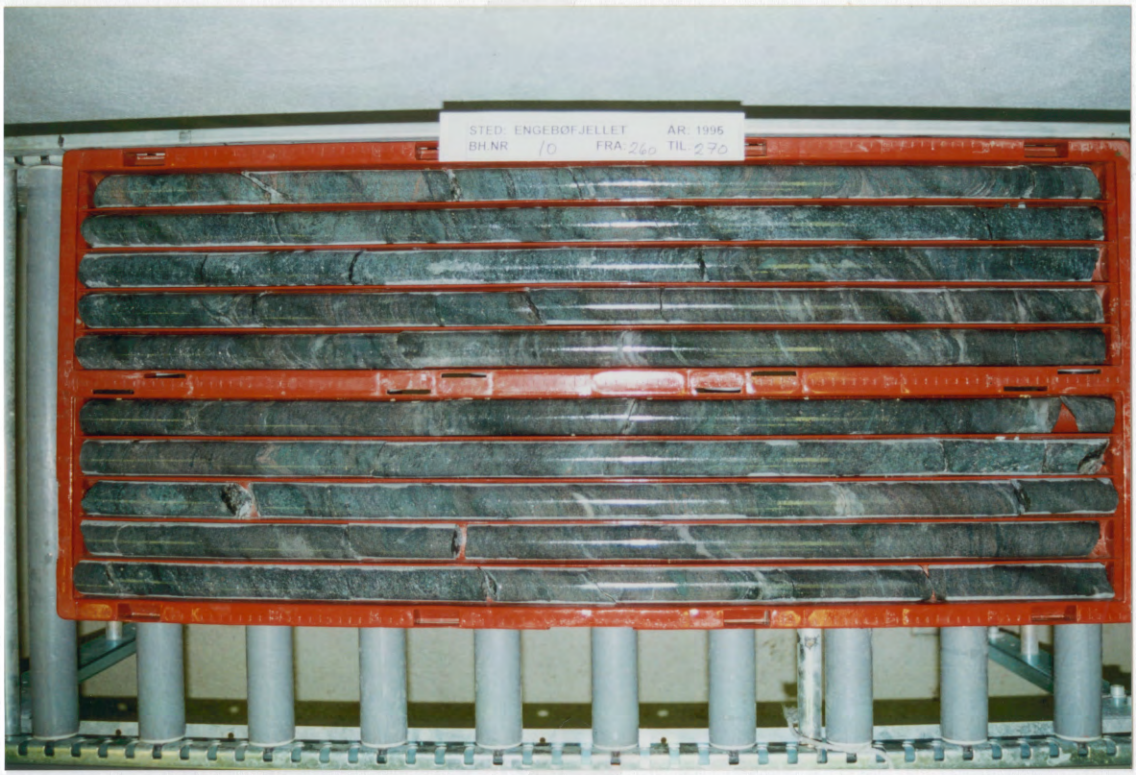
STED: ENGEBØFJELLET ÅR: 1995
BH.NR 10 FRA: 260 TIL: 270

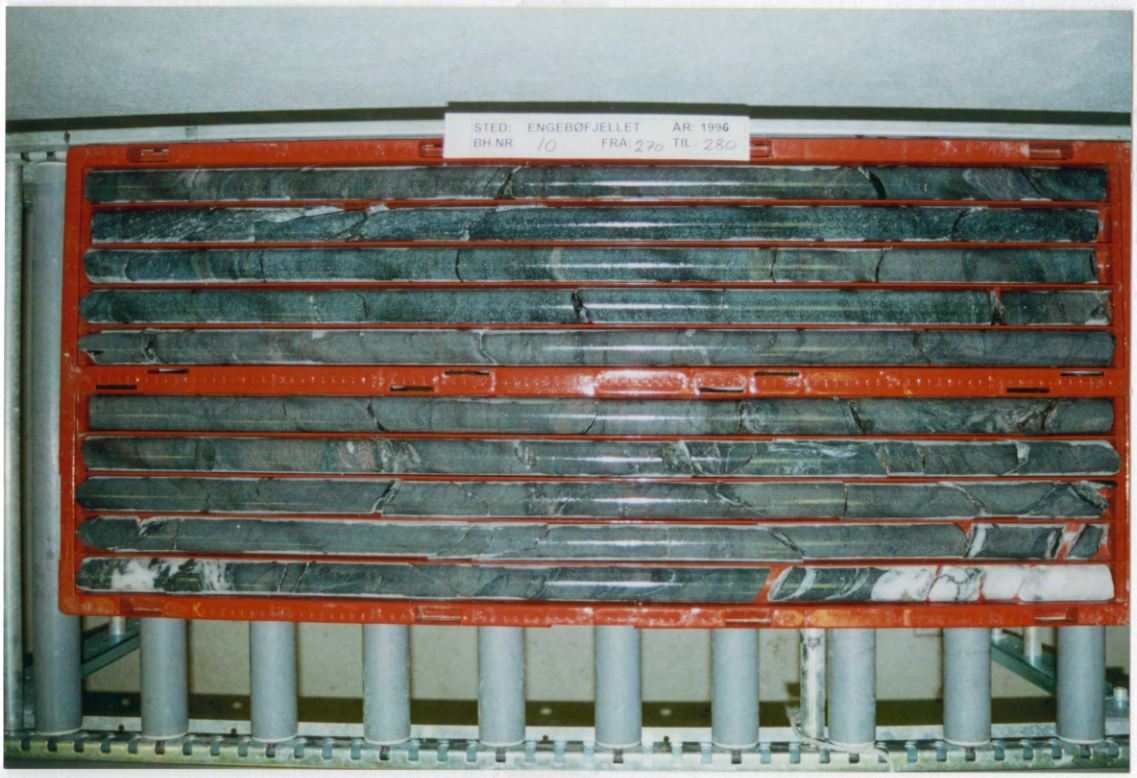
STED: ENGEBØFJELLET ÅR: 1996
BH.NR 10 FRA: 270 TIL: 280

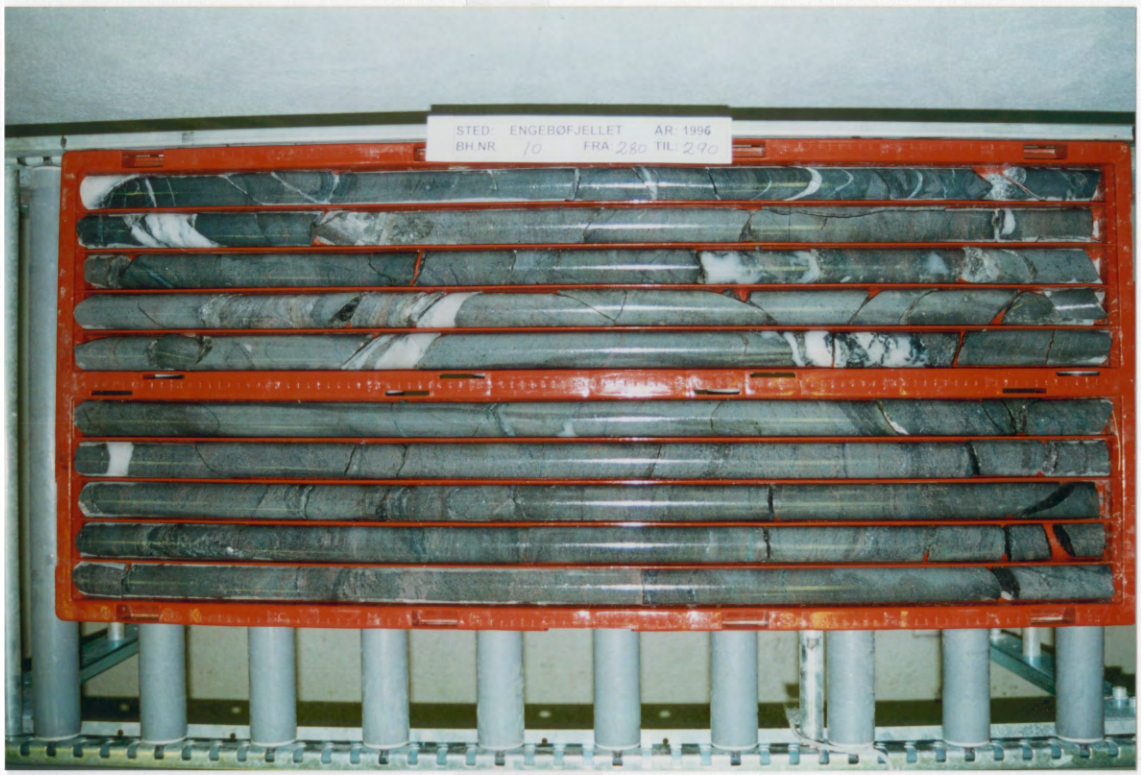
STED: ENGEBØFJELLET ÅR: 1996
BH.NR 10 FRA: 280 TIL: 290

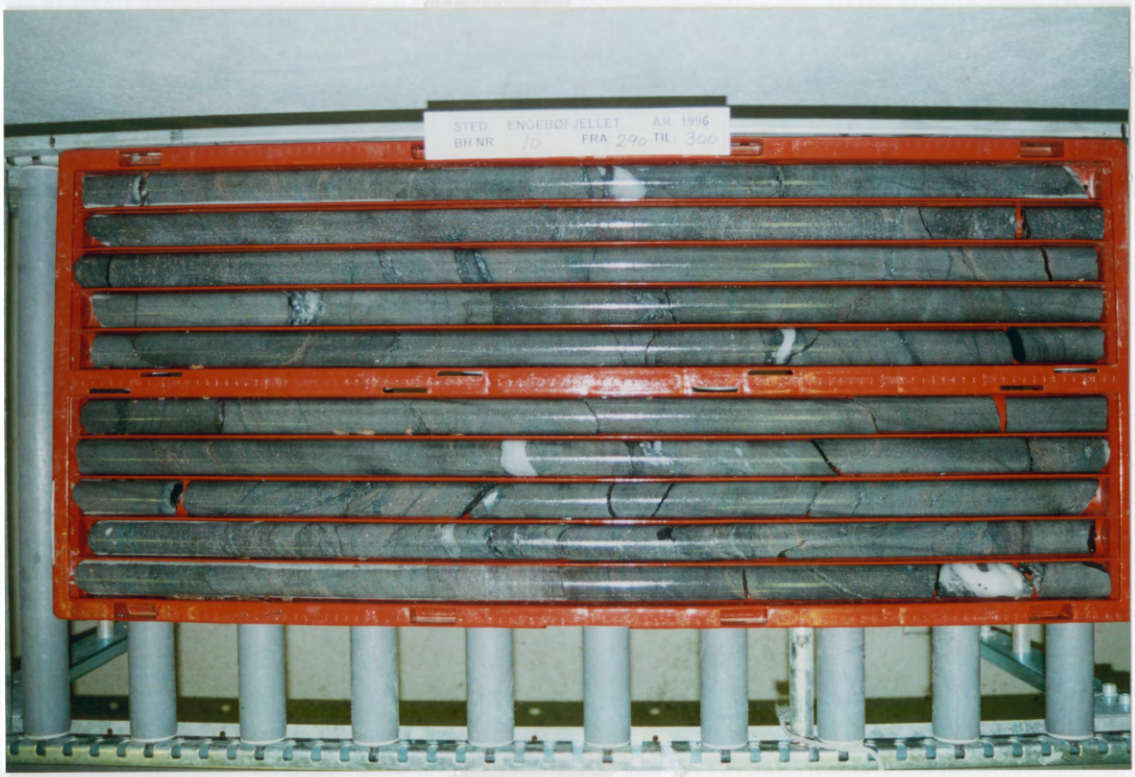
STED: ENGEBØFJELLET ÅR: 1996
BH.NR 10 FRA: 290 TIL: 300

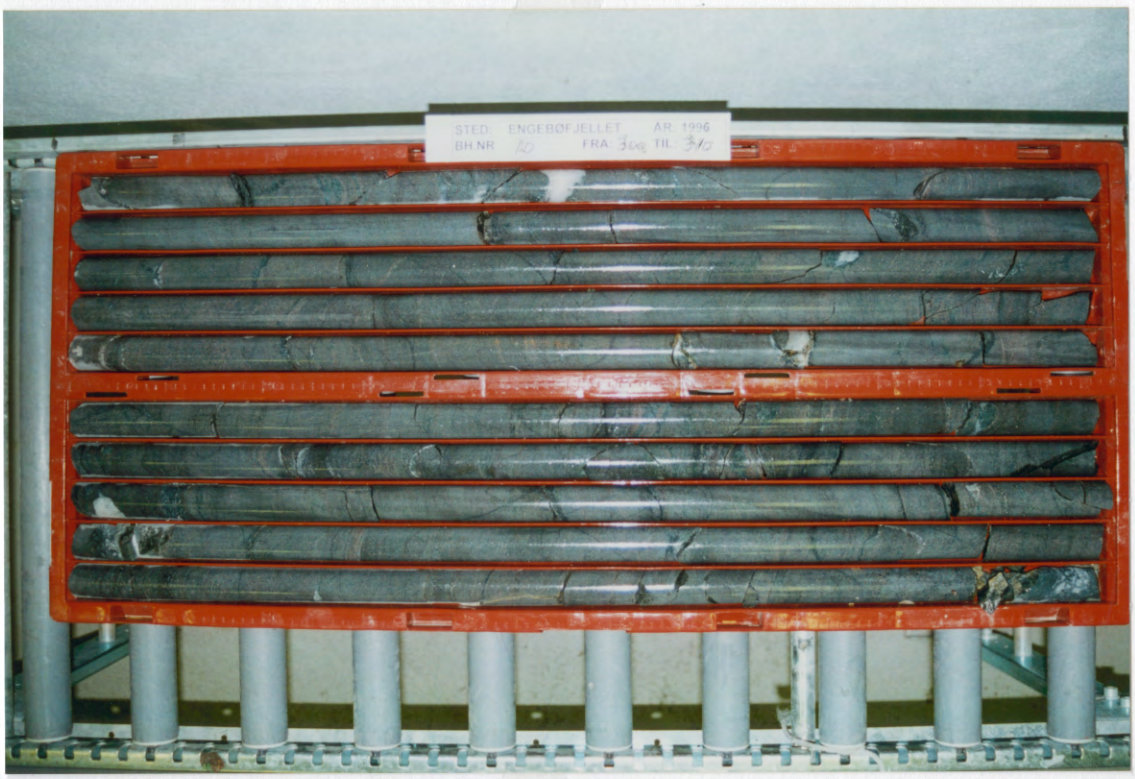
STED: ENGEBØFJELLET ÅR: 1996
BH.NR 10 FRA: 308 TIL: 317

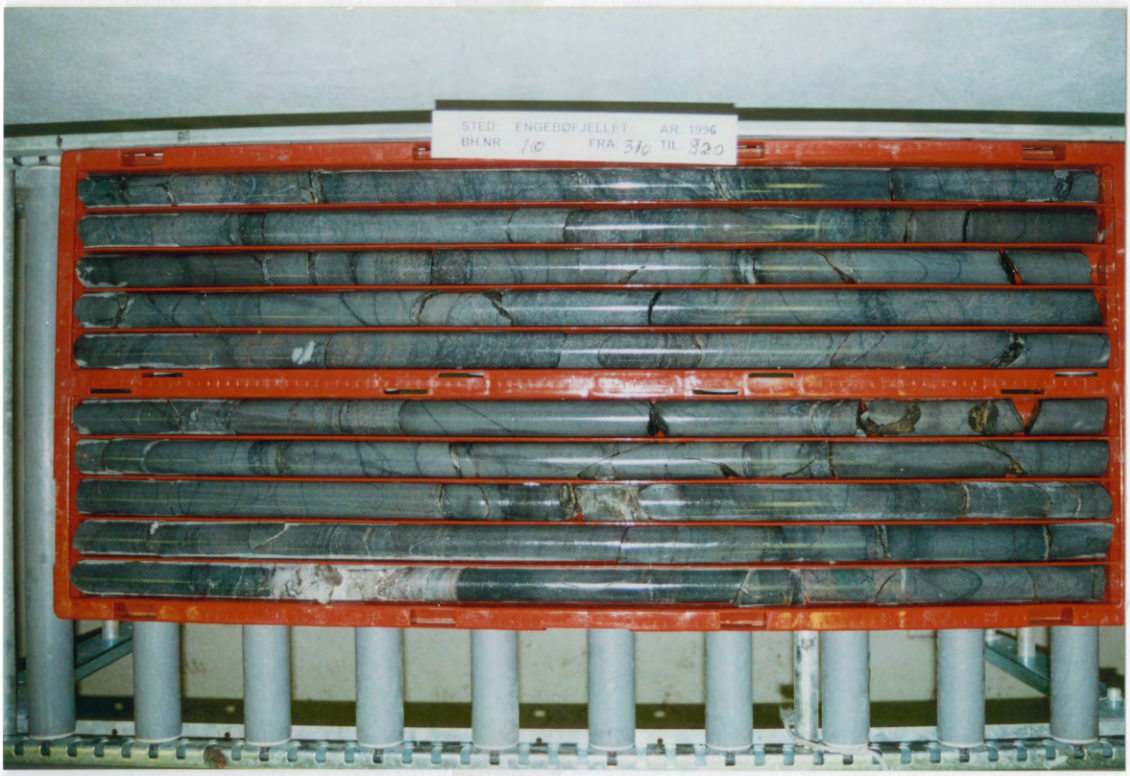
STED: ENGEBØFJELLET ÅR: 1996
BH.NR 10 FRA: 317 TIL: 327

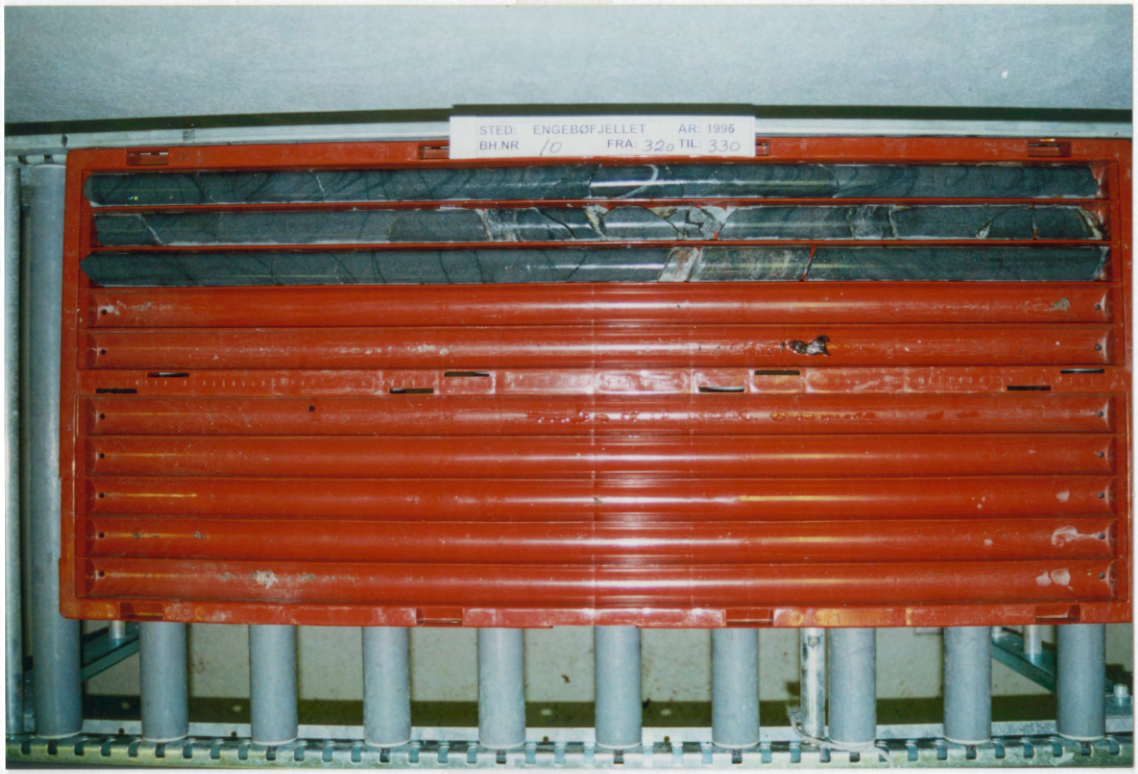
STED: ENGEBØFJELLET ÅR: 1996
BH.NR 10 FRA: 320 TIL: 330

Appendix 8f:

Photographs of 10m core sections

Dh3

(continued; se report 96.062 for Dh3 0-163m)

Photographed at NGU's core storage at Løkken


ENGEBØFJELLET
BH 3 163,1 - 170 m
163
164
169
170
STED: ENGEBØFJELLET AR: 1996
BH.NR 3 FRA: 163,1 TIL: 170

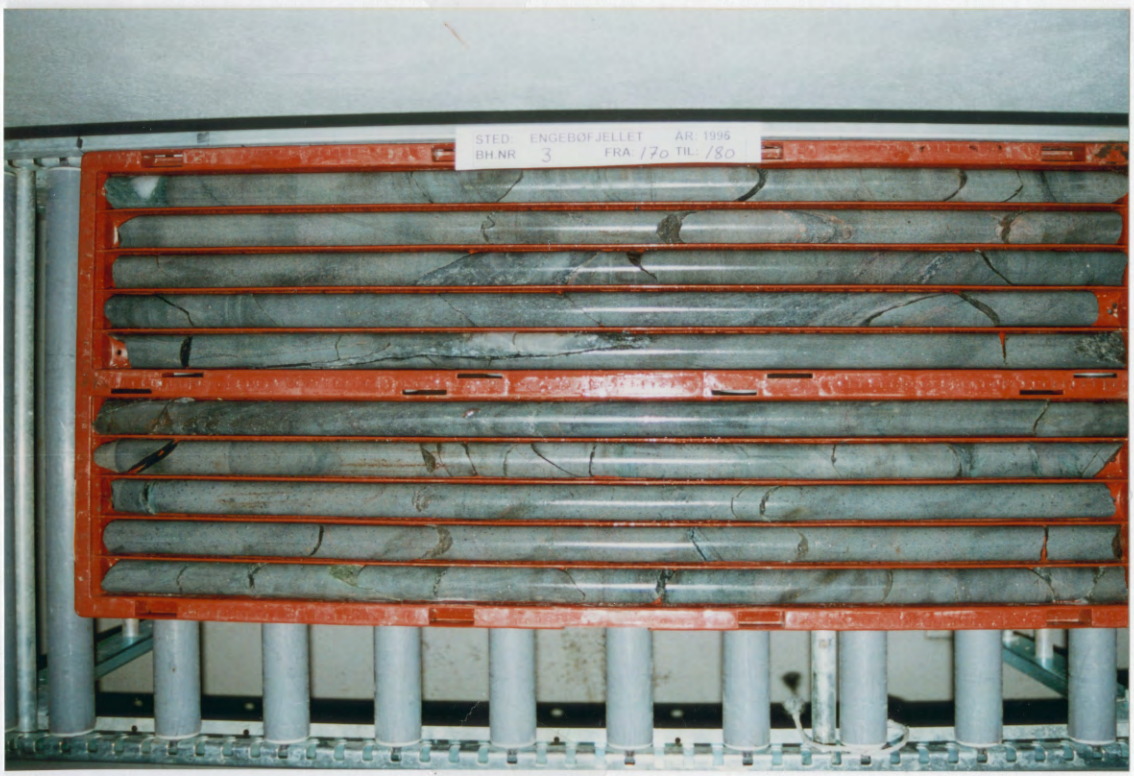
STED: ENGEBØFJELLET AR: 1996
BH.NR 3 FRA: 170 TIL: 180

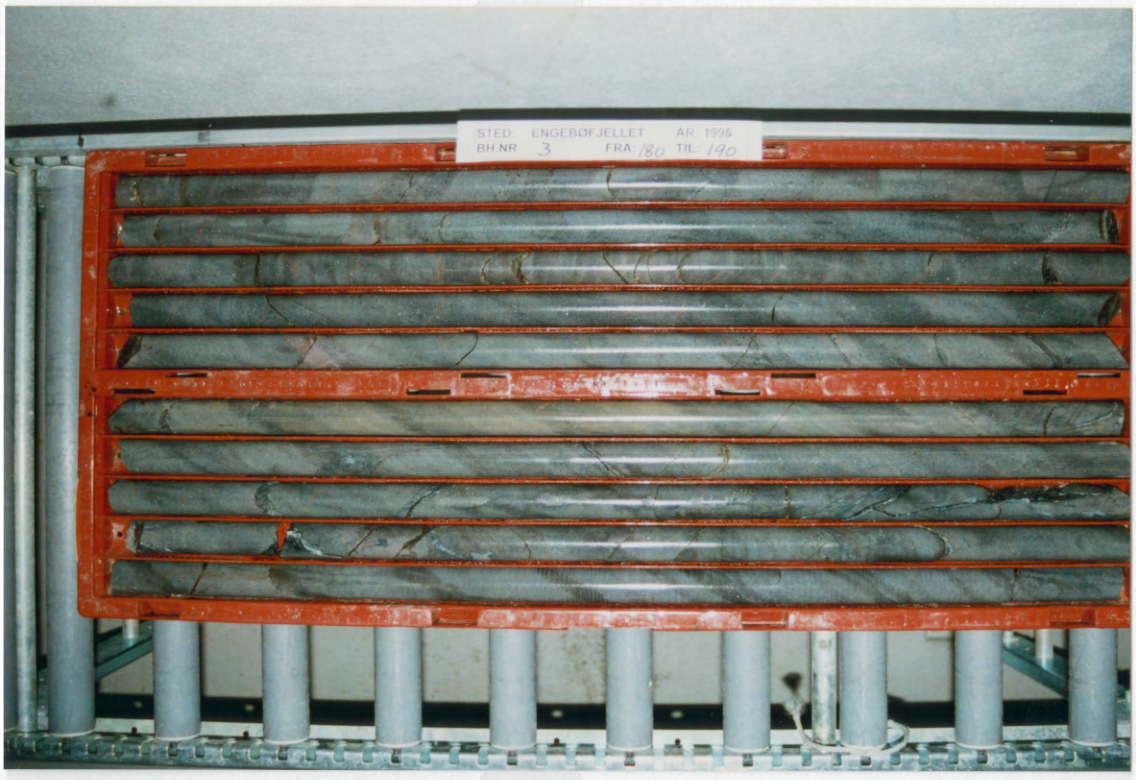
STED: ENGEBØFJELLET ÅR: 1996
BH.NR 3 FRA: 180 TIL: 190

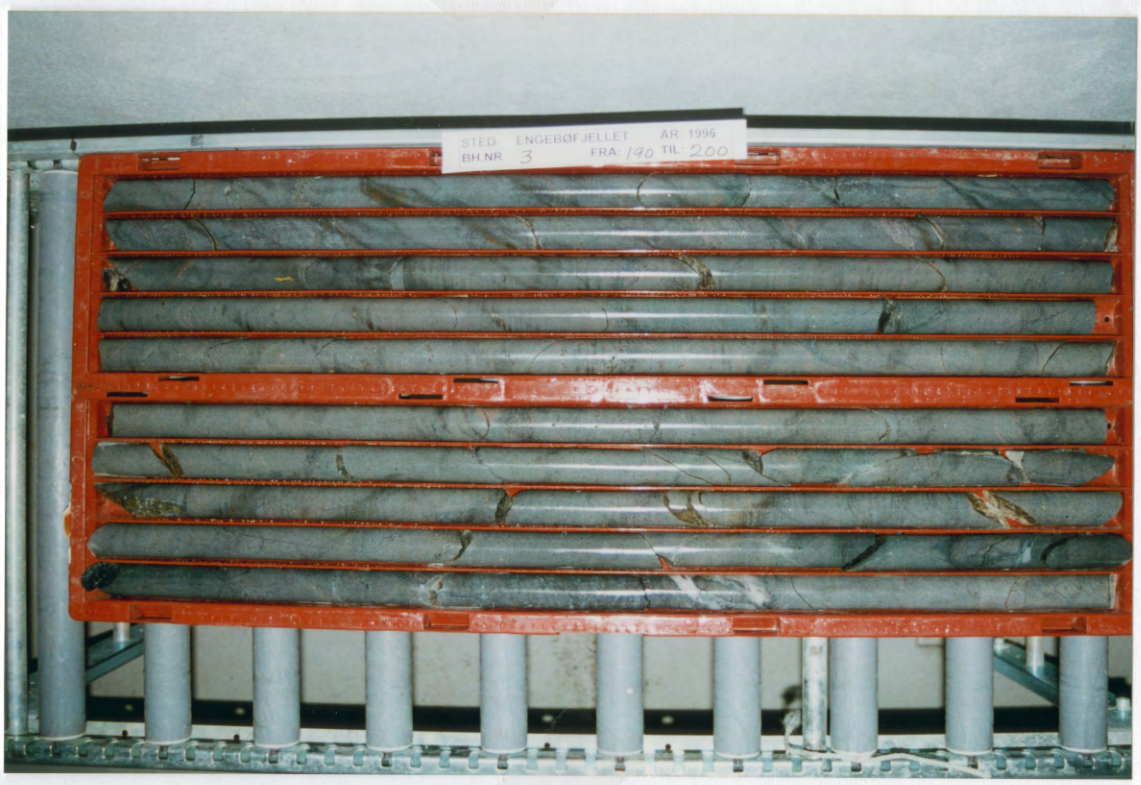
STED: ENGEBØFJELLET ÅR: 1996
BH.NR 3 FRA: 190 TIL: 200

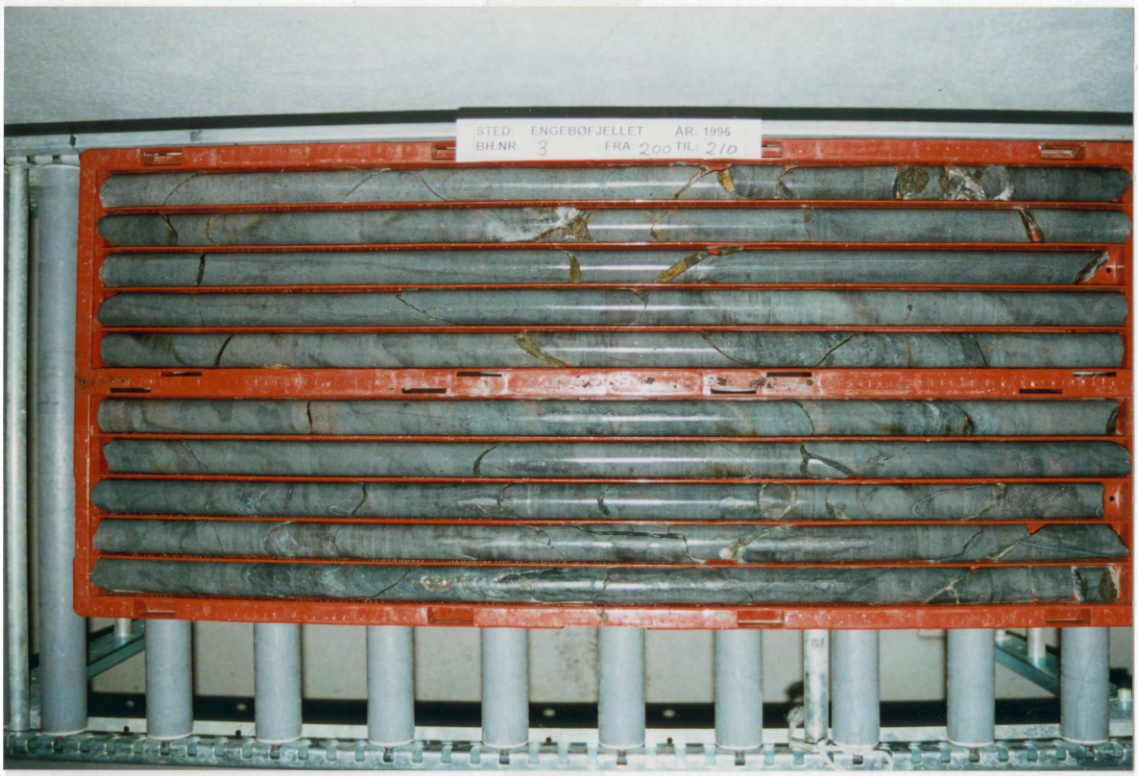
STED: ENGEBØFJELLET ÅR: 1996
BH.NR. 3 FRA: 200 TIL: 210

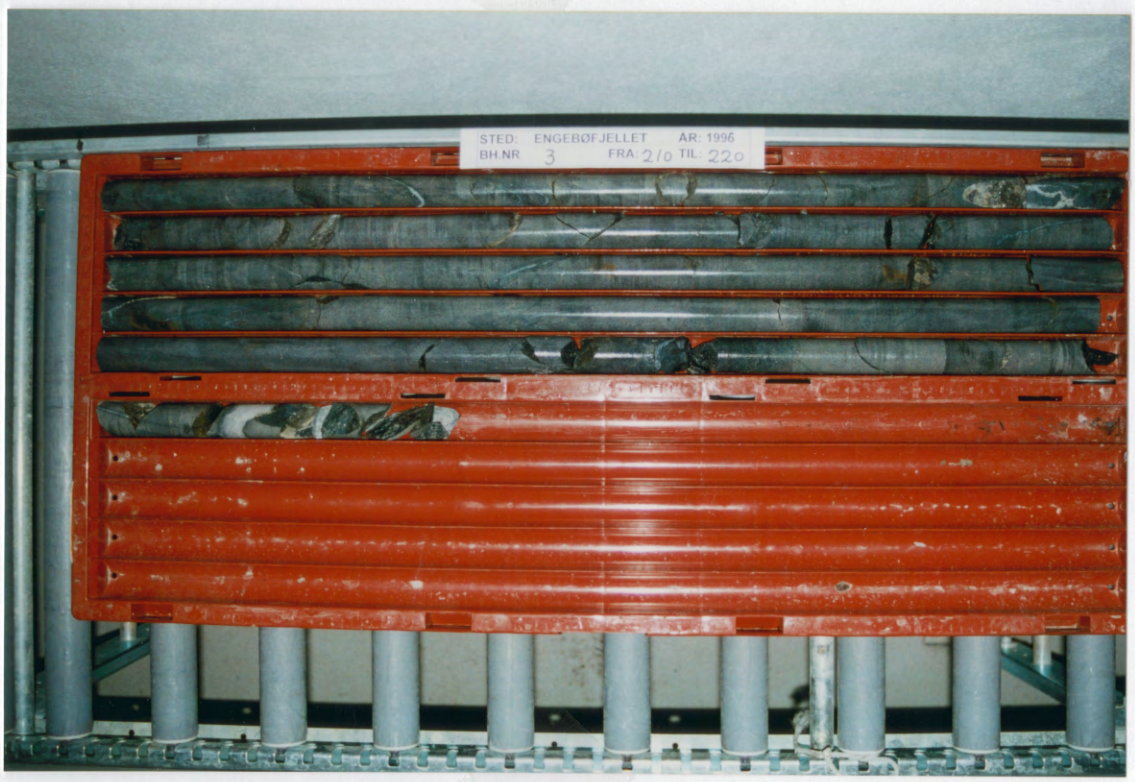
STED: ENGEBØFJELLET ÅR: 1996
BH.NR. 3 FRA: 210 TIL: 220